



Johnson, Sile Ann (2018) The local tumour immune response following systemic Salmonella enterica serovar Typhimurium infection. PhD thesis, University of Glasgow. PhD thesis.

<https://theses.gla.ac.uk/8982/>

Copyright and moral rights for this work are retained by the author

A copy can be downloaded for personal non-commercial research or study, without prior permission or charge

This work cannot be reproduced or quoted extensively from without first obtaining permission in writing from the author

The content must not be changed in any way or sold commercially in any format or medium without the formal permission of the author

When referring to this work, full bibliographic details including the author, title, awarding institution and date of the thesis must be given

Enlighten: Theses

<https://theses.gla.ac.uk/>  
[research-enlighten@glasgow.ac.uk](mailto:research-enlighten@glasgow.ac.uk)



# University of Glasgow

A thesis submitted to the University of Glasgow for the degree of  
Doctor of Philosophy

The local tumour immune response following systemic  
*Salmonella enterica* serovar Typhimurium infection

**Síle Ann Johnson**  
**BSc, MRes**

Submitted September, 2017

Institute of Infection, Immunity and Inflammation  
College of Medical, Veterinary and Life Sciences  
University of Glasgow

# Declaration

I hereby declare that this thesis is the result of my own work and has been composed for the degree of PhD at the University of Glasgow. This work has not been submitted for any other degree at this or any other institution. All work presented was performed by myself unless otherwise stated. All sources of information and contributions to the work have been specifically acknowledged in the text.

---

Síle Johnson

September 2017

Col, we always knew it, but now it's official: I'm smarter than you.

## Acknowledgments

Dónal ‘Dó-Dawg’ Wall; thank you for putting up with me and letting me run wild (although I’m not sure you had much choice in the matter). I probably have a lot of things to apologise for, but where’s the fun in that?? It is what it is.

Annie; thank you for knowing what I needed before I even knew myself. You run this joint, so thanks for looking after me and keeping me right over the years.

Slasher; you are a big reason I came to this lab group, and my leap of faith was paid back, even with just the orange drizzle cake alone. You have been such a great companion to have during this whole PhD business, and I am so grateful for that.

MJO; sound.

Hannah Banana; what an adventure! A big shout out to Darren and Olwyn, of course, for putting us together. I honestly wouldn’t know what FlowJo was, or what to do with a flow cytometer (I still don’t) if it wasn’t for you.

A big thanks to all of the people who gave me technical assistance over the years. Thank Margaret for the EM, Shauna and Jim for the histology. A big thank you to Diane in FCF for her patience and support with those big scary machines! Because of you, flow cytometry was a pleasure (most of the time), which isn’t something everyone can say. Also thank you to all of the Biological Services staff. Thanks to Craig, Stuart and Dennis for the IVs. Colin, you’re a wizard.

The Mowlings deserve a statue for their momentous contribution to this thesis. A special thanks to Allan for the meetings which really shaped my understanding (or lack there-of) of many concepts.

It would be remiss of me not to mention the Banter Bus, which has been central to the whole process. New Orleans changed everything (‘She gon’ get beat up’). It was the beginning of the Dream Team, and I will always be grateful to the City of Muffuletta for that. The Wallie Group was revolutionized, the likes of which had never been seen before; the squeaks; the tunes; the harvests; the poo; the

lols. I could write a whole thesis on the Dream Team, but then I'd have to write another acknowledgements section, and wouldn't know what to say. Unfortunately, the end is nigh, a pineapple, pepperoni and BBQ sauce pizza beckons. It is at this point I must hand over the mantle to you, Watson, and let you run the show. I must ask that you refrain from winking and pulling kissy-faces at barmen though.

The place will never be the same again. I give you the keys to the Banter Bus. Use them wisely! (but obviously not with anyone else).

The biggest thanks really have to go to main man, my Michael. Since you have been able to tolerate me in these last few days, I think we can get through anything. Thank you for coming to visit me in the FACS room on the late nights. Thank you for helping me with CFU plating when I needed it. Thank you for coming back in with me in the middle of the night when I needed to harvest plates. Thank you for making me get up early when I told you I needed to get up, and for bringing me coffee. Thank you for feeding me (lots of cereal!). Thank you for helping me with this final push (ugh) to get this thing printed (in spite of interspersed bouts of song) and getting me lots of wine.

## **Presentations and publications**

Johnson, SA *et al.*, **Weapons of tumour mass destruction; the use of *S. Typhimurium* as a cancer killer.** Poster Presentation at the Society of General Annual Conference, 30<sup>th</sup> March - 2<sup>nd</sup> April, 2015, Birmingham, United Kingdom.

Johnson, SA *et al.*, **Weapons of tumour mass destruction; the use of *S. Typhimurium* as a vehicle to deliver apoptotic genes to cancer cells.** Poster Presentation. American Society for Microbiology General Meeting, 2015, New Orleans, USA.

Johnson, SA *et al.*, **Trials and Tribu-filamentations of *S. Typhimurium* as a vehicle for therapeutic gene delivery to cancer cells.** Poster Presentation at the 'The New Bacteriology', Royal Society, 28<sup>st</sup> -29<sup>th</sup> January, 2016, London, United Kingdom.

Johnson, SA *et al.*, **Trials and Tribu-filamentations of *S. Typhimurium* as a vehicle for therapeutic gene delivery to cancer cells.** Oral Presentation at the Microbiology Society Annual Conference, 21<sup>st</sup> -24<sup>th</sup> March, 2016, Liverpool, United Kingdom.

Johnson, SA *et al.*, **Trials and Tribu-filamentations of *S. Typhimurium* as a vehicle for therapeutic gene delivery to cancer cells.** Poster Presentation at the Young Microbiologists Symposium, 29<sup>th</sup> - 30<sup>th</sup> June, 2016, Dundee, United Kingdom.

Johnson, SA *et al.*, ***S. Typhimurium*-mediated cancer therapy; a role for monocytes?** Oral Presentation at the Tumour Immunology conference, 3<sup>rd</sup> - 5<sup>th</sup> September, 2017.

Ormsby MJ, Johnson SA, Wall DM. 2016. **Draft genome sequence of the commensal *Escherichia coli* strain F-18.** Genome Announcements, 4(6):e01416-16.

Johnson SA, Ormsby MJ, Wall DM. 2017. **Draft genome sequence of the tumor-targeting *Salmonella enterica* serovar Typhimurium strain SL7207.** *Genome Announcements*, 5:e01591-16

Ormsby, MJ, Johnson, SA, Meikle, LM, Goldstone, RJ, McIntosh, A, Wessel, H, Hulme, HE, McConnachie, C, Fitzgerald, E, Gerasimidis, K, Morrison, D, Smith, DGE and Wall, DM.. 2017. **The short chain fatty acid antimicrobial propionic acid enhances the virulence of Crohn's disease associated adherent-invasive *Escherichia coli*.** *(Under review at PNAS)*

## Summary

In recent years, there is renewed interest in the potential of bacteria as an alternative cancer therapeutic strategy. *Salmonella enterica* serovar Typhimurium is arguably the most well studied strain of bacteria for cancer therapy, examined in both pre-clinical and clinical settings. Many of the studies which have demonstrated a role for *S. Typhimurium* in tumour growth inhibition or regression have focused on increasing the tumour-specific localisation of the bacteria, or enhancing the efficacy of the treatment modality. However, the exact mechanisms underlying *S. Typhimurium*-mediated tumour growth inhibition are incompletely elucidated, particularly with respect to the myeloid-derived immune cells, such as monocytes and macrophages.

The current study intended to address the dearth of information in the literature pertaining to the overall tumour-local immune response to systemically administered *S. Typhimurium*. This was achieved through the development of an *in vivo* tumour model and the optimisation of the *S. Typhimurium* administration protocol to maximise therapeutic effect. This allowed for the investigation of changes in multiple immune cell types in the tumour, both in number and functional phenotype, following infection. It was found that following systemic SL7207 infection, there was an increase in the secretion of pro-inflammatory mediators in the tumour milieu. This was accompanied by the activation of both neutrophils and monocytes, and possibly increased migration of tumour-associated dendritic cells. Interestingly, we found evidence to suggest that resident tumour-associated macrophages (TAMs) do not participate in mediating the pro-inflammatory tumour microenvironment following infection, which is suggested in some published reports. We were also interested in the types of T cell responses stimulated in the tumour following infection. This investigation revealed increases in the frequency of tumour-associated T helper (T<sub>H</sub>)1, but also T<sub>H</sub>17 cells following infection. There was also a concomitant decrease in the frequency of the tumour-promoting, T regulatory (Treg), cells in the tumour mass. To our knowledge, this is the first report to suggest a role for either T<sub>H</sub>17 or Tregs in playing a role in bacterial-mediated cancer therapy.

Given the phenotypic changes in the tumour-associated monocytes following infection, we chose to assess the contribution of this cell population to *S.*

Typhimurium-mediated tumour growth inhibition. This was attempted through the employment of transgenic mice lacking circulating monocytes and clodronate liposome-mediated depletion of monocytes/macrophages. Both of these approaches were proficient in depleting tumour monocytes in the uninfected state, with TAMs also affected by clodronate liposome-treatment. However, we found that neither of these approaches was sufficient to mediate the depletion of tumour-recruited monocytes following systemic *S. Typhimurium* infection. Interestingly, clodronate liposome treatment abrogated the *S. Typhimurium*-induced tumour growth inhibitory effects anyway. Upon further investigation, it was observed that the spleens of clodronate liposome-treated mice that were systemically infected with *S. Typhimurium* did not experience splenomegaly like their control PBS liposome-treated counterparts. As the spleen is a source of systemic inflammatory mediators following infection and splenic monocytes contribute to the tumour monocyte/macrophage population, the current hypothesis is that the splenic monocytes mediate tumour-growth inhibition in *S. Typhimurium* infected mice. This concept antagonises the prevailing ideology in the literature that tumour-local immune cells are the effectors of bacterial-mediated tumour growth arrest.

This study also sought to enhance the tumour arrest effects of *S. Typhimurium* through transformation of the bacteria with a eukaryotic expression vector encoding tumour inhibitory genes, destined for transfer to the tumour cells. However, through this investigation, it was discovered that the bacteria transformed with such a plasmid exhibited an aberrant morphology and phenotype, which we subsequently discovered was due to a phage origin of replication encoded in the plasmid.

The data generated in this thesis provides valuable information pertaining to the general immune response in the tumour following systemically administered *S. Typhimurium*. Furthermore, we propose a role for monocytes, possibly of splenic origin, in mediating the effects of *S. Typhimurium*-induced tumour growth inhibition. Finally, we identified a feature of eukaryotic expression plasmid, a phage origin of replication, which is not compatible with *S. Typhimurium* and should be avoided for bactofection, and other bacteriological, studies.

# Table of Contents

Declaration.....	II
Acknowledgments.....	IV
Presentations and publications .....	VI
Summary.....	VIII
Table of Contents .....	X
List of Figures .....	XIV
List of Tables .....	XVI
Abbreviations.....	XVII
<b>1 Introduction.....</b>	<b>1</b>
<b>1.1 <i>Salmonella enterica</i> serovar Typhimurium .....</b>	<b>1</b>
1.1.1 Incidence and pathology.....	1
1.1.2 <i>S. Typhimurium</i> epithelial cell invasion and persistence .....	1
1.1.3 Stress responses of <i>S. Typhimurium</i> .....	3
1.1.4 Innate Immune Response to <i>S. Typhimurium</i> .....	4
1.1.5 Adaptive immune response to <i>S. Typhimurium</i> .....	12
<b>1.2 Cancer.....</b>	<b>17</b>
<b>1.3 The role of the immune system in preventing and promoting cancer .....</b>	<b>18</b>
1.3.1 Inflammation and cancer initiation .....	18
1.3.2 The immunosuppressive microenvironment.....	19
1.3.3 Cancer immunotherapy; enhancing anti-tumour immunity.....	28
<b>1.4 Bacterial-mediated cancer therapy .....</b>	<b>30</b>
1.4.1 Tumour specific localisation and proliferation of systemically administered bacteria	31
1.4.2 Native and enhancement of bacterial tumour toxicity.....	35
1.4.3 Bactofection.....	38
1.4.4 <i>Salmonella</i> strains for bacterial mediated cancer treatment .....	41
1.4.5 Bacterial-mediated cancer therapy: immune cell activation.....	43
1.4.6 The contributions of local versus systemic tumour-inflammation in anti-tumour effects of bacteria .....	47
1.4.7 Limitations of bacteria for the purposes of cancer therapy .....	47
<b>1.5 <i>In vitro</i> and <i>in vivo</i> models to study bacterial mediated cancer therapy .....</b>	<b>50</b>
1.5.1 <i>In vitro</i> tumour spheroid models .....	50
1.5.2 <i>In vivo</i> cancer models .....	51
1.5.3 <i>In vivo</i> cancer models employed for bacterial mediated cancer therapy studies .....	52
<b>1.6 Hypotheses and aims .....</b>	<b>56</b>
<b>2 Methods and Materials.....</b>	<b>58</b>
<b>2.1 Animals.....</b>	<b>58</b>
<b>2.2 Bacterial strains, plasmids and cancer cell lines.....</b>	<b>58</b>
<b>2.3 Bacterial growth, cell culture and infection .....</b>	<b>60</b>
2.3.1 Bacterial growth curves .....	60
2.3.2 <i>In vitro</i> monolayer infection and harvest .....	61
<b>2.4 Gram staining and bacterial cell length measurement.....</b>	<b>61</b>
<b>2.5 Harvesting bacteria for fluorescent imaging .....</b>	<b>62</b>
<b>2.6 <i>In vitro</i> cell death analysis .....</b>	<b>62</b>
<b>2.7 Tumour spheroid generation <i>in vitro</i> and infection .....</b>	<b>63</b>
<b>2.8 Harvesting tumour spheroids .....</b>	<b>63</b>
2.8.1 Fluorescent imaging to investigate bacterial invasion and bactofection .....	63

2.8.2	Scanning electron microscopy to investigate bacterial localisation .....	64
2.8.3	Transmission electron microscopy to investigate biofilm formation .....	64
<b>2.9</b>	<b>Generation of bioluminescent SL7207 strain .....</b>	<b>65</b>
<b>2.10</b>	<b>B16F10 transplantable model and SL7207 infection protocol .....</b>	<b>65</b>
<b>2.11</b>	<b><i>In vivo</i> imaging of SL-Lux .....</b>	<b>66</b>
<b>2.12</b>	<b><i>In vivo</i> tissue harvest following infection for CFU counts .....</b>	<b>66</b>
<b>2.13</b>	<b>Hematoxylin and eosin staining of tumour sections .....</b>	<b>67</b>
2.13.1	Tissue harvest and digest .....	67
2.13.2	Intracellular cell stimulation .....	68
2.13.3	Surface staining .....	68
2.13.4	Intracellular staining.....	68
2.13.5	Assessment of phagocytosis.....	69
<b>2.14</b>	<b>Immunoblot analysis.....</b>	<b>70</b>
2.14.1	Immunoblot analysis of prokaryotic cells.....	70
2.14.2	Immunoblot analysis of eukaryotic cells .....	71
<b>2.15</b>	<b>Enzyme-linked immunosorbent assay (ELISA).....</b>	<b>71</b>
<b>2.16</b>	<b>Photoconversion of immune cells in Kaede mice .....</b>	<b>72</b>
<b>2.17</b>	<b>Clodronate-mediated depletion of monocytes and macrophages.....</b>	<b>73</b>
<b>2.18</b>	<b>Generation of the pACYC-EGFP plasmid .....</b>	<b>73</b>
2.18.1	Plasmid isolation (Miniprep) .....	73
2.18.2	Polymerase chain reaction .....	74
2.18.3	Restriction digest.....	75
2.18.4	Agarose gel electrophoresis .....	76
2.18.5	Gel purification of DNA bands.....	76
2.18.6	Ligation .....	77
<b>2.19</b>	<b>Generation of the pEGFLacZ plasmid using NEBuilder<sup>®</sup> Hifi DNA Cloning .....</b>	<b>77</b>
<b>3</b>	<b>Development of the B16F10 tumour model and <i>S. Typhimurium</i> infection protocol</b>	<b>79</b>
<b>3.1</b>	<b>Introduction.....</b>	<b>79</b>
3.1.1	Aims .....	80
<b>3.2</b>	<b>Results .....</b>	<b>81</b>
3.2.1	Optimisation of tumour cell seeding density for subcutaneous tumour growth .....	81
3.2.2	Optimisation of <i>S. Typhimurium</i> SL7207 infectious dose .....	82
3.2.3	Understanding the dynamics of SL7207 tumour infection .....	84
3.2.4	Effects of SL-Lux on tumour growth .....	88
3.2.5	Effects of SL-Lux on tumour cell death and tumour cell replicative capacity..	90
3.2.6	<i>In vitro</i> tumour cell killing capacity of SL-Lux.....	94
<b>3.3</b>	<b>Discussion .....</b>	<b>96</b>
3.3.1	Why is the choice of tumour mouse model important for understanding and interpreting the data? .....	96
3.3.2	Implications of colonisation represented as CFU/g .....	97
3.3.3	Why investigate the optimal conditions for SL7207 infection of tumour-bearing mice? .....	99
3.3.4	How does the tumour growth inhibition of SL7207 compare with other studies? ..	100
3.3.5	Host welfare: is it safe to use <i>S. Typhimurium</i> on cancer patients? .....	101
3.3.6	SL7207-mediated tumour growth arrest: tumour cell death or cell cycle inhibition? ..	102
3.3.7	Concluding remarks .....	104
<b>4</b>	<b>Characterisation of the local immune response in the tumour following systemic administration of SL7207.....</b>	<b>105</b>
<b>4.1</b>	<b>Introduction.....</b>	<b>105</b>
4.1.1	Aims .....	106
<b>4.2</b>	<b>Results .....</b>	<b>107</b>

4.2.1	Leukocyte content of tumour during steady state .....	107
4.2.2	Changes in the production of pro-inflammatory mediators in the tumour following systemic SL7207 infection .....	109
4.2.3	Changes in the total number of leukocytic cell infiltrates in tumours infected with SL7207 .....	111
4.2.4	Effects of systemic SL7207 infection of tumour-associated neutrophils.....	112
4.2.5	Tumour-associated DC number and activation following systemic SL7207 infection .....	114
4.2.6	Changes in the T cell infiltrate into the tumour and tdLN following infection .....	121
4.2.7	T <sub>H</sub> 1 responses detected in the tumour and tdLN following SL7207 infection .....	122
4.2.8	T <sub>H</sub> 17 responses in the tumour following SL7207 infection.....	124
4.2.9	Changes in the frequency of CD4 <sup>+</sup> Foxp3 <sup>+</sup> Tregs in the tumour following SL7207 infection.....	125
<b>4.3</b>	<b>Discussion .....</b>	<b>127</b>
4.3.1	Why was there no change in the number of tumour-associated leukocytes following infection? .....	127
4.3.2	What role might tumour-associated neutrophils be playing in SL7207-mediated tumour growth inhibition? .....	129
4.3.3	What role might the DCs be playing following SL7207 infection?.....	130
4.3.4	Why is it important to understand the type of T cell response in the infected tumour? .....	133
4.3.5	Concluding Remarks .....	135
<b>5</b>	<b>The role of the monocyte/macrophage compartment in SL7207-mediated tumour growth inhibition .....</b>	<b>136</b>
<b>5.1</b>	<b>Introduction .....</b>	<b>136</b>
5.1.1	Aims .....	137
<b>5.2</b>	<b>Results .....</b>	<b>139</b>
5.2.1	Tumour-associated monocyte/macrophage subsets in the B16F10 tumours in steady state .....	139
5.2.2	Effects of systemic SL7207 infection on tumour-associated monocytes.....	142
5.2.3	Effects of systemic SL7207 infection on TAMs .....	148
5.2.4	Contributions of resident and recruited precursors to MHCII <sup>+</sup> TAMs .....	155
5.2.5	Effects of SL7207 in monocyte deficient <i>CCR2</i> <sup>-/-</sup> mice .....	161
5.2.6	The effects of clodronate liposome-mediated monocyte/macrophage depletion on tumour inhibition by SL7207 .....	166
<b>5.3</b>	<b>Discussion .....</b>	<b>172</b>
5.3.1	Why is it important to define and characterise immune cell subsets in the tumour? .....	172
5.3.2	Why is there an accumulation of Ly6C <sup>+</sup> MHCII <sup>+</sup> cells, and why might this promote anti-tumour effects?.....	175
5.3.3	What do the changes in TAM phenotype following infection mean, and why is this important? .....	177
5.3.4	Why was the Kaede data not informative and how could this experiment be improved?.....	179
5.3.5	Why was the <i>CCR2</i> <sup>-/-</sup> murine strain not effective at removing monocytes during SL7207 infection? .....	180
5.3.6	What can be concluded from the clodronate liposome infected mice? .....	183
5.3.7	Concluding remarks .....	185
<b>6</b>	<b><i>S. Typhimurium</i> transformed with an eukaryotic expression plasmid to mediate bactofection in tumour spheroid cells <i>in vitro</i>.....</b>	<b>186</b>
<b>6.1</b>	<b>Introduction.....</b>	<b>186</b>
6.1.1	Aims .....	187
<b>6.2</b>	<b>Results .....</b>	<b>188</b>

6.2.1	The generation of three dimensional tumour spheroids <i>in vitro</i> .....	188
6.2.2	Invasion and biofilm forming capacities of VNP20009 with tumour spheroids .....	189
6.2.3	Selection of VNP20009 through serial reisolations to increase tumour invasion capacity <i>in vitro</i> .....	191
6.2.4	Bactofection capacities of <i>S. Typhimurium</i> -pEGFP .....	192
6.2.5	Morphological characterisation of <i>S. Typhimurium</i> transformed with pEGFP .....	194
6.2.6	Effects of pEGFP transformation on <i>E. coli</i> strains .....	196
6.2.7	Effects of filamentation on growth and invasion of SL-pEGFP .....	198
6.2.8	Stress responses induced in pEGFP-transformed <i>S. Typhimurium</i> cultures .....	199
6.2.9	The contribution of the f1 ori in pEGFP to the filamentous phenotype of SL-pEGFP	201
<b>6.3</b>	<b>Discussion .....</b>	<b>205</b>
6.3.1	Why employ tumour spheroids for the preliminary <i>in vitro</i> study? .....	205
6.3.2	Why were there still VNP20009 cells on the surface of the tumour spheroid following gentamycin treatment, and why is this a concern?.....	206
6.3.3	Why increase the tumour cell invasion potential of <i>S. Typhimurium</i> ?.....	207
6.3.4	What is the relevance of the attenuated replication and invasion features of the filamentous cultures? .....	209
6.3.5	What is the role of the f1 ori in eukaryotic expression plasmids and how might it be inducing filamentation?.....	210
6.3.6	Concluding remarks.....	211
<b>7</b>	<b>Conclusions and future perspectives .....</b>	<b>213</b>
<b>8</b>	<b>References.....</b>	<b>219</b>
<b>9</b>	<b>Appendix .....</b>	<b>268</b>

# List of Figures

Figure 1.1 PRR signaling in response to PAMPs	5
Figure 1.2 Development of mature tissue macrophages from bone marrow precursors	9
Figure 1.3 Polarized CD4 <sup>+</sup> T <sub>H</sub> subsets	13
Figure 1.4 Origin of tumour-associated macrophages	21
Figure 1.5 Proposed mechanisms contributing to tumour-specific localisation and proliferation of bacteria following systemic infection	33
Figure 1.6 <i>S. Typhimurium</i> have multiple features which make them amenable for bacterial-mediated cancer therapy	42
Figure 3.1 Optimisation of the tumour cell seeding density for tumour development	82
Figure 3.2 Optimisation of the infectious dose to induce tumour growth inhibition	83
Figure 3.3 Growth and invasion characteristics of SL-Lux compared to wild type	84
Figure 3.4 <i>In vivo</i> localisation of SL-Lux	85
Figure 3.5 Colony forming unit (CFU) counts from multiple organs following SL-Lux infection	86
Figure 3.6 Optimisation of tumour size for SL-Lux infection	88
Figure 3.7 Effects of SL-Lux on tumour growth and survival of tumour-bearing mice	89
Figure 3.8 Effects of SL-Lux on tumour fold growth and weight	90
Figure 3.9 While tumour viability and tumour cell gating strategy	91
Figure 3.10 Effects of SL-Lux on whole tumour viability	92
Figure 3.11 Effects of SL-Lux on tumour cell viability	93
Figure 3.12 Effects of SL-Lux on tumour cell proliferation	94
Figure 3.13 Effects of SL-Lux on tumour cell viability <i>in vitro</i>	95
Figure 4.1 Gating strategies for immune cells in the tumour and tdLN	108
Figure 4.2 Tumour immune cells at indicated time points	109
Figure 4.3 Effects of SL7207 on the production of pro-inflammatory cytokines in the tumour	110
Figure 4.4 Effects of SL7207 on the tumour CD45 <sup>+</sup> immune cell content	111
Figure 4.5 Effects of SL7207 on tumour neutrophil content	112
Figure 4.6 Effects of SL7207 on the activation of tumour neutrophils	114
Figure 4.7 Effects of SL7207 on tumour DC content	115
Figure 4.8 Effects of SL7207 on tumour DC MHCII and CD80 expression	116
Figure 4.9 Revised gating strategy for tumour and tdLN cDCs	117
Figure 4.10 Effects of SL7207 on tumour cDC1 and cDC2 content	118
Figure 4.11 Effects of SL7207 on tdLN cDC1 and cDC2 content	119
Figure 4.12 Effects of SL7207 on migratory cDCs in tdLN	120
Figure 4.13 Effects of SL7207 on tumour T cell content	121
Figure 4.14 Effects of SL7297 on tdLN T cell content	122
Figure 4.15 Effects of SL7207 on T <sub>H</sub> 1 response in the tumour	123
Figure 4.16 Effects of SL7207 on T <sub>H</sub> 1 response in tdLN	124
Figure 4.17 Effects of SL7207 on T <sub>H</sub> 17 response in the tumour	125
Figure 4.18 Effects of SL7207 on Treg response in the tumour and tdLN	126
Figure 5.1 Monocyte/macrophage populations in steady state B16F10 tumours	140
Figure 5.2 Functional features of MHCII <sup>+</sup> and MHCII <sup>-</sup> TAMs in B16F10 tumours	141
Figure 5.3 Phagocytic capacities of MHCII <sup>-</sup> and MHCII <sup>+</sup> TAMs	142
Figure 5.4 Effects of SL7207 infection on tumour Ly6C <sup>+</sup> MHCII <sup>-</sup> monocyte content	143
Figure 5.5 Effects of SL7207 infection on the functional phenotype of tumour Ly6C <sup>-</sup> MHCII <sup>+</sup> monocytes	144
Figure 5.6 Effect of SL7207 infection on the phagocytic capacity of tumour Ly6C <sup>-</sup> MHCII <sup>+</sup> monocytes	145
Figure 5.7 Effects of SL7207 infection on tumour Ly6C <sup>+</sup> MHCII <sup>+</sup> monocyte content	146
Figure 5.8 Effects of SL7207 infection functional phenotype of tumour Ly6C <sup>+</sup> MHCII <sup>+</sup> monocytes	147
Figure 5.9 Effect of SL7207 on the phagocytic capacity of tumour Ly6C <sup>-</sup> MHCII <sup>+</sup> monocytes	148
Figure 5.10 Effects of SL7207 infection on TAM content	149
Figure 5.11 Effect of SL7207 infection on total TAM MHCII expression	150
Figure 5.12 Effects of SL7207 infection on CD206 expression on TAM populations	151
Figure 5.13 Effects of SL7207 infection on the replicative potential of TAM populations	152
Figure 5.14 Effects of SL7207 infection on functional phenotype of TAM populations	154
Figure 5.15 Effects of SL7207 on phagocytic capacities of TAM populations	155
Figure 5.16 Gating strategy for tumour monocyte/macrophages in tumour-bearing Kaede mice	157
Figure 5.17 Optimisation of photoconversion protocol	158
Figure 5.18 Effects of SL7207 infection on tumour-bearing Kaede mice	159

Figure 5.19 Effects of SL7207 infection on Kaede red <sup>+</sup> monocytes/macrophages in the tumour	160
Figure 5.20 B16F10 tumour growth in CCR2 <sup>-/-</sup> mice	161
Figure 5.21 Monocyte and macrophage populations in the CCR2 <sup>-/-</sup> mice	163
Figure 5.22 Effects of SL7207 on tumour growth and body weight in tumour-bearing CCR2 <sup>-/-</sup> mice	164
Figure 5.23 Effects of SL7207 on the tumour monocytes in CCR2 <sup>-/-</sup> mice	165
Figure 5.24 Effects of Clod Lipo on tumour monocyte/macrophage population	167
Figure 5.25 Effects of Clod Lipo on B16F10 tumour growth and body weight	168
Figure 5.26 Effects of Clod Lipo on SL7207 infection tumour-bearing mice	169
Figure 5.27 Effects of SL7207 on the tumour monocyte/macrophage compartment in Clod Lipo treated, SL7207-infected mice	171
Figure 6.1 In vitro tumour spheroids	188
Figure 6.2 VNP20009 invasion of tumour spheroids	190
Figure 6.3 VNP20009 biofilm formation on tumour spheroids	190
Figure 6.4 Serial reisolation of infective VNP20009 colonies to increase cumulative infective capacity	192
Figure 6.5 Bactofection capacity of <i>S. Typhimurium</i> -pEGFP	193
Figure 6.6 Bactofection capacity of SL7207-pEGFP and SL7207-pLuc	194
Figure 6.7 Morphology of SL7207-pEGFP	195
Figure 6.8 Morphology of other <i>S. Typhimurium</i> strains transformed with pEGFP	196
Figure 6.9 Morphology of <i>E. coli</i> strains transformed with pEGFP	197
Figure 6.10 Variability in cell length of SL-pEGFP compared to wild type	198
Figure 6.11 Growth and invasion characteristics of SL-pEGFP	199
Figure 6.12 Stress response activation in <i>S. Typhimurium</i> -pEGFP	200
Figure 6.13 Effect of the removal of f1 from pEGFP on cell length with resultant plasmid, pEGFP <sub>LacZ</sub>	202
Figure 6.14 Effects of other plasmid features on the pEGFP-induced filamentous phenotype	204
Figure 7.1 Proposed mechanism for Clod Lipo abrogating SL7207 tumour growth inhibition	217
Figure 9.1 Long term SL7207 infection in tumour-bearing mice	268
Figure 9.2 Effects of SL7207 infection on size of tdLN	268
Figure 9.3 Contribution of blood-borne monocyte/macrophages to total monocyte/macrophage population in tumour preparation	269
Figure 9.4 CD11c expression in the Ly6C <sup>+</sup> MHCII <sup>+</sup> monocyte population following SL7207 infection	269
Figure 9.5 Effects of Clod Lipo on spleens from infected tumour-bearing mice	270

## List of Tables

<i>Table 1.1 Summary of the roles of multiple cell types in cancer and S. Typhimurium infection</i>	27
<i>Table 1.2 In vivo models employed in published bacterial-mediated cancer therapy studies</i>	54
<i>Table 2.1 Details of bacterial strains used in this study</i>	58
<i>Table 2.2 Details of plasmids used in this study</i>	60
<i>Table 2.3 Antibodies used for flow cytometry</i>	69
<i>Table 2.4 Primers used in this study</i>	74
<i>Table 2.5 PCR programme for DNA amplification</i>	75

# Abbreviations

APC	antigen presenting cells
ATCC	American type culture collection
ATP	Adenosine triphosphate
BCG	<i>Bacillus Calmette-Guerin</i>
BCG-CWS	BCG cell wall skeleton
BM	Bone marrow
BMM	Bone marrow-derived macrophages
bp	Base pairs
BSA	Bovine serum albumin
CCR	C-C chemokine receptor
CD	Cluster of differentiation
cDC	Conventional dendritic cell
CFUs	Colony forming units
CMP	Common myeloid progenitor
CMV	Cytomegalovirus
CO <sub>2</sub>	Carbon dioxide
CRF	Central Research Facility
CSF	Colony stimulating factor
CTL	cytotoxic T cells
CTLA	cytotoxic T lymphocyte antigen
Cx43	connexin 43
DAMP	Damage-associated molecular pattern
DC	Dendritic cell
dH <sub>2</sub> O	Distilled water
DMEM	Dulbecco's modified eagle medium
°C	Degrees Celsius
DNA	Deoxyribonucleic acid
dNTP	Deoxyribonucleoside triphosphate
Dpi	Days post infection
DTR	Diphtheria toxin receptor
EDTA	Ethylenediaminetetraacetic acid
EGF	epidermal growth factor
EGFP	Enhanced green fluorescent protein
ELISA	Enzyme linked immunosorbent assay
<i>et al.</i>	<i>et alios</i> (and others)
F1 <i>ori</i>	Filamentous phage 1 <i>ori</i>
FACS	Fluorescence activated cell sorting
FB	Flow cytometry buffer
FCS	Foetal calf serum
FlaB	flagellin B
FoxP3	Forkhead box binding protein 3
FSC	Forward scatter
g	Gram(s)
GALT	Gastrointestinal associated lymphoid tissue
GFP	Green fluorescent protein
GM-CSF	Granulocyte macrophage colony-stimulating factor
GTPases	Guanosine triphosphate phosphohydrolases
h	Hour(s)
Hpi	Hours post infection
HRP	Horseradish-peroxidase
HSC	Haematopoietic stem cell
HXA <sub>3</sub>	hepoxilin A <sub>3</sub>
i.v.	Intravenous
IFN	Interferon
Ig	Immunoglobulin
IL	Interleukin
iNOS	Inducible Nitric oxide synthases
iTreg	Induced Tregs
IVIS	<i>In vivo</i> imaging system
JRF	Joint Research Facility

Kb	Kilo base pairs
KCl	Potassium chloride
kDa	Kilo Dalton
kV	Kilovolts
l/L	Litre(s)
LB	Luria broth
LP	Lamina propria
LPS	Lipopolysaccharide
M	Molar
MAM	Metastasis-associated macrophages
MAPK	mitogen-activated protein kinase
MCA	methylcholanthrene
MFI	Median fluorescence intensity
mg	Milligram
mg L <sup>-1</sup>	Milligrams per litre
MHC	Major histocompatibility complex
min	Minute(s)
ml	Millilitre
mM	Millimolar
mm	Millimetre(s)
Moi	Multiplicity of infection
Ms	Milliseconds
MyD88	Myeloid Differentiation primary response 88
NC3R	National Centre for the Replacement, Refinement and Reduction of Animals in Research
NCBI	National Centre for Biotechnology information
NEB	New England Bioscience
NETs	neutrophil extracellular traps
NF-κB	nuclear factor kappa-light-chain-enhancer of activated B cells
ng	Nanogram
ng L <sup>-1</sup>	Nanograms per litre
NK	Natural killer
NLR	Nod-like receptor
NLRC	Nod-like receptor complex
NO	Nitric oxide
No.	Number
NOD	Nucleotide-binding oligomerisation domain
NSCLC	non-small cell lung carcinoma
nTreg	natural Tregs
OD <sub>600</sub>	Optical density at 600 nm
PAMP	Pathogen associated molecular pattern
PBS	Phosphate buffered saline
PCR	Polymerase chain reaction
PCR	Polymerase chain reaction
PD-L	Programmed Death-Ligand
pDC	Plasmacytoid dendritic cell
PE	Phycoerythrin
PFA	Paraformaldehyde
pH	A measure of solution acidity
PMA	Phorbol 12-myristate
PP	Peyer's patches
PRR	Pathogen recognition receptor
PyMT	Polyoma-middle T antigen oncoprotein
RIP	receptor-interacting serine/threonine-protein
RNA	Ribonucleic acid
ROD	Ribose ornithine deoxycholate
ROR	RAR-related orphan receptor gamma
RORgt	Retinoic acid receptor-related orphan receptor gamma
rpm	Revolutions per minute
RPMI	Roswell Park Memorial Institute 1640 medium
RT-PCR	Reverse transcriptase polymerase chain reaction
s	Second(s)
S. Typhimurium	<i>Salmonella enterica</i> serovar Typhimurium
SCV	<i>Salmonella</i> -containing vacuoles

SD	Standard deviation
SDS	Sodium dodecyl sulphate
SDS-PAGE	Sodium dodecyl sulphate-polyacrylamide gel electrophoresis
Sem	Standard error of the mean
SEM	Scanning electron microscopy
SIP	Stock isotonic Percoll®
SipA	<i>Salmonella</i> invasion protein A
SipC	<i>Salmonella</i> invasion protein C
SL-CD	<i>Salmonella</i> cytosine deaminase
SL-Lux	Bioluminescent SL7207
SPI-1	<i>Salmonella</i> pathogenicity island-1
ss	Single stranded
SSC	Side scatter
STAT	Signal transducer and activator of transcription
SV40	Simian Virus 40
T3SS-1	type three secretion system 1
TAE	Tris, acetic acid, Ethylenediaminetetraacetic acid
TAM	Tumour-associated macrophage
TCR	T cell receptor
TEM	Transmission electron microscopy
TGF	Transforming growth factor
TH1	T helper 1
TH17	T helper 17
TH2	T helper 2
TIP-DCs	TNF- and inducible nitric oxide synthase producing DCs
TIR	toll/interleukin-1 receptor
TLR	Toll like receptor
TNF	Tumour necrosis factor
TPS	Two-partner secretion
TRAIL	tumour necrosis factor-related apoptosis-inducing ligand
Treg	T regulatory cell
TRIF	TIR-domain-containing adapter-inducing interferon- $\beta$
Tris	2-amino-2-(hydroxymethyl) 1,3-propanediol
TRP2	Tyrosine related protein 2
TTSS	Type three secretion system
V	Volt(s)
v/v	Volume per volume
VEGF	Vascular endothelial growth factor
VNP20009	Vion Pharmaceuticals 20009
w/v	Weight per volume
$\Delta$	Deletion
$\mu\text{g}$	Microgram
$\mu\text{l}$	Microlitre
$\mu\text{M}$	Micromolar
$\mu\text{m}$	Micrometre

# 1 Introduction

## 1.1 *Salmonella enterica* serovar Typhimurium

### 1.1.1 Incidence and pathology

*Salmonella* is a Gram-negative facultative anaerobe belonging to the Enterobacteriaceae family. Non-typhoidal *Salmonella* serotypes are a common cause of food poisoning worldwide (Rabsch *et al.*, 2001). It is estimated that there are 93.8 million cases of gastroenteritis annually for which non-typhoidal *Salmonella* is responsible, resulting in an estimated 155,000 deaths (Majowicz *et al.*, 2010). Non-typhoidal *Salmonella* causes a local enteric disease characterised by diarrhoea, intestinal cramping, fever and the presence of neutrophils in stool samples (Harris *et al.*, 1972). *Salmonella enterica* serovar Typhimurium (*S.* Typhimurium) is one of more than 2,500 serovars of the *Salmonella enterica* species, and has been determined to be the leading cause of human non-typhoidal gastroenteritis in the United States (Scallan *et al.*, 2011). As well as being an enteric pathogen, attenuated strains of *S.* Typhimurium have also been investigated for their potential in mediating tumour growth inhibition and regression in pre-clinical and clinical trial settings (Clairmont *et al.*, 2000; Crull *et al.*, 2011a; Toso *et al.*, 2002; Zhang *et al.*, 2015; Zheng *et al.*, 2017a).

### 1.1.2 *S.* Typhimurium epithelial cell invasion and persistence

Much of the evidence available describing the invasion of *S.* Typhimurium into host cells comes from studies involving infection via the mucosal route. Following oral infection, the major route of *S.* Typhimurium mucosal barrier breach is thought to be across the Microfold (M) cells, which overlie the gut-associated lymphoid tissue (Clark *et al.*, 1996; Jones *et al.*, 1994). *S.* Typhimurium can also gain access to the epithelium by type three secretion system 1 (T3SS-1)-mediated entry, which is under the control of the *Salmonella* pathogenicity island-1 (SPI-1) (Galán & Curtiss, 1989). The T3SS is a needle-like complex which traverses the bacterial cell envelope, to deliver effector proteins directly into the host cell cytoplasm (Ginocchio *et al.*, 1994). SPI-1 is a 40-kilobase segment at centisome 63 of the bacterial chromosome, which contains more than 25 genes encoding structural components and effector proteins of T3SS-1 (Galán & Ginocchio, 1994; Mills *et al.*, 1995).

Upon contact with enterocytes, *S. Typhimurium* can translocate secreted effector proteins into host cells. The effector proteins SopE, SopE2 and Sop2 initiate the process of bacterial cell invasion by promoting the activation of host Rho-Guanosine triphosphate phosphohydrolases (GTPases) priming entry (Friebel *et al.*, 2001; Stender *et al.*, 2000). These activities also result in the activation of the nuclear factor kappa-light-chain-enhancer of activated B cells (NF- $\kappa$ B) and the associated inflammatory response (Henry *et al.*, 2006). *Salmonella* invasion protein C (SipC) plays a role in interacting with the host cell cytoskeleton, while SipA also interacts with the host cell cytoskeleton by promoting actin polymerization (McGhie *et al.*, 2001). The combined efforts of SipA and SipC result in actin filament bundling which leads to the formation of membrane ruffles that allow for the engulfment of the associated bacterium.

Following invasion, intracellular phagosomes, known as *Salmonella*-containing vacuoles (SCVs) are formed from early endosomes, to allow for intracellular bacterial replication (Richter-Dahlfors *et al.*, 1997; Salcedo *et al.*, 2001). There are at least 30 known effector proteins that are translocated by a second T3SS, T3SS-2, across the SCV membrane into the host cell cytoplasm (Figueira & Holden, 2012). During SCV maturation, *Salmonella*-induced filaments (Sifs) play an important role in the proper positioning of the compartment within the host cell (Beuzón *et al.*, 2000). Sifs are long filamentous glycoprotein-containing membrane tubules which extend from the SCV surface along microtubules at around 4-6 hours post host cell invasion. The appearance of Sifs coincides with bacterial replication in the SCV, although *Salmonella* replication can also occur in the cytoplasm (Beuzón *et al.*, 2002).

*S. Typhimurium* has evolved a number of mechanisms to modulate the host immune response following invasion. Another effector protein, SptP antagonises SopE and SopE2 function and reverses the host-cell membrane perturbations as early as three hours post *Salmonella* host cell infection (Fu & Galán, 1998). SptP, along with SspH1, downregulates interleukin (IL)-8 and inhibits NF- $\kappa$ B-dependent gene expression, which suggests that down-regulation of pro-inflammatory responses might be important in establishing the intracellular *Salmonella* niche (Figueira and Holden, 2012). *S. Typhimurium* effector proteins employ a strategy of molecular mimicry to antagonise host cell functions (Haraga & Miller, 2003).

SseL, a de-ubiquitinating enzyme similar to those found in the host, inhibits the degradation of the inhibitor of NF- $\kappa$ B, I $\kappa$ B $\alpha$  (Rytkönen *et al.*, 2007), a negative regulator of the NF- $\kappa$ B pathway, thus limiting inflammation. AvrA also performs this function as well as de-ubiquitinating  $\beta$ -catenin to further modulate inflammation (Collier-Hyams *et al.*, 2002).

### 1.1.3 Stress responses of *S. Typhimurium*

*S. Typhimurium* is predisposed to stress responses following multiple stimuli such as nutrient deprivation, acidification, temperature fluctuations, plasmid carriage and the presence of single stranded (ss) DNA in the cytosol (Humphrey, 2004). The general stress response reacts to stimuli such as osmotic stress, carbon starvation, hyperosmotic stress and heat shock, amongst others (Lee *et al.*, 1995; McMeechan *et al.*, 2007). RpoS ( $\sigma^E$ ) is the master regulator which coordinates these responses (Erickson & Gross, 1989; Humphreys *et al.*, 1999). The SOS stress response is induced in reaction to genomic instability, notably the generation of ssDNA. This can be as a consequence of genotoxic damage from UV irradiation (Quillardet *et al.*, 2003) but also from phage-induced ssDNA generation (Campoy *et al.*, 2006; Higashitani *et al.*, 1995). The activation of the SOS response results in the expression of at least 30 genes. The SOS response is negatively regulated by the LexA protein which binds to the promoter sequence of the SOS-response genes (Brent & Ptashne, 1981). DNA damage causes stalling of the DNA replication fork, exposing ssDNA fragments, to which the SOS-related protein RecA binds (Roca & Singleton, 2003). Activated RecA-ssDNA triggers the self-catalytic properties of LexA, relieving the SOS promoter, and transcriptional operon, of the LexA-inhibitory effects (Little, 1984). One of the consequences of SOS response activation is the sequestration of the FtsZ cell division protein by Sula, which subsequently results in the inhibition of cell septation (Cordell *et al.*, 2003; Justice *et al.*, 2000; Trusca *et al.*, 1998). Notably, bacterial growth can continue in the absence of septation, with the formation of elongated cells, characteristic of SOS-induction (Justice *et al.*, 2008). When the DNA insult is resolved, Sula is degraded by Lon protease, LexA-mediated suppression of SOS gene expression is restored and septation resumes (Ishi *et al.*, 2000; Justice *et al.*, 2008; Mizusawa & Gottesman, 1983). Interestingly, the SOS response has been implicated in the virulence of uropathogenic *Escherichia coli* (*E. Coli*) in a

murine model of cystitis (Li *et al.*, 2010) and in macrophage-residing *Salmonella in vitro* (Eriksson *et al.*, 2003).

### 1.1.4 Innate Immune Response to *S. Typhimurium*

The innate immune system provides the host's immediate defence against invading pathogens. This comprises a collection of molecules and cells, which are activated upon recognition of the insult, and creates an environment non-permissive to pathogen propagation as well as activating the adaptive arm of the immune response. The innate immune system recognises and responds to pathogens in a non-specific way that does not provide long-lasting immunity to the host. *S. Typhimurium* infection is a highly immunostimulatory process, and as such, has profound effects on the innate immune system

#### 1.1.4.1 Recognition and inflammation

*S. Typhimurium* contains an array of detectable molecules that the host immune system has evolved to recognise. Many immune cells, most notably antigen presenting cells (APCs), express a collection of germ-line encoded pathogen recognition receptors (PRRs) to detect pathogen-associated molecular patterns (PAMPs) (Figure 1.1) (Vance *et al.*, 2010). The Toll-like receptor (TLR) family plays a major role as PAMPs with both extracellular (TLR1, 2, 4, 5, 6 and 10) and intracellular vesicular members (TLR3, 7, 8, 9, 11 and 13). TLRs can detect specific extracellular and endosomal PAMPs such as lipopolysaccharide by TLR4 (Chow *et al.*, 1999), flagellin protein, FliC by TLR5 (Hayashi, 2001) or the CpG-rich repetitive elements in bacterial DNA by TLR9 (Chuang *et al.*, 2002). The absence of one or more of these TLRs can lead to severely compromised bacterial clearance. For example, *TLR4*<sup>-/-</sup> mice demonstrate increased susceptibility to *S. Typhimurium* infection (Arpaia *et al.*, 2011) and this is even more severe in *TLR4*<sup>-/-</sup>*TLR5*<sup>-/-</sup> mice (Feuillet *et al.*, 2006).

TLR signalling mostly occurs through the adaptor molecule Myeloid Differentiation primary response 88 (MyD88) which activates NF-κB signalling, controlling an array of pro-inflammatory cytokine genes, including IL-1β and IL-18 (Figure 1.1). There are however, MyD88-independent signalling cascades following TLR activation. TLR3 and sometimes TLR4 can signal through

toll/interleukin-1 receptor (TIR) domain containing adaptor inducing interferon- $\beta$  (TRIF), in a MyD88-independent manner which leads to the production of Type I interferons (Yamamoto *et al.*, 2003).

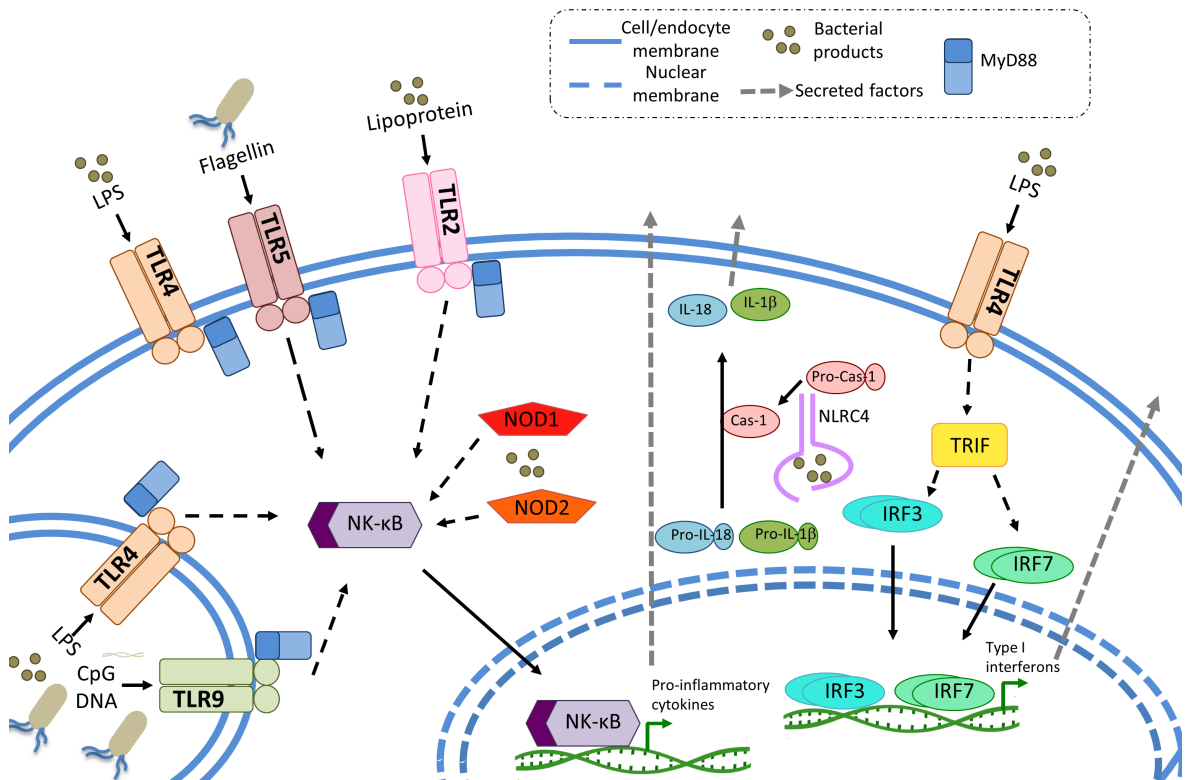


**Figure 1.1 PRR signaling in response to PAMPs**

*S. Typhimurium* mediates the activation of a number of TLRs, both extracellular and endocytic, which mostly signal via the adaptor protein MyD88 to activate the NF- $\kappa$ B transcriptional programme. This includes the production of pro-IL-1 $\beta$  and pro-IL-18 which are cleaved via caspase-1 following cytosolic NLRC4 activation in response to cytosolic bacterial products. NOD1 and NOD2 can be activated via cytosolic bacterial products to induce NF- $\kappa$ B signaling. TLR4 can also signal in a MyD88-independent signaling pathway through TRIF, which leads to the production of Type I interferons. IL, interleukin; IRF, interferon response element; LPS, lipopolysaccharide; NF- $\kappa$ B nuclear factor kappa-light-chain-enhancer of activated B cells; NLRC4, NOD-like receptor complex 4; NOD, nucleoside oligomerisation domain; TLR, Toll-like receptor; TRIF, toll/interleukin-1 receptor -domain-containing adapter-inducing interferon- $\beta$ .

Although *Salmonella* residing in the SCV are somewhat protected from these PRRs, immune cells have evolved other mechanisms to recognise PAMPs in the cytosol. The nucleotide-binding oligomerisation domain (NOD)-like receptor (NLR) family of proteins can recognise cytosolic PAMPs and stimulate a responsive signalling cascade (Fritz *et al.*, 2006). NLRs contain multiple protein domains, which can stimulate multimerisation and subsequent transcriptional activation. For example, NOD1/2 can recognise bacterial products such as

muramyl dipeptide (Inohara *et al.*, 2003) and peptidoglycan (Girardin *et al.*, 2003), interact with receptor-interacting serine/threonine-protein (RIP)2 kinase and lead to NF- $\kappa$ B activation (Figure 1.1), which is an important activator of innate immune defence against invading pathogens (Ogura *et al.*, 2001). In fact, mice deficient in NOD1/2 or RIP2 displayed attenuated inflammatory responses and increased colonisation of mucosal tissue when orally challenged with *S. Typhimurium* (Geddes *et al.*, 2010). NLRs also form complexes, NLRs, which can lead to the cleavage and activation of caspase-1 (Franchi *et al.*, 2009) (Figure 1.1).

#### 1.1.4.2 Polymorphonuclear neutrophils control bacterial dissemination

Neutrophils are highly phagocytic cells and often reported to be one of the first cell types to migrate to sites of infection, and arrive en masse (Barthel *et al.*, 2003; Rydström & Wick, 2009). Following phagocytosis, neutrophils can kill the pathogen using anti-bacterial proteins such as cathepsins and lysozyme, or utilise reactive oxygen species (Segal, 2005). Neutrophils are granulocytes, meaning they can release cytotoxic-molecule containing granules to kill invading pathogens. Neutrophils can also produce neutrophil extracellular traps (NETs) which are detrimental to invading bacteria (Brinkmann *et al.*, 2004). These are composed of chromatin DNA to which histones and cytotoxic granule proteins attach (Delgado-Rizo *et al.*, 2017). These web-like structures function to trap pathogens, and can mediate direct killing of the entrapped cargo. NETs were found to be four times more efficient at trapping bacteria in the circulation than Kupffer cells, the liver-resident macrophage (McDonald *et al.*, 2012). Furthermore, blockade of NET formation resulted in greater bacterial dissemination *in vivo*. The importance of neutrophils in controlling *S. Typhimurium* infection is evident as mice exhibiting neutropenia had an increased systemic *S. Typhimurium* infection following oral application (Cheminay *et al.*, 2004).

Neutrophil recruitment is induced via the IL-23/IL-17 axis (Wu *et al.*, 2007). These cytokines lead to the stimulation of granulopoiesis in the bone marrow by inducing the production of granulocyte colony-stimulating factor, G-CSF (Lord *et al.*, 1989; Smith *et al.*, 2007). The *S. Typhimurium* effector proteins SopE, SopE2 and SopB induce Cdc42 activation which in turn triggers multiple mitogen-

activated protein kinase (MAPK) pathways (Henry *et al.*, 2006). The initiation of these pathways culminates in the activation of NF- $\kappa$ B which induces IL-8 secretion. Neutrophil recruitment to the infected intestine is dependent on basolateral IL-8 secretion (McCormick *et al.*, 1995), as well MyD88 signalling (Rydström & Wick, 2009). SipA is another effector protein which contributes to neutrophil recruitment (Wall *et al.*, 2007). SipA regulates arachidonic acid metabolism in host epithelial cells which leads to the apical release of hepxilin A<sub>3</sub> (HXA<sub>3</sub>) (Mrsny *et al.*, 2004). HXA<sub>3</sub> establishes a gradient along intercellular epithelial junctions which functions as a signal for neutrophil recruitment at the apical surface.

#### **1.1.4.3 Monocytes and macrophages phagocytose *S. Typhimurium* and produce inflammatory cytokines**

Macrophages are phagocytic cells, which engulf apoptotic cellular debris as well as invading organisms. Their derivation is tissue dependent (Epelman *et al.*, 2014), with some seeding during developmental processes, and others derived from circulating monocytes (Bain *et al.*, 2014). They are important for containing bacterial spread through phagocytosis. Macrophages are adept at producing cytokines following bacterial infection, including IL-6, IL-12, IL-23, IL-1 $\beta$  and tumour necrosis factor (TNF)- $\alpha$  (Yrlid *et al.*, 2000).

Phagocytosis is a critical element for the containment of bacterial spread (Kaufmann and Dorhoi, 2016). Following phagocytosis, *S. Typhimurium* develop the SCV in macrophages. However, there are other members of the NLR family which are capable of responding to *S. Typhimurium* infection through the formation of a large multi-protein signalling complex known as the inflammasome, such as NLRC4 (Fritz *et al.*, 2006) (Figure 1.1). NLRC4 detects flagellin and effector proteins in the cytosol of the host cell (Franchi *et al.*, 2006; Miao & Warren, 2010). Assembly of the complex leads to the recruitment of pro-caspase-1, which is auto-cleaved and activated following dimerization (Franchi *et al.*, 2009). Mature activated caspase-1 cleaves the inactive, pro-forms of IL-1 $\beta$  and IL-18, which creates a positive feedback loop for the continual production of these pro-inflammatory cytokines (Sansonetti, 2001). Furthermore, *Salmonella*-induced caspase-1 initiates a pro-inflammatory form of controlled cell death in macrophages called pyroptosis (Brennan & Cookson,

2000; Hersh *et al.*, 1999; Monack *et al.*, 1996). Pyroptosis is dependent on caspase-1 as *Casp1*<sup>-/-</sup> mice employ alternative mechanisms of cell death (Jesenberger *et al.*, 2000). During pyroptosis, pores form in the pyroptotic macrophage, which release cytosolic pro-inflammatory cytokines into the vicinity, amplifying the inflammatory response (Fink & Cookson, 2006). Caspase-1 activation is an important event in *S. Typhimurium* host response. *Casp1*<sup>-/-</sup> mice exhibit higher bacterial burdens than wild type mice and succumb to *S. Typhimurium* infection more quickly (Lara-Tejero *et al.*, 2006; Raupach *et al.*, 2006). These defects are due, at least in part, to the loss of IL-1 $\beta$  and IL-18 as mice deficient in either cytokine are also more susceptible to *S. Typhimurium* infection than wild type mice. NLRC4 is not required for inflammasome activation as NLRC3 can also activate caspase-1. Only ablation of both NLRP3 and NLRC4 lead to higher bacterial loads in the mesenteric lymph node, spleen and liver similar to caspase-1 deficient mice, suggesting that NLRP3 and NLRC4 play redundant roles in host defence (Broz *et al.*, 2010). Following pyroptosis, the majority of the phagocytosed bacteria remain within pyroptotic bodies where they are subject to efferocytosis by recruited neutrophils (Jorgensen *et al.*, 2016).

Monocyte recruitment is characteristic of *S. Typhimurium* and is believed to be heavily reliant on the C-C chemokine receptor (CCR)2-CCL2 axis (Rydstrom & Wick, 2007; Rydström & Wick, 2009). In steady state, in tissues such as the intestine and tumour, monocytes with high expression of the monocyte marker, Ly6C, termed Ly6C<sup>hi</sup> monocytes constantly replenish resident tissue macrophages (Bain *et al.*, 2014; Franklin *et al.*, 2014; Movahedi & Van Ginderachter, 2016). This has been described to involve a differentiation process where Ly6C<sup>hi</sup> monocytes acquire the expression of the antigen presenting complex, major histocompatibility complex (MHC)II, and downregulate Ly6C expression (Bain *et al.*, 2013; Bain *et al.*, 2014) (Figure 1.2).

This acquisition of Ly6C<sup>hi</sup> monocytes is amplified following inflammation (Bain *et al.*, 2013; Zigmund *et al.*, 2012). CCL2 is rapidly up-regulated in the Peyer's Patches and mesenteric lymph nodes of orally *S. Typhimurium*-infected mice (Rydström & Wick, 2009). It has been demonstrated that CCR2 is required for the recruitment of Ly6C<sup>hi</sup> monocytes into tissues during persistent *S.*

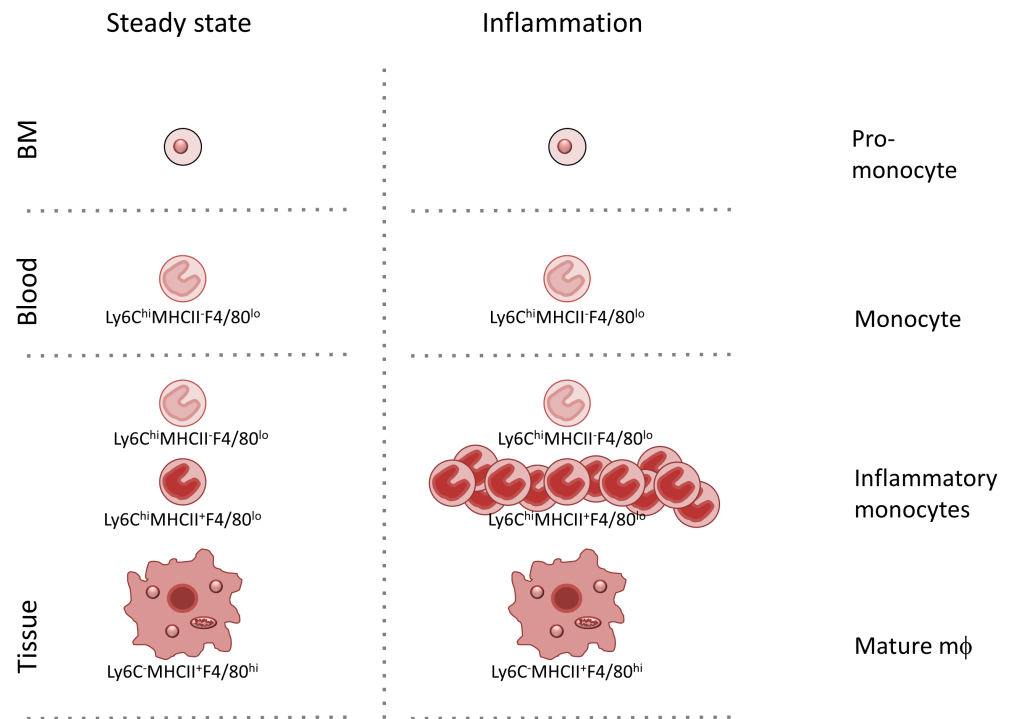


**Figure 1.2 Development of mature tissue macrophages from bone marrow precursors**

In steady state, pro-monocytes from the bone marrow give rise to blood monocytes, characterised by  $Ly6C^{hi}MHCII^{-}F4/80^{lo}$  cell surface expression. These cells subsequently migrate into tissues, such as colon or tumour, and through a differentiation process, give rise to mature  $Ly6C^{-}MHCII^{+}F4/80^{hi}$  macrophages. During inflammation, there is an expansion of the  $Ly6C^{hi}MHCII^{-}F4/80^{lo}$  population, termed 'inflammatory monocytes'.

Typhimurium infection (Van der Velden *et al.*, 2015). Furthermore, this report demonstrated that CCR2- and CCL2-deficient mice were more susceptible to *S. Typhimurium* infection than wild type. In certain contexts, such as inflammation,  $Ly6C^{hi}$  monocytes do not differentiate into macrophages, but instead seem to stall at the  $Ly6C^{+}MHCII^{+}$  phenotype (Bain *et al.*, 2013) (Figure 1.2). These cells appeared to have greater TNF- $\alpha$  production than resident macrophages and are more responsive to TLR stimulation, suggesting that they are the major contributors to inflammation in this setting (Bain *et al.*, 2013). The removal of the pro-inflammatory function of monocytes using a TLR2-peptide resulted in a significant decrease in inflammation associated pathology in a colitis model further evidencing their role in inducing a pro-inflammatory environment (Shmuel-Galia *et al.*, 2016).

The role of macrophages and monocytes in antigen presentation is debated (Jakubzick *et al.*, 2017). It is generally accepted that macrophages are tissue resident, and do not migrate to the lymph (Yrlid *et al.*, 2006). However, they can stimulate the secondary activation of antigen-specific T cells in the lamina

propria (Rossini *et al.*, 2014). Ly6C<sup>+</sup>MHCII<sup>+</sup> cells which accumulate in tissues following inflammation have alternatively been ascribed as TNF- and inducible nitric oxide synthase producing DCs (TIP-DCs) on account of their CD11c expression in the absence of CD14 and F4/80 as well as their ability to prime naïve alloreactive T cells *in vivo* (Hohl *et al.*, 2010; Serbina *et al.*, 2003). However, the factors which underlie the accumulation of either inflammatory monocytes or TIP-DCs are unknown.

#### **1.1.4.4 Dendritic cells activate T cell responses following *S. Typhimurium* infection**

Dendritic cells (DCs) are a population of myeloid immune cells which are capable of capturing, processing and presenting antigens to T cells, earning them the title of professional APCs (Banchereau & Steinman, 1998). DCs constantly traffic to tissue-draining lymph nodes, but migration is increased in response to microbial stimuli (MacPherson *et al.*, 1995; Turnbull *et al.*, 2005). DCs are separated into classical DCs (cDC) and non-classical DCs (Merad *et al.*, 2013). Within the cDCs, there are two subsets and both are important for the host's response to *S. Typhimurium* infection: cDC1, characterised by the expression of CD8<sup>+</sup>/CD103<sup>+</sup> and cDC2s, which are CD11b<sup>+</sup> (Merad *et al.*, 2013).

DCs are recruited to *S. Typhimurium*-infected tissue (Johansson *et al.*, 2006). DCs express an array of endocytic and phagocytic receptors (Platt *et al.*, 2010) and are proficient at capturing antigen from infected dying cells, such as pyroptotic macrophages (Tam *et al.*, 2008). Furthermore, they can capture and present pathogen-derived antigens from viable infected or tumour cells by acquiring preformed MHC I in a process known as trogocytosis (Joly & Hudrisier, 2003; Zhang *et al.*, 2008). It has also been reported that DCs can capture bacterial antigen from the lumen (Niess, 2005).

DC maturation can be achieved by direct bacterial interaction and activation of PRRs but also through inflammatory signals from the environment (Tam *et al.*, 2008). Maturation is accompanied by acidification of the lysosomal compartment for optimised antigen processing, up-regulation of co-stimulatory molecules for T cell activation and cell surface expression of MHCII for antigen presentation (Cella *et al.*, 1997; Platt *et al.*, 2010). Following maturation, which is also

accompanied by cytokine production, the DC migrates to the lymph node in a CCR7-dependent fashion (Jang *et al.*, 2006), where in the T cell zone it can encounter and activate cognate T cells. In order to activate T cells, T cells require at least three distinct stimuli: cognate MHC-antigen encounter, co-stimulatory signals provided by B7 family members and instructing cytokines (Bousso, 2008). After antigen presentation, DCs are thought to undergo apoptosis (Chen *et al.*, 2006), as thoracic duct lymph nodes does not contain DCs under steady state (Pugh *et al.*, 1983).

‘Cross-presentation’ is the term given when a cell presents antigen via MHCI to a CD8<sup>+</sup> T cell. Although various MHCI-expressing cells, including macrophages, are capable of cross presenting model antigens *in vitro*, it is evident that cDC1s are the most proficient cross-presenting APC *in vivo* (den Haan *et al.*, 2000). cDC1s are also known to be a critical source of IL-12 following acute parasitic infection or lipopolysaccharide (LPS) stimulation (Mashayekhi *et al.*, 2011; Reis e Sousa *et al.*, 1997).

Early after oral *S. Typhimurium* infection cDC2s are found associated with bacteria in the sub-epithelial dome of the lamina propria (Tam *et al.*, 2008). cDC2s express high levels of TLR2 and TLR4 and are proficient at producing IL-12 and IL-23 upon activation, as well as stimulation T<sub>H</sub>17 responses (Schlitzer *et al.*, 2013). cDC2s are known to be inefficient at cross presentation, but are superior to cDC1s in activating T<sub>H</sub> cells which are critical for host immunity to *S. Typhimurium* (Dudziak *et al.*, 2007).

Within the non-conventional DC subset are plasmacytoid DCs (pDCs) and monocyte-derived DCs (moDCs). There is high levels of expression of TLR7 and TLR9 on pDCs and these cells play an important role in anti-viral responses through type I interferon production (Ito *et al.*, 2005; Kato *et al.*, 2005). Monocyte-derived DCs, also known as TIP-DCs are derived from inflammatory monocytes, which are recruited to inflamed tissue (Hohl *et al.*, 2010; Serbina *et al.*, 2003).

### 1.1.5 Adaptive immune response to *S. Typhimurium*

DCs bridge the gap between the innate and adaptive immune responses by stimulating T cell activation in the secondary lymph organs. The adaptive immune response also consists of antibody-producing B cells. T cells, also called T lymphocytes, recognise foreign antigens through surface expressed T cell receptors (TCR). The majority of T cells express the  $\alpha\beta$  TCR, with a small percentage expressing the  $\gamma\delta$  TCR. There are two major types of T cells; T helper cells ( $T_H$  cells) and cytotoxic T cells (CTLs), both of which are implicated in the resolution of *S. Typhimurium* infection. It is generally understood that the initial  $CD4^+$  T cell-priming step in the lymph node drives the phenotypic skewing of the  $T_H$  cells to one of four main lineage subsets (Figure 1.3). The phenotypic skewing is largely dependent on the signals received from the DC in the form of cytokines or other mediators. Naive  $CD8^+$  T cells are also activated in the lymph node (Mempel *et al.*, 2004).

#### 1.1.5.1 $T_H1$ and $T_H2$ $CD4^+$ T cells

The  $T_H1$   $CD4^+$  T cell lineage is induced by IL-12 (Macatonia *et al.*, 1995). Tbet is the central transcription factor responsible for driving the function of these cells, of which interferon (IFN)- $\gamma$  production is a hallmark (Szabo *et al.*, 2000). Other cytokines associated with  $T_H1$  responses are TNF- $\alpha$  and IL-6. Although  $T_H1$  cells have homeostatic functions, they are better known for being major responders to viral and bacterial infection. For example, following *S. Typhimurium* infection, IFN- $\gamma$  is necessary for the expansion of both  $CD4^+$  and  $CD8^+$  T cells which are required for pathogen clearance (Bao *et al.*, 2000). Tbet expression in  $CD4^+$  T cells is necessary for resistance to systemic *S. Typhimurium* infection (Ravindran *et al.*, 2005). In this study the absence of  $CD4^+Tbet^+$  cells in *S. Typhimurium*-infected hosts severely attenuated the production of IFN- $\gamma$  and bacterial clearance. IFN- $\gamma$  plays an important role in the killing of intracellular bacteria which have been phagocytosed by macrophages (MacMicking, 2012). IFN- $\gamma$  also has a role in stimulating the transcription of GTPases that are involved in inflammasome assembly (Kim *et al.*, 2011).

$T_H2$   $CD4^+$  T cells are characterised by the transcription factor G-A-T-A binding protein 3 (GATA3) (Zheng & Flavell, 1997). These cells are associated with the

production of IL-4 and IL-13.  $T_H2$  cells play an important role in directing an immune response against helminth infections (McSorley & Maizels, 2012).

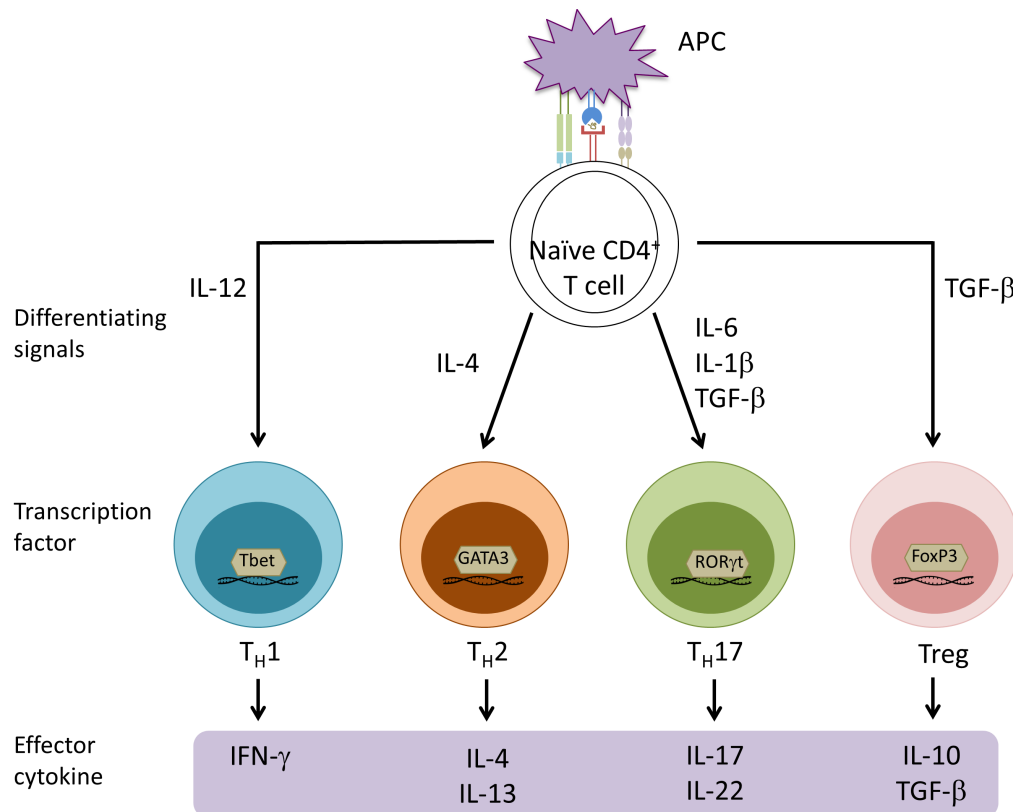


**Figure 1.3 Polarized  $CD4^+$   $T_H$  subsets**

Each  $CD4^+$  T cell subset can be defined by the cytokines which induce their lineage-specific differentiation phenotype, the transcription factors which drive their transcriptional programme and the effector cytokines they secrete. APC, antigen presenting cell; FoxP3, forkhead box protein 3; GATA3, G-A-T-A binding protein 3; IFN- $\gamma$ , interferon- $\gamma$ ; IL, interleukin; ROR $\gamma$ t, retinoic acid receptor-related orphan receptor-related; TGF- $\beta$ , transforming growth factor- $\beta$ ;  $T_H$ , T helper.

### 1.1.5.2 $T_H17$ $CD4^+$ T cells

$T_H1$  and  $T_H2$  cells were long thought to be the quintessential T cell types, readily inducible *in vitro* through the exposure of naïve T cells to either IL-12 or IL-4, respectively. However, it was demonstrated that the stimulation of isolated  $T_H$  cells with *Borrelia burgdorferi*, the spirochete that causes Lyme disease, resulted in the significant production of IL-17 from the cells in the absence of either IFN- $\gamma$  or IL-4 (Infante-Duarte *et al.*, 2000). Therefore, these cells did not fit the prototypical  $T_H1$  or  $T_H2$  lineage-specific profile, and a new area of T cell biology was spawned. These cells, now termed  $T_H17$  cells, are characterised by

the transcription factor retinoic acid receptor-related orphan receptor-related (ROR) $\gamma$ t and the production of IL-17 (Ivanov *et al.*, 2006).

T<sub>H</sub>17 cells have been found to be critical immune mediators to bacterial infection. Oral inoculation with *Citrobacter rodentium* (*C. rodentium*) induces a robust T<sub>H</sub>17 response in the mucosa (Symonds *et al.*, 2009). T<sub>H</sub>17 cells are also induced following oral *S. Typhimurium* infection. In an ileal loop model in rhesus macaques, T<sub>H</sub>17-associated cytokines dominated the early gene expression profiles of *S. Typhimurium*-infected samples compared to uninfected controls, with significant increases in IL-17, Lipocalin-2, and CXC chemokine ligand (CXCL)10 (Raffatellu *et al.*, 2008). IL-22 and GM-CSF are also associated with T<sub>H</sub>17 responses, with important roles in granulopoiesis and neutrophil recruitment (Ye *et al.*, 2001). IL-22 is vital for bacterial clearance as it was seen that IL-22-deficient mice succumbed to oral *C. rodentium* infection whilst wild type mice did not (Zheng *et al.*, 2008). This is possibly explained by the finding that IL-22 plays an important role in maintaining the integrity of the intestinal epithelia barrier and mediating antimicrobial production in the epithelial cells (Sonnenberg *et al.*, 2010).

There have been multiple reports describing the cytokine requirements for the differentiation of T<sub>H</sub>17 cells from naïve T cells. Transforming Growth Factor (TGF)- $\beta$  and IL-6 have been found to be capable of driving T<sub>H</sub>17 differentiation (Bettelli *et al.*, 2006; Veldhoen *et al.*, 2006). However, another study found that in the absence of TGF- $\beta$ , IL-6 and IL-1 $\beta$  were sufficient to induce T<sub>H</sub>17 differentiation (Ghoreschi *et al.*, 2010). T<sub>H</sub>17 cell maintenance has been found to be due to IL-23 (Stritesky *et al.*, 2008).

### 1.1.5.3 T regulatory cells

Another type of T cell is the T regulatory cell (Treg), the role of which is more in keeping with immunoregulation, supporting oral tolerance to food antigens and the commensal microbiota. The removal of CD4<sup>+</sup>CD25<sup>+</sup> T cells (which are now appreciated as Tregs) from a CD4<sup>+</sup> preparation adoptively transferred into an athymic mice resulted in multiple spontaneous autoimmune pathologies (Sakaguchi *et al.*, 1995). In contrast, the early reconstitution of the CD4<sup>+</sup>CD25<sup>+</sup> cells into the same mice prevented the development of autoimmune symptoms.

Similar results were found in thymectomised mice (Asano, 1996), with both studies concluding that the CD4<sup>+</sup>CD25<sup>+</sup> T cells had an immunosuppressive role. Tregs are characterised by the expression of the transcription factor forkhead box protein 3 (FoxP3), and can also be defined by the expression of cytotoxic T lymphocyte antigen (CTLA)-4 and IL-10 and TGF- $\beta$  production (Fontenot *et al.*, 2003; Jago *et al.*, 2004; Uhlig *et al.*, 2006).

There are two distinct populations of Tregs dependent on tissue origin for differentiation. Most FoxP3<sup>+</sup> cells differentiate in the thymus from immature CD4<sup>+</sup>CD8<sup>+</sup> precursor cells, termed natural Tregs (nTreg) (Fontenot *et al.*, 2003). Induced Tregs (iTreg) differentiate in the periphery from conventional CD4<sup>+</sup> T cells into FoxP3<sup>+</sup> Tregs via APC-expressed B7 (Liang *et al.*, 2005) and TGF- $\beta$  signalling (Chen *et al.*, 2003). Many factors can induce this 'conversion' including commensal bacteria and antigenic tolerance (Apostolou & von Boehmer, 2004; Atarashi *et al.*, 2011; Lathrop *et al.*, 2011).

Mice with increased Treg cells are more susceptible to *S. enterica* infection (Pejic-Karapetrovic *et al.*, 2007; Rowe *et al.*, 2011). The immunosuppressive potency of Tregs changes during the course of infection and has been found to be mediated by the expression of CTLA4 which suppresses activated T cell proliferation (Johanns *et al.*, 2010). APCs are also inhibited by Treg expression of CTLA4 and programmed death ligand (PD-L)1/2, as well Treg-mediated IL-10 production (Uhlig *et al.*, 2006). Granzyme B, a serine protease that can induce mitochondrial pathway-dependent apoptosis in target cells via proteolysis of the anti-apoptosis protein Bid (Pinkoski *et al.*, 2001), is produced by Tregs and can induce apoptosis in conventional T cells. Tregs also express CD25 highly, which sequesters local IL-2, depleting reserves for other T cells (Benoist & Mathis, 2012; Sakaguchi *et al.*, 2010). FoxP3 antagonises T<sub>H</sub>17 cell cytokine induction by antagonising ROR $\gamma$ t function (Yang *et al.*, 2008).

#### 1.1.5.4 CD4<sup>+</sup> T<sub>H</sub> cell plasticity

CD4<sup>+</sup> cells are highly plastic, and multiple reports have demonstrated that differentiated CD4<sup>+</sup> T cells can alter their phenotype to become more similar to other lineages. This has been shown for T<sub>H</sub>17 cells, which can become T<sub>H</sub>1-like in a IL-17-induced colitis model through the Tbet transcription factor and IFN- $\gamma$

production (Harbour *et al.*, 2015). Another study also showed this same T<sub>H</sub>17-to-T<sub>H</sub>1 phenomenon by fate mapping T<sub>H</sub>17 cells in a model of experimental autoimmune encephalomyelitis (Hirota *et al.*, 2011). Newly polarized T<sub>H</sub>1 cells have been demonstrated to transform their phenotype similar to that of a T<sub>H</sub>2 cell *in vivo* following IL-4 administration or helminth infection (Panzer *et al.*, 2012). Conversely, stably committed GATA3<sup>+</sup> T<sub>H</sub>2 cells have been forced to adopt a GATA3<sup>+</sup>Tbet<sup>+</sup> and IL4<sup>+</sup>IFN- $\gamma$ <sup>+</sup> phenotype *in vivo* following infection with lymphocytic choriomeningitis virus (Hegazy *et al.*, 2010).

Of all the T<sub>H</sub> cells, Tregs are possibly the most often associated with plastic potential. FoxP3<sup>+</sup> expression in Tregs has been found to be unstable (DuPage & Bluestone, 2016). Through the employment of FoxP3<sup>+</sup>YFP<sup>+</sup> reporter mice, there was a significant portion of the FoxP3<sup>+</sup> cells, which had down-regulated or completely lost FoxP3 expression (Zhou *et al.*, 2010). These ‘ex-FoxP3’ cells were mostly activated-memory phenotype and produced inflammatory cytokines. Their conversion to ‘exFoxP3’ cells was enhanced in an autoimmune setting. Human Tregs have been shown to convert to T<sub>H</sub>17 cells when stimulated with allogenic antigen in the presence of exogenous IL-2 and IL-15, *ex vivo* (Koenen *et al.*, 2008). Another report demonstrated that *in vitro* stimulated iTregs could be converted to IL-17-producing T cells when treated with IL-6 and TGF- $\beta$ , and this was enhanced with the addition of IL-1 and IL-23 (Yang *et al.*, 2008). Thymus-derived nTreg-to-T<sub>H</sub>17 cell conversion has also been reported following IL-6 treatment *in vitro* (Xu *et al.*, 2007). It is worth noting that some studies have demonstrated that Tregs can also remain constant as evidenced by FoxP3 stability in adoptively transferred Tregs, *in vivo* (Gavin *et al.*, 2007; Williams & Rudensky, 2007).

#### 1.1.5.5 CD8<sup>+</sup> T cells

CD8<sup>+</sup> T cells are important for killing infected and malignant cells. CD8<sup>+</sup> T cells are capable of clearing many different parasitic, viral, fungal and bacterial infections (Perry *et al.*, 1997; Rothstein *et al.*, 1978). This can be achieved by killing infected host cells but also through direct killing of extracellular microbes.

CTL-mediated killing requires the direct interaction between the CTL-TCR and the peptide-MHCI complex on the target cell, for the formation of the cytolytic immune synapse (de la Roche *et al.*, 2016). CTLs have a number of cytotoxic mediators for their cell-killing functions. Granulysin is a CTL product which is capable of directly killing a broad spectrum of pathogens by mediating membrane permeability of targets (Ernst *et al.*, 2000). Perforin creates pores in the target cell membrane (Keefe *et al.*, 2005) and can be endocytosed into the target cell along with the potent cytotoxic mediator granzyme B (Shi *et al.*, 2005). CTLs are very effective at killing target cells. Single CD8<sup>+</sup> T cells can kill many target cells in a process identified *in vitro* as 'serial killing' (Halle *et al.*, 2017; Rothstein *et al.*, 1978).

CTLs are important for bacterial clearance. CTLs produce the T<sub>H</sub>1 cytokine, IFN- $\gamma$ , in response to intracellular infection (Perry *et al.*, 1997). The production of IFN- $\gamma$  is critical for bacterial clearance as evidenced when IFN- $\gamma$ -deficient mice were unable to resolve *Chlamydia trachomatis* infection (Lampe *et al.*, 1998). It has also been shown that mice lacking the Class-IIa molecule or perforin/granzyme B were unable to resolve primary infection of *S. Typhimurium* as effectively as wild type mice (Lee *et al.*, 2012).

## 1.2 Cancer

Cancer is a disease in which normal body cells develop the ability to grow uncontrollably. In their seminal review, Hanahan and Weinberg (2000) built on the prevailing ideology that the transition of a normal cell to a malignant cell was a multistep process. They argue that this process was analogous to Darwinian evolution, in which successive steps conferred growth advantages and culminated in this transformation. They identified six traits which a cell must acquire in this transformation process to become malignant: sustained proliferative signalling, insensitivity to growth suppression, limitless replicative potential, sustained angiogenesis, evasion of apoptosis and finally, tissue invasion and metastatic potential. Hanahan and Weinberg updated this review in 2011, in light of advances in cancer biology to include emerging and enabling traits such as dysregulation of cellular energetics, genome instability, immune evasion and tumour-promoting inflammation (Hanahan & Weinberg, 2011).

According to the most up-to-date statistics at the time of writing, Cancer Research UK reported that there were 356,860 cases of cancer in the United Kingdom in 2014, of which 163,444 patients died. (<http://www.cancerresearchuk.org/health-professional/cancer-statistics>). It is predicted that 1 in 2 people in the United Kingdom born after 1960 will be diagnosed with cancer in their lifetime. The main types of cancer treatment available are surgery, radiation and chemotherapy. The suitability and efficacy of these treatments differ depending on multiple factors including tumour origin, type and accessibility. A new type of cancer therapy, immunotherapy, has recently prevailed in the clinical context (Phan *et al.*, 1993; van Elsas *et al.*, 1999), with the advances in our understanding of the role the immune system plays in the prevention, progression or rejection of tumours.

### **1.3 The role of the immune system in preventing and promoting cancer**

The immune system plays many roles in a cancer setting. Sir McFarlane Burnet and Lewis Thomas first put the role of the immune system in cancer prevention forth in 1957, with their ‘cancer immunosurveillance’ hypothesis (Burnet, 1957). They postulated that neoplasias may develop spontaneously throughout a lifetime, but that emerging tumours could possess tumour-specific antigens, provoking a protective immune response thus preventing clinical presentation of a tumour. Although this is indeed true in some cases, the removal of neo-antigen-expressing tumour cells allows for the selection of antigen-lacking tumour cells which subsequently escape immune clearance (Dunn *et al.*, 2004).

#### **1.3.1 Inflammation and cancer initiation**

Evidence for an association between inflammation and tumourigenesis comes from epidemiological data showing that chronic inflammation predisposes individuals to various types of cancer (Balkwill & Mantanovi, 2001). Inflammatory cells and mediators are present in most, if not all tumours irrespective of the factors that led to cellular transformation (Mantovani *et al.*, 2008). Myeloid-derived pro-inflammatory cytokines, such as IL-6, induce the activation of the transcription factor NF- $\kappa$ B in tumour cells, leading to the promotion of proliferation and suppression of apoptosis (Greten *et al.*, 2004). TNF- $\alpha$  has been

associated with the initiation and progression of multiple cancer types (Greten *et al.*, 2004; Popivanova *et al.*, 2008). Several cytokines, including TNF- $\alpha$ , IL-1 $\beta$ , IL-13 and TGF- $\beta$  can lead to genome destabilisation by the induction of activation-induced cytidine deaminase (AID) which has been demonstrated to mutate tumour suppressor genes such as *TP53* and *MYC*, promoting oncogenesis (Endo *et al.*, 2008).

### 1.3.2 The immunosuppressive microenvironment

The progression of tumourigenesis is accompanied by an immunosuppressive microenvironment, which limits the ability of the immune system to reject the tumour (Rodriguez *et al.*, 2004). Chief amongst the mechanisms which allow this is the production of anti-inflammatory cytokines to inhibit the functions of tumour-infiltrating lymphocytes (Boehmer *et al.*, 2005). These cytokines also lead to the accumulation of immunosuppressive immune cells such as Tregs (Strauss *et al.*, 2007). Stromal cells are also implicated in perpetuating the anti-inflammatory environment. In a model of non-small cell lung carcinoma (NSCLC) a subset of isolated fibroblasts constitutively expressed the immune checkpoint molecules, PD-L1 and PD-L2 (Nazareth *et al.*, 2007). The deletion of fibroblasts attenuated tumour growth significantly in a model of Lewis Lung Carcinoma, even though the fibroblast-associated protein- $\alpha^+$  cells comprised only 2% of the tumour mass (Kraman *et al.*, 2010).

#### 1.3.2.1 Neutrophils promote many features of tumourigenesis

The role of neutrophils in cancer is becoming of increasing interest, as this innate immune cell type is expanding its repertoire of reported functions. Neutrophils have tumour-promoting characteristics. Neutrophil elastase is able to enter tumour cells and liberate phosphatidylinositol-3-kinase, which can drive cancer cell proliferation (Houghton *et al.*, 2010). Neutrophil elastase can also promote angiogenesis via the production of matrix metalloproteinase (MMP)-9 and vascular endothelial growth factor (VEGF) (Deryugina *et al.*, 2014; Wada *et al.*, 2007). Blocking neutrophil elastase using a small molecule inhibitor, Sivelestat, attenuated tumour cell proliferation *in vitro* and reduced the growth of human tumour xenografts *in vivo* (Wada *et al.*, 2006, 2007). A recent study described how c-Kit $^+$  neutrophils were associated with the promotion of

metastasis (Coffelt *et al.*, 2015). These neutrophils were induced by IL-17 production from  $\gamma\delta$ T cells and suppressed CTL activity *in vivo*. These findings are somewhat contradictory to a study by Andzinski and colleagues, whereby activated, IFN- $\beta$ -stimulated, pro-inflammatory neutrophils had a greater capacity to kill tumour cells directly *in vitro*, and the removal of these pro-inflammatory neutrophils resulted in reduced tumour killing capacity by the neutrophil population (Andzinski *et al.*, 2016). These data suggest that the phenotype of the neutrophils may be dictating the contribution of neutrophils to either tumour development or protection (Coffelt *et al.*, 2016).

### 1.3.2.2 TAMs stimulate multiple stages of tumourigenesis

It has been demonstrated that in up to 80% of clinical studies of cancer progression, macrophage density was associated with poor prognosis (Bingle *et al.*, 2002). TAMs are associated with defective expression of inflammatory cytokines, and a pre-disposition to produce immunosuppressive cytokines such as IL-10 (Saccani *et al.*, 2006). Macrophages play functionally diverse roles at multiple stages of cancer progression as well as adopting distinct roles in different tumour microenvironments (Qian & Pollard, 2010).

TAMs are derived from circulating CCR2<sup>+</sup> bone marrow-derived monocytes (Franklin *et al.*, 2014) (Figure 1.4). It has also been reported that TAMs can arise from splenic progenitors (Cortez-Retamozo *et al.*, 2012), but the mechanisms underlying the requirements for monocyte egress from the spleen are incompletely elucidated. However, there is some evidence to suggest a role for CCR2 and Angiostatin-2 in mediating splenic monocyte egress (Cortez-Retamozo *et al.*, 2012; Swirski *et al.*, 2009).

TAMs are capable of directly stimulating tumour cell proliferation through the production of epidermal growth factor (EGF) (Sullivan *et al.*, 1993). TAMs can also stimulate neo-vascularisation in the growing tumour. Tie2<sup>+</sup> macrophages have been directly implicated in stimulating angiogenesis in tumours (De Palma *et al.*, 2005). These macrophages are found aligned with the endothelial cells through interaction with Angiostatin-2, the Tie2 ligand. In humans, these cells express higher levels of pro-angiogenic genes including *Vegf-a*, *Mmp9* and *Cyclooxygenase (Cox)2* than Tie2<sup>-</sup> monocytes/macrophages (Coffelt *et al.*, 2010).

## Specific targeting of Tie2 interrupts the macrophage-endothelial interaction and inhibits

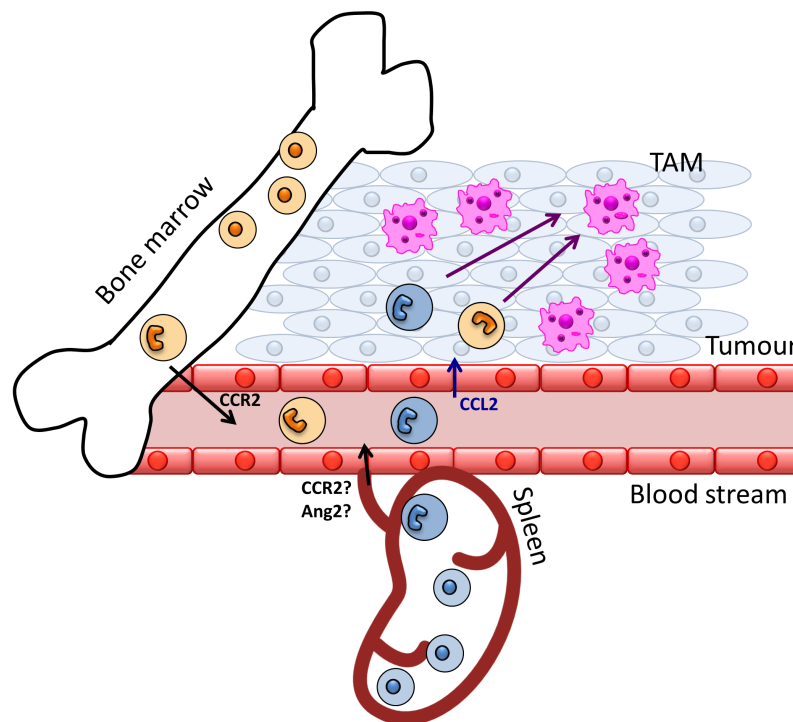


**Figure 1.4 Origin of tumour-associated macrophages**

Ly6C<sup>hi</sup> monocytes egress from the bone marrow in a manner dependent on CCR2. The spleen can also be a source for TAMs, and egress may be dependent on CCR2 and Angiostatin-2 (Ang2). Ly6C<sup>hi</sup> monocytes can migrate into the tissue and differentiate into mature TAMs which lose Ly6C expression, and exhibit variable MHCII expression. TAMs are capable of secreting many cytokines and chemokines to propagate the immunosuppressive tumour microenvironment.

angiogenesis in various cancer models (Coffelt *et al.*, 2011; Mazziari *et al.*, 2011). It has been found that Colony Stimulating Factor (CSF)-1, most likely from tumour cells, can promote Tie2 expression on TAMs (Coffelt *et al.*, 2011). Furthermore, the Tie2<sup>+</sup> TAMs have been found to express increased levels of IL-10 and stimulate Treg cell expansion.

TAMs can also promote tumourigenesis by secreting an array of cytokines and chemokines, which promote immunosuppressive cell recruitment. One such example is TAM-mediated CCL22 secretion which has been shown to recruit Tregs in an ovarian carcinoma model (Curiel *et al.*, 2004; Facciabene *et al.*, 2011). Furthermore, it has been shown that macrophages can induce iTregs by the production of IL-10 and TGF- $\beta$  (Murai *et al.*, 2009; Schmidt *et al.*, 2016). IL-10 inhibits T<sub>H</sub>1 cytokine production (Del Prete *et al.*, 1993; Fiorentino *et al.*, 1989; Fiorentino *et al.*, 1991). TGF- $\beta$  inhibits the expression of CTL effector function-associated gene products perforin, granzyme A, granzyme B, Fas ligand

and IFN- $\gamma$  (Thomas & Massagué, 2005), as well as inhibits T<sub>H</sub>1 cell differentiation and proliferation (Gorelik, 2002).

TAMs can also express molecules which arrest infiltrating effector T cells, such as PD-1 and PD-L1 (Belai *et al.*, 2014). The immunomodulatory cytokines CSF-1 and IL-4 induce the expression of PD-L2 in macrophages (Loke & Allison, 2003). Furthermore, TAMs in hypoxic regions of a tumour up-regulate PD-L1 due to hypoxia inducible factor 1 $\alpha$  (HIF-1 $\alpha$ ) signalling (Noman *et al.*, 2014). TAM PD-1 expression increases over time in mouse models and has been found to increase with increasing disease stage in human cancers (Gordon *et al.*, 2017). It has been shown that TAM PD-1 expression negatively correlates with tumour phagocytic potential, and blockade of PD-1/PD-L1 axis abrogated this functional deficiency and led to increased survival of mice bearing subcutaneous tumours (Gordon *et al.*, 2017).

The CTLA-4 ligands are the B7 family members. The expression of B7-H4 on TAMs correlates with the clinical stage of lung carcinoma and gastric cancer (Chen *et al.*, 2012; Matsunaga *et al.*, 2011). B7-H4 expression on TAMs in human ovarian cancer suppressed antigen-specific T cell activation (Kryczek *et al.*, 2006). Furthermore, the inhibition of B7-H4 resulted in tumour regression, further proving the immunosuppressive function of this ligand and TAMs (Kryczek *et al.*, 2006).

TAMs can also suppress T cell activity through the depletion of L-arginine in the tumour microenvironment, which is required for T cell function (Rodriguez *et al.*, 2004). The depletion of L-arginine inhibits the re-expression of CD3 after internalisation caused by antigen stimulation and T cell receptor signalling (Zea *et al.*, 2004). Pro-tumoural TAMs secrete arginase-1 which is an enzyme which metabolises, and depletes, L-arginine in the tumour microenvironment, leading to T cell suppression (Bak *et al.*, 2008; Sica *et al.*, 2008).

As well as promoting tumour growth at the original site, TAMs are also complicit in promoting tumour cell extravasation and metastasis. Tie2<sup>+</sup> TAMs have been directly implicated in assisting tumour cells to escape from the original site of

tumourigenesis (De Palma *et al.*, 2005, 2008). TGF- $\beta$  is also implicated in promoting metastasis (Padua *et al.*, 2008).

Beyond extravasation, macrophages can promote metastasis by enhancing tumour cell seeding at distal sites. TAMs are capable of migrating with invasive carcinoma cells *in vivo* (Dovas *et al.*, 2013; Ojalvo *et al.*, 2009). In fact, the migration of these invasive carcinoma cells is dependent upon the co-migration of TAMs. Metastasis-associated macrophages (MAMs) are critical in the formation of the pre-metastatic niche (Ojalvo *et al.*, 2009). VEGF and CCL2 production by MAMs increases vascular permeability at the metastatic site, which promotes tumour cell extravasation from the circulatory system (Qian *et al.*, 2012). Furthermore, MAMs expressing VEGFR promote tumour cell survival following metastatic seeding. In a spontaneous model of mammary epithelial cancer, genetic or chemical ablation of VEGFR in MAMs decreased metastatic tumour cell seeding and growth (Qian *et al.*, 2015).

Macrophages have been reported to be highly plastic cells, which can alter their phenotype depending on specific immunological stimuli (Sica *et al.*, 2008). This was first demonstrated *in vitro* where macrophages could be skewed towards a T<sub>H</sub>1 or T<sub>H</sub>2 phenotype through the addition of exogenous IFN- $\gamma$  or IL-4 respectively (Mantovani *et al.*, 2002; Mosser & Edwards, 2008). As such, 'M1' and 'M2' were employed as a categorisation of macrophages based on their production of either T<sub>H</sub>1-associated or T<sub>H</sub>2-associated cytokines, respectively. However, based on limited phenotypic information which does not encompass the complex transcriptional profile of the multiple different types of TAMs, this nomenclature is superseded by phenotypic descriptions of the cells including cell surface and intracellular markers (Murray *et al.*, 2014). However, there is some suggestion that this switch from one phenotype to another also occurs *in vivo* (Guiducci *et al.*, 2005). In the report, it was unclear if this process was actually resident macrophages experiencing re-polarisation from the T<sub>H</sub>2-like phenotype to the T<sub>H</sub>1-like phenotype, or simply if inflammatory monocytes (Ly6C<sup>+</sup>MHCII<sup>+</sup>) were populating the tissue as T<sub>H</sub>1 macrophages. Another, more convincing, study demonstrated that differentiated macrophages can be reprogrammed when transferred into a new environment (Lavin *et al.*, 2014). This was evidenced when adoptively transferred peritoneal macrophages into lung tissue resulted in

these cells adopting an alveolar macrophage-like chromatin landscape, distinct from their original phenotype. These data demonstrate that the environmental niche can influence macrophage behaviour, but this plasticity has not yet been demonstrated in the tumour microenvironment.

### **1.3.2.3 Tumour-associated DCs exhibit attenuated maturation and T cell activation**

DCs play an important role in anti-tumour responses. The CD103<sup>+</sup> cDC1 population are responsible for transporting tumour antigen to the draining lymph, for both spontaneous and implantable tumour models (Fuertes *et al.*, 2011; Roberts *et al.*, 2016). cDC2s fail to present tumour antigen in tumour draining lymph nodes but the reason for this is unknown, in spite of the fact that cDC1 and cDC2s appear to migrate in equal numbers (Roberts *et al.*, 2016). It is speculated that one contributing factor might be their decreased expression of endocytic receptors such as Clec9a, which would reduce their ability to take up antigen from apoptotic or necrotic cells (Gardner & Ruffell, 2016).

Tumour-associated DCs are attenuated in their ability to activate T cells (Flies *et al.*, 2016) and were unable to stimulate tumour antigen-specific T cells *ex vivo* (Stoitzner *et al.*, 2008). Tumour-associated molecules are largely responsible for the inhibition of DC maturation and activation. VEGF inhibits DC maturation *in vitro* and *in vivo*, in part through blocking NF- $\kappa$ B function in hemopoietic progenitor cells (Gabilovich *et al.*, 1998; Gabilovich *et al.*, 1996). The blockade of VEGF-R2 resulted in increased tumour-associated DCs in a pre-clinical model of breast cancer (Roland *et al.*, 2009). Tumour-derived TGF- $\beta$  has been shown to down-regulate DC maturation markers CD86, CD80 and MHCII (Kel *et al.*, 2010) and suppress the production of pro-inflammatory cytokines associated with DC maturation (Lievens *et al.*, 2013). IL-10 is also suppressive of tumour DC function, e.g. inhibiting the expression of co-stimulatory molecules such as CD40 (Shurin *et al.*, 2002). Systemic IL-10 blockade in tumour-bearing mice resulted in an increase of CD103<sup>+</sup> cDC1 and CD11b<sup>+</sup> cDC2 in tumours (Ruffell *et al.*, 2014). IL-10 produced by TAMs can also inhibit IL-12 production by CD103<sup>+</sup> cDC1s (Ruffell *et al.*, 2014). It is also possible that the degree of metabolic dysfunction within the tumour impacts upon DC function. Both lactic acid and hypoxia have been reported to suppress DC activation *in vitro* (Doedens *et al.*,

2010; Gottfried *et al.*, 2013). This immunosuppressive DC phenotype can be characterised by decreased expression of co-activation markers and increased expression of regulatory markers such as PD-L1 (Harimoto *et al.*, 2013; Krempski *et al.*, 2011). DCs are also complicit in perpetuating the immunosuppressive immune environment through further secretion of IL-10 (Llopiz *et al.*, 2016).

#### **1.3.2.4 Effector T cells are critical for tumour clearance but are suppressed in the tumour microenvironment**

Tregs have also been implicated in tumourigenesis, with IL-10 and TGF- $\beta$  production particularly permissive to tumour development. High infiltration of Tregs is associated with poor prognosis for breast cancer patients (Bates *et al.*, 2006; Gobert *et al.*, 2009). The removal of peripheral CD4<sup>+</sup>CD25<sup>+</sup> T cells from a transplantable tumour model resulted in tumour eradication (Shimizu *et al.*, 1999). Tregs are attracted to the tumour microenvironment through the secretion of chemoattractants. The systematic blockade of the tumour-associated chemokine, CCR5, resulted in a significant attenuation of Treg migration into tumours in a model of pancreatic cancer and tumourigenesis was compromised (Tan *et al.*, 2009). Furthermore, tumour hypoxia has been reported to drive Treg recruitment through the production of CCL22 in ovarian cancer (Curiel *et al.*, 2004). Effector T cells, those with anti-tumour function, are suppressed in the tumour microenvironment. Tregs produce TGF- $\beta$  which can suppress CTL functional molecules and T cell expansion (Chen *et al.*, 2005; Gorelik, 2002; Thomas & Massagué, 2005). Tregs express immune checkpoint molecules such as PD-1 and CTLA-4, which serve to arrest infiltrating effector T cells, particularly CTLs (Han *et al.*, 2014; Wang *et al.*, 2009).

T<sub>H</sub>1 cells and T<sub>H</sub>1-associated cytokines are strongly associated with good clinical outcome for nearly all cancer types. In a study of colorectal cancer patient samples, it was found that patients with high T<sub>H</sub>1 cytokine production experienced prolonged survival (Tosolini *et al.*, 2011). In a study of epithelial ovarian cancer, high levels of T cell-mediated IFN- $\gamma$  production was correlated with longer overall survival of patients (Marth *et al.*, 2004). Furthermore, it has been found that the relative levels of T<sub>H</sub>1:T<sub>H</sub>2 cytokine expression in favour of the former was a predictor of prognosis in multiple stages of human epithelial ovarian cancer (Kusuda *et al.*, 2005). IFN- $\gamma$  is an important T<sub>H</sub>1-associated

cytokine and plays an important role in tumour immunity. *Ifngr1<sup>-/-</sup>* mice develop spontaneous and MCA-induced tumours more readily than wild type (Kaplan *et al.*, 1998; Shankaran *et al.*, 2001). IFN- $\gamma$  can inhibit cancer cell proliferation (Bromberg *et al.*, 1996) as well as induce cancer cells to undergo apoptosis both *in vitro* and *in vivo* (Burke *et al.*, 1999; Wall *et al.*, 2003). T<sub>H</sub>1-derived IFN- $\gamma$  was shown to induce macrophages to directly kill cancer cells *in vivo* and produce angiostatic chemokines CXCL9 and CXCL10 (Haabeth *et al.*, 2011).

T<sub>H</sub>2 cells have been implicated in supporting tumourigenesis in pancreatic cancers, resulting in reduced patient survival (De Monte *et al.*, 2011; Tassi *et al.*, 2008). Furthermore, this T<sub>H</sub>2 phenotype is propagated through a complex crosstalk involving T<sub>H</sub>2 cells, thymostromal lymphotoxin protein, cancer associated fibroblasts and DCs (De Monte *et al.*, 2011). IL-4 has been reported to increase the proliferative capacity of multiple prostate cancer cell lines *in vitro* (Roca *et al.*, 2012). However, there is also evidence to suggest an anti-tumour role for T<sub>H</sub>2 cells. In one study, the expression of the T<sub>H</sub>2-associated transcription factor, GATA3, correlated positively with breast cancer patient survival and responsiveness to therapy (Parikh *et al.*, 2005).

There have been mixed reports pertaining to the contributions of T<sub>H</sub>17 to tumourigenesis. T<sub>H</sub>17 cells have been found to correlate with increased patient survival in esophageal squamous cell carcinoma (Lv *et al.*, 2011) whereas in a study of ovarian cancer, T<sub>H</sub>17 cell density correlated with poor prognosis (Tosolini *et al.*, 2011). In melanoma studies, T<sub>H</sub>17 cells have demonstrated significant anti-tumour immunity, in part through the generation of tumour-specific CTLs (Martin-Orozco *et al.*, 2010; Muranski *et al.*, 2008). These data suggest that the role of T<sub>H</sub>17 cells in cancer is cancer type-dependent.

As there are many roles for the multiple cell types discussed both during cancer and in response to *S. Typhimurium*, the major contributions of specified cell types are summarised in Table 1.1.

**Table 1.1 Summary of the roles of multiple cell types in cancer and *S. Typhimurium* infection**

Immune cell type	Key marker(s)	Role in cancer	Role in responding to <i>S. Typhimurium</i> infection
Neutrophil	Ly6G	<u>Promotion:</u> Angiogenesis, tumour cell proliferation, metastasis, suppress CTLs  <u>Rejection:</u> ROS production, H <sub>2</sub> O <sub>2</sub> production, T cell recruitment	Phagocytosis of extracellular bacteria and cellular debris, NET production, degranulation, pro-inflammatory cytokine secretion, granulopoiesis
Monocyte/macrophage	F4/80, Ly6C	<u>Promotion:</u> tumour cell proliferation, angiogenesis, metastasis, immunosuppressive molecule production, Treg recruitment, effector T cell suppression  <u>Rejection:</u> T cell recruitment	Phagocytosis of extracellular bacteria and cellular debris, pyroptosis, pro-inflammatory cytokine secretion, immune cell recruitment, antigen presentation
DC	CD11c MHCII	<u>Promotion:</u> Immunosuppressive cytokine secretion, abrogated T cell activation  <u>Rejection:</u> Phagocytosis, tumour antigen presentation, lymph node migration, T cell activation, pro-inflammatory cytokine secretion	Phagocytosis, trogocytosis, antigen presentation, lymph node migration, T cell activation, pro-inflammatory cytokine secretion.
T <sub>H</sub> 1 cells	CD3  CD4  Tbet	<u>Promotion:</u> not well defined  <u>Rejection:</u> Tumour cell killing, pro-inflammatory cytokine secretion	Pro-inflammatory cytokine secretion, T cell expansion, CTL stimulation, inflammasome assembly
T <sub>H</sub> 2 cells	CD3  CD4  GATA3	<u>Promotion:</u> tumour cell proliferation, immunosuppression  <u>Rejection:</u> not well defined	Not well defined
T <sub>H</sub> 17 cells	CD3  CD4  ROR $\gamma$ t	<u>Promotion:</u> Angiogenesis  <u>Rejection:</u> pro-inflammatory cytokine secretion, recruitment of anti-tumour cells	Pro-inflammatory cytokine secretion, granulopoiesis, neutrophil recruitment
Tregs	CD3	<u>Promotion:</u> Effector T cell arrest,	Antagonise <i>S. Typhimurium</i> immune

	CD4  FoxP3	APC arrest,  <u>Rejection:</u> pro-inflammatory cytokine secretion, recruitment of anti-tumour	response
CTL	CD3  CD8	<u>Promotion:</u> Not well defined  <u>Rejection:</u> pro-inflammatory cytokine secretion, direct tumour cell killing	Infected-cell killing, directly bacteria killing

### 1.3.3 Cancer immunotherapy: enhancing anti-tumour immunity

Cancer immunotherapy, the modulation of the immune system to eradicate cancer, has become a clinically relevant therapeutic modality in light of the cancer immunology research generated over the last two decades.

DCs are a promising target for cancer therapy (Gardner & Ruffell, 2016). Therapeutic vaccination for cancer depends on the ability of DCs to present tumour antigen to T cells. This can be achieved by loading DCs with tumour-specific antigens *ex vivo*, increasing tumour-specific lymphocyte response and reducing tumour development (Palucka & Banchereau, 2013). Another strategy for enhancing tumour immunity via DCs is to use agonists to activate the DCs directly. This approach has been investigated using a variety of TLR agonists to stimulate DCs, which have resulted in tumour growth arrest *in vivo* associated with increased DC maturation and an enhanced CD8<sup>+</sup> T cells response (Ohkuri *et al.*, 2014; Vicari *et al.*, 2002).

Tregs are also a target of immunotherapies. CTLA-4 was the first immune-checkpoint receptor to be clinically targeted. CTLA-4 is expressed exclusively on T cells and counteracts the activity of the co-stimulatory receptor CD28 (Pardoll, 2012; Schwartz, 1992). CTLA-4 is constitutively expressed on Tregs (Jago *et al.*, 2004) and seems to inhibit T cell activation and APCs through binding to the B7 ligands, CD80 and CD86, arresting effector functions (Linsley *et al.*, 1991; Linsley *et al.*, 1995). Treg-specific knockdown of CTLA-4 significantly inhibits their ability to antagonise tumour immunity (Peggs *et al.*, 2009). Preclinical studies demonstrated the significant efficacy of CTLA4 antibodies on partially

immunogenic tumours, whereas combination therapy with GM-CSF was required to mediate rejection of poorly immunogenic tumours (van Elsas *et al.*, 1999). Ipilimumab, a humanized CTLA-4 antibody, began clinical testing in 2000. It was found that 21% of melanoma patients produced objective cancer regression, but with autoimmune clinical manifestations including colitis and dermatitis in 35% of patients (Phan *et al.*, 2003). Another study demonstrated an objective tumour response of 14% but was accompanied by similar autoimmune side effects (Beck *et al.*, 2006).

PD-1 is another promising target for immunotherapy. PD-1 is induced when T cells become activated (Keir *et al.*, 2006) and limits T cell activity in peripheral tissues following inflammation to limit autoimmunity through ligand engagement (Freeman *et al.*, 2000; Keir *et al.*, 2006). PD-1 is also expressed on other immune cells such as NK cells and macrophages (Gordon *et al.*, 2017; Terme *et al.*, 2011). There are two ligands for PD-1: PD-L1 and PD-L2. PD-L1 has been shown to be up-regulated on cancer cells (Dong *et al.*, 2002; Konishi *et al.*, 2004), as well as myeloid cells in the tumour environment (Brown *et al.*, 2003; Kuang *et al.*, 2009). PD-L1 overexpression correlates poorly with prognosis for multiple cancer types (Nakanishi *et al.*, 2007; Nomi *et al.*, 2007; Ohigashi *et al.*, 2005; Thompson *et al.*, 2004). *In vivo* studies have demonstrated increased anti-tumour immunity following PD-L1 blockade (Blank *et al.*, 2004; Iwai *et al.*, 2002). The first clinical study employing the humanised monoclonal antibody against PD-1 saw objective tumour responses of 28% for melanoma, 27% for renal carcinoma and 18% for NSCLC, with 14% of patients suffering autoimmune side effects (Topalian *et al.*, 2012). Another study demonstrated a survival rate of one year with 42% of patients with advanced squamous-cell NSCLC treated with nivolumab compared to 24% of patients treated with docetaxel. In this study, only 7% of patients suffered grade 3 or 4 treatment-related adverse effects (Brahmer *et al.*, 2015). The US Food and Drug Administration (FDA) has approved nivolumab for patients with metastatic melanoma, NSCLC, renal cell carcinoma and non-Hodgkins lymphoma. However, there are more PD-1 signal inhibitors besides nivolumab. At the time of writing, according to the clinical trials database managed by the U.S. National Institute for Health, there are 636 clinical trials recruiting patients for studies utilising an intervention of the PD-1-PD-L1/2 axis (clinicaltrials.gov).

## 1.4 Bacterial-mediated cancer therapy

The link between bacterial infection and anti-cancer effects was employed for clinical use at the end of the 19<sup>th</sup> century by the head of the Bone Tumour Service at the Memorial Hospital in New York (McCarthy, 2006). Dr William Coley's interest in bacterial mediated cancer therapy was stimulated when a sarcoma patient with an inoperable tumour experienced tumour regression following 'a severe attack of erysipelas' (Coley, 1883). Erysipelas is characteristic of an upper dermal infection, most commonly caused by *Streptococcus pyogenes* infection (Bonnetblanc & Bédane, 2003). Intense investigation of the literature provided Coley with several references to a relationship between infection and tumour regression (Starnes, 1992). Coley went on to conclude:

*'If erysipelas, a disease produced by a specific organism, could cure a case of undoubted sarcoma when occurring accidentally, it seemed fair to presume that the same benign action would be exerted in a similar case if erysipelas could be artificially produced.'*

It was not long after that Coley had an opportunity to induce erysipelas in a hopeless case of sarcoma. When this patient, who was treated with *Streptococcus*, experienced tumour free survival, Coley endeavoured a career in bacterial-mediated cancer therapy, unknowing that he had founded the field of immunotherapy. From reports which have retrospectively analysed the progression of Coley's career, there is a consensus that Coley's treatment modality was overshadowed by the emerging modalities of chemotherapy and radiation therapy treatment, as well as a general scepticism in the credibility of his studies (Coley Nauts *et al.*, 1946; McCarthy, 2006). The combination of these resulted in bacterial cancer therapy being a neglected area of research interest for decades.

In the last two decades, research into the potential of bacteria as a legitimate cancer treatment option has grown exponentially (Forbes, 2010). Many genera of bacteria have been investigated for their anti-cancer effects such as *Escherichia*, *Clostridium*, *Bifidobacterium*, *Listeria*, *Streptococcus* and *Salmonella* (Clairmont *et al.*, 2000; Cronin *et al.*, 2010; Dang *et al.*, 2001; Kasinskas & Forbes, 2007;

Maletzki *et al.*, 2008; Pijkeren *et al.*, 2010; Stern *et al.*, 2015). This resurrection may be in part from the success of an attenuated bacterial strain in clinical trials, *Bacillus Calmette-Guerin* (BCG). BCG is a strain of *Mycobacterium* and is the first line of post-operative therapy for high-risk non-muscle invasive urothelial carcinoma (Babjuk *et al.*, 2011). This therapeutic strategy was first published in 1976 when it was found that nine patients suffering from recurrent superficial bladder tumour responded favourably (Ingersoll & Albert, 2013; Morales *et al.*, 1992). BCG has proven to be a very effective therapy in this setting, succeeding in >50% of patients in reducing recurrence and diminishing disease progression (Babjuk *et al.*, 2011). Given the success of BCG in the clinic, it is surprising that the mechanisms governing the anti-tumour effects of BCG, and other strains, have only come to be appreciated in the last decade.

This resurrection of interest in bacterial-mediated cancer therapy has largely focused on improving bacterial localisation to the tumour to maximize therapeutic potential (Clairemont *et al.*, 2000; Low *et al.*, 1999) or to use the bacteria as a vehicle for therapeutic molecules (Loeffler *et al.*, 2008, Zheng *et al.*, 2017b). However, there is a sense that these studies are somewhat removed from Coley's original understanding of the underlying mechanism behind the success of bacteria or bacterial products in cancer therapy: the immune response (Coley, 1883).

#### **1.4.1 Tumour specific localisation and proliferation of systemically administered bacteria**

Systemically administered bacteria often exhibit tumour specific colonisation and proliferation but the mechanisms underpinning these are incompletely elucidated (Forbes, 2010). It has been speculated that the most prominent contributing factors include aberrant vasculature, chemotaxis towards chemical gradients in the tumour, tumour-specific nutrients, oxygenation and immune evasion (Figure 1.5).

During tumourigenesis, tumours need to synthesise new blood vessels to support tumour cell proliferation and survival. The resulting vessels are often chaotic and differ substantially from vessels in other tissues and are characterised by aberrant, disorganised and leaky blood vessels, resulting in tumour-specific

decreases in blood flow rates (Azzi *et al.*, 2013). It has been observed that *S. Typhimurium* are capable of attaching to the tumour vasculature *in vitro*, which was more prominent with lower flow rates (Forbes *et al.*, 2003). Therefore, there is greater opportunity for the bacteria to adhere and invade in the tumour vasculature compared to other tissues. Systemic *S. Typhimurium* administration has been reported to be accompanied by a spike in levels of TNF- $\alpha$  in the blood (Leschner *et al.*, 2009). This increase in TNF- $\alpha$  led to a large influx of blood into the tumour, which contributed to tumour colonisation.

The tumour microenvironment has been reported to contain physiologically distinct regions characterised by differential nutrient accumulation (Kasinskas & Forbes, 2006). Bacteria, including *S. Typhimurium*, contain multiple receptors for some of these nutrients, which include aspartate, serine and glucose. The loss of the aspartate receptor, Tar, inhibited tumour cylindroid accumulation of the  $\Delta tar$  strain whereas the wild type strain consistently colonised the periphery of the cylindroid (Kasinskas & Forbes, 2007). These data suggest a specific nutrient repertoire playing a role in mediating tumour-specific colonisation of bacteria. However, parallel studies *in vivo* have not been carried out. Motility is argued to be a significant advantage of bacteria compared to chemotherapeutic molecules which are limited by diffusional gradients. Motility was essential for bacterial accumulation within *in vitro* tumour cylindroids as the loss of flagella machinery reduced bacterial accumulation in the cylindroid model (Kasinskas & Forbes, 2007). This is in contrast to another study which demonstrated that strains lacking critical motility machinery,  $\Delta cheY$  and  $\DeltafliGH$ , were equally competent at bacterial colonisation as the wild type strain (Crull *et al.*, 2011a). The discrepancy between these findings may be due to the fact that Kasinskas *et al.*, (2007) looked at distribution within the tumour whereas Crull and colleagues only looked at total colonisation. Therefore, although motility might not be necessary for initial tumour invasion, it likely plays a role in tumour penetration which may in turn affect anti-tumour effects and long-term survival therein. Glycoprotein expression has also been identified as a potential mechanism for tumour-specific localisation, as *Salmonella* preferentially bound to neoplastic-associated glycoproteins *in vitro* (Wang *et al.*, 2016).

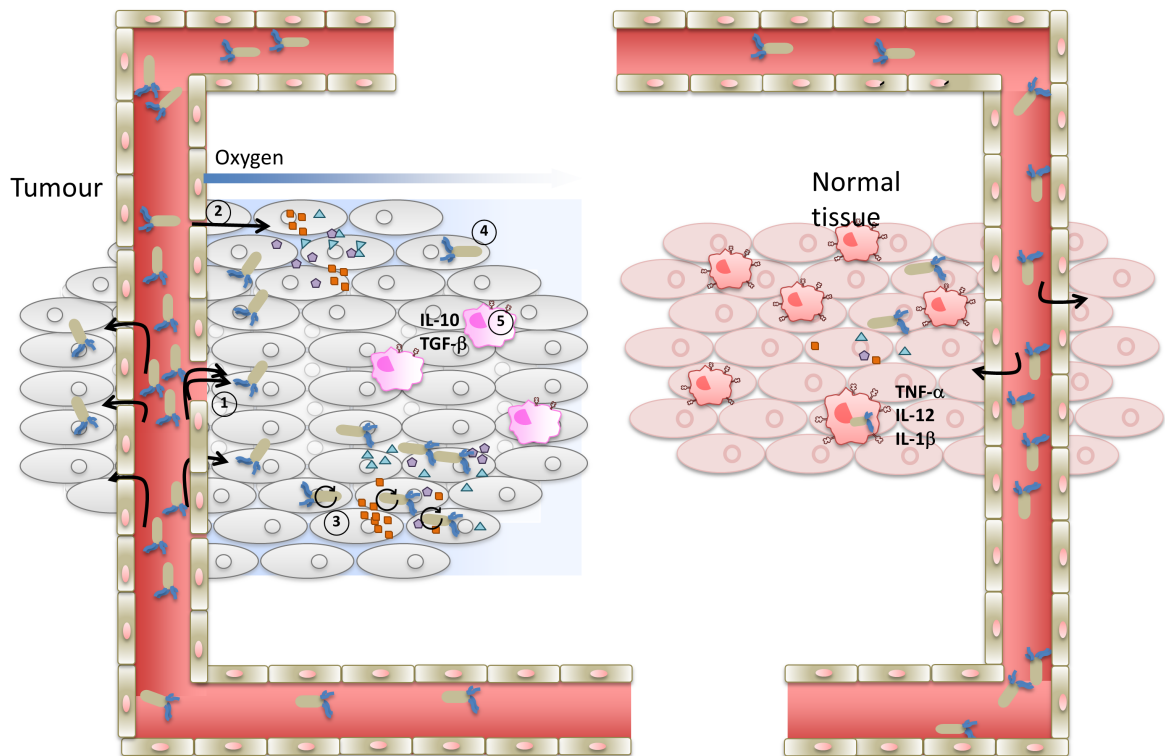


**Figure 1.5 Proposed mechanisms contributing to tumour-specific localisation and proliferation of bacteria following systemic infection**

Tumour specific bacterial localization and colonization has been reported in the literature. The proposed mechanisms for these phenomena are: 1. Aberrant tumour-specific vasculature, including altered blood flow and leaky vessels, are conducive to bacterial migration out of the blood stream. 2. Tumour-specific nutrients induce bacterial chemotaxis out of the vasculature. 3. Tumour-specific nutrients promote bacterial replication. 4. Tumour hypoxia allows for the proliferation of anaerobic and facultatively anaerobic bacterial strains. 5. The immunosuppressive tumour environment allows for bacterial immune evasion

Tumour-specific growth has been reported for multiple bacterial strains following systemic administration *in vivo* (Low *et al.*, 1999; Pijkeren *et al.*, 2010; Stern *et al.*, 2015). Furthermore, these tumour-specific nutrients have been suggested to support tumour-specific bacterial growth. Many strains employed for the purposes of bacterial cancer therapy are attenuated strains, commonly auxotrophic for certain nutrients. The *S. Typhimurium* cancer therapy strain, VNP20009, is an example whereby a *purl* deletion renders this strain auxotrophic for purines, which can be found in abundance in the necrotic regions of the tumour (Low *et al.*, 1999).

Tumours often exhibit various states of oxygenation: normoxia (normal), hypoxia (low) and anoxia (oxygen depleted) (Hockel & Vaupel, 2001). These features of the tumour allow for the tumour-specific colonisation of certain bacterial strains which employ anaerobic respiration, such as *Clostridia* strains. This has proved a

successful strategy whereby the administration of *Clostridium novyi* spores were demonstrated to germinate specifically within avascular regions of *in vivo* tumours and mediate tumour cell death (Dang *et al.*, 2001). In this study, there were no germinating spores recovered from the spleen, kidney, lung or liver of inoculated mice. Other bacterial species, such as *Salmonella*, are facultative anaerobes which means they can survive in other normoxic and hypoxic conditions. This feature increases the range of tumour environments the bacteria can reside in, but also negatively affects the tumour-specific localisation of the systemically administered bacteria. This limitation was addressed with the creation of an anaerobic *S. Typhimurium* strain, YB1 (Yu *et al.*, 2012). This SL7207-derivative had the essential gene, *asd*, under the control of the anaerobic promoter, *pepT*. This strategy increased tumour-specific localisation compared to wild type SL7207 and other *S. Typhimurium* cancer strains, demonstrating that hypoxia is a potent feature for bacterial tumour specific targeting.

The final feature credited with playing a role in tumour-specific colonisation of systemically administered bacteria is immune evasion. Tumours are widely regarded as immune privileged environments (Streilein, 1995). This phenomenon means that bacteria which localise therein are able to replicate and disseminate in the absence of the immune clearance mechanisms which exist to eliminate them (Westphal *et al.*, 2008). However, as discussed below, it is widely hypothesised that the tumour microenvironment can be transformed following bacterial accumulation, which may serve to alert the immune system to the presence of the tumour, leading to anti-cancer effects.

Tumour-specific localisation of bacteria, as well as serving as a therapeutic intervention, can also be employed for diagnostic purposes. Multiple studies have generated bacterial strains which can be imaged *in vivo* using relatively non-invasive techniques (Baban *et al.*, 2012; Cronin *et al.*, 2010). These technologies also enable the tracking of bacterial localisation *in vivo* in tumour models, possibly for the detection of metastases (Panteli *et al.*, 2015).

### 1.4.2 Native and enhancement of bacterial tumour toxicity

Multiple studies have reported that systemically administered bacteria are capable of direct anti-tumour behaviour and that native bacterial toxicity is sufficient to regress tumours (Dang *et al.*, 2001; Low *et al.*, 1999; Stern *et al.*, 2015).

*S. Typhimurium* mediates invasion of epithelial cells through the concerted action of the T3SS-1 (Galán & Curtiss, 1989; Galán & Ginocchio, 1994). One of the proteins which is passed through the injectisome into the host cell is SipA (Kaniga *et al.*, 1995). This protein has a caspase-3 cleavage site, which when cleaved, can produce two functional proteins (Srikanth *et al.*, 2010), providing scope to potentially overexpress and enhance the caspase-3 activation of cancer cells (McIntosh *et al.*, 2017). VNP20009 was demonstrated to directly kill B16F10 tumour cells *in vitro* (Jia *et al.*, 2007). SL3261, an attenuated derivative of SL1344 was also seen to be capable of mediating tumour cell death of Lewis Lung Carcinoma and mammary carcinoma 4T1 cells *in vitro* (Fu *et al.*, 2008). These results were similarly seen *in vivo* where systemically administered VNP20009 co-localised with apoptotic tumour cells (Chen *et al.*, 2012). Other bacterial species are also capable of mediating tumour cell death. An attenuated strain of *C. novyi* has been demonstrated to directly kill tumour cells at the interface between the viable rim and necrotic regions of subcutaneous B16 tumours (Dang *et al.*, 2001).

Although bacteria alone exhibit native anti-tumour effects, multiple strategies have been employed to enhance the tumour inhibitory effects of bacterial cancer therapies. These strategies generally employ the bacteria as a vehicle for the delivery of chemotherapeutic drugs, cytotoxic proteins, cytokines or genetic material to the tumour tissue.

Bacteria have been employed to mediate the conversion of systemically administered pro-drugs into their active cytotoxic forms in the tumour-specific locale. This has been demonstrated whereby tumour-targeting *S. Typhimurium*, expressing the *E. coli* cytosine deaminase enzyme (SL-CD), were capable of converting non-toxic 5-fluorocytosine into the active chemotherapeutic 5-fluorouracil (King *et al.*, 2002). The combinatorial administration of SL-CD and

pro-drug 5-fluorocytosine to tumour-bearing mice *in vivo*, resulted in greater tumour specificity of 5-fluorouracil as well as significantly reduced tumour growth compared to the bacteria or the pro-drug alone.

Multiple studies have employed the use of bacteria to deliver apoptosis-inducing products to cancer cells (Guan *et al.*, 2013; Jeong *et al.*, 2014; Zigmond *et al.*, 2012). One of these studies engineered VNP20009 to secrete tumour necrosis factor-related apoptosis-inducing ligand (TRAIL) using a plasmid-based system (Chen *et al.*, 2012). The study employed the use of a hypoxia promoter, *nirB*, to restrict *TRAIL* expression to regions of hypoxia, resulting in tumour-specific production of the cytotoxic protein. The therapeutic effect of VNP2009-pTRAIL was greater than VNP20009 transformed with a control plasmid and induced significantly greater tumour cell death *in vitro*.

Bacteria have also been employed as a means to perpetuate their native immunostimulatory potential via the production of eukaryotic cytokines or the overproduction of immunostimulatory bacterial proteins. VNP20009, transformed with a prokaryotic plasmid encoding the mammalian cytokine LIGHT, was demonstrated to significantly impair tumour progression and lung metastasis in an *in vivo* model of colon carcinoma (Loeffler *et al.*, 2007). LIGHT has been demonstrated to be capable of stimulating activation and lymph node-migration of DCs (Morel *et al.*, 2001; Schneider *et al.*, 2004). Another strategy is to overexpress prokaryotic proteins that stimulate the immune system. This process was employed by Zheng *et al.* (2017) in which the attenuated *S. Typhimurium* strain, SHJ2037, was engineered to overexpress flagellin B (FlaB) from *Vibrio vulnificus* (SL-pFlaB). The therapeutic consequence of this strategy in a transplantable tumour model was highly significant: SL-FlaB-infected tumours were prevented from growing up to 45 days post tumour challenge. This was in contrast to the SL-pEmpty-treated mice whose tumours seemed to have reached clinical endpoint 20 days previous. More than half of the SL-pFlaB infected mice were alive at 120 days following tumour challenge whereas all of the SL-pEmpty mice reached clinical endpoint before day 40 (Zheng *et al.*, 2017b). This report, and others, demonstrated the potency of enhancing the therapeutic effects of bacteria through immunostimulation.

It is also possible to couple the native toxicity of bacteria to other treatment modalities, such as chemotherapy. In a screen of more than 30 chemotherapeutic drugs, it was found that combination with *E. coli* (Nissle 1917) increased the efficacy of six of the drugs *in vitro* (Lehouritis *et al.*, 2015). In a transplantable *in vivo* model, co-administration of *E. coli* and the alkylating agent CB1954 produced more potent anti-tumour effects than either treatment modality alone. This same study also demonstrated that certain bacteria can *decrease* the efficacy of common cancer chemotherapeutics which is important to consider for future studies (Lehouritis *et al.*, 2015). Another study demonstrated that the combination of *S. choleraesuis* and the chemotherapeutic drug cisplatin resulted in greater tumour inhibitory effects and enhanced survival compared to either bacterial or cisplatin treatment alone (Lee *et al.*, 2005). *S. Typhimurium* has also been coupled to radiation as a synergistic treatment option (Avogadri *et al.*, 2008; Ganai *et al.*, 2009). Radiation treatment coupled to intra-tumoural *S. Typhimurium* treatment exhibited greater therapeutic potential than either modality alone, generating an anti-tumour CD8<sup>+</sup> T cell response (Avogadri *et al.*, 2008). This is possibly explained by radiation-induced increased expression of MHC I on tumour cells, which was demonstrated *in vitro*. Radiation treatment was also coupled to *S. Typhimurium* in another study of bacterial mediated therapy (Ganai *et al.*, 2009). Here, *S. Typhimurium* was transformed with radiation-inducible prokaryotic promoter upstream of TRAIL, limiting the expression of this cytotoxic protein to the area treated with radiation.

*S. Typhimurium* has also emerged as an attractive combinatorial therapy for multiple immune therapy treatment strategies. Adoptive T cell therapy has emerged as a promising treatment option for multiple cancers (Fesnak *et al.*, 2016). This treatment involves a combination of the isolation, genetic alteration and propagation *ex vivo* of tumour-specific T cells for re-introduction into the donor, but instances of tumour relapse following treatment have been reported (Thomas *et al.*, 2009). In one study, it was found that adoptive T cell transfer effectively prevented tumour relapse, but only when A1-R was co-administered (Binder *et al.*, 2016). This group also demonstrated that the combination of *S. Typhimurium* strain A1-R expressing tumour antigen plus the checkpoint inhibitor

antibody against PD-L1 resulted in 80% long-established melanomas being rejected *in vivo* up to 240 days post tumour challenge (Binder *et al.*, 2013).

### 1.4.3 Bactofection

‘Bactofection’ is the term used to describe the use of bacteria to transfer eukaryotic nucleic acids to eukaryotic cells for expression therein (Powell *et al.*, 1999; Schaffner, 1980). This strategy has been employed in a number of studies to enhance the anti-tumour effects of therapeutic strains (Guan *et al.*, 2013; Yuhua *et al.*, 2001).

#### 1.4.3.1 Proposed mechanisms of bactofection

The exact molecular mechanism of bactofection are incompletely elucidated. For some bacteria such as *Listeria*, it was believed that plasmids were liberated from the bacteria following bacterial lysis in the cytosol (Weiss, 2003). The bacterial lysis was believed to be due to metabolic auxotrophy, a suicide system or compromised cell wall integrity due to antibiotic treatment (Dietrich *et al.*, 1998; Hense *et al.*, 2001; Sizemore *et al.*, 1995; Weiss, 2003). However, this explanation does not suffice to describe how vacuole-residing species such as *Salmonella* were capable of bactofection (Darji *et al.*, 1997). Furthermore, intracellular invasion is not strictly a pre-requisite for mediating inter-kingdom DNA transfer, as the soil pathogen *Agrobacterium tumefaciens* was reported to transfer DNA to HeLa cells *in vitro* (Kunik *et al.*, 2001). Interestingly, the *Agrobacterium* attached to the HeLa cells, but did not invade them.

There have been multiple strategies employed to increase the degree of bactofection in bacterial DNA delivery vectors. One such strategy was the use of antibiotics to compromise the integrity of the bacterial cell wall, such as ampicillin or polymyxin B (Jones *et al.*, 2013; Pijkeren *et al.*, 2010). An alternative approach has been to induce the expression of a lysis phage or lysis gene upon cellular entry to facilitate plasmid expulsion into the cytosol (Chung *et al.*, 2015). This was achieved through the employment of a heterologous protein expression of listeriolysin and LyE to weaken the bacterial membrane (Chung *et al.*, 2015). These strategies are presumed to involve the liberation of

the plasmid from the bacterium, providing circumstantial evidence that plasmid cytosolic-residency is required for nuclear uptake and transgene expression.

Although the mechanisms resulting in exogenous DNA reaching the cytosol are incompletely understood, once the DNA is in the cytosol, the mechanisms underpinning DNA uptake to the nucleus have been heavily studied. It has been demonstrated that certain DNA sequences are required for cytosolic DNA entry into the nucleus (Dean, 1997). The most important of these was shown to be the Simian Virus 40 (SV40) sequence. The absence of the SV40 sequence was shown to arrest microinjected DNA in the cytosol, even 12 hours after injection, whereas all SV40 sequence-containing DNA localised to the nucleus within eight hours. Further inspection into the SV40 sequence demonstrated that the 72-base pair repeat promoter/enhancer region provided the majority of the nuclear import function (Dean *et al.*, 1999). Another study reported that a repetitive NF- $\kappa$ B binding sites cloned into a reporter plasmid enhanced transfection up to 12-fold in multiple cell types *in vitro* (Mesika *et al.*, 2001). To get to the nucleus, the plasmid DNA migrates to the nucleus along microtubules, most likely dynein, through adaptor molecules which recognise specific sequences on the plasmid (Vaughan & Dean, 2006). In particular, cytoplasmic transcription factors which recognise the consensus sequence on the plasmid DNA can bind and facilitate nuclear import through the nuclear pore in concert with importins such as Importin  $\beta$ 1 and Importin 7, as well as histone H2B and NM23-H2 supported plasmid nuclear entry (Miller *et al.*, 2009; Munkonge *et al.*, 2009). Interestingly, it is possible to restrict plasmid transfer to specific cell types (Miller & Dean, 2009; Vacik *et al.*, 1999). This strategy would be particularly beneficial to employ in the context of cancer therapy to limit the efficacy of a given gene therapy to cancer cells alone, whilst leaving other non-cancerous cells unaffected by the treatment. There are reports which claim to have identified tumour-specific promoters (Kim *et al.*, 1994; Lu *et al.*, 2005), opening the possibility to exploit this system to limit the effects of gene therapy to cancer cells alone.

#### **1.4.3.2 Applications, efficiency and efficacy**

Bactofection can be employed in multiple tissues to replace silenced or mutated genes. A preliminary *in vitro* study demonstrated that *Listeria monocytogenes*

can mediate the bactofection of the cystic fibrosis transmembrane conductance regulator (CFTR) gene in eukaryotic cells (Krusch *et al.*, 2002). An *in vivo* model looked specifically at bactofection of lung epithelial cells, and found that *E. coli* transformed with a eukaryotic expression plasmid could mediate transgene expression in murine lung tissue (Larsen *et al.*, 2013).

Bactofection is increasingly becoming an attractive therapeutic option for cancer treatment. Bactofection studies for the purposes of enhancing bacterial mediated cancer therapy has been investigated using multiple bacterial species including *S. enterica*, *E. coli*, and *L. monocytogenes* (Byrne *et al.*, 2014; Guan *et al.*, 2013; Pijkeren *et al.*, 2010; Pilgrim *et al.*, 2003; Yuhua *et al.*, 2001). It was demonstrated that the *S. Typhimurium* strain, SL7207, was most proficient at DNA vaccine delivery in a mouse model for neuroblastoma, when compared to gene gun application and viral-mediated delivery (Berger *et al.*, 2013).

There have been variable frequencies of bactofection reported. In one study, intratumoural injection of *E. coli* strain K12, transformed with a eukaryotic FLAG reporter plasmid, resulted in 17.2% of total live tumour cells being FLAG<sup>+</sup> 48 hours post infection (hpi) (Byrne *et al.*, 2014). Another study found that *in vitro*, infection with *L. monocytogenes* at a multiplicity of infection (MOI) of 50:1 yielded a proportion of macrophages expressing the fluorescent reporter plasmid gene was in the region of 10<sup>-2</sup>, which is much less than that observed by Byrne and colleagues (Dietrich *et al.*, 1998). Even with this low efficiency, the macrophages which delivered the antigen protein-encoded plasmid had detectable levels of T cell activation, *in vitro*. In contrast to Dietrich and colleagues, up to 30% of primary peritoneal macrophages infected with *S. Typhimurium* were successfully transfected with a eukaryotic expression plasmid (Darji *et al.*, 1997). The employment of bactofection to transfer GM-CSF on a eukaryotic expression plasmid from *Salmonella* to cancer cells enhanced the anti-tumour effects of the bacteria as more than 70% of tumour-bearing mice to 60 days post tumour cell inoculation (Yuhua *et al.*, 2001). The control group with a GFP-encoding plasmid did not survive past day 35. Taken together, these studies and others have provided evidence that bactofection is an effective strategy in transferring eukaryotic genes to eukaryotic cells and can also enhance the native anti-tumour effects of bacteria.

#### 1.4.4 *Salmonella* strains for bacterial mediated cancer treatment

There are many bacterial genera and strains which have been investigated for bacterial-mediated cancer therapy. The most commonly employed genus is *Salmonella*, with many attributes lending to its suitability as a bacterial cancer therapy (Forbes, 2010) (Figure 1.6).

*Salmonella* has been demonstrated to exhibit tumour specific colonisation and growth (Crull *et al.*, 2011a; Zhao *et al.*, 2005). Although multiple strains of *Salmonella* have been demonstrated to induce tumour growth arrest when administered alone, *Salmonella* is also capable of delivering therapeutic molecules, such as chemotherapeutics, DNA and RNA to tumours. Furthermore, *Salmonella* has been shown to be able to express anti-cancer agents such as immunostimulatory cytokines (Loeffler *et al.*, 2007, 2009) or non-native tumouricidal bacterial products (Zheng *et al.*, 2017b). Although this enhanced tumouricidal bacteria could potentially lead to greater systemic toxicity, this eventuality has been circumvented in multiple studies by the employment of tumour-specific promoter systems (Leschner *et al.*, 2012; Yu *et al.*, 2012). *S. Typhimurium* has also been demonstrated to increase the efficacy of some chemotherapeutics when co-administered (Lehouritis *et al.*, 2015). This effect might be due in part to the fact that *S. Typhimurium* functionally down-regulates P-glycoprotein, a multidrug resistance protein responsible for the efflux of many cancer drugs, in intestinal cancer epithelial cells (Siccardi *et al.*, 2008).

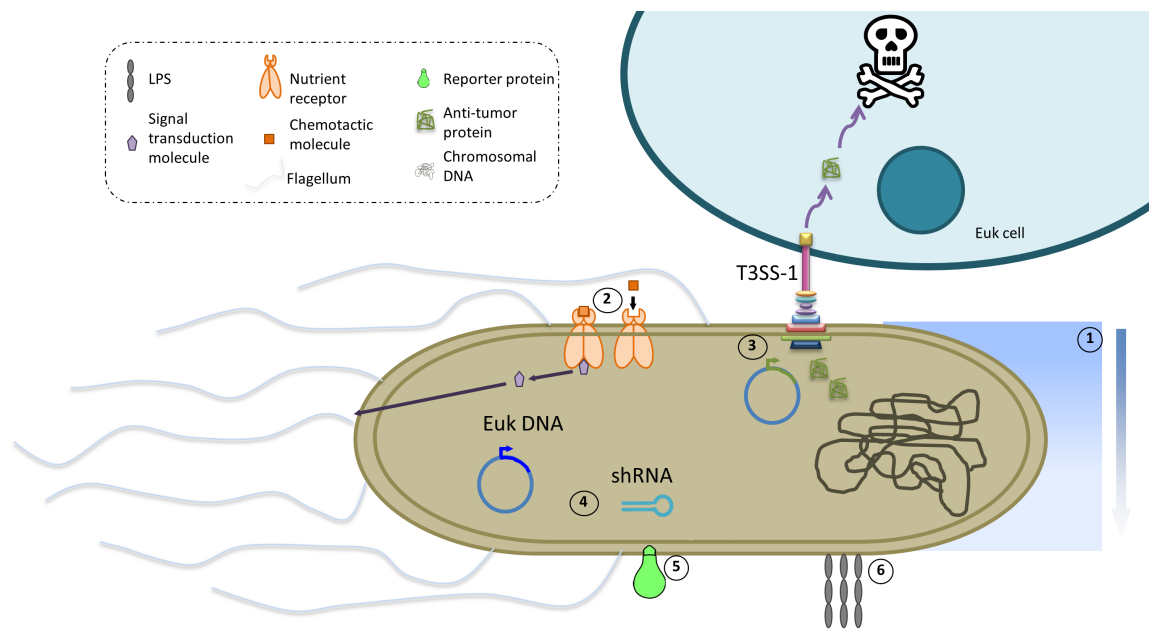


**Figure 1.6 *S. Typhimurium* have multiple features which make them amenable for bacterial-mediated cancer therapy**

*S. Typhimurium* is an attractive strain for bacterial mediated cancer therapy. 1. *S. Typhimurium* is a facultative anaerobe so can survive in multiple states of oxygenation. 2. *S. Typhimurium* is motile, and can receive signals from the environment to chemotax towards defined areas of the tumour. 3. *S. Typhimurium* can carry plasmids encoding cytotoxic or immunostimulatory molecules which it can deliver to the eukaryotic cell via the Type 3 Secretion System-1 (T3SS-1). 4. *S. Typhimurium* can carry eukaryotic DNA and shRNA encoding anti-tumour genes which can be delivered to the eukaryotic cell, most likely upon spontaneous lysis. 5. *S. Typhimurium* can be engineered to be visualised to enable *in vivo* tracking. 6. *S. Typhimurium* is highly immunostimulatory so can elicit an immune response which is not conducive to tumour growth.

There are multiple cancer therapy strains of *S. Typhimurium*, most notably VNP20009 ( $\Delta msbB$ ,  $\Delta purI$ ), SL7207 ( $\Delta aroA$ ) and A1-R (Leucine-arginine auxotroph) (Hoiseth & Stocker, 1981; Low *et al.*, 1999; Zhao *et al.*, 2006). Each of these strains is attenuated in some way which reduces their systemic toxicity in the host. In employing a strain for bacterial cancer therapy, it is pivotal to balance between an attenuated strain which is not toxic to the host with maintaining sufficient virulence to infect and antagonise the tumour. VNP20009 was highly successful in mediating anti-tumour effects in mouse models of cancer, but when it was taken to Phase I clinical trials, there was tumour colonisation but no effect on tumour growth (Low *et al.*, 1999; Toso *et al.*, 2002). It was concluded that the strain, which is auxotrophic for purines and has an attenuated LPS component, was overly attenuated and thus ineffective. Another report compared the tumour specific colonisation, anti-tumour effects and survival of tumour-bearing mice following infection with VNP20009 or A1-R, and found the latter to be more beneficial in every parameter investigated (Zhang *et al.*, 2015). However, the A1-R strain is not widely available.

SL7207 is a highly effective anti-cancer agent. It has a full LPS (in comparison to VNP20009) so is suitably virulent but has a 1,194-bp deletion in the *aroA* gene rendering the strain auxotrophic for  $p$ -aminobenzoic acid and 2,3-dihydroxybenzoate (Hoiseh & Stocker, 1981; Johnson *et al.*, 2017). Neither of these molecules is available in mammalian tissue, which means that in theory, the bacteria can only survive a finite number of replications, *in vivo* (Hoiseh & Stocker, 1981). *AroA* mutants have been demonstrated to be more immunostimulatory, susceptible to penicillin and sensitive to phagocytosis compared to *aroA*-competent controls, *in vivo* (Felgner *et al.*, 2016). All of these attributes are beneficial for bacterial mediated cancer therapy.

#### **1.4.5 Bacterial-mediated cancer therapy: immune cell activation**

As is evident from Sections 1.1.4 and 1.1.5, *S. Typhimurium* is highly immunostimulatory. Therefore, there has been intense investigation into the immune activation status of models subjected to bacterial mediated cancer therapy. However, it is pertinent to note that not all bacterial agents might act as immunotherapy agents. For example, some strains are highly effective in inhibiting tumour growth in immunocompromised mice (Zhao *et al.*, 2005; Zhao *et al.*, 2006). Furthermore, some strains might only be effective anti-cancer agents when carrying appropriate cargo to be delivered to the tumour (Forbes, 2010)

Direct evidence for immune involvement in bacterial mediated cancer therapy comes from the studies which have demonstrated the failure of tumours to establish upon secondary challenge following bacterial-mediated clearance of a primary tumour (Agrawal *et al.*, 2004; Stern *et al.*, 2015). These studies suggest a role for immune memory in blocking the establishment of the secondary tumour.

For the first well studied bacterial immunotherapy, BCG, a number of reports have evidenced an increase in immune cells following therapy (Bisiaux *et al.*, 2009; De Boer *et al.*, 1991; Suttman *et al.*, 2006b). Many studies have pointed towards a  $T_H1$ -biased immune response following BCG therapy in bladder cancer patients and mouse models. Urine analyte analysis of superficial bladder cancer patients found that following BCG treatment, there was a significant increase in

the production of pro-inflammatory cytokines such as TNF- $\alpha$ , IL-8, IL-6, IL-1 $\beta$  (Bisiaux *et al.*, 2009). Another study found similar results where there was increased secretion of IL-1 $\beta$ , IL-6, IL-8, TNF- $\alpha$  and IFN- $\gamma$  into the urine of carcinoma *in situ* bladder cancer patients following repeated BCG treatments (Jackson *et al.*, 1999). In fact, IL-12 and IFN- $\gamma$  are essential for BCG anti-tumour efficacy in an orthotopic murine bladder cancer model (Riemensberger *et al.*, 2002). The BCG cell wall skeleton (BCG-CWS), a non-infectious material consisting of peptidoglycan, arabinogalactan and mycolic acids, has been investigated in other cancer types such as lung and ovarian cancers (Hayashi, 1998; Yamamura *et al.*, 1979). It was reported that BCG-CWS treatment might stimulate DCs to mature and promote the secretion of TNF- $\alpha$  and IL-1 $\beta$  in a manner dependent on TLR2 and TLR4 (Tsuji *et al.*, 2000).

Looking at the immune infiltrates into the tumour following BCG treatment, there was found to be an increased number of granulocytes, monocytes, macrophages and lymphocytes in the urine of patients 24 hours after BCG instillation (De Boer *et al.*, 1991). Another study of 17 patients of superficial bladder cancer found that there was an increase in granulocytes, monocytes and lymphocytes four hours following a patient's first BCG instillation, and this increase was further enhanced following the third treatment (Bisiaux *et al.*, 2009). In these studies granulocytes were found to heavily infiltrate following treatment, and in fact, this was required for the mediation of BCG anti-tumour effects (Suttman *et al.*, 2006a).

Interestingly, the blockade of neutrophils in a *S. Typhimurium*-treated cancer model enhanced the therapeutic effect of the bacteria by propagating the spread of the bacteria within the tumour (Westphal *et al.*, 2008). Neutrophils have been reported to accumulate in tumours following bacterial mediated tumour therapy in a number of transplantable tumour models (Lee *et al.*, 2008; Lizotte *et al.*, 2014). Neutrophils were also found to be essential for *S. Typhimurium* biofilm formation on tumours, *in vivo* (Crull *et al.*, 2011b).

DCs are arguably the most well characterised myeloid derived immune cell in the context of bacterial mediated immunity. DCs are recruited to the tumour as soon as two days post *S. Typhimurium* infection *in vivo* (Avogadri *et al.*, 2005).

DCs from infected tumours had enhanced cross presentation of tumour antigen to CD8<sup>+</sup> T cells *ex vivo* compared to uninfected. In a follow up study, it was demonstrated that DCs from the tumour-draining lymph node of intratumourally *S. Typhimurium* injected mice could produce more IL-6, IL-1 $\beta$  and TNF- $\alpha$  than DCs harvested from control mice (Avogadri *et al.*, 2008). These DCs also expressed a more activated phenotype evidenced by increased MHCI, Fas and CD86 expression compared to control DCs. Another study demonstrated that *S. Typhimurium* treatment of tumour-bearing mice resulted in the increased expression of connexin 43 (Cx43), a gap junction pore-forming protein which facilitated the movement of tumour associated antigen from tumour cells to DCs (Saccheri *et al.*, 2010). In fact, the silencing of Cx43 resulted in severely attenuated anti-tumour efficacy of *S. Typhimurium*, demonstrating the importance of DC-mediated antigen loading for the anti-tumour effects.

Many studies which have examined the cytokine profiles of *Salmonella*- and *E. coli*-infected tumour-bearing mice, either in the blood or the tumour itself, have evidence for the increase in the production of T<sub>H</sub>1-associated cytokines or factors such as TNF- $\alpha$ , IFN- $\gamma$ , inducible nitric oxide synthase (iNOS), IL-6, (Lee *et al.*, 2008; Leschner *et al.*, 2009; Lizotte *et al.*, 2014; Stern *et al.*, 2015). This has also been seen following treatment with *C. novyi* NT spores (Agrawal *et al.*, 2004). Interestingly, there has been little or no evidence to suggest the involvement of the T<sub>H</sub>17 response in bacterial mediated tumour therapy.

Looking at lymphocyte involvement, many studies have also demonstrated the tumour infiltration of CD4<sup>+</sup> and CD8<sup>+</sup> T cells following bacterial infection of tumour-bearing mice (Cronin *et al.*, 2010; Kuan & Lee, 2016; Lee *et al.*, 2011, 2008), but the reports have provided somewhat contradictory evidence for the roles of these cells. In one study, the blockade of CD4 with an anti-CD4 antibody did not significantly affect the tumour growth inhibitory effects of *E. coli*, whilst the blockade of CD8 completely abolished the anti-tumour efficacy (Stern *et al.*, 2015). Furthermore, the adoptive transfer of tumour-educated CD8<sup>+</sup> T cells resulted in tumour rescue in uninfected, tumour-bearing mice. In another study, either CD4 or CD8 blockade only mildly abrogated the anti-tumour effects of *S. choleraesuis* (Lee *et al.*, 2011). Furthermore, CD4, as opposed to CD8, was credited with being the major producer of IFN- $\gamma$  in this study. Given the number

of reports which support a role for T cells in mediating the anti-tumour effects of *Salmonella*, it was therefore surprising that there are also reports in which *S. Typhimurium* has been effective in treatment of athymic nude mice (Zhang *et al.*, 2015; Zhao *et al.*, 2005; Zhao *et al.*, 2006). Therefore, other immune cells may be the effectors of bacterial-mediated tumour growth inhibition. Furthermore, tumour-specific bacterial colonisation was demonstrated to be greater in athymic mice than immunocompetent mice in a *Bifidobacterium breve* infected transplantable tumour model (Cronin *et al.*, 2010).

It is apparent that TLRs play an important role in bacterial mediated cancer treatment. *Tlr4*<sup>-/-</sup> resulted in decreased anti-tumour efficacy of *S. choleraesuis* in a transplantable tumour model (Lee *et al.*, 2008). *Tlr4* depletion also decreased the recruitment of immune cell types including neutrophils, macrophages, CD4 and CD8 T cells, as well as decreasing the production of intratumoural IFN- $\gamma$ . Some of these results were also seen in *S. Typhimurium*-treated tumour models (Zheng *et al.*, 2017b). In addition, the loss of the adaptor molecule MyD88 had detrimental effects to anti-tumour efficacy of *S. Typhimurium*, supporting a critical role for these pathways in *S. Typhimurium*-mediated tumour immunity (Kaimala *et al.*, 2014; Zheng *et al.*, 2017b).

Macrophages have not been significantly considered in the bacterial mediated cancer therapy literature. This is surprising given the central role these cells play in mediating the innate immune response to oral *S. Typhimurium* infection (Rydstrom & Wick, 2007; Rydström & Wick, 2009; Yrlid *et al.*, 2000). A number of studies have reported an increase in the number or proportion of macrophages in the tumour following systemic bacterial infection (Lee *et al.*, 2008; Lizotte *et al.*, 2014). One report suggested a macrophage expansion within the tumour following systemic *L. monocytogenes* infection, but given that the only obvious marker for these ‘macrophages’ was CD11b, it is difficult to conclude with confidence that these were indeed macrophages alone (Lizotte *et al.*, 2014). The activation of TAMs following systemic *S. Typhimurium* infection was evidenced by the up-regulation of the co-activation marker CD86 following infection (Zheng *et al.*, 2017b). There was also the suggestion that the TAMs were moving away from the ‘M2’ phenotype due to the decreased expression of the scavenger receptor CD206. These data suggest a transformation in the

immune signature of the tumour microenvironment following bacterial administration to a phenotype not compatible with tumour progression.

#### **1.4.6 The contributions of local versus systemic tumour-inflammation in anti-tumour effects of bacteria**

It is apparent that there are many immune cells which may play a role in bacterial-mediated anti-tumour effects. However, it is unclear if this immune response is driven by tumour-local or systemic inflammation.

Many studies have attributed the anti-tumour effects of intravenously injected bacteria to the tumour-specific localisation and proliferation of the bacteria (Low *et al.*, 1999; Zhao *et al.*, 2005). Another study has demonstrated that increased tumour-specific *S. Typhimurium* localisation was associated with greater anti-tumour effects (Zhao *et al.*, 2006). Multiple studies which have attested to the fact that bacteria can kill tumour cells directly *in vitro* and *in vivo*, further provide evidence that the bacteria have a local anti-tumour effect (Fu *et al.*, 2008; Kuan & Lee, 2016; Lee *et al.*, 2008). Furthermore, direct intratumoural injection of *S. Typhimurium* leads to tumour growth inhibition and regression (Avogadri *et al.*, 2008; Din *et al.*, 2016; Roberts *et al.*, 2014). However, it was found that in some cases, direct intratumoural injection can result in systemic inflammation (Avogadri *et al.*, 2008), but whether this was due to bacterial dissemination of tumour-propagated immune mediators was not reported.

It is likely that both systemic and local responses play a role in mediating bacterial tumour-growth inhibition. It was demonstrated that systemic infection with pro-inflammatory mediators LPS and TNF- $\alpha$ , was sufficient to inhibit the tumour growth of certain cancer types, but not all (Kocijancic *et al.*, 2017). This evidence suggests that the contribution of tumour localisation of the bacteria versus the systemic inflammatory effects might be cancer type dependent.

#### **1.4.7 Limitations of bacteria for the purposes of cancer therapy**

Although multiple bacteria have been promising in various *in vivo* settings, several considerations must be addressed prior to further human clinical trials.

The most implicit limitations of bacteria as a cancer therapy are treatment related adverse effects and antibiotic resistance.

In Phase I clinical trials with systemically administered VNP20009 on patients with metastatic melanoma, tumour localisation was reported, however there were no anti-tumour effects (Heimann & Rosenberg, 2003; Toso *et al.*, 2002). In another study, VNP20009 capable of expressing the *E. coli* cytosine deaminase gene was administered intratumourally in combination with the cytosine deaminase substrate, 5-fluorocytosine (Cunningham & Nemunaitis, 2001). In two out of the three patients, there was an objective response at the tumour site. In all of these studies, adverse effects were reported. According to the National Cancer Institute's Cancer Therapy Evaluation Programme, Grade 3 adverse effects are 'severe and undesirable adverse events; and Grade 4 are 'life-threatening or disabling adverse events' ([www.fda.gov](http://www.fda.gov)). The most consistent symptoms reported following bacterial administration included fever, nausea and vomiting (Cunningham & Nemunaitis, 2001; Heimann & Rosenberg, 2003; Toso *et al.*, 2002). In the initial study, 8% of the 25 patients exhibited Grade 3 toxicity which included fever and anaemia (Toso *et al.*, 2002). There were no Grade 4 toxicities observed. It could be speculated that the adverse effects reported following bacterial-treatment in cancer patients is less severe than those following chemotherapy regimens. In a study of patients receiving the chemotherapeutic 5-hydroxytryptamine 3 and corticosteroid, severe nausea occurred in 23.8% of patients and vomiting occurred in 20.8% of the 240 patients (Escobar *et al.*, 2015). Another study of 1,008 patients with various carcinomas found that 25.5% of patients experienced both nausea and vomiting following treatment with various chemotherapeutics (Chopra *et al.*, 2016). In 12.9% of cases, the adverse effects required patient hospitalisation. However, the studies regarding bacterial-mediated cancer therapy have employed small sample sizes and relatively short-term treatment regimens so further studies are warranted to provide convincing data pertaining to the long-term effects following this treatment modality.

As these studies have touched on, but what is also evident in many pre-clinical trials is the immune-stimulatory potential of multiple bacterial strains, particularly when administered systemically (Lizotte *et al* 2014; Stern *et al.*,

2015; Zheng *et al.*, 2017b). This is a great cause for concern going forward, as cytokine storm and the related sepsis might not be well tolerated by the host, removing the therapeutic potential of the treatment modality.

A more general concern associated with bacterial-mediated cancer therapy is antibiotic resistance. Although the bacteria may be beneficial for tumour growth inhibition, antibiotic-resistant bacteria are a major safety concern, particularly when cancer patients are often immune-compromised (Hübel *et al.*, 1999; Klastersky & Aoun, 2004; Viscoli *et al.*, 2005). Evidence in favour of the safety profile of bacteria comes from multiple studies. In a Phase I clinical trial, systemically administered VNP20009 was completely cleared from the bloodstream within six hours of treatment (Cunningham & Nemunaitis, 2001). It was also demonstrated that SL7207 could be almost completely cleared from tumour-bearing mice with administration of ciprofloxacin immediately following infection (Crull & Weiss, 2011). Furthermore,  $\Delta$ *aroA* mutants are more sensitive to penicillin and phagocytosis (Felgner *et al.*, 2016). However, there is currently no data to predict the emergence of resistant strains in these models. This is potentially the greatest hurdle bacteria have to overcome to be taken further into human clinical trials.

However, there are strategies that can remove these limitations whilst maintaining the anti-tumour effects of the bacteria, or bacterial products. It has been demonstrated that in some cases, heat-killed bacteria are equally capable of mediating tumour growth inhibition as viable bacteria (Kocijancic *et al.*, 2017; Mathé *et al.*, 1977). Binder *et al.* (2013) demonstrated that administration of heat killed bacteria in conjunction with adoptive T cell therapy mediated sustained tumour cell rejection. These findings provide an incentive to isolate the anti-tumour effectors of the bacteria to examine if they can be used in isolation to mediate tumour growth inhibition. One study employed the use of the effector protein SipA, which has been demonstrated to activate the apoptosis-inducing enzyme caspase-3 and down-regulate the multidrug resistance protein, P-glycoprotein (Siccardi *et al.*, 2008; Srikanth *et al.*, 2010; Wall *et al.*, 2007). This effector protein was isolated and used for cancer therapy in the absence of its bacterial shell (Mercado-Lubo *et al.*, 2016). Another study has compared the efficacy of the pro-inflammatory mediators

(responsible for many of the immunogenic features of *S. Typhimurium* infection) LPS and TNF- $\alpha$  to SL7207 in a similar quest to remove the toxicity of the bacteria *in vivo* (Kocijancic *et al.*, 2017). The inflammatory mediators alone were comparably as efficacious as the bacteria in some tumour models. They were, however, ineffective for certain tumour types, suggesting alternative mechanisms of bacterial-mediated tumour growth inhibition other than those induced by LPS and TNF- $\alpha$ . These studies support the possibility for other bacterial cell products to have anti-cancer effects without the detrimental systemic effects such as weight loss and the risk of antibiotic resistance.

## **1.5 *In vitro* and *in vivo* models to study bacterial mediated cancer therapy**

Studies employing bacterial mediated cancer therapies often use a combination of both *in vitro* cell culture and *in vivo* tumour models.

### **1.5.1 *In vitro* tumour spheroid models**

The mainstay of *in vitro* studies for cancer therapy and bacterial infection is to employ two dimensional (2D) monolayer culture. However, these cultures do not exhibit many features of tumours *in vivo*, such as region-specific molecular gradients and differential oxygen tension (Sutherland *et al.*, 1996). This limitation can be addressed by the employment of *in vitro* tumour spheroid cultures. Tumour spheroids exhibit multiple features of *in vivo* tumours, and the *in vivo* tumour microenvironment. Tumour spheroids exhibit regions of hypoxia, which plays an important role in promoting angiogenesis and tumour-permissive macrophages (Movahedi & Van Ginderachter, 2016; Sutherland *et al.*, 1986). Tumour spheroids exhibit pseudo-glandular structures reminiscent of *in vivo* carcinoma tissue (Sutherland *et al.*, 1986). In tumour spheroids greater than 500-600  $\mu\text{m}$  in diameter, central necrosis can develop surrounded by a viable rim of actively proliferating cells. Necrosis is believed to be induced by metabolic cell death due to the attenuated transport of oxygen, nutrients and waste (Carlsson & Acker, 1998). Necrosis is a feature of tumours *in vivo* which correlates with poor prognosis and plays a role in propagating chronic inflammation that drives tumourigenesis (Edwards *et al.*, 2003; Freyer, 1988).

Tumour spheroids also demonstrate atypical mitochondrial function compared to 2D monolayers (Bredel-Geissler *et al.*, 1992).

### **1.5.2 *In vivo* cancer models**

There are many different cancer mouse models available, which would be suitable to investigate the effects of bacteria on the tumour immune response. Mouse models can be characterised into at least three groups: transplantable, genetically engineered and carcinogen-induced (Zitvogel *et al.*, 2016).

Arguably, the most commonly employed model in cancer immunology is the inoculation of histocompatible tumour cell lines into mice; the transplantable tumour model (Suggit & Bibby, 2005). Most often, this technique consists of subcutaneous injection of a defined number of syngeneic tumour cells into the back flank of the mouse. Orthotopic and intravenous application are also routinely carried out. These models are highly attractive as tumour development is easily monitored, either by palpation or using *in vivo* imaging technologies. This approach yields highly reproducible tumour growth dynamics. However, utilisation of clonal tumour cells grown *in vitro* is not reflective of the diversity of tumour cells found in human cancer (Ngiow *et al.*, 2016). Furthermore, these tumour cells, and the associated leukocytes, have not experienced the chronic inflammatory processes, which select tumour and stromal cells during tumour development in humans (Mantovani *et al.*, 2008). However, these tumours have played an important role in multiple discoveries in cancer research such as the identification of immune checkpoint inhibitors to inhibit tumour development and metastasis, which have been hailed as a major breakthrough in cancer treatment (Iwai *et al.*, 2002).

An alternative strategy to transplantable tumours is the use of genetically engineered mouse models (Zitvogel *et al.*, 2015). These most often utilise the transgenic overexpression of oncogenes or the inactivation of tumour suppressor genes to drive spontaneous oncogenesis. This model overcomes many of the limitations of the transplantable model, as the tumour cells are highly heterogeneous with respect to their development, progression and antigenic makeup. However, these models often take months for the mice to develop tumours, which may not be possible to monitor by eye. Furthermore, germ-line

mutations of certain potent oncogenes can result in widespread transformations occurring at multiple sites, thus overwhelming the immune system, a phenomenon which may or may not be occurring in humans. This limitation can be overcome by designing the genetic alteration to be tissue specific, such as Polyoma-middle T antigen oncoprotein (PyMT) under the control of mouse mammary tumour virus long terminal repeat (MMTV-LTR) which is restricted to expression in mammary epithelial cells (Guy *et al.*, 1992; Muller *et al.*, 1988). Genetically engineered mouse models have contributed substantially to our understanding of tumour development, as well as the role certain immune effectors have in this process. For example, the *PPF*<sup>-/-</sup> mouse strain, which lacks perforin, has been shown to experience accelerated progression of multiple cancers demonstrating an important role for perforin-producing immune cells in anti-tumour immunity (Smyth *et al.*, 2000).

Carcinogen-induced mouse models involve the use of a carcinogen, such as ultraviolet light or methylcholanthrene (MCA), to induce transformation of healthy cells (Abel *et al.*, 2009). These neoplasias often offer genetically diverse tumours, which is reflective of the human cancer environment. However, a limitation of these models is the absence of defined genetic transformations as well as long treatment protocols in some cases (Zitvogel *et al.*, 2016).

### **1.5.3 *In vivo* cancer models employed for bacterial mediated cancer therapy studies**

Most studies that have investigated the effects of bacteria on tumours have employed the use of transplantable tumour models in either the C57BL/6 or BALB/c backgrounds (Suggit & Bibby, 2005) (Table 1.2).

C57BL/6 and BALB/c strains differ greatly in their immune responses to different stimuli. These strains have been reported to be prototypical T<sub>H</sub>1- and T<sub>H</sub>2-type mouse strains, respectively (Mills *et al.*, 2000; Santos *et al.*, 2006). When macrophages from each mouse strain were challenged with bacterial products, macrophages from C57BL/6 were more potent producers of TNF- $\alpha$  and IL-12, both pro-inflammatory T<sub>H</sub>1 cytokines, than the cells from BALB/c mice. BALB/c mice also failed to facilitate bacterial clearance *in vivo* (Watanabe *et al.*, 2004). In one study, systemic infections of tumour-bearing mice in both C57BL/6 and

BALB/c strains were carried out with *S. choleraesuis*. The bacteria significantly inhibited tumour growth compared to the uninfected controls in both models, but the therapeutic effects of the bacteria were more apparent in the BALB/c model (Kuan & Lee, 2016). Given that there are such robust differences in the ability of these mice to respond to bacterial infection, it is tempting to speculate that the differential responsiveness observed in bacterial-mediated tumour inhibition is due to immune mediators. Therefore, in choosing just one of the strains for a study, it is possible to bias the results in favour of the strain's phenotype, possibly masking other phenotypic responses explaining a given outcome. This was seen in a model of chemical induced asthma, where the mouse strain had considerable and variable impacts on a wide range of parameters pertaining to the asthma phenotype under evaluation (de Vooght *et al.*, 2010).

For experiments involving genetically manipulated mice, there are few available on the BALB/c background, whereas there is an abundance of genetically modified C57BL/6 mice. Therefore, the selection of the BALB/c strain would require the use of blocking antibodies alone to ablate specific cell types or functions, whereas the employment of the C57BL/6 mice allows for both this approach as well as genetic ablation. Furthermore, Kaede mice, whose green fluorescent cells can be photoconverted to Kaede red using UV light to enable tracking of cellular movement *in vivo*, are only available on the C57BL/6 background (Ando *et al.*, 2002; Torcellan *et al.*, 2017).

The most commonly employed cell line in the transplantable tumour model in C57BL/6 mice is the B16 cell line. This is a murine melanoma line which was created following the chemical induction of cancer in C57BL/6 mice (Fidler, 1973). The most popular clones from this line are B16F1 and B16F10 (Fidler & Nicolson, 1976). The latter is characterised by high metastatic potential and aggressive growth. However, given the speed of cell growth *in vivo* with mice surviving only 2-4 weeks following tumour cell induction, there is limited scope for long-term analysis following therapeutic intervention (Sharma *et al.*, 2015). B16F10 cells are highly immunogenic, with high levels of targetable epitopes associated with melanoma such as tyrosinase related protein 2 (TRP2) and gp100 (Bloom *et al.*, 1997).

**Table 1.2 *In vivo* models employed in published bacterial-mediated cancer therapy studies**

Mouse strain	Tumour cell type	Bacterial species	Bacterial strain	Reference	
BALB/c	CT26	<i>S. Typhimurium</i>	SL7207	(Stern <i>et al.</i> , 2015; Crull <i>et al.</i> , 2010; Crull <i>et al.</i> , 2011a; Crull <i>et al.</i> , 2011b; Leschner <i>et al.</i> , 2009; Leschner <i>et al.</i> , 2012;	
			ATCC 14028	Jeong <i>et al.</i> , 2014)	
			SF200	(Kocijancic <i>et al.</i> , 2017)	
			SL3261 LB500	(Yuhua <i>et al.</i> , 2001)	
			<i>E. coli</i>	Nissle 1917	(Lehouertis <i>et al.</i> , 2015)
				TOP10	(Stern <i>et al.</i> , 2015)
	D2F2	<i>S. Typhimurium</i>	VNP20009	(Loeffler <i>et al.</i> , 2007; Loeffler <i>et al.</i> , 2009)	
	4T1	<i>S. Choleraesuis</i>	ATCC 15480	(Kuan & Lee 2015)	
	RenCA	<i>S. Typhimurium</i>	SF200 UK-1	(Kocijancic <i>et al.</i> , 2017)	
	F1A11	<i>S. Typhimurium</i>	SF200 UK-1	Kocijancic <i>et al.</i> , 2017	
	HepG2	<i>S. Typhimurium</i>	SL7207	(Li <i>et al.</i> , 2012)	
	MC38	<i>S. Typhimurium</i>	SHJ2037	(Zheng <i>et al.</i> , 2017)	
	4T1	<i>S. Typhimurium</i>	VNP20009	Ganai <i>et al.</i> , 2009)	
C57BL6	B16F1	<i>S. Typhimurium</i>	BRD509E	(Kaimala <i>et al.</i> , 2014)	
	B16F10	<i>S. Typhimurium</i>	VNP20009	(Loeffler <i>et al.</i> , 2009; Chen <i>et al.</i> , 2012)	
			SL3261AT	(Avogadri <i>et al.</i> , 2005, 2008; Saccheri <i>et al.</i> , 2010)	
			BRD509E	(Yoon <i>et al.</i> , 2011)	
			SHJ2037	(Zheng <i>et al.</i> , 2017b)	
		<i>Clostridium novyi</i>	<i>C. novyi</i> NT	(Dang <i>et al.</i> , 2001)	

		<i>Bifidobacterium breve</i>	UCC2003	(Cronin <i>et al.</i> , 2010)
		<i>S. Choleraesuis</i>	Not specified	(Lee <i>et al.</i> , 2011)
	LLC	<i>S. Typhimurium</i>	SL1344 $\Delta invA$ SL3261AT SL3261AT $\Delta invA$	(Avogadri <i>et al.</i> , 2005)
	EG7	<i>L. monocytogenes</i>	10403S	(Lizotte <i>et al.</i> , 2014)
	ID8- <i>Defb29/Vegf-A</i>	<i>S. Typhimurium</i>	A1	(Zhao <i>et al.</i> , 2005)
Nude	PC3	<i>S. Typhimurium</i>	A1 A1-R	(Zhao <i>et al.</i> , 2006)
	MARY-X	<i>S. Typhimurium</i>	SL7207 VNP20009 YB1	(Yu <i>et al.</i> , 2012)
	MDA-MB-231	<i>S. Typhimurium</i>	A1-R VNP20009	(Zhang <i>et al.</i> , 2015)
	LLC	<i>Clostridia novyi</i>	<i>C. novyi</i> NT	(Dang <i>et al.</i> , 2001)
	HCT116	<i>S. Choleraesuis</i>	Not declared	(Lee <i>et al.</i> , 2008)
C3H/HeN	K175	<i>S. Typhimurium</i>	SL1344 $\Delta phoPQ$ SL1344 $\Delta phoPQ \Delta aroA$	(Danino <i>et al.</i> , 2012)
A/J	NXS2	<i>S. Typhimurium</i>	SL7207	(Berger <i>et al.</i> , 2013)

## 1.6 Hypotheses and aims

The intention of this thesis was to provide a more comprehensive overview of the changes in the tumour immune environment and cellular composition following systemic *S. Typhimurium* infection, with a specific focus on the monocyte/macrophage compartment. Furthermore, it was intended to enhance the anti-tumour effects of *S. Typhimurium* through transformation of the bacteria with a eukaryotic expression vector (tumour-associated antigen or immunostimulatory genes) destined for transfer to and expression in the tumour cells.

As the development of a tumour model was novel to the laboratory group, it was first pertinent to develop a reproducible *in vivo* tumour mouse model. Following this, it was important to optimise the infection protocol which would allow for bacterial-mediated tumour growth inhibition, whilst preserving the welfare of the mice. It was hypothesised that *S. Typhimurium* would exhibit differential efficacy at different stages of tumour growth, so it was desired to characterise the time point at which the tumour growth inhibitory effects were maximal. It was believed that in doing so, we would increase the likelihood of identifying critical cellular and molecular mediators in the process of bacterial-mediated tumour growth inhibition.

As the tumour is generally characterised as an immunosuppressive environment, and *S. Typhimurium* is highly immunostimulatory, it was hypothesised that systemic administration of the bacteria in a tumour-bearing mouse model would lead to a change in the inflammatory status in the tumour microenvironment, with a pro-inflammatory phenotype which is non-permissive to tumour progression (Bromberg *et al.*, 1996; Wall *et al.*, 2003). It was sought to investigate the cellular components of the innate and adaptive immune system which may be complicit in this phenotype. The innate immune responders of particular interest were neutrophils, macrophages and dendritic cells as these are implicated as critical players in response to oral *S. Typhimurium* infection (Wick, 2011). It was hypothesised that there would be a massive immune cell influx into the tumour following infection, as has been reported following oral infection and inflammatory settings (Barthel *et al.*, 2003; Johansson *et al.*, 2006; Rydstrom & Wick, 2007; Rydström & Wick, 2009). Furthermore, it was

hypothesised that the recruited cells would produce pro-inflammatory cytokines which would contribute to the inflammatory immune environment.

The adaptive immune response was also an area of interest for this study. Various studies have suggested a role for T<sub>H</sub>1 cytokines in mediating anti-tumour immunity following bacterial infection (Lee *et al.*, 2008; Stern *et al.*, 2015). However, *S. Typhimurium* are also competent at inducing T<sub>H</sub>17 responses in the mucosa (Raffatellu *et al.*, 2008) which have proven to be highly tumour protective in melanoma studies (Martin-Orozco *et al.*, 2010; Muranski *et al.*, 2008). Furthermore, Tregs are associated with poor prognostic outcome for multiple cancer types, but can be stimulated to adapt T<sub>H</sub>1 and T<sub>H</sub>17 phenotypes following stimulation with pro-inflammatory cytokines such as IL-6 (Bettelli *et al.*, 2006; Ghoreschi *et al.*, 2010; Veldhoen *et al.*, 2006). Therefore, it was hypothesised that T<sub>H</sub>17 responses, as well as T<sub>H</sub>1 responses, would be associated with *S. Typhimurium*-mediated tumour growth inhibition, which would coincide with decreased frequency of Tregs in the tumour.

Tumour-associated macrophages (TAMs) are capable of stimulating multiple stages of tumour development (Qian & Pollard, 2010). They are also implicated in being critical for host defence to *S. Typhimurium* infection (Wick, 2011). Given this dual role, it was hypothesised that the TAMs would experience phenotypic changes following *S. Typhimurium* infection, resulting in cells that were no longer conducive to tumour growth and propagated anti-tumour immune responses. The TAM progenitors, monocytes, were suspected to play a role in these processes also. It was postulated that these cells were critical for the mediation of bacterial immune response. To test this hypothesis, it was endeavoured to remove the monocyte cellular compartment from the tumour microenvironment.

The final aim of this thesis was to investigate the ability of multiple strains of *S. Typhimurium* to mediate bactofection. It was hypothesised that the transformation of the bacteria with eukaryotic expression plasmids encoding immunostimulatory or apoptotic genes would enhance the therapeutic outcome of *S. Typhimurium* as a bacterial mediated cancer treatment both *in vitro* and *in vivo*.

## 2 Methods and Materials

### 2.1 Animals

Animals were maintained at the Central Research Facility (CRF) and the Joint Research Facility in the University of Glasgow, except for initial training which was undertaken in the Animal Facility in the Beatson Institute for Cancer Research. Female, 7-9 week old C57BL/6 mice were obtained from Charles River. *Ccr2*<sup>-/-</sup> mice, bred in the CRF, were kindly provided by Prof Simon Milling, having been originally purchased from Jackson Laboratories (Maine, USA). Kaede mice, bred in the CRF, were also kindly provided by Prof Simon Milling. All animal procedures were carried out in keeping with Home Office regulations (Project License No. 70/8584). Animal welfare was in keeping with guidelines laid out by the NC3Rs and in Workman *et al*, (2010).

### 2.2 Bacterial strains, plasmids and cancer cell lines

Full details of bacterial strains used in this study are listed in Table 2.1. Bacterial cultures were maintained on Luria broth (LB) agar, supplemented with antibiotics as appropriate at the following concentrations: kanamycin, 50 µg/ml; ampicillin, 100 µg/ml; chloramphenicol, 500 µg/ml or erythromycin, 50 µg/ml.

**Table 2.1 Details of bacterial strains used in this study**

<u>S. Typhimurium</u>	<u>Relevant genotype</u>	<u>Source/Reference</u>
VNP20009	<i>S. Typhimurium</i> $\Delta$ <i>purl</i> $\Delta$ <i>msb</i>	Kindly provided by Dr John Pawelek (Yale University)
SL7207	<i>S. Typhimurium</i> $\Delta$ <i>aroA</i>	Kindly provided by Dr Siegfried Weiss (Helmholtz Centre for Infection Research)
LT2	Laboratory <i>S. Typhimurium</i> strain	Kindly provided by Dr Gillian Douce (University of Glasgow)
SL1344	<i>hisG</i> mutant of 4/74	Kindly provided by Dr Gillian Douce (University of Glasgow) (Hoiseh & Stocker, 1981)
JH3010	SL1344 <i>prgH'</i> - <i>gfp</i>	Kindly provided by Prof Jay

JH3016	SL1344- <i>rpsM'gfp</i>	Hinton (University of Liverpool). (Hautefort <i>et al.</i> , 2003)
<u><i>Escherichia coli</i></u>		
K12	Laboratory <i>E. Coli</i> strain	Kindly provided by Dr Andrew Roe (University of Glasgow)
LF82	Adherent Invasive <i>E. Coli</i>	Kindly provided by Prof Daniel Walker (University of Glasgow)
F18	Commensal <i>E. coli</i>	Kindly provided by Prof Beth McCormick (Ormsby <i>et al.</i> , 2016)
DH5 $\alpha$	See manufacturer's instructions	NEB C2987
StrataClone SoloPack competent cells	See manufacturer's instructions	Agilent

Plasmids are detailed in the Table 2.2. Electrocompetent cells were transformed by electroporation with Eppendorf Eporator<sup>®</sup> at 1.75 kilovolts with a discharge time of 5.0 milliseconds. Chemically competent cells were transformed by heat shock at 42 °C for 30 seconds. Following transformation, samples were recovered on ice for two minutes. Samples were then supplemented with 950  $\mu$ l of warmed LB and incubated at 37 °C (unless otherwise stated) for 1 hour, before being plated out on antibiotic-containing LB agar.

MDA-MB-231 cells were obtained from American Type Culture Collection and were maintained in Roswell Park Memorial Institute (RPMI)-1640 (Gibco<sup>®</sup>, 12633) supplemented with 10% foetal calf serum (FCS), 1 mM L-glutamine, 2 mM sodium pyruvate and 100 I.U/ml penicillin/streptomycin (all Sigma) at 37 °C and 5% CO<sub>2</sub>. B16F10 and B16F10-mCherry cells were kind gifts from Prof Gerry Graham (University of Glasgow) and were maintained in Dulbecco's Modified Eagle Serum (DMEM; Gibco<sup>®</sup>, 12491) supplemented with 10% FCS, 1 mM L-glutamine, 2 mM sodium pyruvate and 100 I.U/ml penicillin/streptomycin at 37 °C and 5% CO<sub>2</sub>. The B16F10-mCherry cells also required the addition of blasticidin (ThermoFisher Scientific, R21001) at a final concentration of 6  $\mu$ g/ml and Geneticin<sup>®</sup> G418 sulphate (ThermoFisher Scientific, 10131035) at a final concentration of 0.25 mg/ml.

**Table 2.2 Details of plasmids used in this study**

<u>Plasmid</u>	<u>Function</u>	<u>Features</u>	<u>Source</u>
pEGFP	Eukaryotic expression vector	Enhanced green fluorescent protein under the control of eukaryotic promoter, cytomegalovirus	Addgene 17700
pUC19	High copy number plasmid Source of lacZ gene	pUC19 origin of replication LacZ gene	New England Bioscience
pLuc	Eukaryotic expression vector similar to pEGFP	Ampicillin resistance, <i>luciferase</i> transgene	Addgene, 45968
pCP25	Prokaryotic GFP reporter plasmid	Constitutive prokaryotic GFP expression	(Jensen & Hammer, 1998)
rpsmGFP	Prokaryotic GFP reporter plasmid	Constitutive prokaryotic GFP expression	(Roe <i>et al.</i> , 2004)
pEGFPLacZ	Test if removal of f1 <i>ori</i> from pEGFP abrogates filamentous phenotype	pEGFP lacking f1 <i>ori</i>	This study
pACYC-EGFP	Test if EGFP can drive filamentation in pACYC184	rpsmGFP plasmid plus EGFP transgene from pEGFP	This study

## 2.3 Bacterial growth, cell culture and infection

### 2.3.1 Bacterial growth curves

Bacteria were grown overnight in LB, 37°C at 180 revolutions per minute (rpm) in a shaking incubator (IKA, KS 4000). In the morning, bacteria were back diluted to an OD<sub>600</sub> of 0.05 in 50 ml of LB culture, supplemented with antibiotics where

appropriate. Cultures were allowed to grow as before with OD<sub>600</sub> readings taken at regular intervals.

### **2.3.2 *In vitro* monolayer infection and harvest**

B16F10 cells were seeded at a concentration of  $5 \times 10^5$  cells/well of a 6-well plate (Corning®) in RPMI supplemented with 3% FCS and 1% L-glutamine (3% media) 24 hours prior to infection. Bacterial cultures were prepared similarly to the *in vitro* growth curve, except 90-120 minutes following back dilution, when cultures were at an OD<sub>600</sub> of 0.6, 100 µl of the culture was added to 3 ml of 3% media. For the uninfected control, 100 µl of LB culture was added to another bijou of 3 ml 3% media. At the time of infection, wells were removed of media and washed twice with PBS to remove debris. Each well received 900 µl of 3%, plus 100 µl of bacterial culture or control culture. Cells remained infected for one hour at which point wells were washed three times with 3% media supplemented with 50 µg/ml of gentamycin. Following these washes, cells were incubated with 1 ml of the gentamycin 3% media until harvest.

For colony forming unit (CFU) counts, cells were washed three times with PBS before 200 µl of 3% Triton™ X-100 (Sigma) in PBS was added to each well to lyse the cells. Cells remained at room temperature for 10 minutes, with lysates being pipetted up and down to improve cell lysis before being removed to ice. From the lysate, 20 µl was transferred to 180 µl of PBS in a 96-well plate (Corning®), which was serially diluted in PBS seven times. Each dilution was plated out twice in two 10 µl spots on LB agar plates with an appropriate antibiotic. LB agar plates were incubated overnight and colonies were counted the next morning.

## **2.4 Gram staining and bacterial cell length measurement**

For Gram stains, all cultures were grown to mid-late log phase before being heat fixed on glass slides (VWR) and gram stained using Fluka Analytical Gram Stain Kit (77730). Briefly, smears of bacteria on glass slides were flooded with Gram's crystal violet solution for one minute, one minute with Gram's iodine solution, five seconds with Gram's decolourizer solution and counterstained with Gram's safranin solution for one minute. Between each of these steps, the slides were gently washed with tap water to remove excess solution, before slides were

allowed to dry overnight. Slides were imaged on a Leica DM2000 microscope. Three biological replicates were imaged, with at least 10 images per slide being taken. Cell length calculation was performed using the Measurement PlugIn on ImageJ (National Institutes of Health).

## 2.5 Harvesting bacteria for fluorescent imaging

Bacterial strains were grown overnight as before. In the morning, cultures were back diluted and grown to an OD<sub>600</sub> of ~0.6. At this time, 1 ml of culture was centrifuged at 8,000 g for 3 minutes, washed twice in PBS before being fixed in 4% paraformaldehyde (PFA) at room temperature for 15 minutes. Samples were washed twice more in PBS before being dried onto coverslips and mounted onto glass slides with DAPI-containing mounting media (VWR). Images were taken using a Leica DMI8 fluorescent microscope.

At least three biological replicates were imaged for each strain, with at least 10 images per coverslip. Images were analysed using the CellCounter PlugIn on ImageJ.

## 2.6 *In vitro* cell death analysis

Bacteria and B16F10 cells were prepared as in Section 2.3.2. As a positive control for B16F10 cell death, staurosporine (final concentration 1  $\mu$ M, Sigma) was added to a well. At the time of harvest, B16F10 cell supernatants were transferred to labelled 15 ml centrifuge tubes. Wells were washed with PBS twice. B16F10 cells were treated with 200  $\mu$ l Trypsin-ethylenediaminetetraacetic acid (EDTA; 0.25%) (Gibco<sup>®</sup>) and incubated at 37°C for 5 minutes to ensure dissociation. The Trypsin-EDTA was neutralised with 2 ml of 3% media and the cells were transferred to their respective tubes. B16F10 cells were centrifuged at 500 g for 5 minutes. B16F10 cells were then resuspended in Fixable Viability Dye eFluor<sup>®</sup> 780 (eBioscience, 65-0865-14) in PBS (dilutes 1:1000) for 20 minutes on ice in the dark. Viability was then measured using a LSRII flow cytometry analyser (BD Bioscience).

## 2.7 Tumour spheroid generation *in vitro* and infection

Tumour spheroids were generated by seeding  $5 \times 10^5$  MDA-MB-231 cells per well in 200  $\mu\text{l}$  of cell media supplemented with 2.5% Matrigel<sup>®</sup> (Corning<sup>®</sup>, 354230; Ivascu & Kubbies, 2006) in Corning<sup>®</sup> 96-well clear bottom ultra-low attachment microplates (Corning<sup>®</sup>, 7007). Plates were centrifuged at 1,000 g for 5 minutes to promote cellular aggregation. After 9 days in culture, with media changes every other day, tumour spheroids of approximate diameter 500  $\mu\text{m}$  were formed. Single colonies of *S. Typhimurium* were grown as described previously. Cultures were diluted appropriately and 100  $\mu\text{l}$  was added per tumour for an MOI of 100:1. Spheroids were incubated with bacteria for 1 hour before 100  $\mu\text{l}$  of 100  $\mu\text{g/ml}$  gentamycin (2X) was added to each well to kill extracellular bacteria. Tumour spheroids were incubated at 37°C for 24 or 48 hours before being subject to further processing.

## 2.8 Harvesting tumour spheroids

At the time of harvest, tumour spheroids were carefully removed from the well using a Pasteur pipette and passed through two washes of PBS.

### 2.8.1 Fluorescent imaging to investigate bacterial invasion and bactofection

For cryofixation, spheroids were placed in cryomoulds filled with Optimal Cutting Temperature<sup>™</sup> (OCT) solution and frozen on dry ice. Samples were stored at -80°C until further processing.

Samples were placed in the cryotome (ThermoScientific) and were brought to -16°C for 30 minutes before being cut into 8  $\mu\text{m}$  sections. Samples were allowed to come to room temperature. Samples were fixed on the coverslip in 4% PFA for 15 minutes, washed twice with PBS. Slides were then incubated with rhodamine phalloidin stain (diluted 1:20) for 5 minutes at room temperature. (ThermoScientific, R415) before being washed in PBS twice and mounted in DAPI-containing mounting media (VectaShield<sup>™</sup>). Images were taken using a Leica DMI8 fluorescent microscope.

### **2.8.2 Scanning electron microscopy to investigate bacterial localisation**

Following the PBS washes, samples were incubated in 4% PFA for 30 minutes at room temperature before being washed in two changes of PBS. Transmission electron microscopy (SEM) sample preparation and imaging was carried out by Mrs Margaret Mullin. The spheroids were fixed for one hour in 2.5% glutaraldehyde/2% PFA in 0.1 M sodium cacodylate buffer before being washed three times in 0.1 M sodium cacodylate buffer alone (Sigma G5882, C0250). Following fixation, cells were rinsed in 1% osmium tetroxide buffer (Sigma, 75633), then rinsed three times in distilled water and stained with 0.5% uranyl acetate (TAAB, U001) for one hour in the dark. Spheroids were dehydrated through an ethanol series of 30%, 50%, 70%, 90% (10 minutes each), 100% (5 minutes, four times) followed by dried 100% ethanol (5 minutes, four times). Spheroids then underwent critical point drying from liquid CO<sub>2</sub> using a Polaron E3000 Critical Point Dryer to preserve the structure of the samples. Spheroids were mounted onto aluminium pin stubs, gold/palladium coated (20 nm thick) using a Q150T high vacuum Sputter coater (Quorum Technologies). The SEM samples were viewed on a Jeol6400 SEM, running at 10 kV and images were captured using Olympus Scandium software.

### **2.8.3 Transmission electron microscopy to investigate biofilm formation**

Tumour spheroids were prepared as above. Scanning electron microscopy (SEM) sample preparation and imaging were carried out by Mrs Margaret Mullin. The spheroids were processed as in Section 2.8.3 to the end of the ethanol series. At this time, the samples were changed in propylene oxide (five minutes, three times). Spheroids were left in 1:1 propylene oxide:araldite/Epon (TAAB 812) resin overnight. The following morning, spheroids were changed through the resin twice and left rotating for five hours. Samples were then embedded in fresh resin in moulds and polymerised at 60°C for 14 hours. Semi-thin sections (350 nm) were cut using a Leica Ultracut UCT Ultramicrotome with a diamond Histo-knife (Leica). Sections were dried on a glass sile on a hot plate (80°C) before being stained with Toluidine Blue (Sigma, 89640) for 15-30 seconds and washed in distilled water. Ultrathin sections (60-70 nm) were also cut, using a diamond Ultramicrotome knife (Leica) and collected on 100 mesh Formvar-

coated copper grids (Agar Scientific) before being contrast stained with 2% methanolic uranyl acetate for five minutes and Reynolds lead citrate for five minutes (Agar Scientific, AGR1210). The TEM samples were viewed on a FEI Tecnai TF20 TEM running at 300 kV. Images were captured using Gatan Digital Micrograph software and a Gatan Multiscan 794 camera.

## 2.9 Generation of bioluminescent SL7207 strain

The bioluminescent strain of SL7207, termed SL-Lux, was generated according to the protocol described previously (Riedel *et al.*, 2007). SL7207 was made competent by five washes with 10 ml ice cold distilled H<sub>2</sub>O. SL7207 was then transformed with p16*Slux* and transformants were obtained by plating on agar plates containing 500 µg/ml erythromycin at 30°C (permissive temperature for plasmid replication) for 24-48 hours. Colonies were checked for light emission using the *In vivo* Imaging System (IVIS) Spectrum (Caliper Life Sciences). Positive clones were grown overnight in LB containing 500 µg /ml erythromycin at 30°C. The next morning, cultures were back diluted and incubated overnight at 42°C (non-permissive temperature to force 16*Slux* to integrate into the chromosome by homologous recombination). Samples were plated out on LB agar supplemented with 500 µg /ml erythromycin, and left to grow at 42°C overnight. Colonies positive for light emission using the IVIS were subjected to colony polymerase chain reaction using the primers listed in Table 2.4.

## 2.10 B16F10 transplantable model and SL7207 infection protocol

B16F10 cells were split 1:4 24 hours pre tumour induction to ensure consistent cell confluency. Cells were washed in PBS before being incubated at 37°C for 3 minutes in 0.05% Trypsin-EDTA to ensure complete cell dissociation. This was neutralised with 5 ml of cell culture media (DMEM supplemented with 10% FCS 1 mM L-glutamine, 2 mM sodium pyruvate and 100 I.U./ml penicillin/streptomycin). Cells were centrifuged at 1,000 g for 3 minutes at room temperature before being suspended in PBS. Cells were counted using a Bright-Line™ hemocytometer (Sigma), and cell solutions of defined cell density were made up in cold PBS. Cells were transferred on ice for transport to the relevant animal facility.

Mice were shaved along their right flank. The cell solution was drawn into a 1 ml syringe (BD Plastipak™) with a 25 gauge needle (Medisave, Teruno AGANI, AN-2516R). From this, 200 µl of cell suspension was injected subcutaneously in the back right flank of the mouse, where a bolus temporarily formed. Tumours were allowed to develop over a set number of days. Mice were monitored regularly and tumour diameters were measured using Fisher Science Education Traceable™ Digital Carbon Fiber Calipers. Tumour volumes were calculated using the formula:  $4/3\pi(hxw^2/8)$  where 'h' was height and 'w' was width (Crull *et al.*, 10).

For *in vivo* infection, SL7207 was prepared as per the *in vitro* infection protocols. When the OD<sub>600</sub> reached ~0.6, the appropriate volume of culture was added to ice cold PBS to generate a defined concentration of either 5x10<sup>5</sup> CFUs/100 µl or 5x10<sup>6</sup> CFU/100 µl. Cultures were incubated on ice for transport to the relevant animal facility. Mice were warmed in a heating chamber for 30 minutes at 38°C prior to infection. Mice were infected with 100 µl of bacterial culture via their tail vein. Mice were weighed daily.

## 2.11 *In vivo* imaging of SL-Lux

Mice were anaesthetised using 4% isofluorane in 100% oxygen in an anaesthetic chamber. Mice were placed in the IVIS and images were acquired for 10-120 second exposures, small or large binning depending on the amount of light produced, 1 f/stop and an open filter. The amount of time mice spent under anaesthesia did not surpass 20 minutes.

## 2.12 *In vivo* tissue harvest following infection for CFU counts

Mice were sacrificed using cervical dislocation. Tissues, tumour, spleen and liver, were carefully resected and placed in ice cold PBS. Tissues were weighed. Tissues were then placed in 1-2 ml of PBS in 5 ml bijoux and homogenised (OMNI International Inc., TM125-220). Homogenates were subject to serial dilution in PBS as above. These dilutions were plated out on LB agar. The volume of the homogenate was assessed using pipettes. Plates were checked for bioluminescent light emission to ensure SL-Lux isolation.

## 2.13 Hematoxylin and eosin staining of tumour sections

Mice were sacrificed using cervical dislocation. Tumours were carefully resected and placed in cryomoulds containing 2.5% carboxymethylcellulose in water (Sigma). Tumours were frozen in a slurry of crushed dry ice and ethanol. Samples were stored at  $-80^{\circ}\text{C}$  until processing. Slides were fixed in ice cold 75% acetone, 25% ethanol for 10 minutes. Slides were stained in Harris Hematoxylin Solution (Sigma, HHS16) for two minutes followed by three minutes in running water. The samples were differentiated in 1% acid/alcohol briefly, running water, Scotts Tap Water Substitute (Atom Scientific, RRSP192-D) and running water again. Slides then counterstained with 1% Eosin Solution Y (Sigma, HT110132) for two minutes followed by a brief wash in running water. Sections were dehydrated by three-minute changes in 70% ethanol, 90% ethanol, 100% ethanol (x 2) and xylene (x 2). Sections were mounted with coverslips from xylene (Sigma) with DPX mountant (Sigma). Slides were left to dry overnight before being imaged using a Leica DM2000 microscope. The processing of samples for hematoxylin and eosin staining was performed with Heather Hulme.

### 2.13.1 Tissue harvest and digest

Mice were sacrificed using cervical dislocation. Tissues were carefully resected, weighed if necessary and placed in ice cold PBS. Tumours were then transferred to digestion media composed of 3 mg/ml Collagenase A (Sigma, 10103586001) and 25  $\mu\text{g}/\text{ml}$  DNase I (Sigma, 10104159001) in DMEM as in (Coffelt *et al.*, 2015). Lymph nodes and spleens were transferred to digestion media composed of Liberase TM (Sigma, 5401119001) and 50  $\mu\text{g}/\text{ml}$  DNase I in RPMI supplemented with 1% v/v L-glutamine and 0.1% v/v  $\beta$ -mercaptoethanol (Sigma, M6250). All tissue was digested at  $37^{\circ}\text{C}$  for 30 minutes before being passed through a 70  $\mu\text{m}$  strainer (VWR, 734-0003) and neutralized with 8% FCS-DMEM buffer. Alternatively, for T cell specific analysis, tissues were directly minced through 100  $\mu\text{m}$  strainers. Tumour and spleen cells were treated with 1 ml red blood cell lysis buffer (Sigma, 11814389001) for 5 minutes at room temperature, neutralised with 10 ml of 8% FCS-DMEM and were centrifuged. Cells were resuspended in flow cytometry buffer (FB): 2% FCS, 3 nM EDTA (Sigma, E9884) in PBS. A portion of the cells were counted using Trypan Blue exclusion dye (Sigma, T8154).

### **2.13.2 Intracellular cell stimulation**

Single cell suspensions were washed and resuspended in FB. For intracellular cytokine analysis, cells were resuspended in 500  $\mu$ l of eBioscience™ Cell Stimulation Cocktail (plus protein transport inhibitors) (00-4975-93) in RPMI media supplemented with 10% FCS, 1% L-glutamine and 0.01%  $\beta$ -mercaptoethanol. These cells remained at 37°C, 5% CO<sub>2</sub> for four hours before being washed in FB, centrifuged and subjected to surface and intracellular staining protocols described below.

### **2.13.3 Surface staining**

Single cell suspensions were washed and resuspended in FB. Cells were first stained in Fixable Viability Dye eFluor® 780 in PBS for 15-20 minutes on ice (note that all steps involving fluorophores were carried out protected from light). Following this incubation, cells were washed in 5 ml of FB and centrifuged. Cells were resuspended in their residual buffer before being incubated with anti-CD16/CD32 ('Fc Block') to reduce non-specific binding to Fc receptors (Biolegend). After 5 minutes, 100  $\mu$ l of extracellular antibody mixes (final dilution of 1:200 for each) were added to the cells 20 minutes on ice before being washed with PBS and pelleted. If cells were required for intracellular staining, they were resuspended in 500  $\mu$ l of Fix/Perm Buffer (eBioscience, Foxp3/Transcription Factor staining buffer set, 00-5523-00) overnight at 4°C. If they were not, they could be analysed using the FACS AriaIII, LSRII analyser or Fortessa analyser (all BD Biosciences). All data generated was analysed using FlowJo software (Tree Star Inc, Oregon, USA).

### **2.13.4 Intracellular staining**

Following overnight incubation in Fix/Perm buffer, cells were washed twice with 2 ml Perm Buffer (eBioscience, Foxp3/Transcription Factor staining buffer set, 00-5523-00). Cells were then resuspended in 200  $\mu$ l of Perm Buffer supplemented with intracellular antibodies (1:200) for 1 hour in the dark. Appropriate isotype controls for intracellular stains were included in all experiments.

### 2.13.5 Assessment of phagocytosis

To measure the phagocytic capacity of myeloid cells, in a 1.5 ml microcentrifuge tube, 80  $\mu$ l of whole tumour single cell suspensions were co-incubated with 20  $\mu$ l of pHrodo™ Red E. coli Bioparticles™ (ThermoFisher Scientific, P35361) for 15 minutes at 37°C. For each sample, a duplicate tube was incubated on ice as a negative control for phagocytosis. Cells that had phagocytosed the particles were positive for phycoerythrin (PE) when analysed by flow cytometry.

**Table 2.3 Antibodies used for flow cytometry**

<u>Marker</u>	<u>Cell type</u>	<u>Clone</u>	<u>Company</u>
<u>Extracellular stains</u>			
CD11b	Myeloid cells	HK1.4	Biolegend
CD11c	Primarily DCs	N4/18	Biolegend
F4/80	Primarily Monocytes/macrophages	BM8	Biolegend
CD206	‘Resident’ macrophages or ‘M2-like’ macrophages	C068C2	Biolegend
Ly6G	Primarily neutrophils	1A8	Biolegend
MHCII	Antigen presenting cells	M5/114.15.2	Biolegend
CD45	Common leukocyte marker	30-F11	Biolegend
CD3	T cells	17A2	Biolegend
CD4	CD4+ T cells	GK1.5	Biolegend
CD8	CD8+ T cells	53_6.7	Biolegend
CD25	Activated T cells	PC61	Biolegend
CD44	Activated T cells	IM7	Biolegend
CD69	Activated T cells	H1.2F3	Biolegend
Ly6C	Monocytes	HK1.4	eBioscience

SiglecF	Eosinophils	E50-2440 (Ruo)	BD Biosciences
<b><u>Intracellular stains</u></b>			
Ki67	Recently replicated cells	16A8	Biolegend
FoxP3	Treg transcription factor	FJK-16S	eBioscience
ROR $\gamma$ T	T <sub>H</sub> 17 transcription factor	AFKJS-9	eBioscience
Tbet	T <sub>H</sub> 1 transcription factor	eBio4B10	eBioscience
$\gamma\delta$ TCR	$\gamma\delta$ T cells	eBIOGL3	eBioscience
IL17A	T <sub>H</sub> 17 cytokine	BD_TCII-18H10	BD Biosciences
IFN $\gamma$	T <sub>H</sub> 1 cytokine	554413	BD Biosciences
IL-6	T <sub>H</sub> 1 cytokine	MP520F3	BD Biosciences
TNF- $\alpha$	T <sub>H</sub> 1 cytokine	MP6-XT22	Biolegend
IL-22	T <sub>H</sub> 1/T <sub>H</sub> 17 cytokine	Poly5164	Biolegend
IL-12/23	T <sub>H</sub> 1 cytokine	C15.6	Biolegend
Pro-IL-1 $\beta$	T <sub>H</sub> 1 zymogen	NJTEN-3	eBioscience

## 2.14 Immunoblot analysis

### 2.14.1 Immunoblot analysis of prokaryotic cells

For prokaryotic immunoblot assays, bacterial strains were grown as described. Some were treated with Mitomycin-C (Sigma, M4287) at a concentration of 5  $\mu$ g/ml for 4 hours at 30°C, 120 rpm. Cells were harvested at mid-late log phase and washed twice in PBS, before being centrifuged and frozen at -80°C overnight. The next morning, cells were resuspended in bacterial lysis buffer (50 mM Tris pH 8.0, 10% v/v glycerol, 0.1% Triton X-100, 100  $\mu$ g/ml lysozyme, DNaseI (3 U/ml), 2 mM MgCl<sub>2</sub>, cComplete™ Mini (EDTA-free) Protease Inhibitor Cocktail (Sigma 11836170001), sonicated at 10 mAmps for 30 seconds three times, syringed five times using a 26G needle to shred DNA and centrifuged at 16,000 g to harvest the protein-containing supernatant. Protein concentrations were determined using a Pierce™ BCA Protein Assay Kit (ThermoFisher Scientific).

Briefly, 25  $\mu$ l of lysate was added to a well of a 96-well plate in triplicate including the provided protein standards (ranging from 0 to 2000  $\mu$ g/ml). To each well, 200  $\mu$ l of Working Reagent (50:1, Reagent A: B) was added and the 96-well plate was incubated at 37°C for up to 1 hour. Absorbance was measured at 562 nm on a FLUOstar OPTIMA Microplate reader (BMG Labtech). Using the protein standards to create a standard curve, protein concentrations of samples were determined. Equal amounts of protein were resolved on a 4-12% Bis-Tris SDS Page gel (Life Technologies) before being transferred to a nitrocellulose membrane using a ThermoScientific Pierce™ Powerblot Cassette. Membranes were blocked in 5% milk in PBS-Tween (PBS-T) (0.05%) for 1 hour prior to incubation with a primary antibody against either RpoS (Biolegend, Clone 1RS1, 663703), RecA (Abcam, ab63797) or GroEL (Abcam, ab90522) overnight at 4°C. Membranes were washed using PBS-T three times before being incubated with a rabbit-horse radish peroxidase (HRP) secondary antibody (ThermoFisher Scientific, 31460) for 1 hour at room temperature. Membranes were again washed three times using PBS-T before being developed using a Licor C-DiGit® Blot Scanner.

#### **2.14.2 Immunoblot analysis of eukaryotic cells**

For eukaryotic immunoblot assays, MDA-MB-231 cells were infected with SL7207 wild type or SL7207-pEGFP for 24 hours as described above. At harvesting, cells were washed with PBS three times before being lysed by 200  $\mu$ l of eukaryotic lysis buffer (2% Triton in PBS supplemented with cOmplete™ Mini (EDTA-free) Protease Inhibitor Cocktail, syringed five times using a 26G needle to shred DNA and centrifuged at 16,000 g to harvest the protein-containing supernatant. Protein concentrations were determined using a Pierce™ BCA Protein Assay Kit, ThermoFisher Scientific. Samples were resolved on a 4-12% Bis-Tris SDS Page gel as described above. Membranes were processed as described above using a GFP (Abcam, ab13970) primary antibody and an anti-chicken-HRP secondary antibody (Abcam, ab6753).

#### **2.15 Enzyme-linked immunosorbent assay (ELISA)**

For the sandwich ELISA protocol, supernatants were harvested from tumour cell suspensions which were stimulated *in vitro* with eBioscience™ Cell Stimulation

Cocktail (00-4970-93) in RPMI media supplemented with 10% FCS, 1% L-glutamine and 0.01%  $\beta$ -mercaptoethanol for four hours. Supernatants were normalised to protein concentration before being subject to an ELISA protocol or TNF- $\alpha$  (Biolegend, 430901), IL-17 (Biolegend, 432501) or IFN- $\gamma$  (Biolegend, 430801), according to the manufacturer's instructions. Briefly, ELISA plates (Nunc<sup>TM</sup> Maxisorp<sup>TM</sup>, 442404) were coated overnight with 100  $\mu$ l of the relevant capture antibody at 4°C. Plates were washed three times with 0.05% PBS-T and incubated with 200  $\mu$ l of Blocking Solution for one hour at room temperature before being washed three times. Samples were then added to the plates, 100  $\mu$ l of each in duplicate, as well as the dilute standards. Plates were incubated for two hours at room temperature before being washed three times with PBS-T. Following these washes, Avidin-Horseradish peroxidase conjugate in Blocking Buffer (1:500 dilution) was added to each well and incubated at room temperature for 30 minutes, before plates were stringently washed five times with PBS-T. TMB Substrate Reagent (1:1 mixture of Reagent A and Reagent B) was added to each well in 100  $\mu$ l for up to 60 minutes for colour development. The optical density of the plates was read at 450 nm on FLUOstar OPTIMA Microplate reader (BMG Labtech).

## 2.16 Photoconversion of immune cells in Kaede mice

Kaede mice cells constitutively express a green fluorescent protein from a stony coral, *Trachyphyllia geoffroyi*, and can be photoconverted to a red fluorescent protein following exposure to light in the range of 350-405 nm (Ando *et al.*, 2002). Kaede mice were inoculated with B16F10 tumours as described above. Photo-conversion of the Kaede mouse tumours was performed using a small mains operated 123xS06J bluray diode with a 405-G-2-glass lens (DTR's Laser Shop). The 405 nm laser diode operated at 600-650 mW. The emission spectrum lies at 405 nm and the diode was not run for more than 10 seconds to protect the tissue. There were two exposure protocols examined in the current study. The first involved the exposure of the tissue to a UV light source for three seconds, three times with five-second breaks between exposures (termed Protocol 1). The second involved one ten second exposure, followed by four five-second exposures with five-second breaks between exposures (termed Protocol

2). For the infection protocol, Protocol 2 was employed one day prior to infection. Tumours were then harvested at three dpi.

## **2.17 Clodronate-mediated depletion of monocytes and macrophages**

C57BL/6 mice were inoculated with B16F10 tumour cells as described above. At four days prior to infection, mice were administered 100  $\mu$ l of Clodronate Liposomes (Clod Lipo; Liposoma) via tail vein (Rooijen & Sanders, 1994; Weisser *et al.*, 2012). This transpires to an approximate concentration of 0.5 mg/20 g mouse weight. At 1 day prior to infection, 1 dpi, 3 dpi and 5 dpi, mice received 200  $\mu$ l Clod Lipo. At these time points, control PBS Lipo was also administered to control PBS Lipo mice. At 7 dpi, tissues were harvested and processed as described.

## **2.18 Generation of the pACYC-EGFP plasmid**

### **2.18.1 Plasmid isolation (Miniprep)**

In order to perform molecular cloning, template plasmids first had to be isolated from bacteria, using QIAprep<sup>®</sup> Spin Miniprep Kit (Qiagen). Briefly, bacterial strains containing the plasmid of interest, pACYC184, had to be grown up overnight in 10 ml LB culture. Bacterial cultures were pelleted following centrifugation at 6,800 g for 3 minutes. Pellets were resuspended in 250  $\mu$ l of Buffer P1 (resuspension buffer) before being transferred to a microcentrifuge tube and 250  $\mu$ l of Buffer P2 was added to lyse bacteria and release plasmid DNA. Lysates were neutralised by adding 350  $\mu$ l of Buffer N3 before being centrifuged in a table top microcentrifuge (ThermoScientific, Heraeus Fresco 21) at 17,900 g for 10 minutes. The DNA-containing supernatant was poured into a QIAprep spin column for a 1 minute centrifugation to bind plasmid DNA to the column. The column was washed by adding 500  $\mu$ l of Buffer PB, centrifuged as before, washed with 700  $\mu$ l of Buffer PE and again, centrifuged as before. The column was then inserted into a fresh collection tube before being centrifuged for 5 minutes at 17,900 g to remove any residual liquid. Finally, 50  $\mu$ l of distilled water was added to the column, the column was placed in a fresh 1.5 ml

microcentrifuge tube and incubated at room temperature for 10 minutes before being centrifuged to elute the plasmid DNA in distilled water. DNA quantification was carried out using a NanoDrop™ 2000/2000c.

## 2.18.2 Polymerase chain reaction

Polymerase chain reaction (PCR) was carried out under standard conditions using the Q5® High-Fidelity DNA Polymerase kit (NEB, M0491L). The primers employed for the amplification of the EGFP transgene are listed in Table 2.4. Reaction mixtures comprised a final concentration 1X reaction buffer, of 0.5 µM of each primer, 0.2 mM of each deoxyribonucleoside triphosphate (dNTP), contained 20-50 ng template DNA, 0.2 units/µl polymerase and nuclease-free water. The reaction cycle was carried out in a thermocycler (Techne, TC-412) and is outlined in Table 2.5.

**Table 2.4 Primers used in this study**

<u>Primer name</u>	<u>Purpose</u>	<u>Sequence</u>
16S_rev_XhoI	Check	CTGATCTCGAGGGC GGTGTGTACAAGG
16S_fwd_int	primers for 16Slux chromoso mal integration	CTGATGAATTCCAGGTGTAGCGGTGAAATG

### Plasmid:

#### pEGFP<sub>LacZ</sub>

pEGFP (w/o f1 ori) F	Amplificati on of vector backbone	CTGGGGTGCCTAATGAGTGATTTTATGTTTCAGGTT CAGGGG
pEGFP (w/o f1 ori) R	Amplificati on of vector backbone	GGTTTTACCGTCATCACCGCAATTAGTCAGCAACCA GGTG
LacZ F	Amplificati on of	TCACTCATTAGGCACCCAG

	insert	
LacZ R	Amplification of vector backbone	CGGTGATGACGGTGAAAAC
<u>Plasmid:</u>		
<u>pACYC-EGFP</u>		
EGFP F	Amplification of CMV-EGFP	CTGCATTAATGCGTTACATAACTTACGGTAAATGG
EGFP R	Amplification of CMV-EGFP	CGACGCATGCACGCGTTAAGATACATTGATGAGTT

**Table 2.5 PCR programme for DNA amplification**

<u>PCR Step</u>	<u>Temperature (°C)</u>	<u>Time (minute)</u>	<u>No. Cycles</u>
Initial denaturation	95	5	1
Denaturation	95	1	30
Annealing	55	1	30
Elongation	72	1	30
Final elongation	72	7	1

### 2.18.3 Restriction digest

pACYC184 was digested with *Asel* and *SphI* to generate a 1.5 kilo base (kb) fragments for a new plasmid (pACYC-EGFP). DNA was digested with the FastDigest Green Buffer system (ThermoFisher Scientific). Reaction mixtures composed of 1X FastDigest Green Buffer, one unit of each restriction endonuclease, 100 ng of template DNA and dH<sub>2</sub>O. Samples were incubated in a 37°C water bath for 15 minutes before being removed to ice.

### 2.18.4 Agarose gel electrophoresis

Agarose gel electrophoresis was employed for the visualisation of DNA following PCR or restriction digest. A working solution of buffer containing Tris, acetic acid, EDTA (TAE) was prepared by dilution of 50x TAE (242 g Tris base, 57.1 ml acetic acid, 100 ml 0.5 M EDTA pH 8.0 made up to 1 L in dH<sub>2</sub>O) 1:20 v/v in dH<sub>2</sub>O. The 1% w/v agarose gel was prepared by adding 0.5 g agarose (Sigma, A9539) to 50 ml of TAE buffer in a conical flask, which was heated until all of the agarose was dissolved. The molten solution was slightly cooled before the addition of GelRed™ (Biotium, 41003) to enhance DNA visualisation. The solution was poured into a gel cast, a multi-well comb was added and the gel was allowed to set at room temperature. When the gel was set, the cast was submerged in a Bio-Rad tank and the comb was removed. Samples were added to the wells, including a 1 kb DNA ladder (NEB, N3232). Following sample loading, the lid was fitted and the gel tank was connected to a Bio-Rad PowerPac300 (Bio-Rad, Hercules, CA, USA). The gel was run at 100 V for 30 minutes to allow the band of interest, 1.5 kb, to resolve.

### 2.18.5 Gel purification of DNA bands

DNA bands were purified using a QIAquick® Gel Extraction Kit (Qiagen). Bands were excised with a scalpel and added to 3x volume of Buffer QG in a 1.5 ml microcentrifuge tube. Tubes were incubated at 50°C until the gel melted (10-15 minutes), vortexing occasionally, to which 1x volume of isopropanol was added to the mixture. Samples were then placed in a QIAquick spin column in a collection tube and centrifuged for 1 minute at 17,900 g, with flow through being discarded after every centrifugation step. The DNA bound to the column was washed with 500 µl of QG buffer and centrifuged as before to remove any remaining agarose. The column was then washed with 750 µl of Buffer PE and centrifuged twice. The column was placed in a fresh 1.5 ml microcentrifuge tube and 30 µl of nuclease free H<sub>2</sub>O was added to the column and incubated at room temperature for 5 minutes. DNA was collected following a 2 minute centrifugation at 17,900 g.

### 2.18.6 Ligation

In the present study, to generate the pACYC-EGFP plasmid, the pACYC184 restriction digest product was ligated into a StrataClone Vector (Agilent technologies). pACYC184 is a low copy number plasmid. The StrataClone vector is a high copy number plasmid which is capable of ligating with DNA inserts via topoisomerase I-mediated DNA strand joining. This therefore allows for the amplification of the pACYC184 backbone in the high copy number plasmid to increase the amount of vector DNA recovered for the final ligation reaction. Briefly, following the gel purification of the pACYC184 digested product, 2  $\mu$ l (~50 ng) of this mixture was co-incubated with 3  $\mu$ l StrataClone Cloning buffer and 1  $\mu$ l StrataClone Vector Mix for five minutes at room temperature to allow for ligation. The ligated product was then cloned into StrataClone SoloPack competent cells via heat shock and plated on antibiotic selection LB agar.

Recovered colonies were grown up, plasmids extracted and digested using *AseI* and *SphI* to generate the 1.5 kb pACYC184 backbone as before, but in greater quantity. The pEGFP PCR product was also digested under the same conditions. The digestion reactions were resolved on a 1% TAE agarose gel, the bands of interest were excised and subject to ligation using New England Biolabs (NEB) T4 Ligase (M0202). The final reaction consisted of the EGFP insert (500 ng), pACYC184 backbone (100 ng), 1x T4 DNA Ligase Buffer, 1  $\mu$ l T4 DNA-Ligase. This reaction was incubated over night at 16 °C before the ligase was heat inactivated at 65 °C for 10 minutes. The samples were recovered on ice before being transformed into competent DH5 $\alpha$  cells. Confirmation of the creation of the pACYC-EGFP plasmid was enabled through restriction digest using *HindIII* generating a defined banding pattern according to the generated plasmid map.

### 2.19 Generation of the pEGFPLacZ plasmid using NEBuilder<sup>®</sup> Hifi DNA Cloning

The NEBuilder<sup>®</sup> Hifi DNA Cloning Assembly Kit system (New England Biosciences, E5520S) was employed to generate the pEGFPLacZ plasmid. Fragments were amplified from pEGFP (vector) and pUC19 (insert) using PCR as described above. Primers are listed in Table 2.3. The primers were designed to provide overlapping sequences between the amplified products to promote homologous

recombination upon ligation. PCR products were resolved on a 1% agarose gel in TAE buffer and products were extracted. The two fragments (0.03-0.2 pmol at a vector: insert ratio of 1:2) were coincubated in the presence of 1x NEBuilder<sup>®</sup> HiFi DNA Assembly Master Mix buffer and dH<sub>2</sub>O in a thermocycler at 50 °C for 15 minutes to allow for plasmid assembly. Samples were then removed to ice and electroporated into competent BL21 *E. coli* cells. Transformants were plated on antibiotic-containing LB agar plates to select bacteria containing the assembled plasmid. Sequencing analysis was employed to confirm successful assembly.

## 3 Development of the B16F10 tumour model and *S. Typhimurium* infection protocol

### 3.1 Introduction

In order to assess the role of *S. Typhimurium* in mediating a tumour immune response, it was first necessary to establish an appropriate tumour mouse model, as well as a *S. Typhimurium* infection protocol.

As evident in Table 1.2, there are many different mouse models of cancer. For the present study, the primary criteria were reproducibility and speed. For these reasons, the transplantable tumour model was selected. There are two primary murine background strains employed for these studies: C57BL/6 and BALB/c. As outlined in Chapter 1, Section 1.5.2, in terms of immunological response, these strains differ in their ability to launch a strong  $T_H1$  response (Mills *et al.*, 2000; Santos *et al.*, 2006). The C57BL/6 strain was also reported to be capable of clearing bacterial infection whereas BALB/c did not, making the C57BL/6 background more attractive for an *S. Typhimurium* infection protocol (Watanabe *et al.*, 2004). Furthermore, there are many genetically manipulated strains available on the C57BL/6 background, which is not the case for BALB/c mice. For these reasons, the C57BL/6 strain was chosen for the present study.

It was also pertinent to decide which strain of *S. Typhimurium* to select for the study. As outlined in Chapter 1, Table 1.2, there are multiple *S. Typhimurium* strains which have been employed for cancer studies. These strains vary in their lipopolysaccharide (LPS) immunostimulatory potency and genetic attenuation. The criteria for a bacterial strain for the present study included tumour-specific localisation, immune activation and host tolerance. SL7207 has been reported to exhibit tumour localisation and tumour-specific growth (Crull *et al.*, 2011a; Leschner *et al.*, 2012). SL7207 also has a fully functional LPS, meaning it is capable of activating TLR signalling which results in potent immunostimulation. This strain has also been demonstrated to be the most efficient DNA delivery vehicle for therapeutic DNA delivery in an *in vivo* glioblastoma model (Berger *et al.*, 2013). This characteristic enables the employment of ‘bactofection’ to

enhance the immunostimulatory properties of the bacteria in the future. For these reasons, SL7207 was selected.

The routes of bacterial administration vary from oral, intraperitoneal, intratumoral and intravenous (Avogadri *et al.*, 2008; Jia *et al.*, 2007; Lee *et al.*, 2008; Lehouritis *et al.*, 2015; Zhao *et al.*, 2005). In one study, the methods of administration were compared and it was found that intraperitoneal and intravenous administration resulted in the greatest bacterial tumour localisation and therapeutic efficacy (Crull *et al.*, 2011a). For the present study, intravenous administration was selected as the optimal route of delivery as this was deemed to be the most clinically relevant method.

The protocols that have been described in bacterial-mediated cancer therapy reports have generally allowed the tumour cells to develop into a tumour for a set number of days, or to a predefined size, at which point bacteria are administered (Crull *et al.*, 2011a; Fu *et al.*, 2008; Kuan & Lee, 2016). However, data has not been provided pertaining to the optimisation process involved in selecting these criteria, warranting optimisation of the protocol in the present study. Therefore, it was essential for the current study to ensure consistency and reproducibility between experiments as well as to maximise the therapeutic potential of the bacterial treatment for subsequent experimental investigations.

### **3.1.1 Aims**

1. To develop the B16F10 C57BL/6 tumour model
2. To optimise the SL7207 infection protocol of the tumour model
3. To assess the effects of SL7207 on tumour growth dynamics and host survival

## 3.2 Results

### 3.2.1 Optimisation of tumour cell seeding density for subcutaneous tumour growth

In employing any tumour model, it is critical to have reproducible tumour growth, to minimise variation between experiments. As the B16F10 melanoma cell line in C57BL/6 was not established in our group, it was important to optimise the cell seeding density, and establish the optimal time point after seeding for *S. Typhimurium* inoculation.

Based on the literature, two different cell densities were investigated (Chen *et al.*, 2012; Kuan & Lee, 2016; Zheng *et al.*, 2017b). These were  $2 \times 10^5$  cells and  $5 \times 10^5$  cells, each in 200  $\mu\text{l}$  of cold phosphate buffered saline (PBS). Mice were monitored daily for weight loss (a surrogate marker for the health status of the mice) and tumour growth. The mice did not lose any weight during the tumour growth period, suggesting there was minimal systemic insult to the animals (Figure 3.1A). For both cell densities, tumours became visible about seven days post seeding and were palpable by eight to nine days. The growth dynamics of the tumours for both groups were similar (Figure 3.1B). In this initial experiment, it was noted that the degree of variation (as assessed by the standard deviation) in tumour size at eight days post inoculation was  $182.9 \mu\text{m}^3$  for  $5 \times 10^5$  cells and  $88.67 \mu\text{m}^3$  for  $2 \times 10^5$  cells (Figure 3.1C). A similar trend was seen at 12 days post inoculation with standard deviations of  $478.5 \mu\text{m}^3$  and  $337.5 \mu\text{m}^3$  for  $5 \times 10^5$  and  $2 \times 10^5$  respectively (Figure 3.1D). As the tumour sizes of the mice inoculated with  $2 \times 10^5$  B16F10 cells had less variation, this was the cell density chosen to proceed with for subsequent *S. Typhimurium* infections.

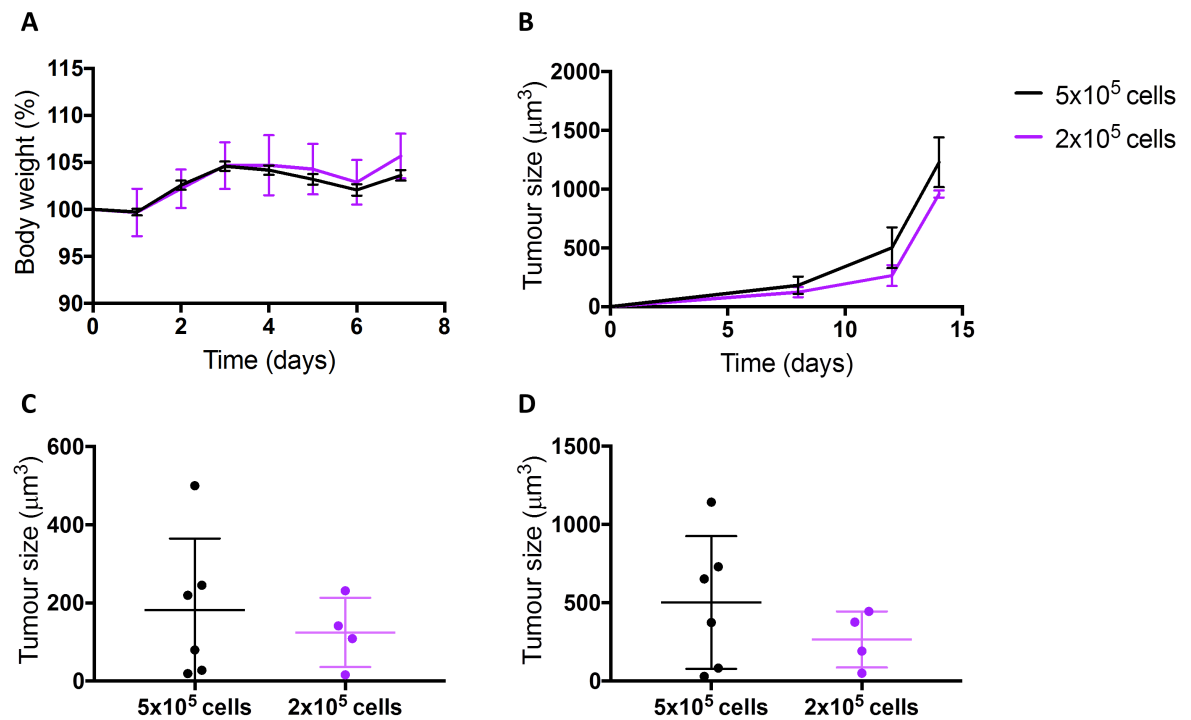


**Figure 3.1 Optimisation of the tumour cell seeding density for tumour development**

B16F10 tumour cells were injected subcutaneously into the back flank of C57BL/6 mice and weight and tumour size were measured over time. **A.** Weight of mice after tumour cell inoculation expressed as a percentage of weight at Day 0. **B.** Tumour size following tumour cell inoculation as measured by Vernier calipers. **C.** Tumour size at eight days post tumour cell inoculation. **D.** Tumour size at 12 days post tumour cell inoculation. Error bars SD.

### 3.2.2 Optimisation of *S. Typhimurium* SL7207 infectious dose

Although SL7207 is an attenuated strain of *S. Typhimurium*, with *in vivo* bacterial administration, it is pertinent to characterise the optimal infectious dose to preserve the welfare of the animals whilst enabling tumour localisation and tumour growth inhibition (Low *et al.*, 1999). Following consultation with the literature, two infectious doses,  $5 \times 10^5$  colony forming units (CFUs) and  $5 \times 10^6$  CFUs of SL7207 were investigated (Crull *et al.*, 2011a; Li *et al.*, 2012). SL7207 was administered systemically via tail vein injection in 100 µl of cold PBS. The mice were monitored daily for changes in weight and tumour size. Mice that were infected with  $5 \times 10^6$  CFUs SL7207 had significant weight loss compared to the uninfected as soon as one day post infection (dpi;  $p < 0.0001^{****}$ ), whereas it took two days for mice infected with  $5 \times 10^5$  CFUs to significantly lose weight compared to uninfected controls ( $p = 0.021^{**}$ ) (Figure 3.2A). At this time point the weight of mice infected with  $5 \times 10^6$  CFUs and  $5 \times 10^5$  CFUs was also significantly different, and the significant differences in weight loss between all three groups continued until the end of the experiment at 7 dpi.

There was a significant difference in tumour size between mice infected with  $5 \times 10^6$  CFUs at 7 dpi versus uninfected mice ( $p < 0.043^*$ ) (Figure 3.2B). There was no significant difference in tumour sizes between the two infected groups at 7 dpi ( $p = 0.09$ ) (Figure 3.2B). There was no significant difference in tumour size between uninfected and mice infected with  $5 \times 10^5$  at any time. Therefore, mice infected with  $5 \times 10^6$  CFU SL7207 experienced tumour growth inhibition whilst their wellbeing remained within acceptable guidelines for the duration of the experiment so this was the protocol employed for subsequent experiments.

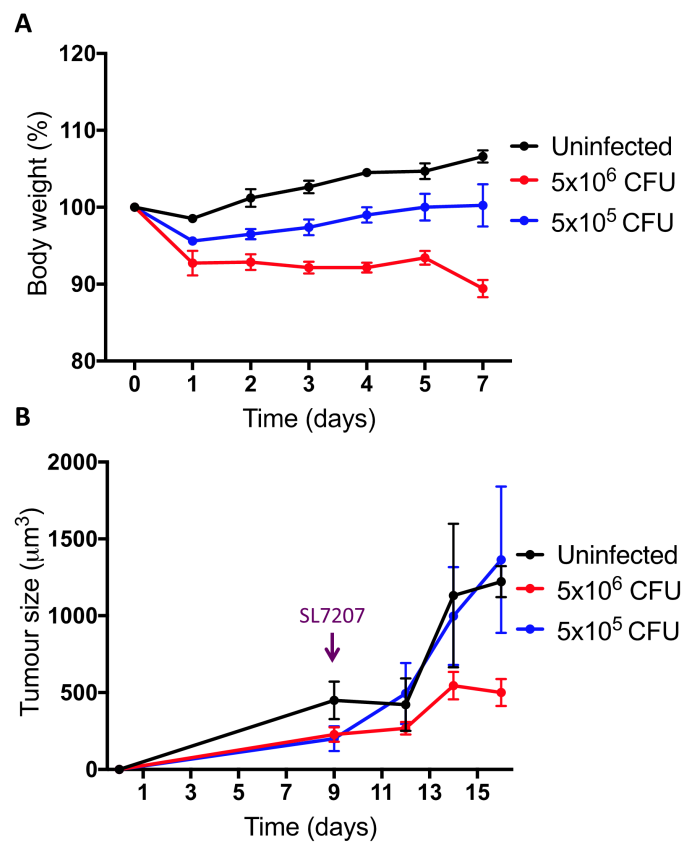


**Figure 3.2 Optimisation of the infectious dose to induce tumour growth inhibition**

Tumour-bearing mice were intravenously inoculated with SL7207 or PBS and weight and tumour sizes were measured over time. **A.** Weight of mice after SL7207 infection at the indicated dose expressed as a percentage of weight at Day 0, when SL7207 was administered. **B.** Tumour size of uninfected mice, and those infected at the indicated dose of SL7207, as measured by Vernier calipers. Purple arrow indicates time point of SL7207 administration. Error bars SEM. Statistical analyses performed using Tukey's multiple comparison test. Stars of significance are omitted due to the high number required, but comparisons of note are detailed in the main text.

### 3.2.3 Understanding the dynamics of SL7207 tumour infection

To understand the infection characteristics of SL7207, it was appealing to construct a strain which could be easily detected *in vivo*. Previous studies have employed the use of bioluminescent reporter strains to identify the *in vivo* localisation of bacteria (Baban *et al.*, 2012; Cronin *et al.*, 2012). Therefore, the 16S*Lux* plasmid-based system to mediate site-directed chromosomal integration of the *luxABCDE* operon derived from *Photobacterium luminescens* into the 16S region of SL7207 was employed (Riedel *et al.*, 2007). Using the *In vivo* Imaging System (IVIS), which is capable of detecting luminescent signal *in vivo*, bioluminescent colonies could be selected. Following the construction of the SL-Lux strain, it was important to verify there were no growth or invasion defects. SL-Lux exhibited a slight lag in growth in comparison to wild type (Figure 3.3A). However, more importantly, the tumour cell invasion of SL-Lux and wild type SL7207 *in vitro* were comparable (Figure 3.3B).

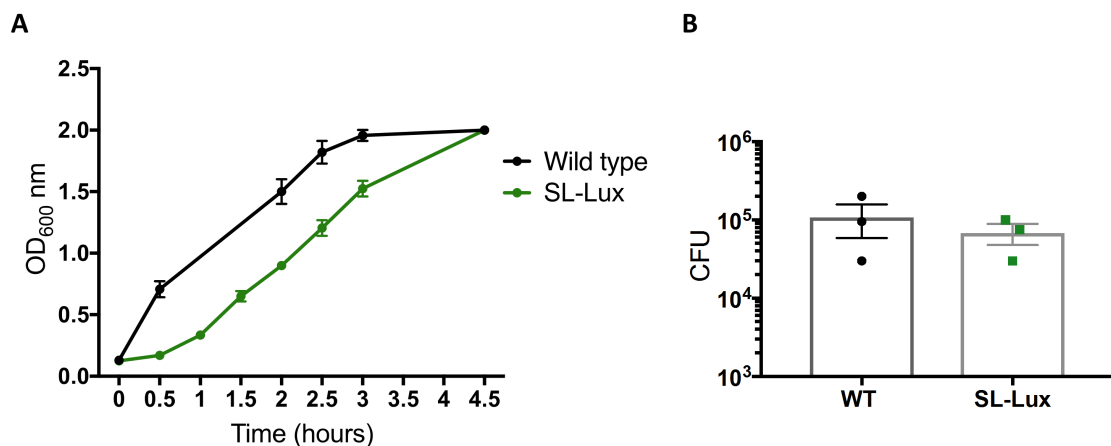


**Figure 3.3 Growth and invasion characteristics of SL-Lux compared to wild type**

Cultures were grown *in vitro*, with regular OD<sub>600</sub> measurements or incubated with B16F10 cells for 2 hours *in vitro* before being subject to CFU counts. **A.** Growth curve of both strains as measured by OD<sub>600</sub>. **B.** CFUs of bacteria recovered from B16F10 tumour cells infected with equal inocula of SL-Lux or wild type SL7207. Error bars SEM. Statistical analysis for B performed using a Student's t test where  $p^* < 0.01$ .

To investigate bacterial localisation *in vivo*, tumour-bearing mice with palpable tumours were infected with  $5 \times 10^6$  CFU SL-Lux via their tail vein. Thereafter, the bioluminescent signal from the tumour as well as the spleen, which is a commonly infected site of systemically administered *S. Typhimurium*, were monitored. According to the IVIS, SL-Lux exhibited high tumour specificity, with

SL-Lux detected in most tumours (Figure 3.4A), whilst there was little or no bioluminescent signal from the spleens (Figure 3.4B).

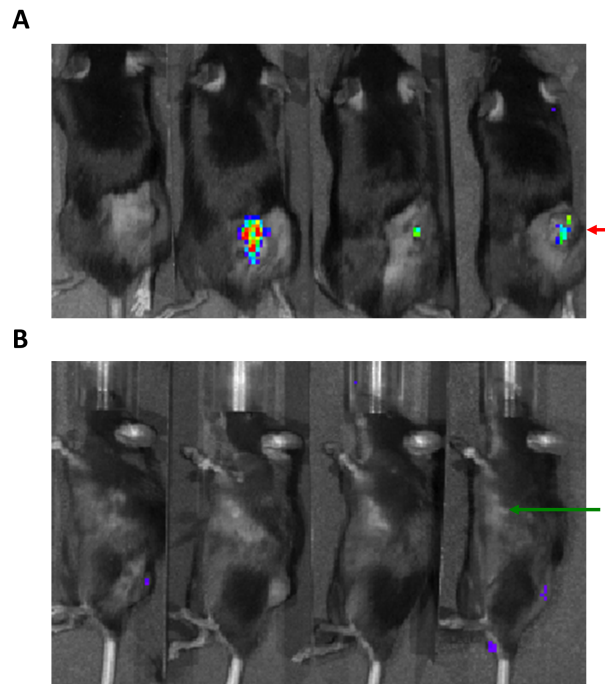


**Figure 3.4** *In vivo* localisation of SL-Lux

Tumour-bearing mice were infected intravenously with SL-Lux and imaged daily using the IVIS to investigate bioluminescent bacterial localization. **A.** Image of the dorsal view of tumour-bearing mice and bioluminescent bacteria. Red arrow indicates the location of the tumour. **B.** Image of the left lateral view of tumour-bearing mice using the IVIS. Green arrow indicates the location of the spleen.

To further investigate the tumour-specific localisation of SL-Lux, the tumour, spleen and liver of infected tumour-bearing mice were harvested at multiple time points, homogenised and serially diluted to acquire the CFU counts of each organ. SL-Lux was capable of infecting all three organs at each time point indicated (Figure 3.5A). There was a significant increase in the CFU/g of SL-Lux in the tumour at 9 dpi compared to either the liver or the spleen. In the tumour, the CFU/g at 9 dpi was also significantly greater compared to 3 and 11 dpi. There were also changes in the CFU/g in the spleen, with an increase at 3 dpi relative to 1 dpi, with subsequent decreases from 3 dpi to both 9 and 11 dpi. The total CFUs for each organ was also assessed (Figure 3.5B). In the tumour, SL7207 infection peaked at 9 dpi and was significantly higher than 1, 3 or 11 dpi. SL7207 infection in the tumour at 9 dpi was also significantly greater than bacterial infection in either the spleen or liver. For the spleen and liver, there was no significant difference in total bacteria recovered between time points.

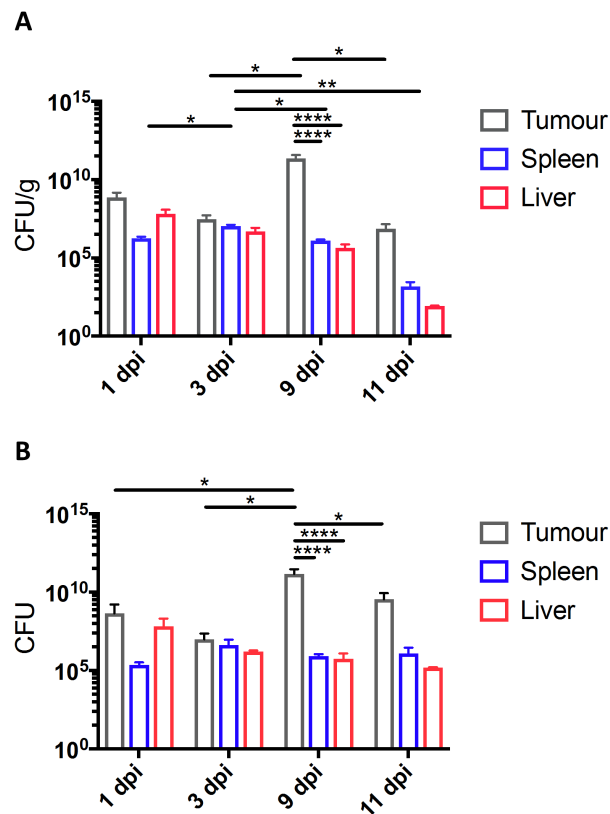


**Figure 3.5 Colony forming unit (CFU) counts from multiple organs following SL-Lux infection**

Tumour-bearing mice were infected intravenously with SL-Lux and specified organs were harvested at the indicated time points and subjected to CFU counts. **A.** Colony forming units (CFUs) of SL-Lux at multiple time points in tumour, liver and spleen, expressed per unit weight, gram (g). **B.** Total CFUs of SL-Lux at multiple time points in tumour, liver and spleen. Statistical analyses performed using Tukey's multiple comparisons tests where  $p < 0.05^*$ ,  $p < 0.01^{**}$ ,  $p < 0.001^{***}$ ,  $p < 0.0001^{****}$ .

There was a degree of variation in the number of CFUs recovered from individual tumours, and it was speculated that there may be a tumour range optimal for tumour colonisation. As such, the tumour size was investigated as a function of tumour colonisation. By comparing the CFUs recovered from a tumour at 1 dpi to the weight of the tumour, there was a positive correlation between tumour weight and CFUs recovered at 1 dpi (Figure 3.6A: R squared value: 0.93,  $p = 0.0001^{***}$ ). SL-Lux was not recovered from tumours weighing less than approximately 100 mg at 1 dpi. This might lead one to hypothesise that as bigger tumours have higher infection burdens, they may be more susceptible to the anti-tumour effects of SL7207. To test this hypothesis, the fold growth of uninfected and infected tumours after 7 days was examined, stratifying the results to tumours in the range of 100-200  $\mu\text{m}^3$  and  $> 200 \mu\text{m}^3$  at the time of infection. For this analysis, tumours less than 100  $\mu\text{m}^3$  were excluded as they were deemed to be less than 100 mg at the time of infection (deduced from interpolation of Figure 3.6B: R squared value: 0.91,  $p < 0.0001^{****}$ ). There was a

significant difference in the fold growth of tumours which were 100-200  $\mu\text{m}^3$  at the time of infection versus uninfected tumours in the same tumour size range (Figure 3.6C). Interestingly, there was no significant difference in fold growth of tumours which were greater than 200  $\mu\text{m}^3$  at the time of infection versus uninfected tumours (Figure 3.6D). The tumour sizes of infected mice were significantly smaller than uninfected mice at 7 dpi, for the tumours within the range of 100-200  $\mu\text{m}^3$  at the time of infection (Figure 3.6E). This is in contrast to the tumours which were  $> 200 \mu\text{m}^3$  at the time of infection, whereby there was no significant difference in the tumour sizes between infected and uninfected samples (Figure 3.6 F). Therefore, although larger tumours were colonised to a greater degree, tumours  $>200 \mu\text{m}^3$  were also less susceptible to the growth arrest effects of SL7207. With this data, it was decided that tumours in the range of 100-200  $\mu\text{m}^3$  at the time of infection were optimal to identify mechanisms for differential growth characteristics of infected and uninfected tumours.

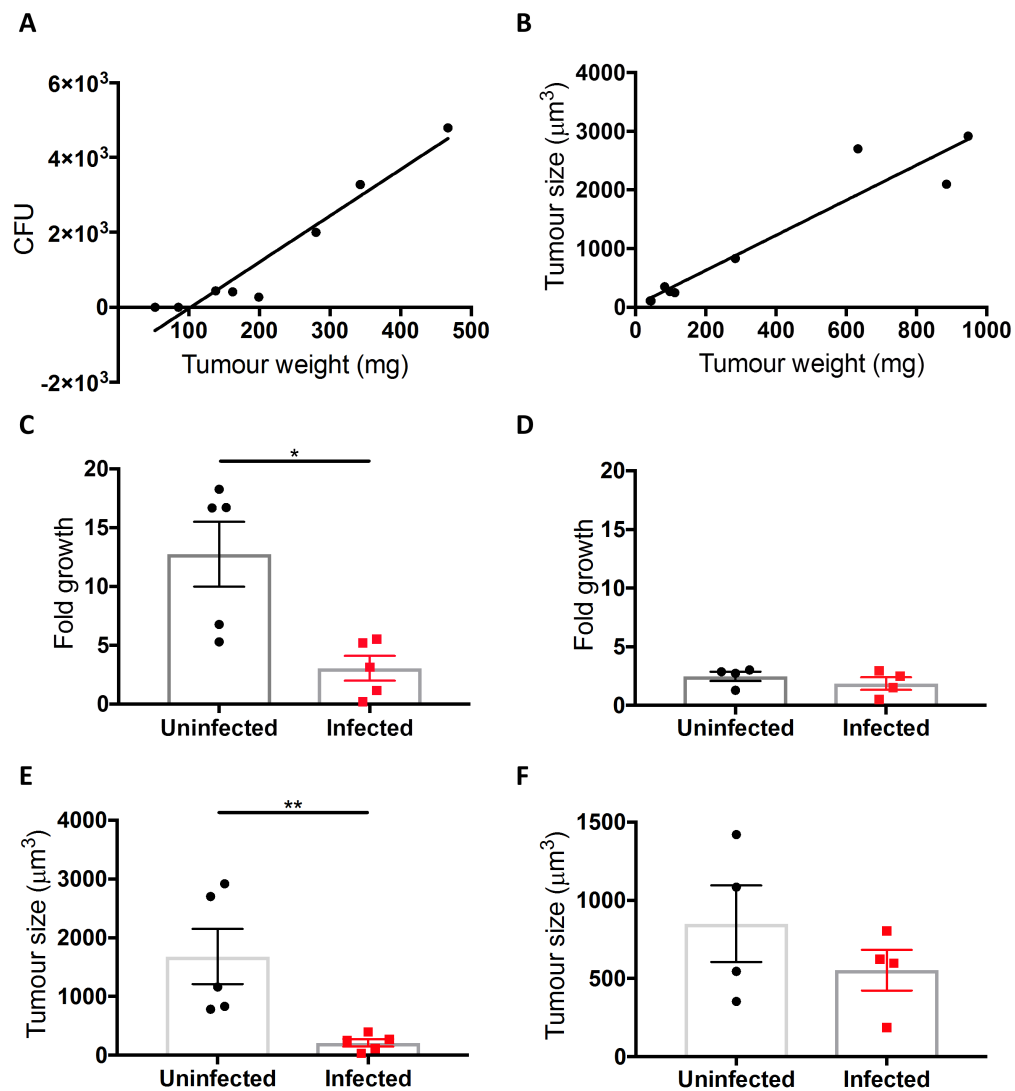


**Figure 3.6 Optimisation of tumour size for SL-Lux infection**

Tumour growth inhibitory effect of SL-Lux was post-hoc analysed by stratifying the tumours into different size categories. **A.** Correlation between CFU recovered at 1 dpi and tumour weight. **B.** Correlation between tumour size and tumour weight. **C.** Fold growth of tumours in the range of 100-200  $\mu\text{m}^3$  (Size at day 7 dpi/Size at day 0) infected with  $5 \times 10^6$  SL-Lux or uninfected. **D.** Fold growth of tumours  $> 200 \mu\text{m}^3$ , infected or uninfected. **E.** Tumour size of infected and uninfected tumours which were of 100-200  $\mu\text{m}^3$  at the time of infection. **F.** Tumour size of infected and uninfected tumours which were of  $> 200 \mu\text{m}^3$  at the time of infection. Error bars SEM (C, D). Statistical analyses performed using a nonparametric Spearman correlation tests (A, B) or Student's t test, (C, D) where  $p < 0.05^*$ .

### 3.2.4 Effects of SL-Lux on tumour growth

After initial analysis of the tumour growth characteristics, the optimal SL-Lux infectious dose and the optimal tumour size for infection to maximise the therapeutic potential, it was appropriate to characterise the therapeutic potential of SL7207. Tumour-bearing mice were infected with  $5 \times 10^6$  CFU SL-Lux at nine days post tumour cell seeding and tumour size was monitored over 7 days. At 5 dpi, there was a significant difference in the tumour size of infected versus uninfected mice ( $p = 0.004^{***}$ ) which continued to 7 dpi ( $p = 0.0032^{**}$ )

(Figure 3.7A). The infected mice also exhibited greater survival ( $p = 0.0004^{***}$ ) than the uninfected group (Figure 3.9B). In fact, it was found that almost half of the infected mice could survive 32 days post tumour cell inoculation, whereas no uninfected mouse was able to survive beyond 17 days. Unsurprisingly, infected mice exhibited splenomegaly (Figure 3.7C). Infected mice significantly lost weight following infection, but their weight began to recover at 3 dpi, and reached pre-infection weight at about 17 dpi (Figure 3.7D).

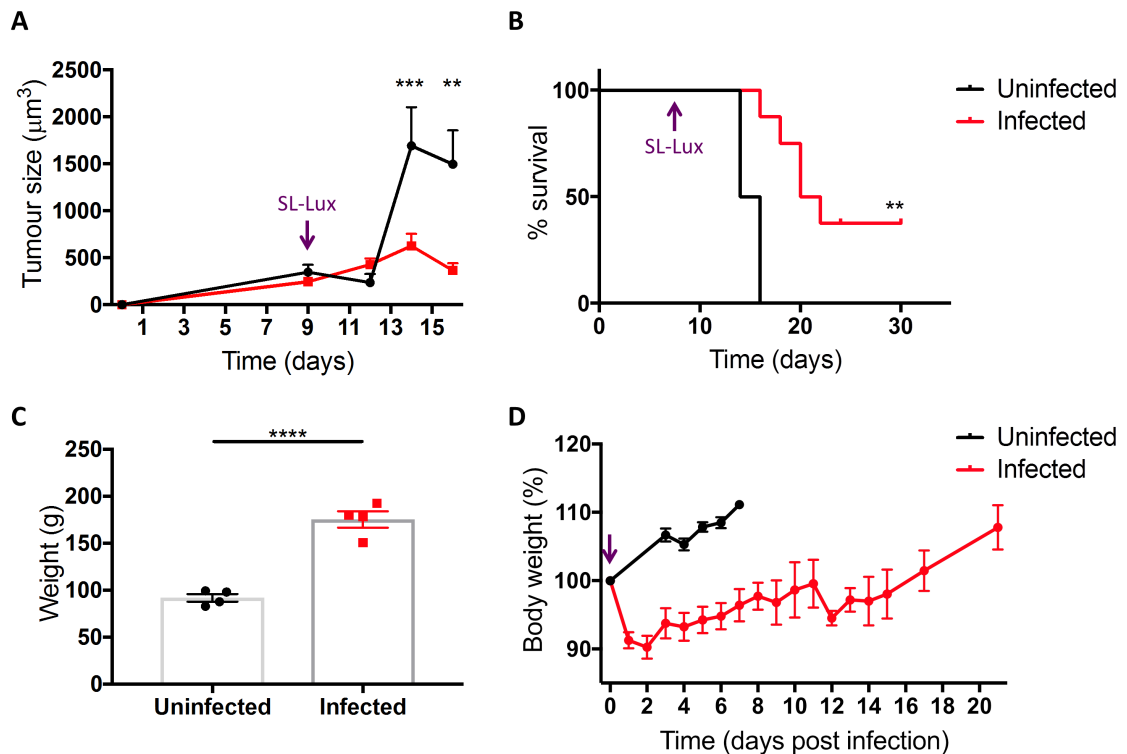


**Figure 3.7 Effects of SL-Lux on tumour growth and survival of tumour-bearing mice**

Tumour-bearing mice were intravenously inoculated with SL-Lux or PBS and tumour size and survival were measured over time. **A.** Tumour sizes of infected and uninfected mice as measured by Vernier calipers. **B.** Kaplan Meier survival curve of tumour-bearing mice infected with SL7207 versus uninfected (purple arrows indicated time point of SL-Lux administration). **C.** Weight of spleens recovered from infected and uninfected mice at 3 dpi. **D.** Weight of mice expressed as a percentage of weight at Day 0 of infection. Error bars SEM. Analysis of A performed using a Sidak's multiple comparisons test. Analysis of B performed using a Log Rank (Mantel-Cox) test. Analysis of C performed using a Student's t test.  $P < 0.05^*$ ,  $p < 0.01^{**}$ ,  $p < 0.001^{***}$ ,  $p < 0.0001^{****}$ .

Furthermore, there was a decrease in tumour fold growth in infected versus uninfected tumours, at 5 and 7 dpi (Figure 3.8A, B). Tumours harvested for analysis at 5 dpi and 7 dpi weighed less for infected tumours than uninfected tumours (Figure 3.8C, D). The differences in tumour size between uninfected tumours and tumours infected for 5 days was also apparent from hematoxylin and eosin staining (Figure 3.8E).

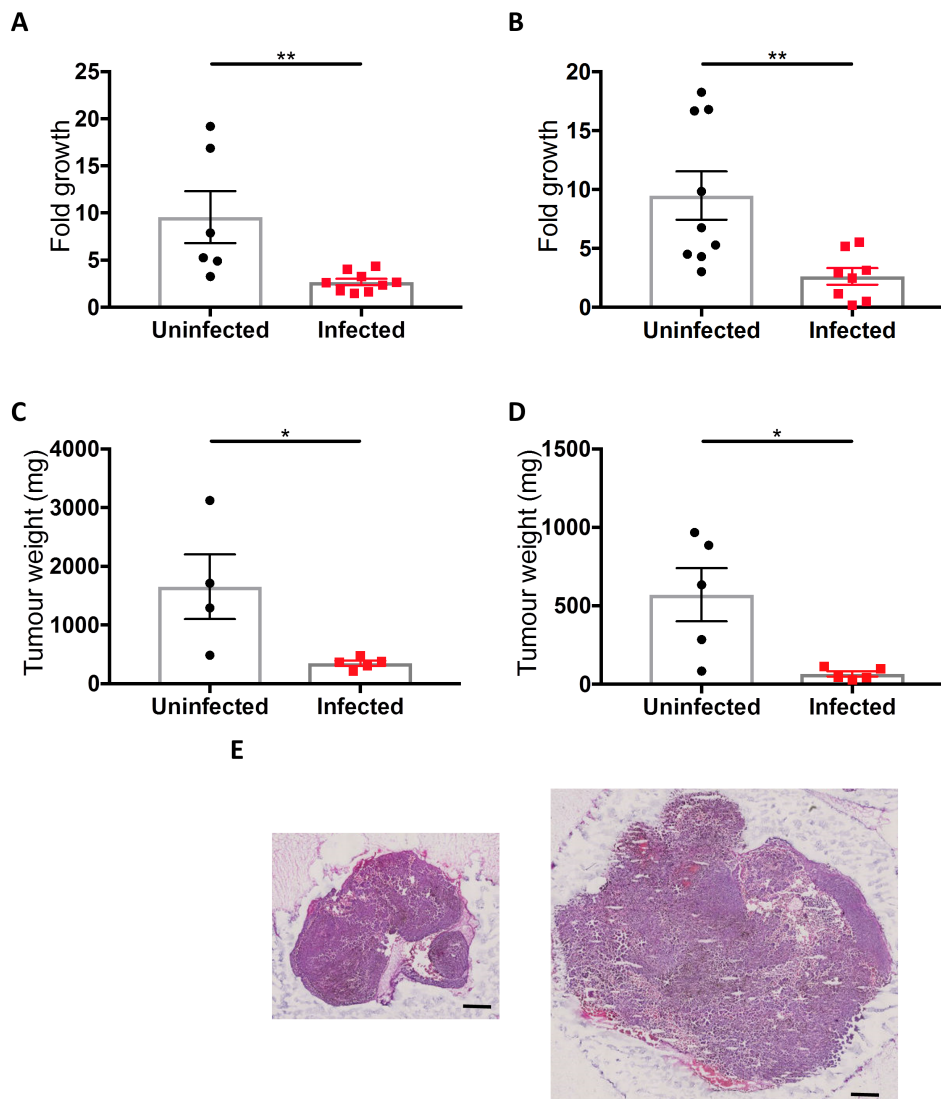


**Figure 3.8 Effects of SL-Lux on tumour fold growth and weight**

Tumour-bearing mice were intravenously inoculated with SL-Lux or PBS and tumour size and weight were analysed. **A.** Fold growth of tumours at the time of harvest 5 dpi compared to tumour size at the time of infection. **B.** Fold growth of tumours at the time of harvest 7 dpi compared to tumour size at the time of infection. **C.** Tumour weight at 5 dpi. **D.** Tumour weight at 7 dpi. **E.** Representative image of hematoxylin and eosin-stained tumours infected (left) and uninfected (right) harvested at 5 dpi (scale bar 1 mm). Statistical analyses performed using Students t test where  $p < 0.05^*$ ,  $p < 0.01^{**}$ .

### 3.2.5 Effects of SL-Lux on tumour cell death and tumour cell replicative capacity

Following SL-Lux administration, tumours did not grow significantly at the time points examined. This could have been due to B16F10 tumour cell death, B16F10 tumour cell replication inhibition or a combination of the two. Both have been reported in the literature (Kuan & Lee, 2016; Yano *et al.*, 2014). In order to investigate the degree of cell viability within the tumour, whole tumours were digested and stained using a viability dye to ascertain the proportion of viable

cells. The samples were then analysed by flow cytometry (gating strategy, Figure 3.9).

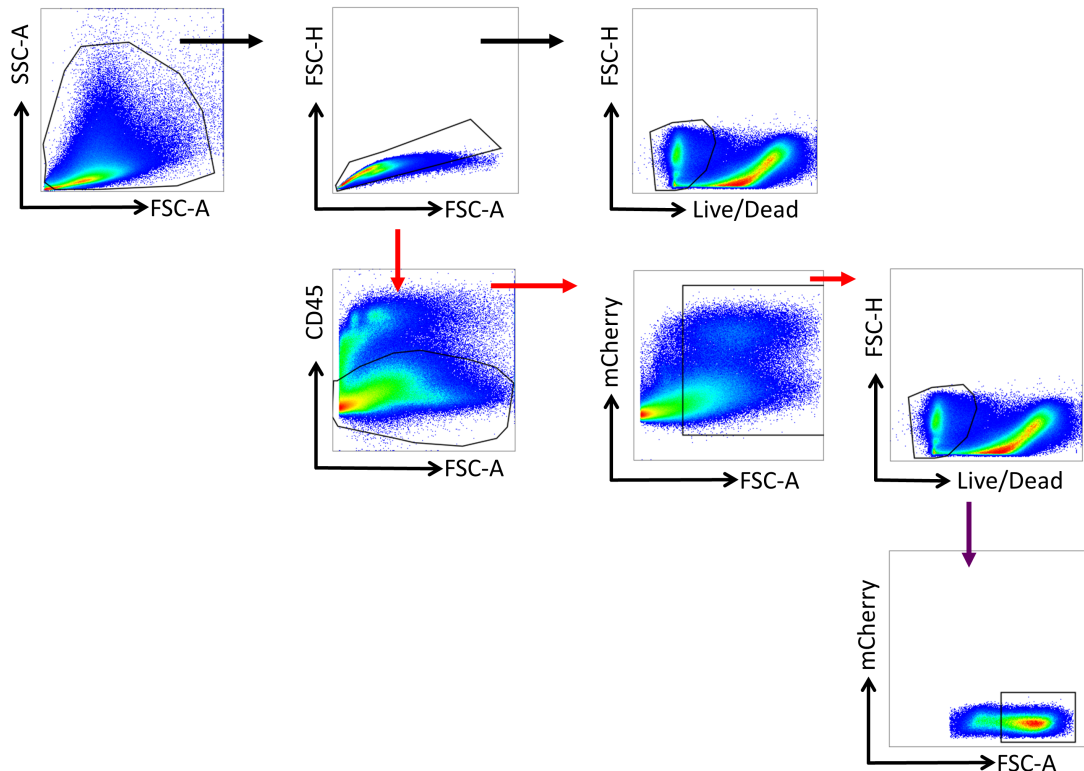


**Figure 3.9 Whole tumour viability and tumour cell gating strategy**

Whole tumours were harvested and analysed flow cytometry. Whole tumour viability (black arrows) was determined by gating on single, live. Live tumour cells (red arrows) gated as single, CD45<sup>+</sup>, FSC-A<sup>hi</sup>, mCherry<sup>+</sup> and live. Ki67<sup>+</sup> tumour cells (red and purple arrows) gated as single, CD45<sup>+</sup>, FSC-A<sup>hi</sup>, mCherry<sup>+</sup>, live, Ki67<sup>+</sup>.

Whole tumours had decreased cell viability at 5 and 7 dpi, but not at 3 dpi (Figure 3.10).

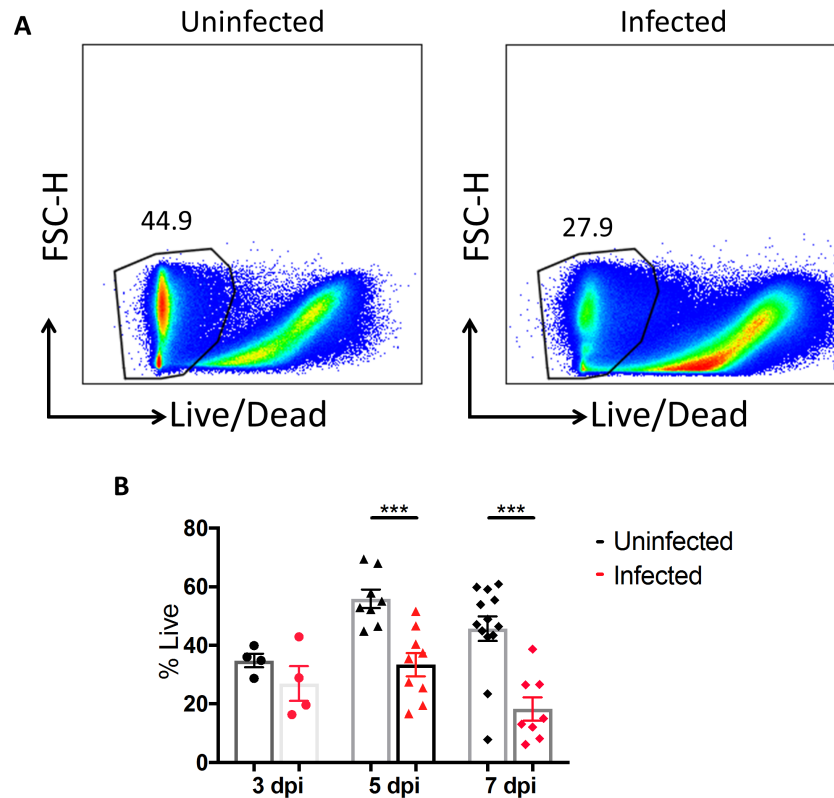


**Figure 3.10 Effects of SL-Lux on whole tumour viability**

Tumour-bearing mice were intravenously inoculated with SL-Lux or PBS and tumours were harvested at defined time points for flow cytometry analysis. **A.** Representative flow cytometry plots show viability tumours from infected and uninfected mice at 5 dpi. **B.** Data are shown as percentage of viable (Live/Dead<sup>+</sup>) cells among total cells at the indicated time points for infected and uninfected samples. Error bars SEM. Statistical analysis performed using Students t test where  $p < 0.05^*$ ,  $p < 0.01^{**}$ ,  $p < 0.001^{***}$ .

To investigate if the B16F10 tumour cells were dying, mCherry-expressing B16F10 cells were employed to accurately gate on the cancer cells according to forward and side scatter characteristics (gating strategy, Figure 3.9). There was a significant decrease in the absolute number of viable B16F10 tumour cells in the infected samples compared to the uninfected at 5 dpi (Figure 3.11A, B). There was also a decrease in the proportion of B16F10 tumour cells among total live cells in the tumour following infection (Figure 3.11C).

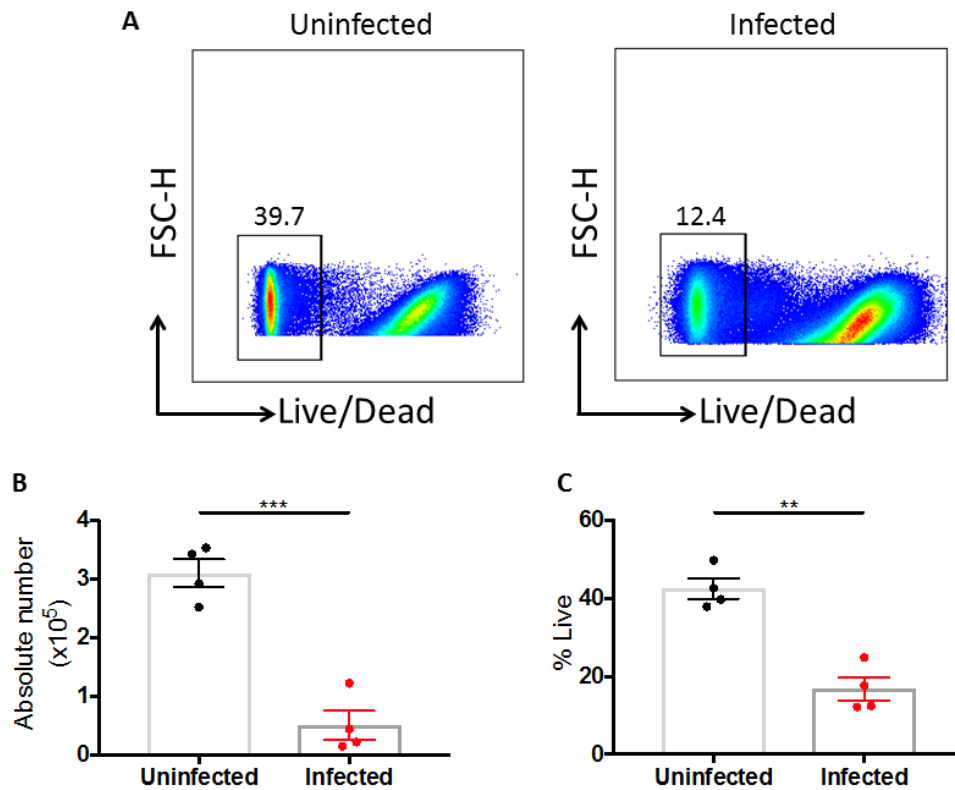


**Figure 3.11 Effects of SL-Lux on tumour cell viability**

Tumour-bearing mice were intravenously inoculated with SL-Lux or PBS and tumours were harvested at 5 dpi for flow cytometry analysis. **A.** Representative flow cytometry plots show viability of infected and uninfected tumour cells. Cells were gated as  $CD45^+$ ,  $FSC-A^{hi}$ . **B.** Quantification of absolute number of tumour cells from infected and uninfected tumours 5 dpi. **C.** Data are shown as percentage of viable (Live/Dead<sup>+</sup>) tumour cells among total tumour cells for infected and uninfected samples. Error bars SEM. Statistical analyses performed using Students t test where  $p < 0.01^{**}$ ,  $p < 0.0001^{****}$ .

B16F10 tumour cell replication was also investigated by staining for Ki67, an intracellular marker which stains recently proliferated cells. By analysing the B16F10 tumour cells staining positive for Ki67, it was apparent that there was no difference in the number of  $Ki67^+$  tumour cells from infected and uninfected samples (Figure 3.12A, B) or the proportion of tumour cells which were  $Ki67^+$  between uninfected and infected samples (Figure 3.12C).

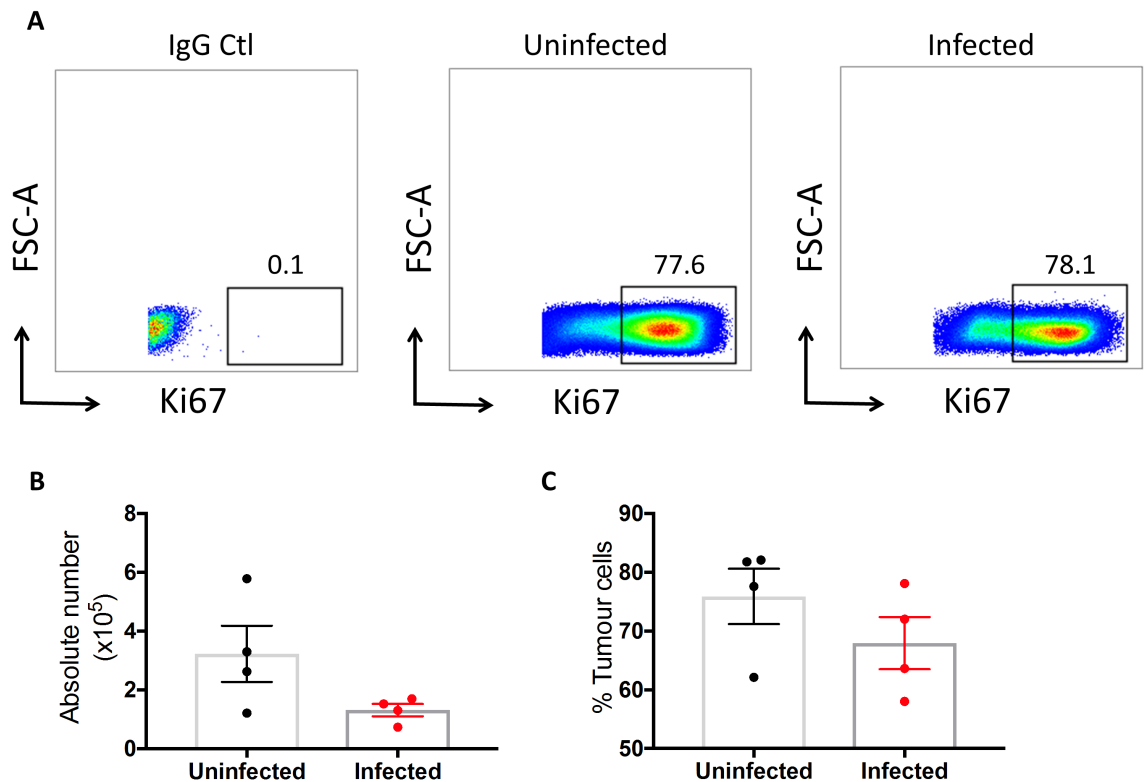


**Figure 3.12 Effects of SL-Lux on tumour cell proliferation**

Tumour-bearing mice were intravenously inoculated with SL-Lux or PBS and tumours were harvested at 5 dpi for flow cytometry analysis. **A.** Representative flow cytometry plots show Ki67<sup>+</sup> tumour cells from infected and uninfected tumours. Cells were gated as single, live, CD45<sup>-</sup>, FSC-A<sup>hi</sup>. **B.** Quantification of the absolute number of Ki67<sup>+</sup> tumour cells from infected and uninfected samples 5 dpi. **C.** Data are shown as percentage of Ki67<sup>+</sup> tumour cells among total live tumour cells from infected and uninfected tumours. Error bars SEM. Statistical analyses performed using Students t test where  $p < 0.05^*$ .

### 3.2.6 *In vitro* tumour cell killing capacity of SL-Lux

Bacteria can directly kill tumour cells *in vitro* and *in vivo* (Chen *et al.*, 2012; Fu *et al.*, 2008). Therefore, it was possible that systemic SL7207 administration could be leading to tumour cell death similarly. To investigate if SL7207 was capable of inducing apoptosis, SL-Lux was co-incubated with B16F10 cells at a multiplicity of infection (MOI) of 100:1 for 24 hours. At this time point, cells were harvested and stained using a viability stain, similar to that described above. There was no significant increase in the proportion of cells which stained positive for the viability dye in the samples infected with either SL7207 or the virulent ancestor SL1344 compared to uninfected control (Figure 3.13).

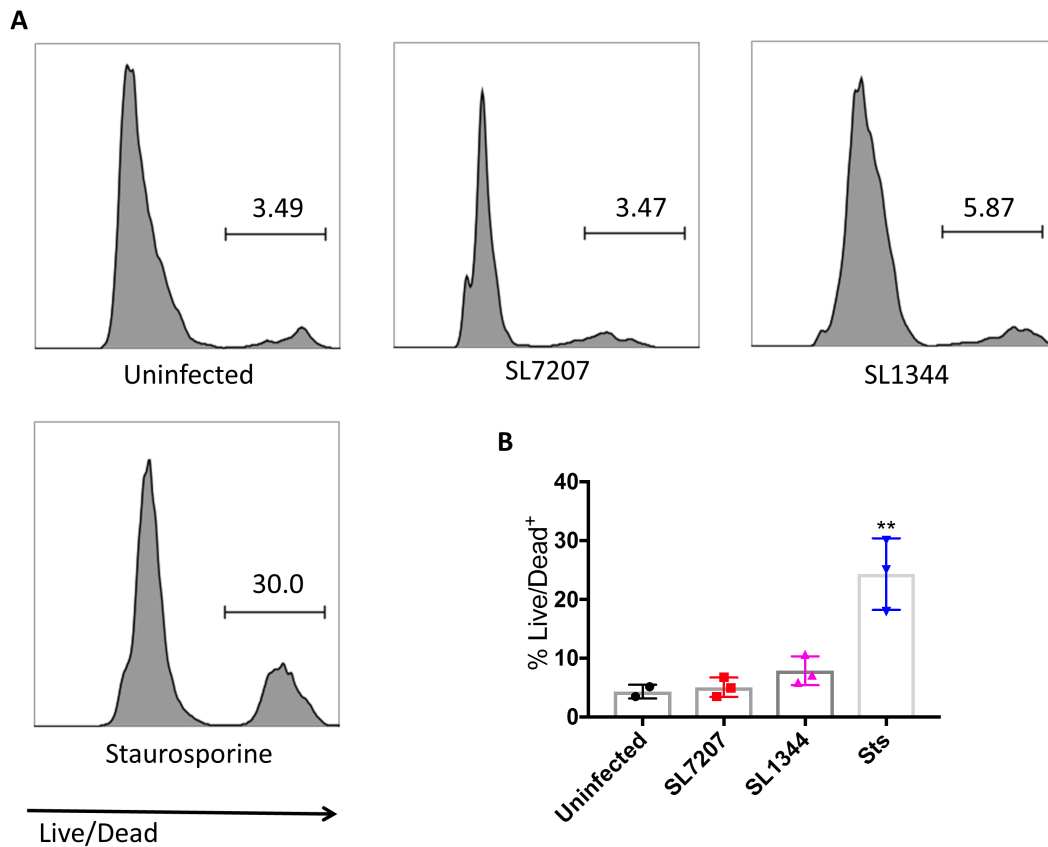


**Figure 3.13 Effects of SL-Lux on tumour cell viability *in vitro***

B16F10 tumour cells were incubated *in vitro* with SL7207 at an MOI of 100:1 for 24 hours before being harvest for flow cytometry analysis. **A.** Representative histograms displaying the expression of Live/Dead viability dye in the indicated samples at 24 hpi. **B.** Data are shown as percentage of dead cells among total cells in each sample. Error bars SEM. Statistical analysis performed using a One Way Anova with multiple comparisons where  $p < 0.05^*$ ,  $p < 0.01^{**}$ .

### 3.3 Discussion

The development of a consistent *in vivo* experimental model is central to testing hypotheses about bacterial-mediated immune responses in cancer. Herein, an *in vivo* tumour model using B16F10 melanoma cells in a C57BL/6 background was developed. Furthermore, the *S. Typhimurium* strain SL7207 was shown to be capable of mediating tumour growth arrest in this model. The optimal bacterial dose and tumour size for infection to maximise the therapeutic effect of the bacteria were identified.

#### 3.3.1 Why is the choice of tumour mouse model important for understanding and interpreting the data?

There are many different tumour mouse models (Zitvogel *et al.*, 2016). It was pertinent that the model chosen for these studies was timely and reproducible. Therefore, it was decided that a transplantable model would be more suitable than a spontaneous model, as with the former, defined time points for experimental manipulation are more apparent and consistent. The two most commonly employed mouse strains for transplantable tumour models are BALB/c and C57BL/6. The latter was chosen for this study for reasons outlined in Section 3.1. However, these mice are skewed towards a  $T_H1$  phenotype which is not directly comparable to humans (Mills *et al.*, 2000; Santos *et al.*, 2006). Humans are extremely heterogeneous in their response to immunological stimuli. Therefore, it is pertinent to note that a single model is rarely sufficient to definitively prove a behaviour or efficacy of a therapeutic intervention. The employment of the C57BL/6 for the present study would likely lead to a bias towards a  $T_H1$  response, which may mask other important immune features of bacterial-mediated tumour growth arrest. This is important to bear in mind in the data described up until now, and for the remainder of the thesis.

Although the transplantable tumour model was highly attractive for the current study, if time had allowed, a spontaneous tumour model would arguably have been more conclusive. The goal of the present study is to identify immune cell responses to the bacteria in the tumour. In human cancer, there is a period of chronic inflammation which can drive transformation and tumourigenesis (Mantovani *et al.*, 2008). Following this period, there is believed to be a

selection process which results in the enrichment of immunosuppressive immune cells dominating the immune landscape of the tumour. These phenomena are reflected in the spontaneous tumour model, but not in the transplantable tumour model (Zitvogel *et al.*, 2016). Therefore, the immune cell infiltrate of the spontaneous tumour model is educated in these processes but the long term effects are uncertain. Furthermore, immune cells of the transplantable tumour model might not reflect the true immune cell infiltrate of a human cancer. Therefore, the data generated from a transplantable tumour model cannot be conclusive without first establishing whether or not there are long term effects on the tumourigenesis-promoting inflammatory process on tumour-resident immune cells. Although interesting, this line of enquiry was outside the remit of the current investigation.

For the present study, these limitations are not apparent as the line of investigation to hand involves determining the change in tumour immune cell phenotype following SL7207 infection, as opposed to characterising these cells in the uninfected state. The hypothesis for the entire study is that the immune cells in the tumour will alter their phenotype from an immunosuppressive phenotype to exhibit pro-inflammatory characteristics. As *S. Typhimurium* is a potent stimulus, it is likely that the immune cells will adopt this phenotype in spite of previous immunological experience. Indeed, it has been demonstrated that both resting and T<sub>H</sub>2-polarised macrophages can adopt a pro-inflammatory, T<sub>H</sub>1 phenotype following LPS treatment *in vitro* (Liu *et al.*, 2013).

### **3.3.2 Implications of colonisation represented as CFU/g**

It was next pertinent to decide upon the dose of bacterial infection. The route of infection was determined to be via intravenous injection, as this is most commonly employed in other bacterial-mediated cancer therapy studies, most likely due to the fact that it is the prospective route of administration in the clinic (Forbes, 2010).

Bacterial dissemination *in vivo* is an important parameter to track to characterise the infection strategy of the bacteria. It was hoped that bacterial dissemination *in vivo* could be monitored through the creation of a

bioluminescent strain of SL7207 (Baban *et al.*, 2012; Riedel *et al.*, 2007). It was possible to visualise the bacteria *in vivo* using the IVIS. There appeared to be tumour-specific localisation in these mice, with little or no bioluminescent signal in the spleen. Furthermore, the degree of colonisation appeared to be variable between mice. However, upon taking these organs, and calculating the CFUs from homogenisation and serial dilutions, it was apparent that the IVIS was unable to definitively determine the location of the bacteria *in vivo*, in contrast to other reports which seemed to be more conclusive (Cronin *et al.*, 2010). All of the organs examined in the present study exhibited bacterial localisation when CFU counts were performed, whether or not there was evident signal from the IVIS. Furthermore, for the tumours, the degree of colonisation reported from the bioluminescent signal using the IVIS was not consistent with the CFU data. Organs were also imaged *ex vivo* (data not shown) but there was no clear correlation between tumour colonisation in terms of CFU and the bioluminescent signal. It was speculated that the most likely explanation for the inaccurate IVIS analyses was the light absorption by the dark B16F10 melanoma cells and the dark skin of the C57BL/6 mice. The combination of these made it more difficult for the light to penetrate the organs and that the bioluminescent signal detected was from bacteria near the surface of the mouse, or at a minimal bacterial density. Therefore, the IVIS data was not used for subsequent analysis.

The CFU counts data was more convincing than the IVIS data as it was evident that the IVIS was not sensitive enough to detect bioluminescent signal in the spleens, in spite of the fact that these were infected. From analysing the CFUs/g isolated from different organs at defined time points following SL-Lux administration, it appeared that the bacteria were capable of replicating in the tumour as well as the spleen. Furthermore, particularly for the liver and spleen, at later time points there appeared to be decreases in the numbers of viable bacteria. However, as it was evident that the infected mice exhibit splenomegaly, this analysis did not control for the possibility that the apparent decreases in bacterial burden may be in fact due to the increasing size of the organ as opposed to the decreasing number of bacteria. To test this hypothesis, the total CFUs of each organ were analysed. This data revealed that there is no significant change in the absolute number of bacteria at any time point in either the liver or spleen. This suggests that the bacteria are not in fact replicating in

the spleen which the CFU/g data would suggest. It also suggests that the bacterial burden in these organs is not decreasing as is often presented in publications as evidence of tumour-specific bacterial localisation and proliferation (Crull *et al.*, 2011a; Low *et al.*, 1999; Stern *et al.*, 2015). By depicting the data as total CFUs, the true bacterial burden of each organ can be seen which clearly depicts the tumour-specific proliferation of SL-Lux.

The investigation of CFU in the tumour was carried out under the assumption that a great degree of tumour-specific localisation is causative of an overall anti-tumour effect. However, this might not necessarily be the case. In Figure 3.2, there looked to be a relationship between the tumour growth inhibitory effects of SL7207 and total body weight loss (suggestive of systemic inflammation). Therefore, possibly tumour localisation is not as important as we initially thought. This is of course assuming that there was still colonisation of the tumour at the lower dose. It would have been informative to measure the CFUs in the tumours of the mice treated with the lower infective dose, to confirm this.

### **3.3.3 Why investigate the optimal conditions for SL7207 infection of tumour-bearing mice?**

In many publications, the principal tumour size for infection is often reported to be within the range of 50-100  $\mu\text{m}^3$  (Crull *et al.*, 2011a; Fu *et al.*, 2008; Kuan & Lee, 2016). However, when analysing the CFUs at 1 dpi, the two smallest tumours (62 and 85 g) did not exhibit bacterial colonisation and the biggest tumour, 467 g, exhibited the greatest. Correlative analysis revealed, unsurprisingly, that there was a strong relationship between the weight of the tumour and the degree of tumour colonisation at 1 dpi (R squared: 0.91). As there was a correlation between tumour size and weight (R squared: 0.91) it was possible to interpolate to identify the minimum size a tumour should be for tumour colonisation by employing a minimum tumour weight of 100 mg. Therefore, only tumours greater than about 100  $\mu\text{m}^3$  were to be used for analysis, refining the previously reported criterion of 50-100  $\mu\text{m}^3$ .

It was tempting to speculate that as the bigger tumours were more susceptible to colonisation, they would also be more susceptible to the tumour growth inhibition effects of the bacteria compared to uninfected controls. Although larger tumours were more colonised, tumours  $> 200 \mu\text{m}^3$  were also less susceptible to the growth arrest effects of SL7207. However, within the tumour size range of 100-200  $\mu\text{m}^3$ , there was a significant difference in the fold growth between infected and uninfected at 7 dpi. This data informed the infection protocol as, henceforth, the optimal range of tumour size for infection was 100-200  $\mu\text{m}^3$  to maximise the differences between infected and uninfected samples so as to easily identify the mechanisms underpinning bacterial-mediated tumour growth inhibition.

These optimal conditions were assessed with a view to keep the parameters within a strict range so as to limit the variability between experiments. Furthermore, by identifying the optimal conditions to maximise SL7207-mediated tumour growth inhibition, it was believed that the therapeutic potential of SL7207 could be more easily identified. The identification of these conditions provided evidence regarding the optimal conditions for treatment in the clinical setting. From the data herein, SL7207 is not effective against larger tumours in the model which suggests that SL7207 might not be a suitable therapeutic option for late-stage tumours. This analysis also alternatively suggests that there were differences in the response of the tumour cells to the bacterial stimulus at different stages of tumour growth. Or possibly represents the possibility that more advanced tumours are more resistant to treatment in general. However, the efficacy of the treatment might be dependent on the cell type, as B16F10 is known to be particularly aggressive. To definitively argue this point, investigations of the tumour growth arrest effects of SL7207 would need to be carried out in other tumour models.

### **3.3.4 How does the tumour growth inhibition of SL7207 compare with other studies?**

With the improved criteria, it was appropriate to fully investigate the effects of SL-Lux on tumour growth in the model. There was a significant difference in the

tumour size of infected and uninfected tumours at 5 and 7 dpi, confirming that SL7207 was capable of inhibiting tumour growth. Furthermore, there was no significant increase in the tumour volume of the infected tumours at 7 dpi from the time of infection, suggesting that the bacteria were mediating tumour growth arrest. In another study which employed the B16F10 model, following systemic infection with a strain of *S. Choleraesuis*, there was a significant difference in the tumour size at 8 dpi, but the difference is not as drastic as it is with the SL-Lux treatment seen herein (Kuan & Lee, 2016). Another study employed the tumour-targeting *S. Typhimurium* strain, VNP20009, and demonstrated that tumour growth was arrested up to 13 days post infection in B16F10 tumour-bearing mice (Luo *et al.*, 2001). The extent of tumour growth inhibition herein was comparable to tumour growth inhibition mediated by other *Salmonella* cancer strains in this, and other mouse models of cancer (Crull *et al.*, 2011a; Luo *et al.*, 2001; Zhang *et al.*, 2015; Zhao *et al.*, 2005). Furthermore, in the present study the infected mice exhibited greater survival than the uninfected mice, with equal or better survival than bacterial therapies reported elsewhere (Yu *et al.*, 2012; Zhang *et al.*, 2015; Zhao *et al.*, 2005; Zhao *et al.*, 2006).

It was also apparent that the major time point of divergence in tumour growth was around 5 dpi, whereas the growth rate of tumours at 5 to 7 dpi were similar between infected and uninfected. This is most likely due to the exponential growth phase of the tumours once they reach a certain size, which was estimated to be 300-500  $\mu\text{m}^3$ . At this phase, the bacteria are capable of having the most therapeutic effect, which is in keeping with the data in Figure 3.6. It is also possible that this is the phase in which the effector cells mediating tumour growth arrest are most active, and points towards these time points as being possibly highly informative for subsequent immune cell analysis.

### **3.3.5 Host welfare: is it safe to use *S. Typhimurium* on cancer patients?**

*S. Typhimurium* is a virulent pathogen. Therefore, there are obviously concerns associated with the safety profile of such a therapeutic treatment. For the present study, the only observable symptoms of SL7207 administration were weight loss and splenomegaly. Splenic cellular infiltration and splenomegaly are

reported to occur following systemic bacterial infection (Johansson *et al.*, 2006), but the possibility that the splenic immune cells, and the pro-inflammatory cytokines they might be secreting systemically has not been considered in any published reports on bacterial-mediated cancer therapy.

Similar to other studies, the infected mice lost weight initially after infection but they appeared to put weight back on 3 dpi, and recover their pre-infection weight at 17 dpi. This recovery in weight is a promising sign for the potential of this strain to be used in the clinic in the future. However, the weight gain of the infected mice seemed to occur at a time when the tumour inhibitory effects of SL7207 were diminished (Appendix, Figure 9.1). Therefore, to maintain the anti-tumour effects of SL7207, it might have been necessary to re-administer, which would mean further weight loss for the subjects. Weight loss in the infected mice in the present study could be mitigated by feeding with treats such as apple flavoured baby food (personal observation). Depending on the type and stage of cancer in question, weight loss can be extremely common with the most cited reason for the weight loss often inappetence (<http://www.cancerresearchuk.org/about-cancer/coping/physically/diet-problems/about/types-of-diet-problems>). In the present study, the most likely explanation for the weight loss observed is systemic inflammation via TNF- $\alpha$  (Di Francia *et al.*, 1994). This therefore raises the possibility that treatment with *S. Typhimurium* could exacerbate the weight loss in cancer patients. Although this hasn't been demonstrated, it is surely an important consideration going forward.

### **3.3.6 SL7207-mediated tumour growth arrest: tumour cell death or cell cycle inhibition?**

The data presented thus far established that SL7207 was capable of mediating tumour growth arrest. However, whether this was due to cell death or attenuation of cell replication remained to be seen. Anecdotally, tumour cell death allows for tumour regression.

Previous reports have shown that different cancer therapy *Salmonella* strains are capable of killing tumour cells (Fu *et al.*, 2008; Kuan & Lee, 2016). In the present study, viability staining of the whole tumour revealed that there was a decrease in viability of the cells in the tumour at 5 and 7 dpi in the infected

samples. However, the tumour is made up of many different cell types including tumour cells, immune cells and stromal cells, which could all be contributing to the decreases viability observed. In order to assess the degree of tumour cell death, it was necessary to be able to identify the tumour cells specifically using flow cytometry. As there are few commercially available antibodies against B16F10 cells for flow cytometry, mCherry-expressing B16F10 tumour cells were acquired. These cells contain a mCherry-expressing plasmid with a resistance cassette ensuring the expression of mCherry in all cells in the population in culture. These cells were seeded into C57BL/6 mice to form tumours, before being infected with SL-Lux for five days. At this time point, (14 days post inoculation), it was likely that in the absence of the antibiotic selection coupled with exponential tumour cell replication, many of the cells would have lost the mCherry expression. Nonetheless, only a small population of mCherry-expressing tumour cells was required to be able to set the gate for *in vivo* tumour cells. It was not possible to use tumour cells directly from *in vitro* culture to determine the gate for *in vivo* tumour cells as the shape and size of cells within the tumour *in vivo* differ from the shape and size *in vitro* (personal observation). Therefore, there was confidence that this gate was of B16F10 tumour cells. However, in order to control for the possibility that there were contaminating CD45<sup>-</sup> stromal cells, there should have been a dump channel for CD31<sup>+</sup> endothelial cells and Vimentin<sup>+</sup>desmin<sup>+</sup> fibroblasts which were possibly contaminating this gate. It is unlikely that these cells were in the gate, as they are much smaller than the large tumour cells and the FSC-A<sup>hi</sup> gating strategy likely excluded them.

It was also of interest whether the bacteria were inhibiting tumour cell replication in this model, as *Salmonella*-mediated tumour cell cycle arrest was previously reported (Yano *et al.*, 2014). To investigate the replication potential of the tumour cells after infection, single cell suspensions were gated for tumour cells as before and the proportion of Ki67<sup>+</sup> replicating cells was analysed. There was no change in the proportion of tumour cells Ki67<sup>+</sup>, suggesting that SL7207 were not affecting the ability of the tumour cells to replicate, either directly or indirectly. This was surprising, as changes in the tumour microenvironment have been reported to have an effect on tumour replication. For example, macrophages are key providers of growth factors which stimulate tumour cell proliferation (Sullivan *et al.*, 1993). Furthermore, it has been postulated that

bacteria in the tumour can compete with tumour cells for nutrients, which should decrease the proliferation capacity of tumour cells (Forbes, 2010).

Multiple *Salmonella* strains have been reported to directly kill tumour cells *in vitro* and *in vivo* (Fu *et al.*, 2008; Kuan & Lee, 2016). The ability of SL7207 to induce tumour cell death in B16F10 melanoma cells was investigated but there was no increase in cell death after 24 hours *in vitro*. As the bacteria are not killing the cells directly, it is possible that other factors are mediating tumour growth inhibition, such as the immune system.

### **3.3.7 Concluding remarks**

The data presented herein provides evidence for a reproducible protocol for an *in vivo* B16F10 tumour model in C57BL/6 mice, which is arrested in growth following systemic SL-Lux infection. Therefore, this was a suitable model to investigate the changes in the hypothesised inflammatory microenvironment of the tumour following infection, and the cell types which might be contributing to, and necessary for this process.

## 4 Characterisation of the local immune response in the tumour following systemic administration of SL7207

### 4.1 Introduction

Multiple reports have provided evidence for the involvement of the immune system in bacterial-mediated cancer therapy (Lee *et al.*, 2008; Saccheri *et al.*, 2010; Stern *et al.*, 2015). There is evidence to support a role for neutrophils and dendritic cells (DCs) in impeding and promoting bacterial-mediated cancer therapy, respectively (Saccheri *et al.*, 2010; Westphal *et al.*, 2008). Macrophages have also been implicated in playing a role in bacterial-mediated cancer therapy, but these will be discussed in detail in Chapter 5. Other studies have focused on the T cell response, providing evidence for the importance of CD4<sup>+</sup> and CD8<sup>+</sup> T cell responses in the tumour for mediating tumour inhibition following infection (Kaimala *et al.*, 2014; Stern *et al.*, 2015). Perhaps the most convincing evidence for immune involvement in bacterial mediated cancer therapy is the finding that CT26 tumour-bearing mice whose tumour was cleared following bacterial treatment are protected from subsequent tumour formation following a second inoculation with CT26 cells, but not control F1A11 tumour cells (Stern *et al.*, 2015). This finding suggests immune memory involvement in the protection against tumour formation.

It has been well documented that the immune system plays an important role in driving and shaping tumourigenesis (Coffelt *et al.*, 2016; Qian & Pollard, 2010). It has also been well documented that the tumour microenvironment develops an immunosuppressive setting which can be highly effective at protecting the tumour from immune detection (Zou, 2005). However, information on the exact nature of the local and systemic overall immune responses to systemically administered *S. Typhimurium* in tumour-bearing mice is currently lacking. Given that the tumour microenvironment is generally regarded as immunosuppressive, and that *S. Typhimurium* is a potent immune activator, it was hypothesised that the tumour microenvironment would become pro-inflammatory following SL7207 administration, which is not permissive to tumour cell growth (Andzinski *et al.*, 2016; Bromberg *et al.*, 1996; Wall *et al.*, 2003). It was also hypothesised that

the tumour would experience increased immune cell infiltration and activated T cell responses following SL7207 infection.

#### **4.1.1 Aims**

1. To characterise the changes in the inflammatory status of the tumour following SL7207 infection
2. To understand immune cell infiltration and the activation of neutrophils and DCs following SL7207 infection
3. To understand the type of T cell response in the tumour following SL7207 infection

## 4.2 Results

### 4.2.1 Leukocyte content of B16F10 tumour

Tumour infiltrating leukocytes play an important role in tumour establishment, development, metastasis of tumour cells, as well as metastatic cell seeding at distal sites (Qian & Pollard, 2010; Zou, 2005). Previous reports have characterised the presence of immune cell infiltrates in the B16F10 melanoma tumour model, including neutrophils, macrophages, dendritic cells, T cells and B cells (Kobayashi *et al.*, 2014; Laoui *et al.*, 2016; Nakahara *et al.*, 2016; Torcellan *et al.*, 2017). It was important to verify that the immune infiltration profile of the tumours in our model corresponded to published data. To do this, mice were allowed to develop tumours for various lengths of time before tumours were excised, enzymatically digested and subjected to flow cytometry analysis of major immune cell constituents of the tumour including eosinophils, neutrophils, DCs, macrophages, monocytes, T cells and B cells (Gating strategy Figure 4.1).

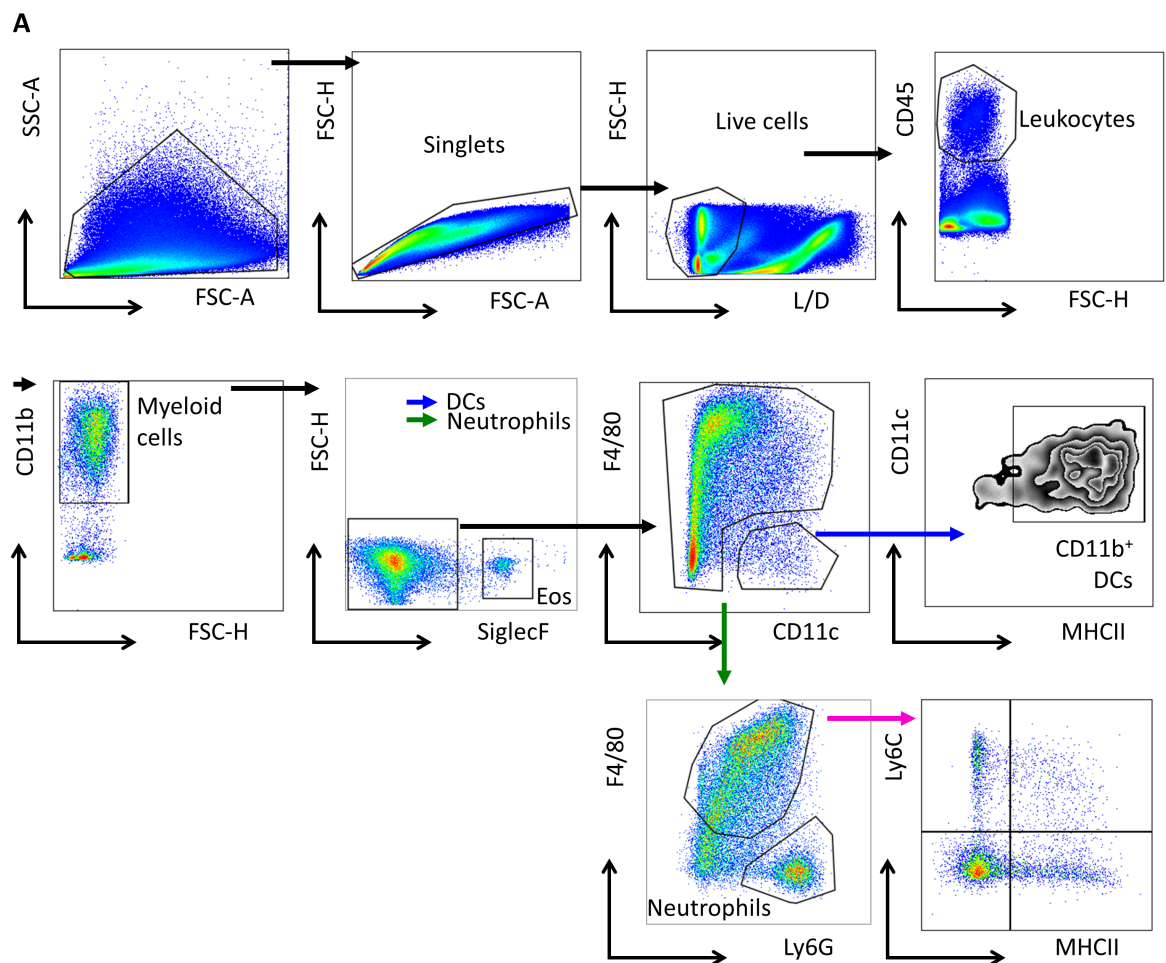
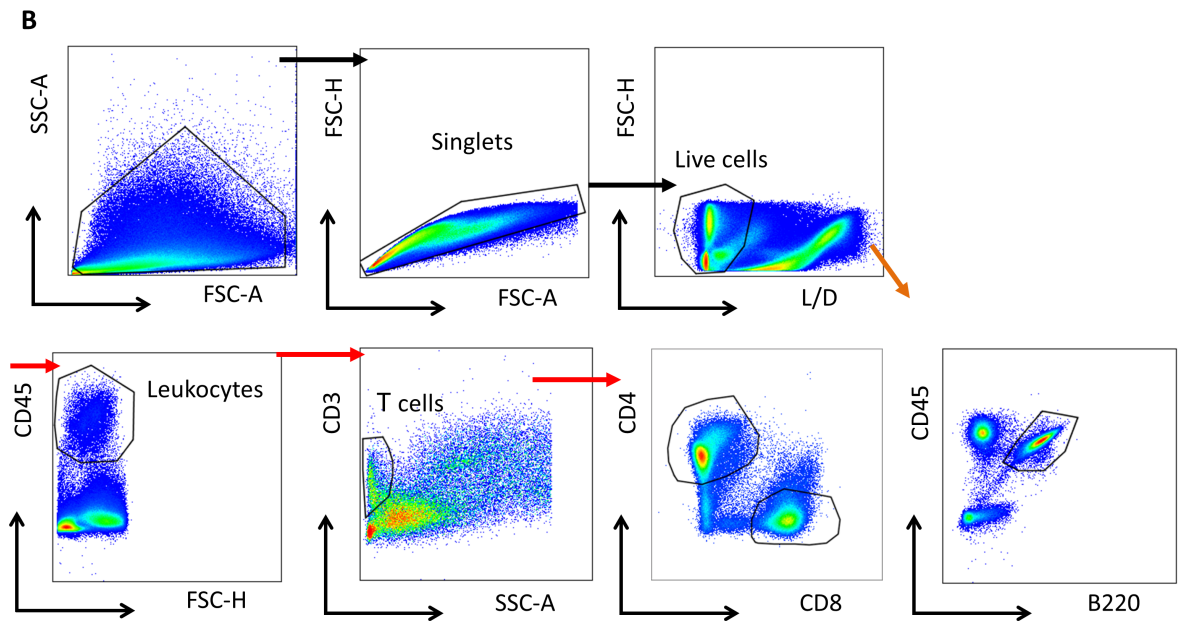


Figure 4.1 continued on the next page



**Figure 4.1 Gating strategies for immune cells in the tumour and tdLN**

**A.** Tumour eosinophils (eos; black arrows) were gated as single, live,  $CD45^+$ ,  $CD11b^+$ ,  $SiglecF^+$ . Tumour neutrophils (black and green arrows) were gated as single, live,  $CD45^+$ ,  $CD11b^+$ ,  $SiglecF^-$  (to exclude eosinophils),  $CD11c^-$  (to exclude DCs),  $F4/80^-$  (to exclude monocytes/macrophages),  $Ly6G^+$ . Tumour DCs (black and blue) were gated as single, live  $CD45^+$ ,  $CD11b^+$ ,  $SiglecF^-$  (to exclude eosinophils),  $F4/80^-$  (to exclude monocytes/macrophages),  $CD11c^+$ ,  $MHCII^+$ . Tumour macrophages and monocytes (black, green and pink arrows) were gated as single, live  $CD45^+$ ,  $CD11b^+$ ,  $SiglecF^-$  (to exclude eosinophils),  $F4/80^+$  and distinguished between monocytes ( $Ly6C^+$ ) and macrophages ( $Ly6C^-$ ). **B.** Tumour and lymph node T cells (black and red arrows) were gated as single, live,  $CD45^+$ ,  $CD11b^+$ ,  $CD3^+$ ,  $SSC^{lo}$  and  $CD4^+$  or  $CD8^+$ . Tumour B cells (black and orange arrows) were gated as single, live,  $CD45^+$ ,  $B220^+$ .

Each of these immune cells has been implicated as being permissive to tumour growth, as well as being targets for therapeutic intervention to inhibit tumour growth. At 12 days post B16F10 tumour cell seeding in C57BL/6 mice, immune cells ( $CD45^+$  cells) made up approximately one-third of all live cells ( $33.43\% \pm 5.49\%$ ) (Figure 4.2A). Consistent with previous reports (O'Sullivan & Lewis, 1994; Williams *et al.*, 2016),  $CD11b^+$   $SiglecF^-$   $F4/80^+$   $Ly6G^-$   $Ly6C^-$  tumour-associated macrophages (M $\phi$ ) were the predominant immune cell population present in the tumour ( $16.4\% \pm 5.6\%$ ) followed by  $CD11b^+$   $SiglecF^-$   $F4/80^+$   $Ly6G^-$   $Ly6C^+$  monocytes (Mo;  $11.28\% \pm 2.61\%$ ) and  $CD11b^+$   $SiglecF^+$  eosinophils (Eos;  $9.81\% \pm 1.57\%$ ) (Figure 4.2B).  $CD11b^+$   $SiglecF^-$   $F4/80^-$   $Ly6G^+$  neutrophils (NT;  $7.87\% \pm 5.13\%$ ) and  $CD11b^+$   $SiglecF^-$   $F4/80^-$   $CD11c^+$   $MHCII^+$  DCs ( $2.30\% \pm 0.318\%$ ) were also quantified. There was also a population of immune cells ( $52.38\% \pm 9.99\%$ ) which were not identified using the antibody panel employed, but were most likely to be made up of B cells, natural killer cells, innate lymphoid cells amongst others. Four days subsequently, at 16 days post tumour cell inoculation,  $CD45^+$  immune cells made up a smaller proportion of the tumour ( $16.8\% \pm 13.19\%$ ), but this was highly variable (Figure 4.2C). Once again, the predominant immune cell population

analysed was the TAMs making up about one-quarter of the immune cell infiltrate ( $26.26\% \pm 2.829\%$ ) (Figure 4.2D). This was followed by T cells ( $T$ ;  $12.48\% \pm 8.99\%$ ), monocytes ( $9.05\% \pm 4.06\%$ ) and neutrophils ( $7.146\% \pm 6.25\%$ ). Eosinophils ( $5.35\% \pm 3.26\%$ ), B cells ( $B$ ;  $3.26\% \pm 2.60\%$ ) and DCs ( $1.41\% \pm 1.02\%$ ) were also accounted for in the tumour mass. There was approximately 35.03% of  $CD45^+$  immune cells which were not accounted for with this panel.

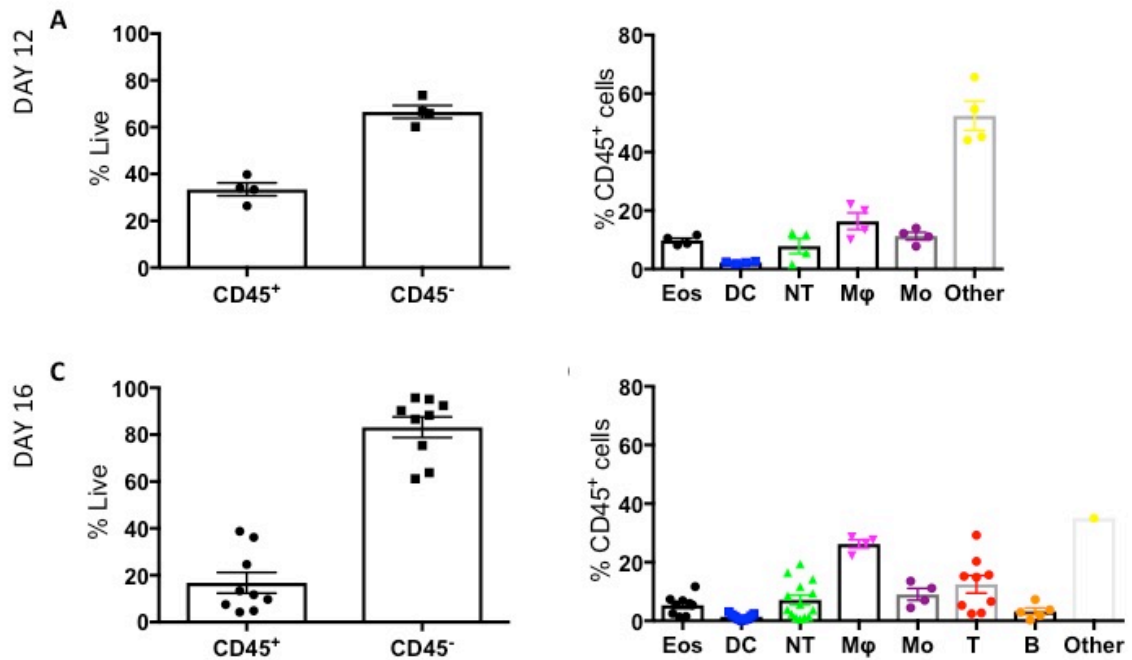


**Figure 4.2 Tumour immune cells at indicated time points**

Tumours were harvested at 12 and 16 days post B16F10 tumour cell seeding in C57BL6 mice for flow cytometry analysis of immune cell populations. **A.** Data are shown as percentage of total live cells at 12 days post tumour cell seeding. **B.** Data are shown as percentage  $CD45^+$  cells for each population. **C.** Data are shown as percentage of total live cells at 16 days post tumour cell seeding. **D.** Data are shown as percentage  $CD45^+$  cells for each population. Error bars SEM.

#### 4.2.2 Changes in the production of pro-inflammatory mediators in the tumour following systemic SL7207 infection

In order to ascertain the changes in the inflammatory status of the tumour following infection, tumours from infected and uninfected mice were harvested at 5 dpi. Whole tumour suspensions were harvested and stimulated *in vitro* for four hours, before the supernatant was collected for enzyme-linked immunosorbent assay (ELISA) analysis. The infected tumours secreted greater quantities of the pro-inflammatory mediator interferon ( $IFN$ )- $\gamma$  at 5 days post infection (dpi) than the uninfected, and appeared to at 7 dpi, but this was not statistically significant (Figure 4.3A). There was also a significant increase in the secretion of tumour necrosis factor ( $TNF$ )- $\alpha$  from the infected tumours compared

to the uninfected at both 5 and 7 dpi (Figure 4.3B). For intracellular cytokine analysis, some of the cells harvested for ELISAs were separately incubated with a protein transport inhibitor to sequester cytokines intracellularly to allow for antibody staining. This analysis revealed an increase in the amount of IL-12p40 in the infected samples compared to the uninfected, but this was not statistically significant ( $p = 0.0506$ , Figure 4.3C, D). IL-12p40 is a subunit of both IL-12 and IL-23, both of which are pro-inflammatory cytokines. However, there was a significant increase in the expression of IL-6 in the infected tumours at this time point (Figure 4.3E, F). These data suggest that the tumour microenvironment adopted an inflammatory phenotype following infection. Unfortunately, neither spleens nor serum samples were harvested at this time for similar analysis.

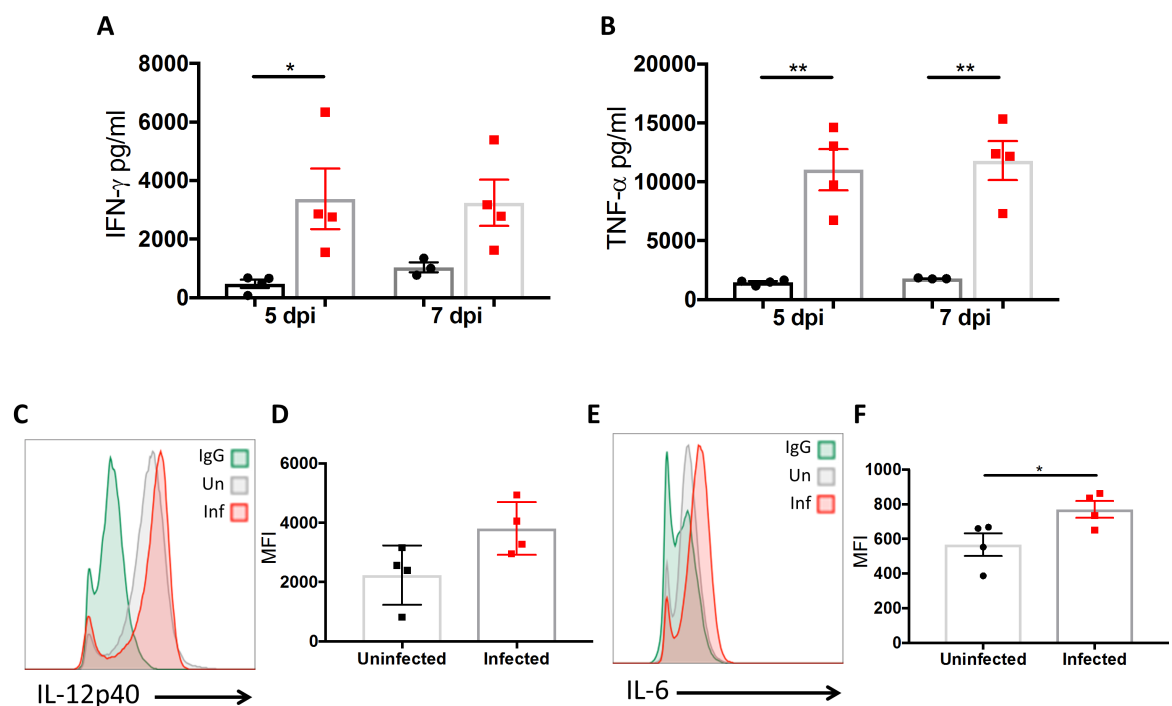


**Figure 4.3 Effects of SL7207 on the production of pro-inflammatory cytokines in the tumour**  
 Tumour-bearing mice were inoculated with SL7207 or PBS and tumours were harvested at 5 dpi, stimulated *in vitro* and the cytokine production analysed by ELISA or flow cytometry. **A.** Whole tumour IFN- $\gamma$  production from infected (red) and uninfected (black) tumours. **B.** Whole tumour TNF- $\alpha$  production from infected (red) and uninfected (black) tumours. **C.** Representative histogram plot of whole tumour IL-12p40 expression from infected and uninfected tumours. Cells were gated on single, live. **D.** MFI of IL-12p40 expression from infected (red) and uninfected (black) tumours. **E.** Representative histogram plot of whole tumour IL-6 expression from infected and uninfected tumours. Cells were gated on single, live. **F.** MFI of IL-6 expression from infected (red) and uninfected (black) tumours. Error bars SEM. Statistical analyses performed using Student's t test were  $p < 0.05^*$ ,  $p < 0.01^{**}$ .

### 4.2.3 Changes in the total number of leukocytic cell infiltrates in tumours infected with SL7207

Given the changes in the production of pro-inflammatory mediators in the tumour, it was hypothesised that infiltrating leukocytes might be contributing to the inflammatory environment established following infection. Therefore, at multiple time points post infection, tumours were harvested and subjected to flow cytometry analysis of immune cell populations. Following SL7207 infection, there was no significant change in the number of CD45<sup>+</sup> immune cells in the tumour at 3, 5 or 7 dpi (Figure 4.4A, B). The number of cells recovered from tumours was variable so this data was transformed ( $Y = \text{Log}(Y)$ ) and represented as such throughout. However, there was an increase in CD45<sup>+</sup> cells as a proportion of live cells at 5 and 7 dpi (Figure 4.4C).

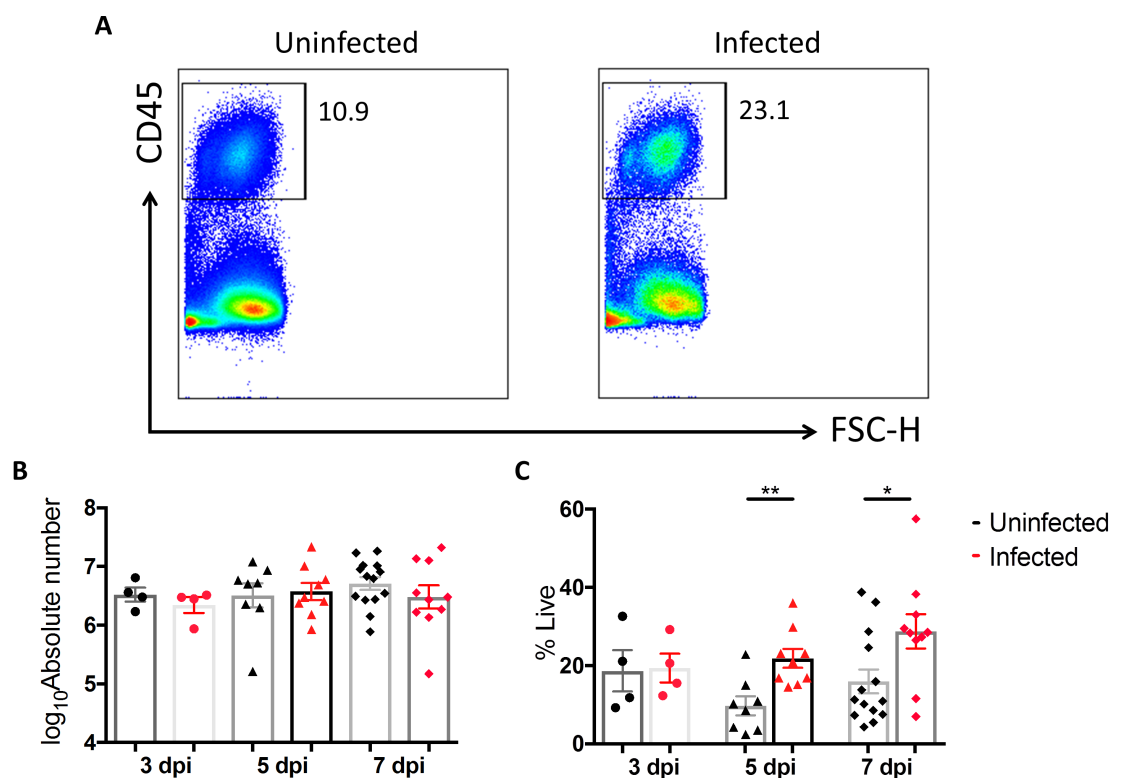
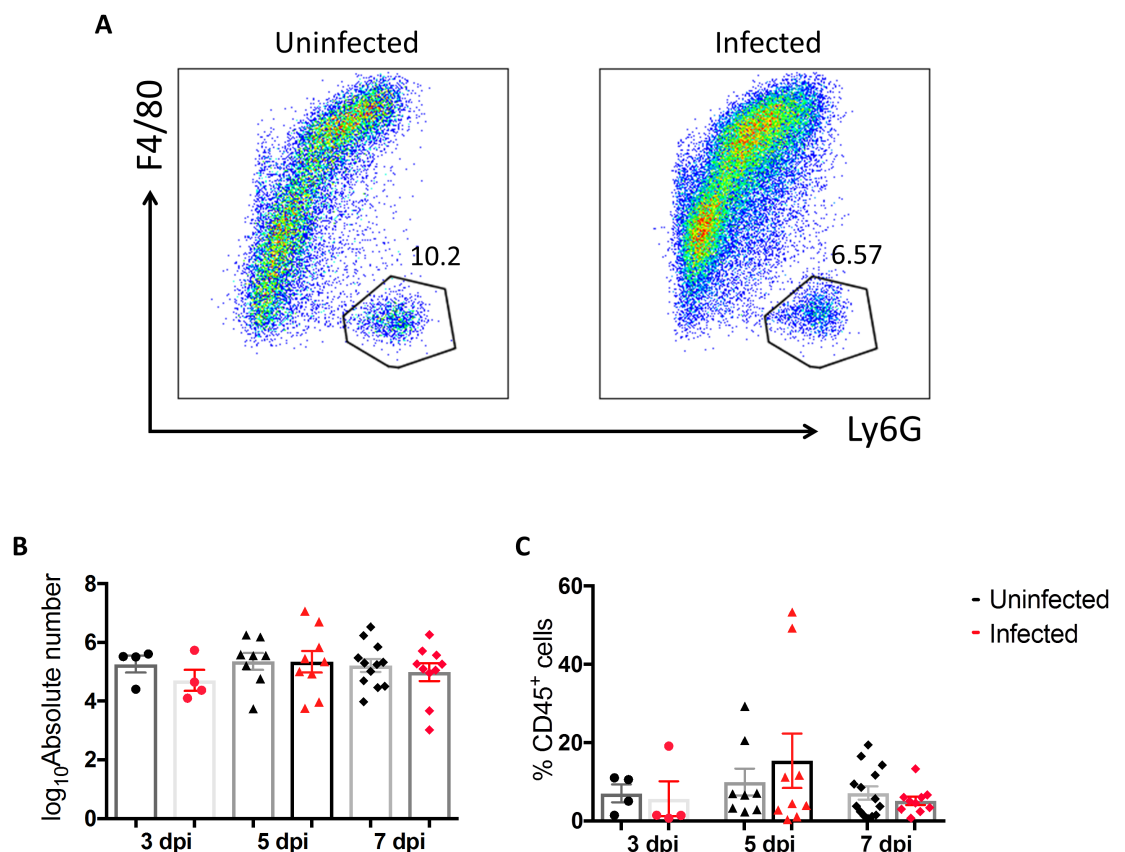


**Figure 4.4 Effects of SL7207 on the tumour CD45<sup>+</sup> immune cell content**

Tumour-bearing mice were inoculated with SL7207 or PBS and tumours were harvested at 3, 5 and 7 dpi for flow cytometry analysis of tumour immune cell content. **A.** Representative flow cytometry plots of CD45<sup>+</sup> cells from infected and uninfected tumours at 5 dpi. Cells were gated on single, live. **B.** Quantification of absolute number of CD45<sup>+</sup> immune cells from infected and uninfected tumours at the indicated time points. **C.** Data shown as percentage CD45<sup>+</sup> of total live cells from infected and uninfected tumours at the indicated time points. Error bars SEM. Statistical analyses performed using Student's t test between infected and uninfected samples at the same time point where  $p < 0.05^*$ ,  $p < 0.01^{**}$ .

#### 4.2.4 Effects of systemic SL7207 infection of tumour-associated neutrophils

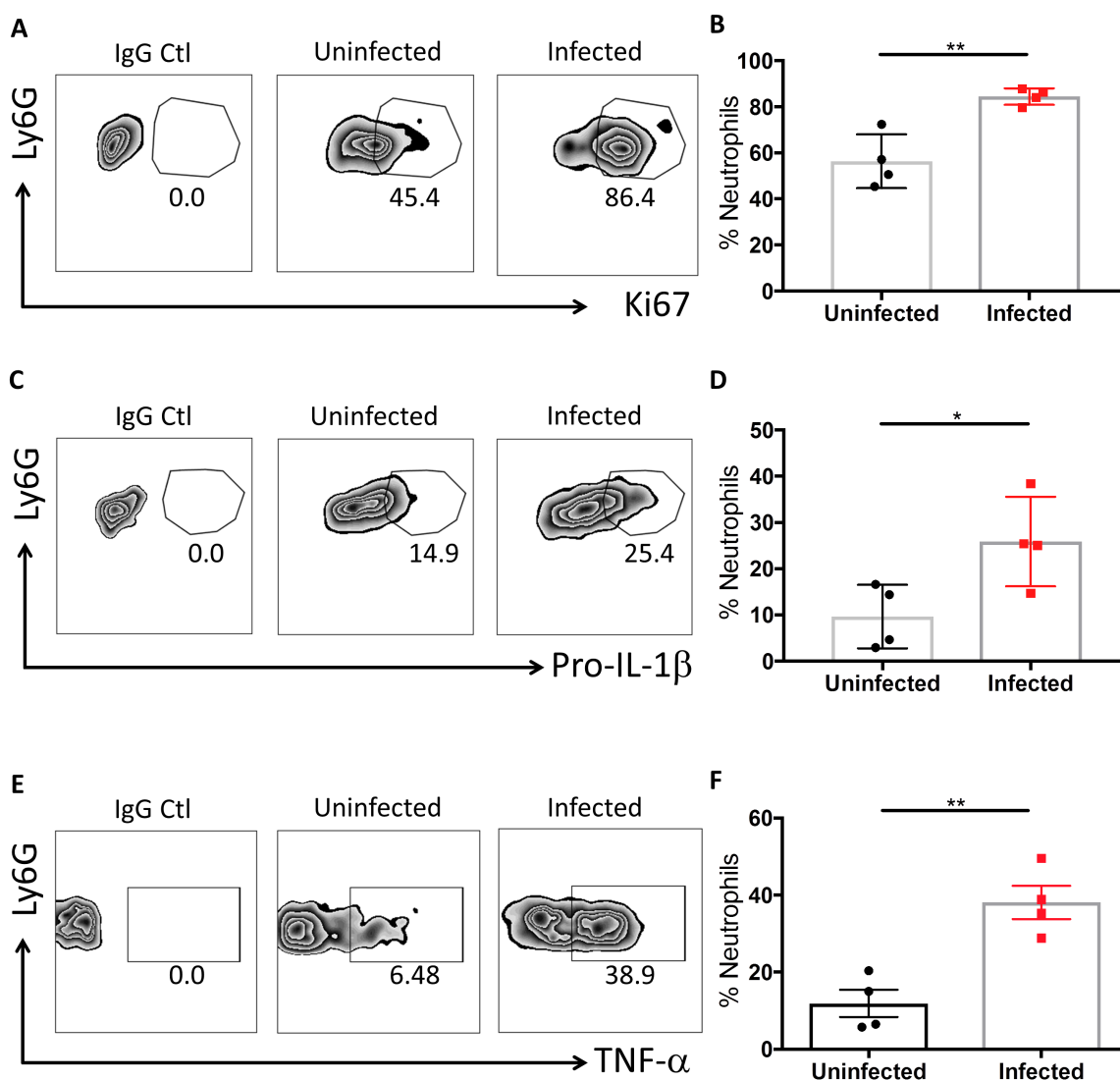
Neutrophils are one of the first immune cells to respond to *S. Typhimurium* infection (Barthel *et al.*, 2003; Rydström & Wick, 2009). In the present study, following SL7207 infection, there was no change in the total number of neutrophils in the tumour (Figure 4.5A, B). However, given that the tumours from the infected mice were much smaller than those in the uninfected, absolute numbers might not be reflective of the expansion of a given cell type following infection. Therefore, to examine if there was an expansion of neutrophils within the total immune cell population, the number of neutrophils amongst total CD45<sup>+</sup> cells was also evaluated. There was not an expansion of the neutrophil population within the leukocyte compartment (Figure 4.5C).



**Figure 4.5 Effects of SL7207 on tumour neutrophil content**

Tumour-bearing mice were inoculated with SL7207 or PBS and tumours were harvested at 3, 5 and 7 dpi for flow cytometry analysis of tumour immune cell content. **A.** Representative flow cytometry plots of Ly6G<sup>+</sup> neutrophils from infected and uninfected tumours at 5 dpi. Cells were gated on single, live, CD45<sup>+</sup>, F4/80<sup>-</sup>. **B.** Quantification of absolute number of neutrophils from infected and uninfected tumours at the indicated time points. **C.** Data shown as percentage Ly6G<sup>+</sup> neutrophils of total CD45<sup>+</sup> cells from infected and uninfected tumours at the indicated time points. Error bars SEM. Statistical analyses performed using Student's t test between infected and uninfected samples at the same time point where  $p < 0.05^*$ .

There was, however, a significantly increased frequency of Ki67<sup>+</sup> neutrophils at 5 dpi in the infected tumours compared to uninfected (Figure 4.6A, B). At this time point, there was also an increase in the proportion of neutrophils producing pro-IL-1 $\beta$  (Figure 4.6C, D) and TNF- $\alpha$  (Figure 4.6E, F). These data are represented as the percentage of neutrophils (% Neutrophils) that were positive for the indicated marker. There was also an up-regulation of IL-22 in the neutrophil population (Figure 4.6G, H). Changes in the phagocytic capacity of the neutrophils was examined through the employment of pHrodo<sup>TM</sup> Red *E. coli* Bioparticles<sup>TM</sup>, which can be taken up by phagocytic cells and assessed through flow cytometry. There was an increase in the phagocytic capacity of tumour-associated neutrophils following infection, as evidenced by the increase in proportion of pHrodo-PE<sup>+</sup> neutrophils in the SL7207 samples compared to uninfected (Figure 4.5I, J).



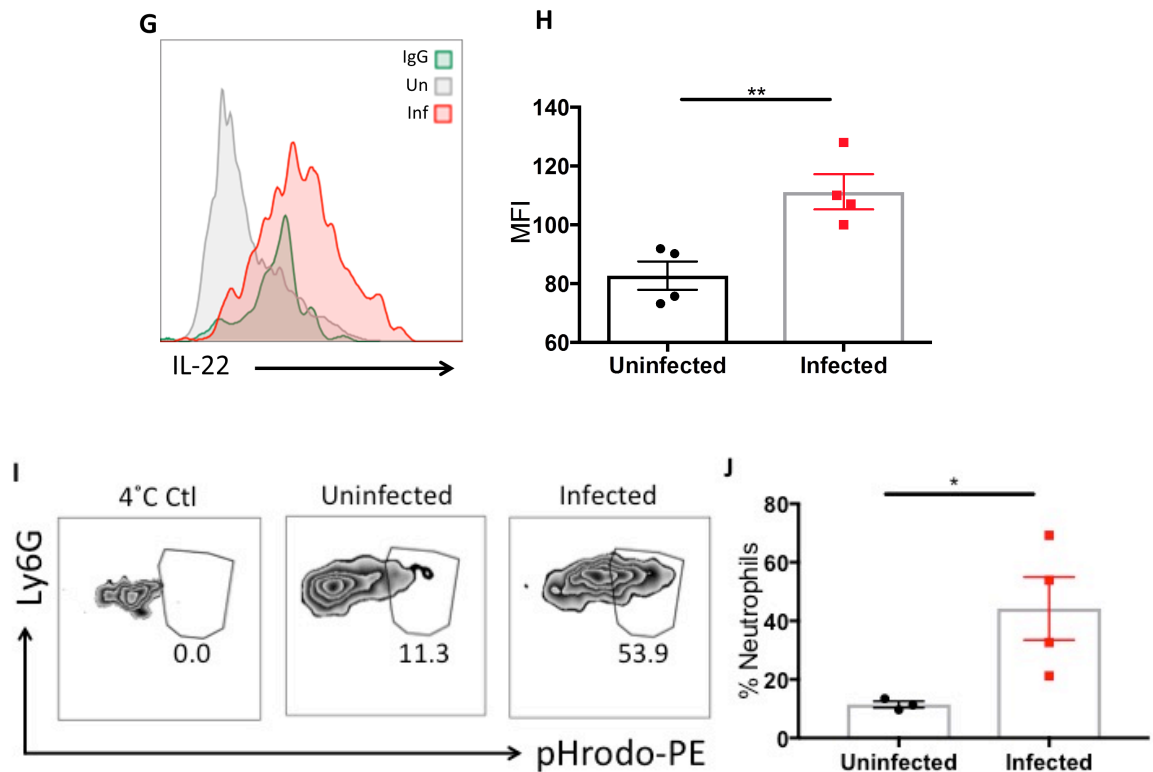


**Figure 4.6 Effects of SL7207 on the activation of tumour neutrophils**

Tumour-bearing mice were inoculated with SL7207 or PBS and tumours were harvested at 5 dpi for *in vitro* stimulation and flow cytometry analysis of activation markers in neutrophils. Cells were gated on . Cells were gated on single, live, CD45<sup>+</sup>, F4/80<sup>-</sup>, Ly6G<sup>+</sup>. **A.** Representative flow cytometry plots showing Ki67<sup>+</sup> Ly6G<sup>+</sup> neutrophils for infected and uninfected samples, including an IgG isotype control. **B.** Data shown as percentage Ki67<sup>+</sup> cells of total Ly6G<sup>+</sup> neutrophils from infected and uninfected samples. **C.** Representative flow cytometry plots showing pro-IL-1 $\beta$ <sup>+</sup> Ly6G<sup>+</sup> neutrophils for infected and uninfected samples including an IgG isotype control. **D.** Data shown as percentage pro-IL-1 $\beta$ <sup>+</sup> cells of total Ly6G<sup>+</sup> neutrophils from infected and uninfected samples. **E.** Representative flow cytometry plots showing TNF- $\alpha$ <sup>+</sup> Ly6G<sup>+</sup> neutrophils for infected and uninfected samples including an IgG isotype control. **F.** Data shown as percentage TNF- $\alpha$ <sup>+</sup> cells of total Ly6G<sup>+</sup> neutrophils from infected and uninfected samples. **G.** Representative histogram plot of Ly6G<sup>+</sup> neutrophil IL-22 production from infected and uninfected samples including an IgG isotype control. **H.** MFI of IL-22 production from Ly6G<sup>+</sup> neutrophils from infected and uninfected samples. **I.** Representative flow cytometry plots showing pHrodo-PE<sup>+</sup> Ly6G<sup>+</sup> neutrophils for infected and uninfected samples, with a 4°C Control. **J.** Data shown as percentage pHrodo-PE<sup>+</sup> cells of total Ly6G<sup>+</sup> neutrophils from infected and uninfected samples. Error bars SEM. Statistical analyses performed using Students t test where  $p < 0.05^*$ ,  $p < 0.01^{**}$ .

#### 4.2.5 Tumour-associated DC number and activation following systemic SL7207 infection

Tumour-associated DCs can play an important role in mediating tumour growth inhibition, mostly through presenting tumour antigens to T cells in the lymph node, which can then recognise and kill the antigen-bearing tumour cells (Liu & Cao, 2015). DCs also play an important role following *S. Typhimurium* infection in the mucosa and spleen, where they are heavily recruited (Johansson *et al.*, 2006) and also perform antigen presentation and T cell activation roles (Tam *et al.*, 2008). Therefore, the number of DCs in the tumour following SL7207 administration was investigated. There was no significant change in the total

number of DCs in the tumour at any time point after infection (Figure 4.7A, B). There was also no change in the proportion of DCs in the CD45<sup>+</sup> immune cell compartment (Figure 4.7C).

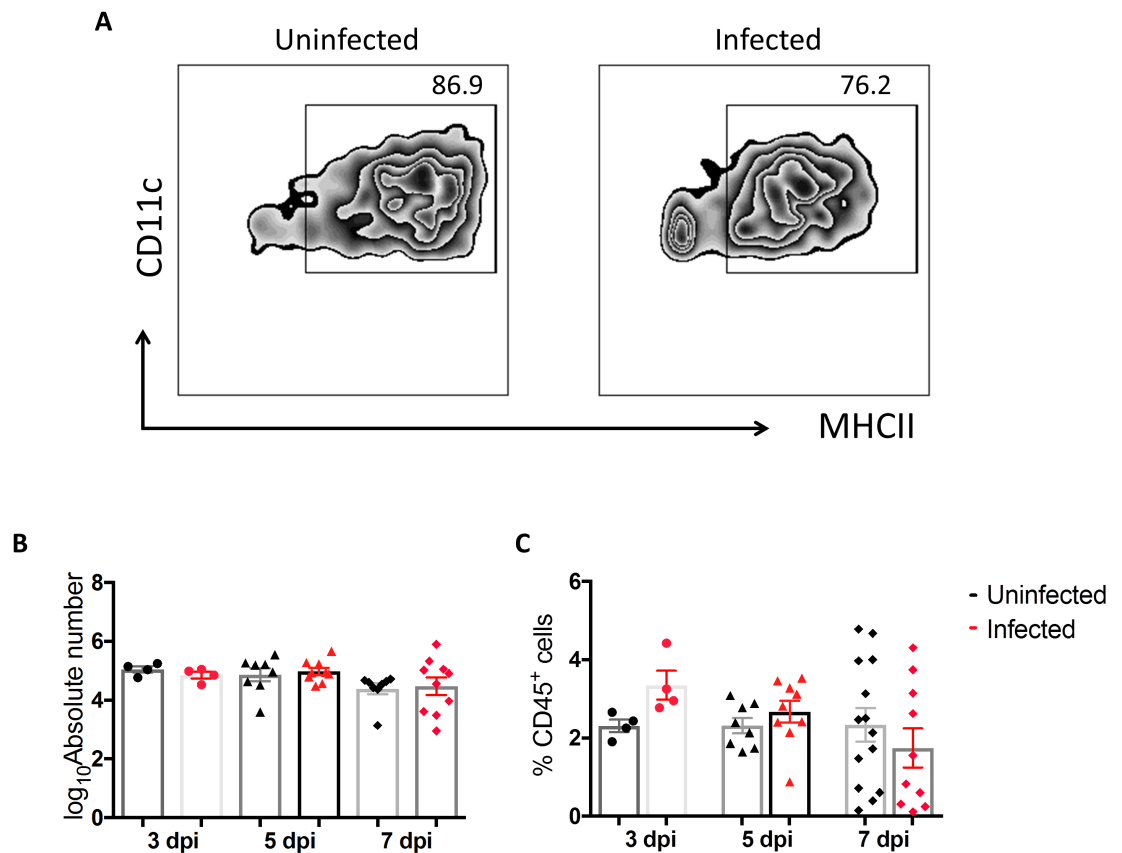


#### Figure 4.7 Effects of SL7207 on tumour DC content

Tumour-bearing mice were inoculated with SL7207 or PBS and tumours were harvested at 3, 5 and 7 dpi for flow cytometry analysis of tumour immune cell content. **A.** Representative flow cytometry plots of MHCII<sup>+</sup> DCs from infected and uninfected tumours at 5 dpi. Cells were gated on single, live, CD45<sup>+</sup>, F4/80<sup>-</sup>, CD11c<sup>+</sup>. **B.** Quantification of absolute number of CD11c<sup>+</sup>MHCII<sup>+</sup> DCs from infected and uninfected tumours at the indicated time points. **C.** Data shown as percentage CD11c<sup>+</sup> MHCII<sup>+</sup> DCs of total CD45<sup>+</sup> cells from infected and uninfected tumours at the indicated time points. Error bars SEM. Statistical analyses performed using Student's t test between infected and uninfected samples at the same time point where  $p < 0.05^*$ .

There was however a change in the phenotype of the DCs. DCs recovered from infected tumours at multiple time points had decreased expression of MHCII (Figure 4.8A, B). Furthermore, there appeared to be a decrease in the frequency of DCs which expressed the co-stimulatory molecule CD80 in the infected compared to uninfected samples at 5 dpi (Figure 4.8C, D).

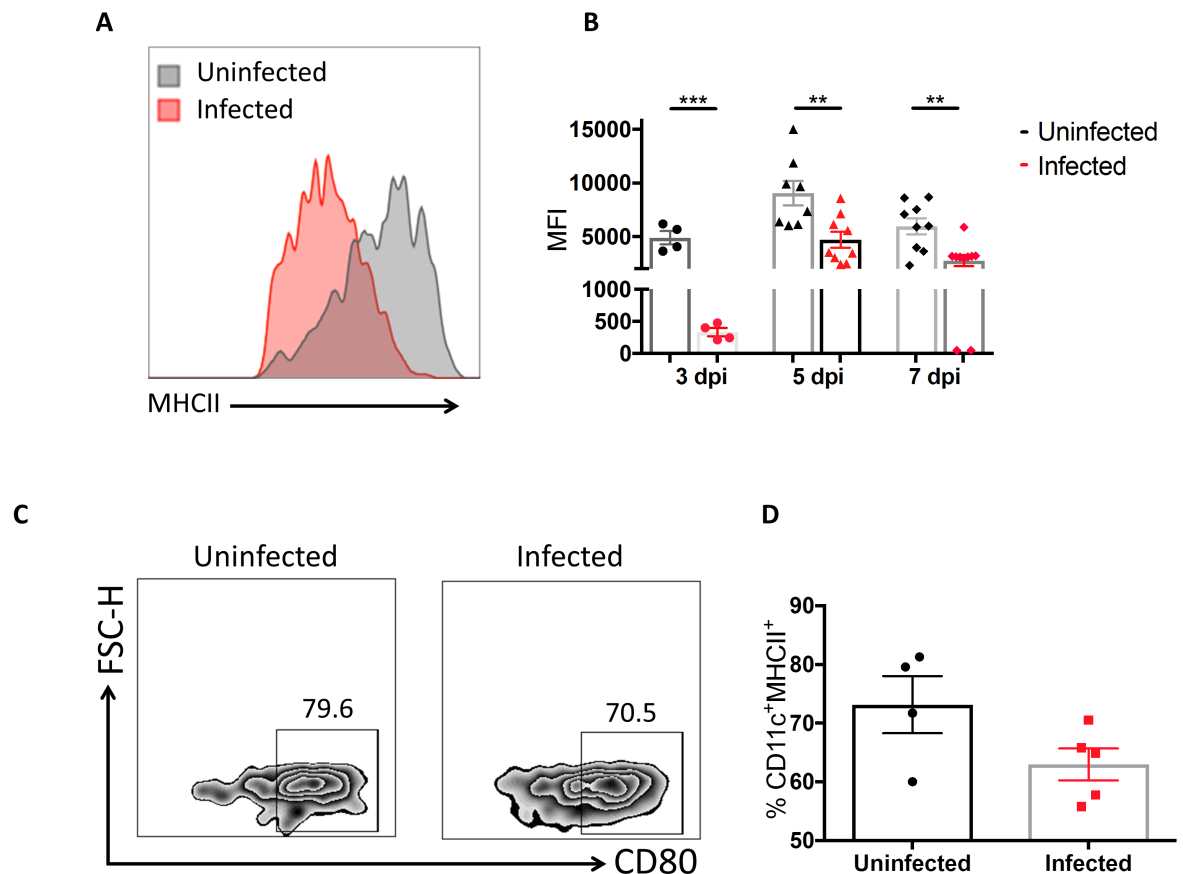


**Figure 4.8 Effects of SL7207 on tumour DC MHCII and CD80 expression**

Tumour-bearing mice were inoculated with SL7207 or PBS and tumours were harvested at 3, 5 and 7 dpi for flow cytometry analysis of tumour immune cell content. **A.** Representative histogram plot of MHCII<sup>+</sup> expression on DCs from infected and uninfected tumours at 5 dpi. Cells were gated on single, live, CD45<sup>+</sup>, F4/80<sup>-</sup>, CD11c<sup>+</sup>. **B.** MFI of MHCII expression on CD11c<sup>+</sup>MHCII<sup>+</sup> DCs from infected and uninfected samples at indicated time points. **C.** Representative flow cytometry plots showing CD80<sup>+</sup> CD11c<sup>+</sup>MHCII<sup>+</sup> DCs from infected and uninfected tumours at 5 dpi. Cells were gated on single, live, CD45<sup>+</sup>, F4/80<sup>-</sup>, CD11c<sup>+</sup>, MHCII<sup>+</sup>. **D.** Data shown as percentage CD80<sup>+</sup> of CD11c<sup>+</sup>MHCII<sup>+</sup> DCs from infected and uninfected samples at 5 dpi. Error bars SEM. Statistical analyses performed using Students t test where  $p < 0.05^*$ ,  $p < 0.01^{**}$ ,  $p < 0.001^{***}$ .

Upon reflection, the gating strategy outlined in Figure 4.1 was insufficient to conclusively analyse classical DCs (cDCs) in the tumour. Firstly, it was possible that there were CD11c<sup>+</sup> B cells included in the 'DC' population. Secondly, this strategy did not include CD103<sup>+</sup>/CD8<sup>+</sup>, cDC1s. Therefore, a revised staining panel and gating strategy was devised (Figure 4.9). The cDC population could be differentiated into cDC1s and cDC2s based on their expression of CD8 or CD11b respectively.

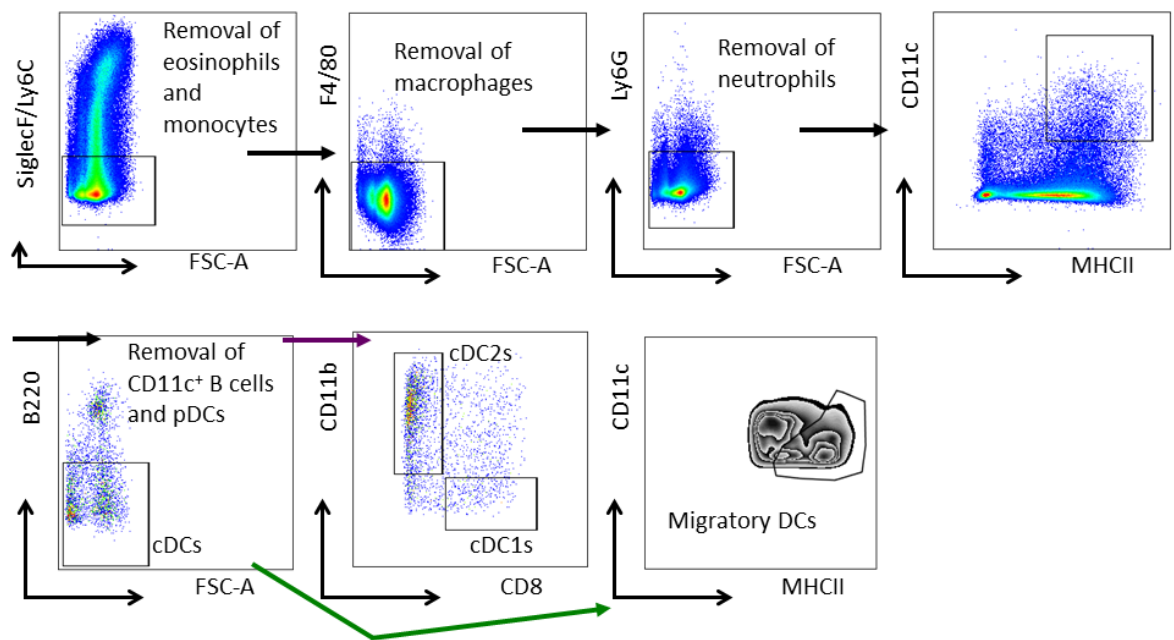


**Figure 4.9 Revised gating strategy for tumour and tdLN cDCs**

Tumour and lymph node cDCs (black and purple arrows) were gated as single, live,  $CD45^+$ ,  $SiglecF^+Ly6C^-$  (removal of eosinophils and monocytes),  $F4/80^-$  (removal of macrophages),  $Ly6G^-$  (removal of neutrophils),  $CD11c^+MHCII^+$ ,  $B220^-$  (removal of  $CD11c^+$  B cells and pDCs) and then differentiated on the basis of CD8 or CD11b expression as cDC1s and cDC2s respectively. To assess the proportion of cDCs which were migratory,  $B220^-$  cDCs were gated on  $MHCII^{hi}$  (green arrow).

The revised DC subset analysis revealed that there was no significant change in the number of cDC1s ( $CD8^+$ ) between infected and uninfected tumours at 5 dpi (Figure 4.10A-C). There was, however, a significant decrease in the number of tumour-associated cDC2s ( $CD11b^+$ ) at 5 dpi following infection (Figure 4.10D). This decrease was also reflected within these cells as a proportion of total tumour-associated  $CD45^+$  immune cells (Figure 4.10E).

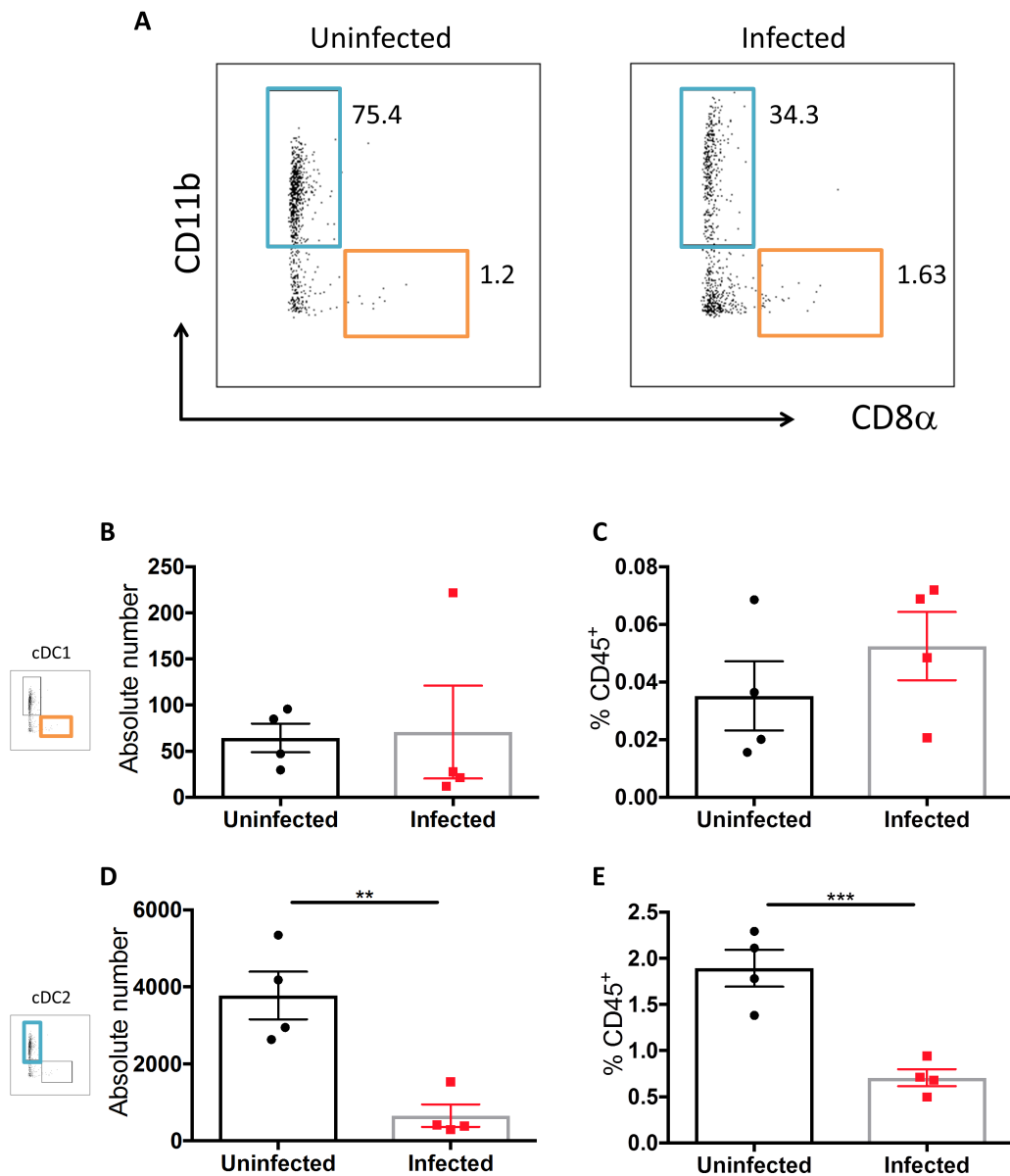


**Figure 4.10 Effects of SL7207 on tumour cDC1 and cDC2 content**

Tumour-bearing mice were inoculated with SL7207 or PBS and tumours were harvested at 5 dpi for flow cytometry analysis of cDC1 and cDC2 content. **A**. Representative flow cytometry plots of cDC1s (CD8<sup>+</sup>, orange boxes) and cDC2s (CD11b<sup>+</sup>, blue boxes) from infected and uninfected tumours. Cells were gated on single, live, CD45<sup>+</sup>, SiglecF<sup>-</sup>, Ly6C<sup>-</sup>, F4/80<sup>-</sup>, Ly6G<sup>-</sup>, CD11c<sup>+</sup>, MHCII<sup>+</sup>, B220<sup>-</sup>. **B**. Quantification of absolute number of CD8<sup>+</sup> DCs from infected and uninfected tumours. **C**. Data shown as percentage CD8<sup>+</sup> DCs of total CD45<sup>+</sup> cells from infected and uninfected tumours. **D**. Quantification of absolute number of CD11b<sup>+</sup> DCs from infected and uninfected tumours. **E**. Data shown as percentage CD11b<sup>+</sup> DCs of total CD45<sup>+</sup> cells from infected and uninfected tumours. Error bars SEM. Statistical analyses performed using Students t test where  $p < 0.05^*$ ,  $p < 0.01^{**}$ ,  $p < 0.001^{***}$ .

It was possible that the observed decreases in frequency and number of tumour-associated cDCs was due to enhanced migration to the draining lymph node. Therefore, the tumour draining lymph nodes (tdLN) were also harvested and the cDC populations therein were analysed to ascertain if there was a concomitant

increase in the number of cDC2s following infection. There was no significant difference between infected and uninfected samples in terms of absolute numbers of cDC1s (Figure 4.11A, B). There was however an increase in cDC1s within the CD45<sup>+</sup> compartment (Figure 4.11C). There was also no significant difference in the number of cDC2s in the tdLN between infected and uninfected samples (Figure 4.11D). There was, however, a highly significant increase in the cDC2 cells amongst total CD45<sup>+</sup> cells (Figure 4.11E).

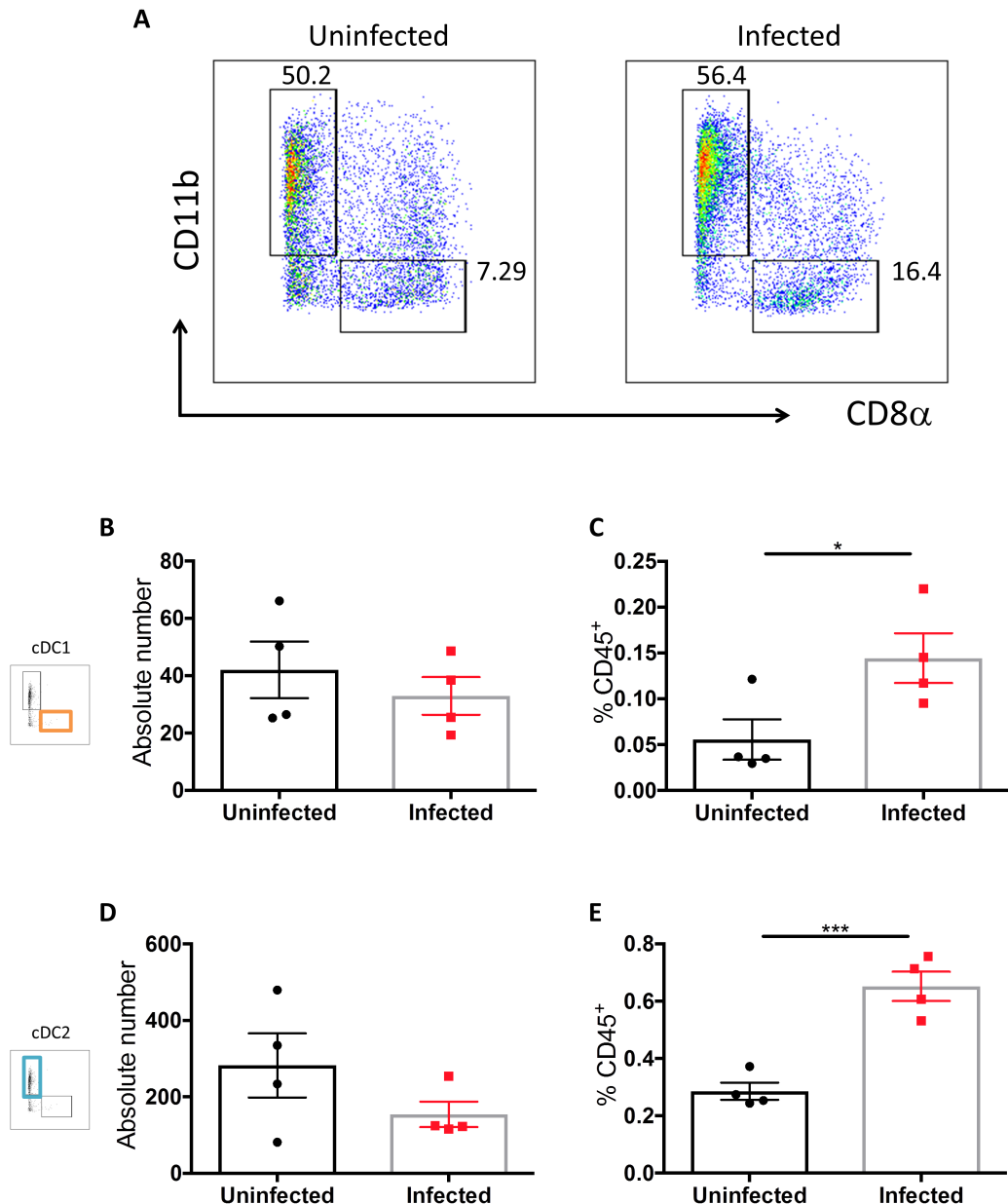


**Figure 4.11 Effects of SL7207 on tdLN cDC1 and cDC2 content**

Tumour-bearing mice were inoculated with SL7207 or and tdLNs were harvested at 5 dpi for flow cytometry analysis of cDC1 and cDC2 content. **A**. Representative flow cytometry plots of cDC1s (CD8<sup>+</sup>, orange boxes) and cDC2s (CD11b<sup>+</sup>, blue boxes) in tdLNs of infected and uninfected tumour-bearing mice. Cells were gated on single, live, CD45<sup>+</sup>, SiglecF<sup>-</sup>, Ly6C<sup>-</sup>, F4/80<sup>-</sup>, Ly6G<sup>-</sup>,

CD11c<sup>+</sup>, MHCII<sup>+</sup>, B220<sup>-</sup>. **B.** Quantification of absolute number of CD8<sup>+</sup> DCs in cells in tdLNs of infected and uninfected tumour-bearing mice. **C.** Data shown as percentage CD8<sup>+</sup> DCs of total CD45<sup>+</sup> cells in tdLNs of infected and uninfected tumour-bearing mice. **D.** Quantification of absolute number of CD11b<sup>+</sup> DCs in tdLNs of infected and uninfected tumour-bearing mice. **E.** Data shown as percentage CD11b<sup>+</sup> DCs of total CD45<sup>+</sup> cells in tdLNs of infected and uninfected tumour-bearing mice. Error bars SEM. Statistical analyses performed using Students t test where  $p < 0.05^*$ ,  $p < 0.01^{**}$ ,  $p < 0.001^{***}$ .

It was also possible to enumerate the number of ‘migratory DCs’ in the tdLN, as these cells are characterised by MHCII<sup>hi</sup> expression (Ohl *et al.*, 2004). If there was an increase in DC migration from the tumour to the tdLN, this would be reflected by an increase in the number of MHCII<sup>hi</sup> DCs. However, there was no difference in the proportion of tdLN cDCs which were migratory between infected and uninfected samples (Figure 4.12).

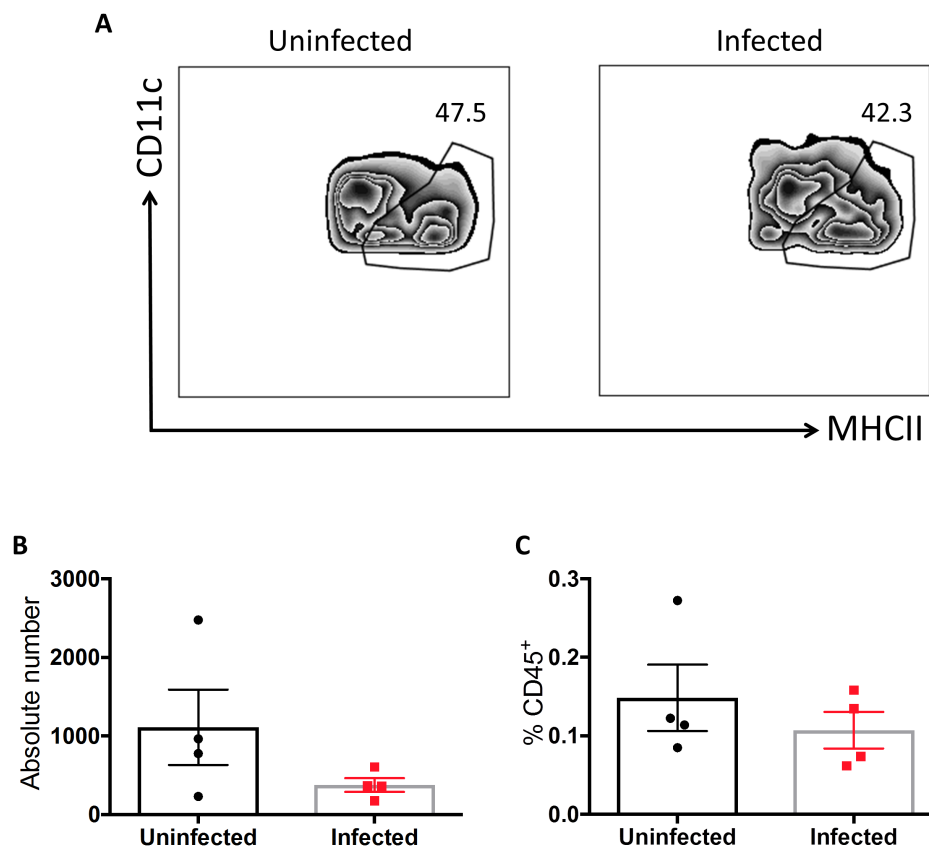


**Figure 4.12** Effects of SL7207 on migratory cDCs in tdLN

Tumour-bearing mice were inoculated with SL7207 or PBS and tdLNs were harvested at 5 dpi for flow cytometry analysis of cDC1 and cDC2 content. **A.** Representative flow cytometry plots showing MHCII<sup>hi</sup> migratory cDCs in the tdLNs of infected and uninfected tumour-bearing mice. Cells were gated on single, live, CD45<sup>+</sup>, SiglecF<sup>-</sup>, Ly6C<sup>-</sup>, F4/80<sup>-</sup>, Ly6G<sup>-</sup>, CD11c<sup>+</sup>, MHCII<sup>+</sup>, B220<sup>-</sup>. **B.** Quantification of the absolute number of MHCII<sup>hi</sup> cDCs in tdLNs of infected and uninfected tumour-bearing mice. **C.** Data shown as percentage MHCII<sup>hi</sup> migratory cDCs of total CD45<sup>+</sup> cells in tdLNs of infected and uninfected tumour-bearing mice. Error bars SEM. Statistical analyses performed using Students t test where  $p < 0.05^*$ .

### 4.2.6 Changes in the T cell infiltrate into the tumour and tdLN following infection

It has been suggested that there is an influx of CD3<sup>+</sup> T cells into the tumour following infection (Avogadri *et al.*, 2005; Cronin *et al.*, 2010; Lee *et al.*, 2011; Lizotte *et al.*, 2014). To investigate this in the present model, infected and uninfected tumours were harvested at indicated time points and analysed by flow cytometry for analysis of T cell populations. The gating strategy is depicted in Figure 4.1. There was a significant decrease in the total number of CD4<sup>+</sup> T cells in the infected tumours compared with the uninfected tumours at 5 dpi, which appeared to be reversed at 7 dpi, but this was not statistically significant ( $p = 0.053$ ; Figure 4.13A,B). There was no change in the number of CD8<sup>+</sup> T cells at either time point between infected and uninfected samples (Figure 4.13C).

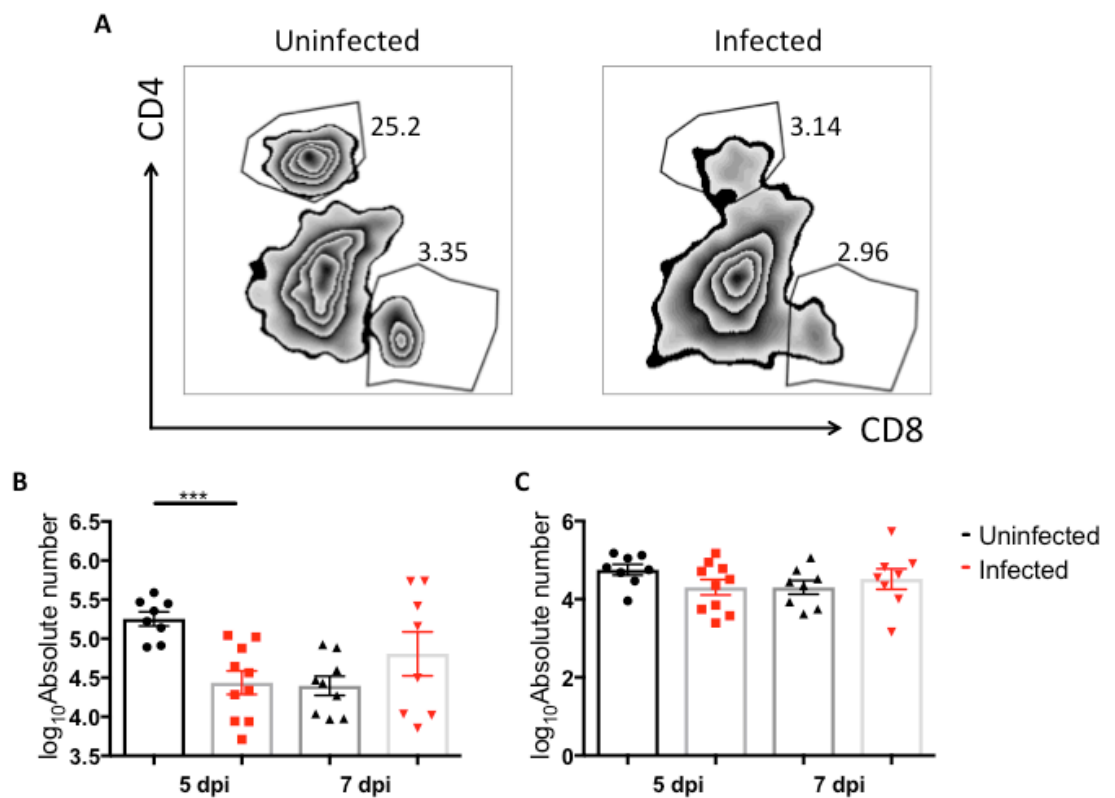


**Figure 4.13 Effects of SL7207 on tumour T cell content**

Tumour-bearing mice were inoculated with SL7207 or PBS and tumours were harvested at 5 and 7 dpi for flow cytometry analysis of tumour T cell content. **A**. Representative flow cytometry plots showing CD4<sup>+</sup> and CD8<sup>+</sup> T cells from infected and uninfected tumours. Cells were gated as CD45<sup>+</sup>, CD3<sup>+</sup>, SSC<sup>lo</sup>. **B**. Quantification of absolute number of CD4<sup>+</sup> T cells from infected and uninfected tumours at the indicated time points. **C**. Quantification of absolute number of CD8<sup>+</sup> T cells from infected and uninfected tumours at the indicated time points. Error bars SEM. Statistical analyses performed using Student's t test between infected and uninfected samples at the same time point where  $p < 0.05^*$ ,  $p < 0.01^{**}$ ,  $p < 0.001^{***}$ .

Looking in the tdLN, there were no significant differences in the number of CD4<sup>+</sup> T cells at either 5 or 7 dpi for infected and uninfected samples (Figure 4.14A, B). There were also no significant differences in the number of CD8<sup>+</sup> T cells between infected and uninfected samples (Figure 4.14C).

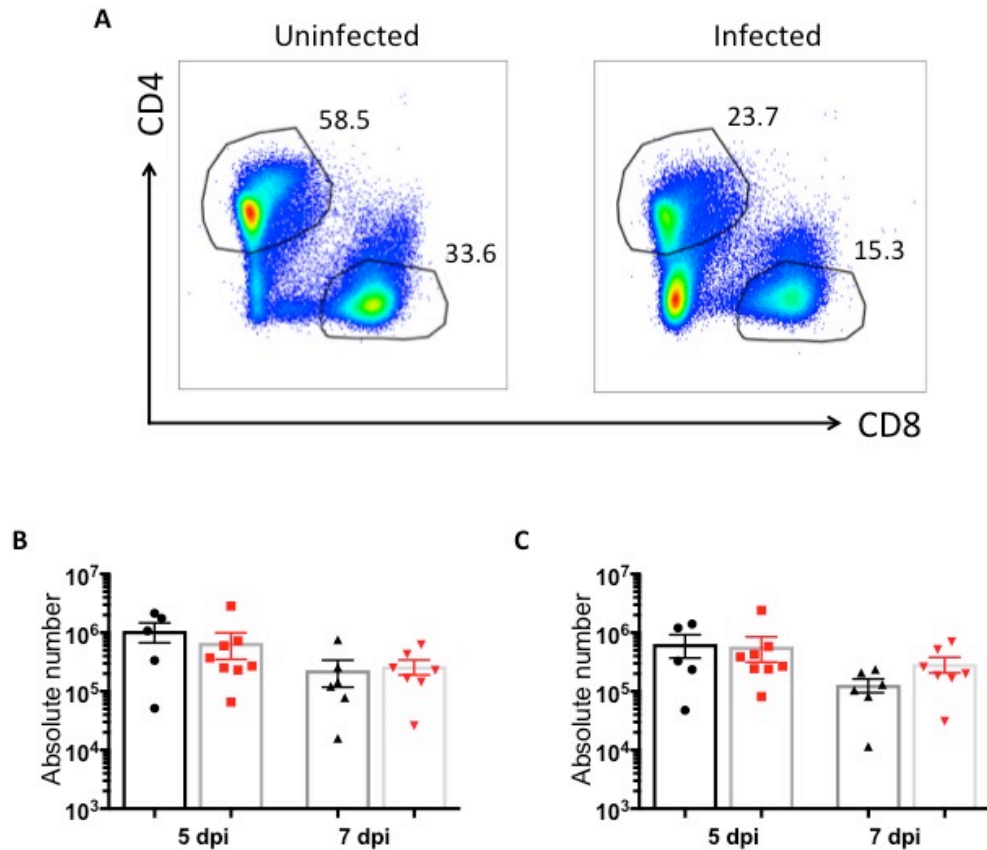


**Figure 4.14 Effects of SL7297 on tdLN T cell content**

Tumour-bearing mice were inoculated with SL7207 or PBS and tdLNs were harvested at 5 and 7 dpi for flow cytometry analysis of tumour T cell content. **A**. Representative flow cytometry plots showing CD4<sup>+</sup> and CD8<sup>+</sup> T cells in tdLNs of infected and uninfected tumour-bearing mice. Cells were gated as CD45<sup>+</sup>, CD3<sup>+</sup>, SSC<sup>lo</sup>. **B**. Quantification of absolute number of CD4<sup>+</sup> T cells in tdLNs of infected and uninfected tumour-bearing mice at the indicated time points. **C**. Quantification of absolute number of CD8<sup>+</sup> T cells in tdLNs of infected and uninfected tumour-bearing mice at the indicated time points. Error bars SEM. Statistical analyses performed using Students t test between infected and uninfected samples at the same time point where  $p < 0.05^*$ .

#### 4.2.7 T<sub>H</sub>1 responses detected in the tumour and tdLN following SL7207 infection

*S. Typhimurium* has been documented to induce a T<sub>H</sub>1 response in the intestine following oral infection (Bao *et al.*, 2000; Ravindran *et al.*, 2005). Furthermore, T<sub>H</sub>1 T cells have been implicated in bacterial-mediated cancer therapy for multiple bacterial genera (Lizotte *et al.*, 2014; Loeffler *et al.*, 2009; Stern *et al.*, 2015). The expression of the T<sub>H</sub>1 lineage-specific transcription factor, Tbet, was examined in CD4<sup>+</sup> T cells. There was an increase in the proportion of tumour

CD4<sup>+</sup> T cells expressing Tbet at 5 dpi (Figure 4.15A, B). There was also an increase in the proportion of CD8<sup>+</sup> T cells producing IFN- $\gamma$ , a T<sub>H</sub>1-associated cytokine, in the infected samples compared with the uninfected at both 5 and 7 dpi (Figure 4.15C, D).

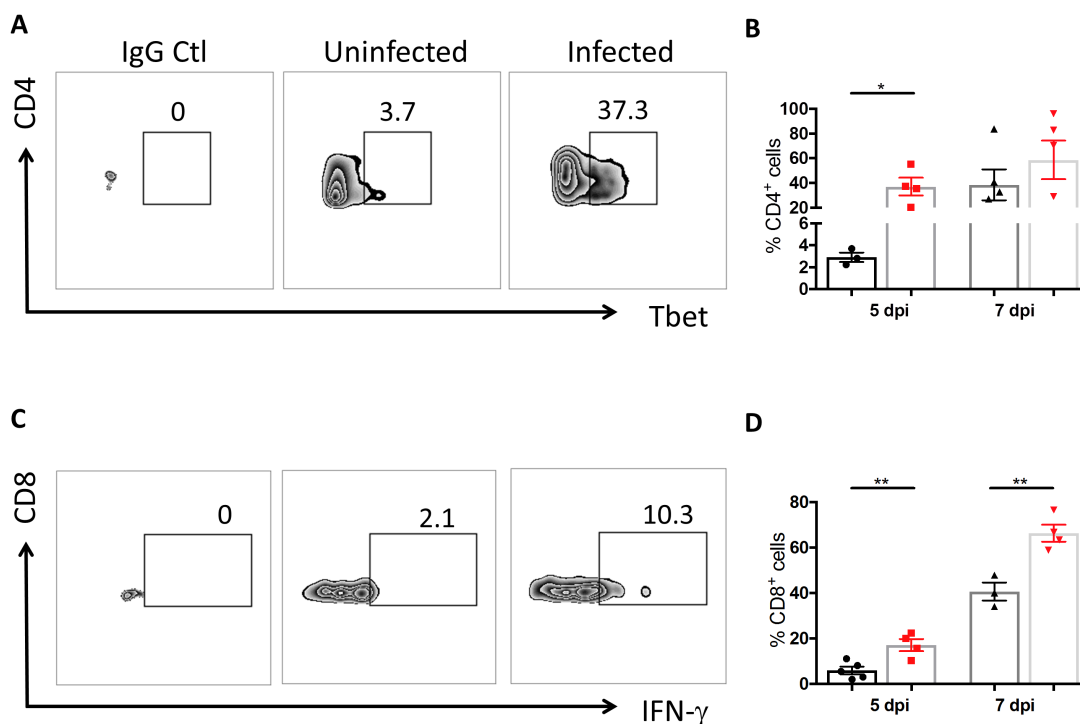


**Figure 4.15 Effects of SL7207 on T<sub>H</sub>1 response in the tumour**

Tumour-bearing mice were inoculated with SL7207 or PBS and tumours were harvested at 5 and 7 dpi for flow cytometry analysis of tumour T cell content. **A.** Representative flow cytometry plots showing Tbet<sup>+</sup> CD4<sup>+</sup> T cells from infected and uninfected tumours, including an IgG isotype control. Cells were gated as CD45<sup>+</sup>, CD3<sup>+</sup>, SSC<sup>lo</sup>, CD4<sup>+</sup>. **B.** Data shown as percentage Tbet<sup>+</sup> of total CD4<sup>+</sup> T cells from infected and uninfected tumours. **C.** Representative flow cytometry plots showing IFN- $\gamma$ <sup>+</sup> CD8<sup>+</sup> T cells from infected and uninfected tumours, including an IgG isotype control. Cells were gated as CD45<sup>+</sup>, CD3<sup>+</sup>, SSC<sup>lo</sup>, CD8<sup>+</sup>. **D.** Data shown as percentage IFN- $\gamma$ <sup>+</sup> of total CD8<sup>+</sup> T cells from infected and uninfected tumours. Error bars SEM. Statistical analyses performed using Students t test between infected and uninfected samples at the same time point where  $p < 0.05^*$ ,  $p < 0.01^{**}$ ,  $p < 0.001^{***}$ .

These T<sub>H</sub>1 T cells were also evident in the tdLN following infection. There was a significant increase in the frequency of CD4<sup>+</sup>Tbet<sup>+</sup> T cells amongst total CD4<sup>+</sup> cells in the infected samples at 5 and 7 dpi (Figure 4.16A, B). There was possibly an increase in the proportion of CD8<sup>+</sup> cells which were IFN- $\gamma$ <sup>+</sup>, at 5 dpi but the low sample size was insufficient to perform statistical analysis (Figure 4.16C, D).

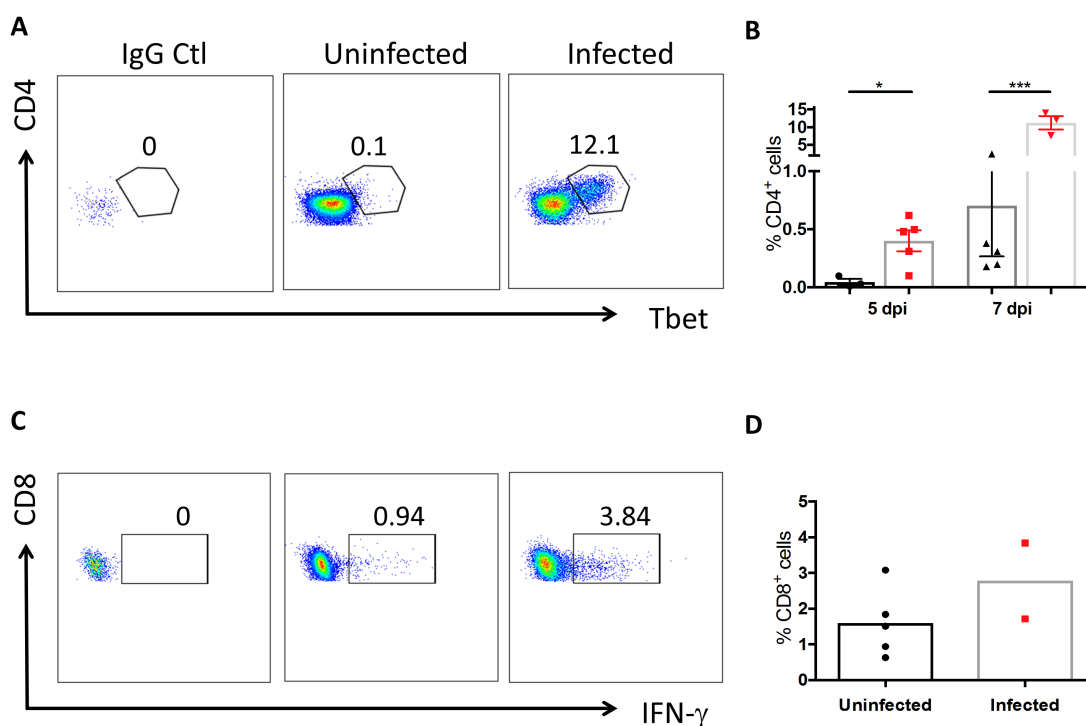


**Figure 4.16 Effects of SL7207 on  $T_H1$  response in tdLN**

Tumour-bearing mice were inoculated with SL7207 or PBS and tdLNs were harvested at 5 and 7 dpi for flow cytometry analysis of tumour T cell content. **A.** Representative flow cytometry plots showing  $Tbet^+ CD4^+$  T cells in tdLNs of infected and uninfected tumour-bearing mice, including an IgG isotype control. Cells were gated as  $CD45^+$ ,  $CD3^+$ ,  $SSC^{lo}$ ,  $CD4^+$ . **B.** Data shown as percentage  $Tbet^+$  of total  $CD4^+$  T cells in tdLNs from infected and uninfected tumour-bearing mice. **C.** Representative flow cytometry plots showing  $IFN-\gamma^+ CD8^+$  T cells in tdLNs of infected and uninfected tumour-bearing mice, including an IgG isotype control. Cells were gated as  $CD45^+$ ,  $CD3^+$ ,  $SSC^{lo}$ ,  $CD8^+$ . **D.** Data shown as percentage  $IFN-\gamma^+$  of total  $CD8^+$  T cells in tdLNs from infected and uninfected tumour-bearing mice. Error bars SEM. Statistical analyses performed using Student's t test between infected and uninfected samples at the same time point where  $p < 0.05^*$ ,  $p < 0.01^{**}$ ,  $p < 0.001^{***}$ .

#### 4.2.8 $T_H17$ responses in the tumour following SL7207 infection

There have been reports that *S. Typhimurium* induces a  $T_H17$  response in the intestine following oral infection (Raffatellu *et al.*, 2008). Therefore, the expression of the  $T_H17$  cytokine, IL-17, was examined in the infected and uninfected tumours. There was an increase in the proportion of  $CD4^+$  T cells producing IL-17 in the infected samples compared with the uninfected samples at 5 dpi (Figure 4.17A,B). There was also an increase in the amount of tumour-produced IL-17 secreted by immune cells present in the infected tumour compared to uninfected following *in vitro* stimulation (Figure 4.17C). These data suggest a  $T_H17$  response in the tumour associated with SL7207 infection.

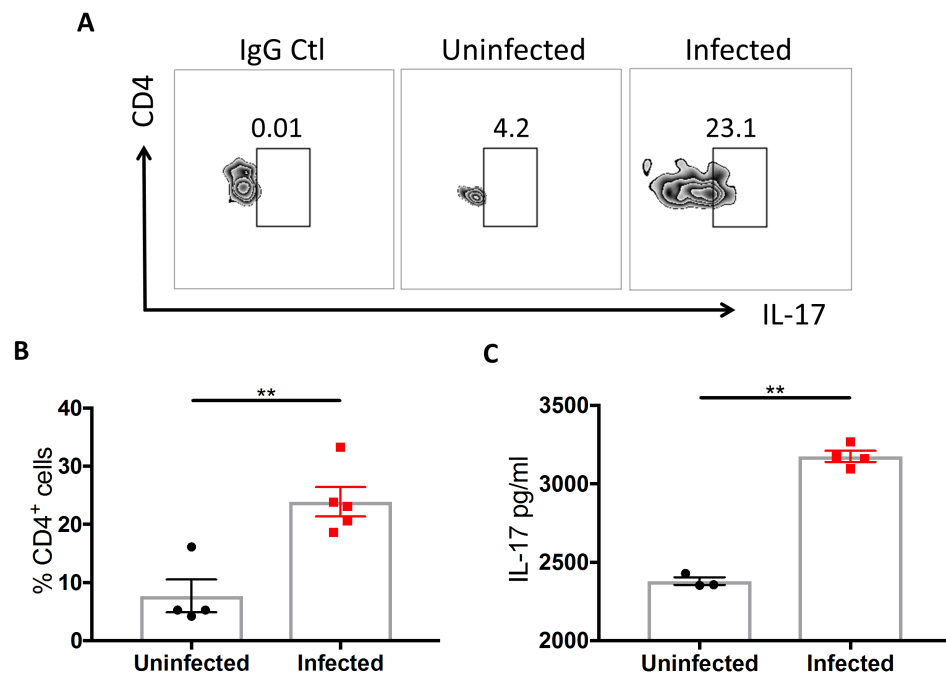


**Figure 4.17 Effects of SL7207 on T<sub>H</sub>17 response in the tumour**

Tumour-bearing mice were inoculated with SL7207 or PBS and tumours were harvested at 5 dpi for flow cytometry analysis of tumour T cell content or ELISA analysis. **A.** Representative flow cytometry plots showing IL-17<sup>+</sup> CD4<sup>+</sup> T cells from infected and uninfected tumours, including an IgG isotype control. Cells were gated as CD45<sup>+</sup>, CD3<sup>+</sup>, SSC<sup>lo</sup>, CD4<sup>+</sup>. **B.** Data shown as percentage IL-17<sup>+</sup> of total CD4<sup>+</sup> T cells from infected and uninfected tumours. **C.** Whole tumour IL-17 production from infected and uninfected tumours. Error bars SEM. Statistical analyses performed using Student's t test between infected and uninfected samples where  $p < 0.05^*$ ,  $p < 0.01^{**}$ .

#### 4.2.9 Changes in the frequency of CD4<sup>+</sup>Foxp3<sup>+</sup> Tregs in the tumour following SL7207 infection

A number of studies have demonstrated a role for Tregs in propagating the immunosuppressive environment of the tumour (Cederbom *et al.*, 2000; Strauss *et al.*, 2007). Therefore, it was interesting to investigate if there was a change in the tumour Treg population following SL7207 infection. There was a decrease in the frequency of CD4<sup>+</sup> T cells which were FoxP3<sup>+</sup> at 5 dpi in the infected samples compared with uninfected control (Figure 5.18A, B). There was also a trend towards a decrease at 7 dpi, but this was highly variable and not statistically significant ( $p = 0.08$ ; Figure 5.18B). There were no differences in the proportion of FoxP3<sup>+</sup>CD4<sup>+</sup> T cells in the tdLN between the treatment groups at either time point post infection (Figure 5.18C, D).

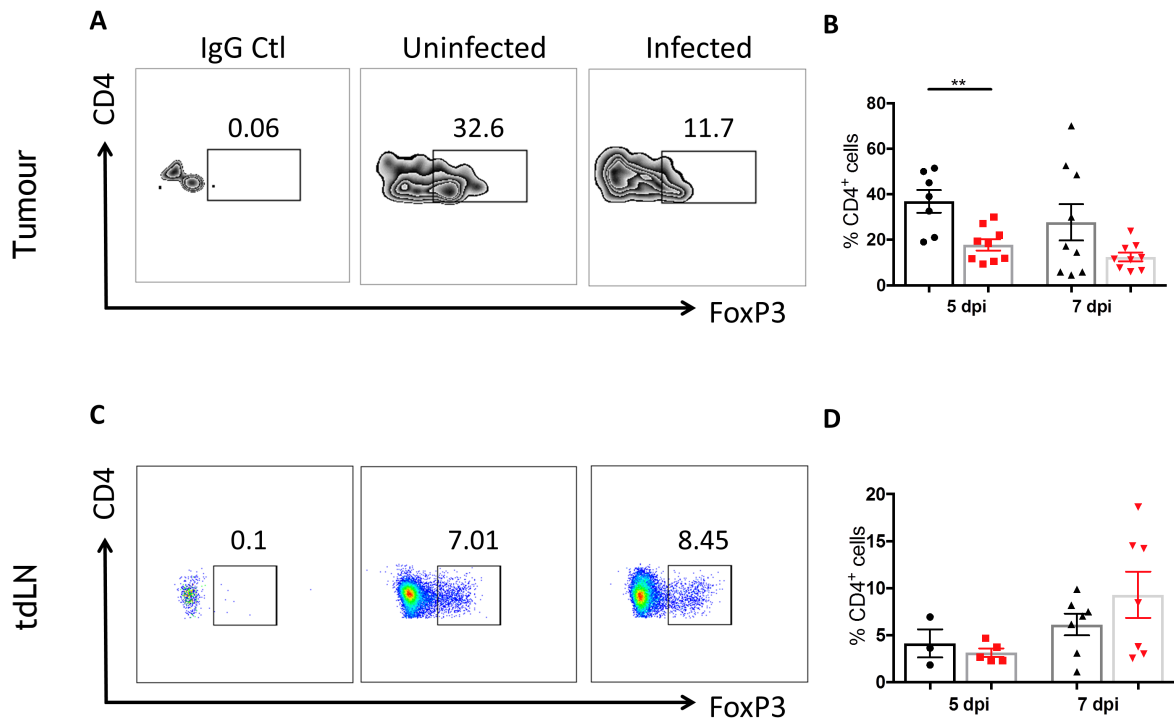


**Figure 4.18 Effects of SL7207 on Treg response in the tumour and tdLN**

Tumour-bearing mice were inoculated with SL7207 or PBS and tumour and tdLNs were harvested at 5 and 7 dpi for flow cytometry analysis of tumour T cell content. **A.** Representative flow cytometry plots showing FoxP3<sup>+</sup> CD4<sup>+</sup> T cells from infected and uninfected tumours, including an IgG isotype control. Cells were gated as CD45<sup>+</sup>, CD3<sup>+</sup>, SSC<sup>lo</sup>, CD4<sup>+</sup>. **B.** Data shown as percentage FoxP3<sup>+</sup> of total CD4<sup>+</sup> T cells from infected and uninfected tumours. **C.** Representative flow cytometry plots showing FoxP3<sup>+</sup> CD4<sup>+</sup> T cells in tdLNs of infected and uninfected tumour-bearing mice, including an IgG isotype control. Cells were gated as CD45<sup>+</sup>, CD3<sup>+</sup>, SSC<sup>lo</sup>, CD4<sup>+</sup>. **D.** Data shown as percentage FoxP3<sup>+</sup> of total CD4<sup>+</sup> T cells in tdLNs from infected and uninfected tumour-bearing mice. Error bars SEM. Statistical analyses performed using Students t test between infected and uninfected samples at the same time point where  $p < 0.05^*$ ,  $p < 0.01^{**}$ .

## 4.3 Discussion

There have been multiple reports which have provided evidence for the implication of tumour-associated immune cells in mediating bacterial-mediated anti-tumour effects (Lee *et al.*, 2011; Stern *et al.*, 2015; Westphal *et al.*, 2008). The focus here was on particular myeloid-derived cells implicated in *S. Typhimurium* infection; neutrophils (Barthel *et al.*, 2003; Rydström & Wick, 2009) and DCs (Tam *et al.*, 2008; Yrlid *et al.*, 2000). There was also an interest in the types of adaptive immune response elicited following infection, given previous findings involving a  $T_H1$  response in bacterial mediated cancer therapy (Lee *et al.*, 2011; Stern *et al.*, 2015). The current study has indeed demonstrated that the tumour immune repertoire is perturbed following systemic *S. Typhimurium* infection, characterised by neutrophil activation and  $T_H1$  and  $T_H17$  responses, with a decrease in the frequency of tumour-associated Tregs following infection.

### 4.3.1 Why was there no change in the number of tumour-associated leukocytes following infection?

It has been reported that there is an influx of immune cells into the gut following oral administration of *S. Typhimurium* to streptomycin-treated mice (Barthel *et al.*, 2003; Johansson *et al.*, 2006; Rydström & Wick, 2009). Therefore, it was hypothesised that there would be a similar influx of  $CD45^+$  immune cells into the tumour following systemic SL7207 infection of tumour-bearing mice. In this report, there was no significant difference in the number of  $CD45^+$  immune cells recovered from infected and uninfected tumours. There was, however, an increase in  $CD45^+$  cells as a proportion of live cells in the infected samples, which is most likely explained by the fact that there is a concomitant decrease in the number of tumour cells. Taken at face value, these data suggest an abrogation in immune recruitment in the tumour following infection.

There are tissue-specific factors which may be underlying the perceived abrogated immune infiltration into the tumour following SL7207 infection. For example, the microbiota in the mucosa play a pivotal role in host response to mucosal infection. Germ-free mice display reduced antigen-specific systemic

immune responses to *S. Typhimurium* (Nardi *et al.*, 1991). As the tumours in this study were taken to be sterile, it is unlikely that local microbiota-host interactions shaped the tumour immune response to systemic SL7207 infection.

Another factor that may play a role in determining the immune infiltration of an infected organ is the stromal cell repertoire. Stromal cells in the gut play an important role in attracting immune cells by propagating inflammation in response to oral *S. Typhimurium* infection (Müller *et al.*, 2009). However, stromal cells in the tumour have been programmed to prevent immune cell infiltration to the tumour. For example, endothelial cells in the tumour often exhibit reduced expression of E-cadherin and multiple integrins such as intercellular-adhesion molecule (ICAM)1 and ICAM2 which lead to impaired lymphocyte recruitment (Griffioen *et al.*, 1996a; Griffioen *et al.*, 1996b). Furthermore, tumour-associated fibroblasts have been demonstrated to promote a tumour-promoting immune landscape (Kraman *et al.*, 2010). Therefore, it might be interesting to investigate if the phenotype of the tumour stroma can play a role in attenuating bacterial-mediated tumour growth inhibition.

Perhaps the most likely explanation for the absence of a CD45<sup>+</sup> cell influx is the immunosuppressive tumour microenvironment. The tumour microenvironment harbours immunosuppressive immune cells such as TAMs that express Programmed Death Ligand-1 (PD-L1) (Gordon *et al.*, 2017) and Tregs (Cederbom *et al.*, 2000; Strauss *et al.*, 2007). Therefore, this environment may not be as responsive to bacterial insult as other tissues, which might be appetising if there wasn't a significant increase in the secretion of pro-inflammatory cytokines in the tumour following infection. However, a limitation of our analysis is that we did not analyse the amount of tumour suppressive cytokines in the tumour following infection, such as IL-10 and TGF- $\beta$ , which may still be present and inhibiting effector cell recruitment.

Given that there is no overall increase in immune cells but still an anti-tumour effect possibly demonstrates that tumour-resident cells are capable of mediating the anti-tumour effects of the bacteria. This is interesting from a clinical point of view because it suggests that patients, who often have a reduced capacity to launch an immune response (Hübel *et al.*, 1999; Klastersky & Aoun, 2004; Viscoli

*et al.*, 2005) may not have to depend on circulating immune cells to mediate the anti-tumour effects of this therapy. Instead, they can rely on the tumour-associated immune cells, which up to the point of treatment have likely played a role in promoting tumourigenesis. Furthermore, it is tempting to speculate that the effects of the immune cells become more potent as the immune cell:cancer cell ratio increases due to tumour cell death. Therefore, if an immune cell is producing anti-tumourigenic molecules such as TNF- $\alpha$  or IFN- $\gamma$ , the remaining tumour cells are being flooded with increasing doses as other tumour cells die. Although this seems intuitive, there is no evidence provided herein to suggest this is the case.

It is also possible that there is indeed immune cell infiltration, but this hasn't been accounted for in the present experimental design. Following *S. Typhimurium* infection, there is immune cell death; for example, macrophages undergo pyroptosis to limit bacterial spread (Monack *et al.*, 1996). If the number of dying immune cells in the tumour environment equals the infiltration following infection, there would be no significant difference in the total number of CD45<sup>+</sup> leukocytes in the tumour following infection, similar to what is seen here. However, this has also been demonstrated to be the case in the intestine following infection, (Barthel *et al.*, 2003; Rydström & Wick, 2009) so does not suffice to explain the absence of a significant immune cell infiltrate in here. Therefore, it would be imperative to investigate the degree of immune cell death before major conclusions pertaining to the perceived abrogation of immune cell infiltration can be drawn.

#### **4.3.2 What role might tumour-associated neutrophils be playing in SL7207-mediated tumour growth inhibition?**

One of the innate immune cell types which has been extensively documented for its tissue infiltration following oral *S. Typhimurium* infection are polymorphonuclear neutrophils (Barthel *et al.*, 2003; Rydström & Wick, 2009). Previous studies have demonstrated that *S. Typhimurium* promotes the migration of neutrophils to the site of infection by the N-terminus domain of the effector protein SipA (Lee *et al.*, 2000; Wall *et al.*, 2007). Bacterial-epithelial interactions subsequently elicit the production of chemoattractants secreted by enterocytes, in the form of chemokines such as IL-8 (Lee *et al.*, 2000).

In the present study, there was no difference in the number of neutrophils or the proportion of neutrophils within the CD45<sup>+</sup> immune cell compartment of the tumour following systemic SL7207 infection compared to uninfected. However, the neutrophils in the tumour displayed increased proliferative capacity and increased production of pro-inflammatory cytokines pro-IL1 $\beta$ , TNF- $\alpha$  and IL-22. It is interesting that the neutrophils increase the expression of Ki67, a marker for replication, yet there is no increase in the overall number of these cells even though they are very likely to be infiltrating the infected tissue. This suggests they may be undergoing cell death.

Given the pro-inflammatory functional phenotype of the neutrophils, it is possible that they are mediating the anti-tumour effects of SL7207. To investigate this, it would be necessary to employ the use of transgenic mice lacking neutrophils or utilise an antibody against neutrophils, such as  $\alpha$ -Ly6G, to inhibit their function and investigate if the local tumour immune response to systemic SL7207 infection is affected. This approach has already been employed in the context of bacterial-mediated cancer therapy, but the major parameter being investigated in that study was the dissemination of *Salmonella* in the tumour (Westphal *et al.*, 2008). The removal of neutrophils allowed for greater bacterial dissemination within the tumour and subsequently a more positive clinical outcome. This therefore suggests that the neutrophils, although they may be contributing to the pro-inflammatory environment, overall are antagonising the effects of the bacteria and therefore may not be the immune cell responsible for the tumour growth inhibitory effects of *S. Typhimurium*. It was for this reason that the role of neutrophils in SL7207-mediated tumour growth inhibition was not further investigated.

### **4.3.3 What role might the DCs be playing following SL7207 infection?**

DCs are critical innate immune responders to mucosal *S. Typhimurium* infection, as well as playing an important role in mediating anti-tumour immunity (Liu & Cao, 2015; Yrlid *et al.*, 2000). There have been many reports regarding the role of DCs in bacterial-mediated tumour growth inhibition (Avogadri *et al.*, 2005, 2008; Saccheri *et al.*, 2010). TdLN DCs have been implicated in playing an important role in mediating anti-tumour immunity following *S. Typhimurium*

(SL3261AT) in the B16F10 tumour-bearing mice by increasing cross-presentation of tumour specific model antigen and stimulating both CD4<sup>+</sup> and CD8<sup>+</sup> T cell proliferation *ex vivo* (Avogadri *et al.*, 2008). The formation of Cx43-dependent gap junctions assisted the delivery of pre-processed antigen from tumour cells to DCs resulting in a cytotoxic T cell response (Saccheri *et al.* 2010). However, in these studies, changes in the DC content of the tumour, or the necessity of DCs were not investigated.

Herein, we analysed the numbers of DCs in the tumour directly. Similar to the neutrophils, there was no difference in the number of total DCs recovered from tumours at any time point after infection. Further probing into the subsets of DCs revealed that there was a decrease in the number of CD11b<sup>+</sup> cDC2s but there was no significant change in the number of CD8<sup>+</sup> cDC1s, though a trend towards decreased numbers was observed. However, as CD103<sup>+</sup> cDCs are the non-lymphoid counterparts of CD8<sup>+</sup> cDC1 (del Rio *et al.*, 2010; Helft *et al.*, 2010), it may have been more informative to stain for CD103 instead of CD8 in the tumour to identify cDC1s. This may also account for why such low numbers of CD8<sup>+</sup> DCs were identified in the tumour (in the range of 12 cells to 221).

There was an increase in CD11b<sup>+</sup> DCs as a proportion of CD45<sup>+</sup> immune cells in the tumour-draining lymph node as well as an increase in CD8<sup>+</sup> DCs, suggesting an increase in DC migration, but these increases were not reflected in terms of absolute numbers. There was no significant change in the number of 'migratory DCs' (MHCII<sup>hi</sup>) in the lymph node. However, as the total number of cells recovered from the infected lymph nodes was significantly less than that recovered from the uninfected samples, (Appendix, Figure 9.2), this might account for the fact that any changes in the increase of migratory cells was not reflected in the quantification of absolute number. Interestingly, this trend of decreased cellular number was also evident in other experiments, which is surprising given that it has been reported that lymph nodes increase in size following systemic infection (Avogadri *et al.*, 2008).

CD11b<sup>+</sup> cDC2s are adept at activating CD4<sup>+</sup> T cells via MHCII presentation (Dudziak *et al.*, 2007). Therefore, an increase in the activation of CD4<sup>+</sup> T cells, discussed below, in the lymph node might be accounted for by an increased

migration of cDC2s. The data herein tentatively points towards that being the case. It would have been interesting to stain for C-C chemokine receptor type 7 (CCR7) in the tumour, which marks DCs ready for migration from the tissue to the lymph node (Jang *et al.*, 2006) to investigate if there was in fact stimulation of DC migration following infection.

The migration of DCs from the tumour to the tdLN might also account for the reported decrease in expression of CD80 and MHCII; it might not necessarily be that *S. Typhimurium* are interfering with the expression of these molecules, but the DCs with the greatest expression of them have already left the tumour to travel to the lymph node. There are mixed reports in the literature about the effects of *S. Typhimurium* on MHCII expression on DCs. The data reported herein contradicts that of Kalupahana and colleagues which looked at monocyte-derived DCs *in vitro*, and demonstrated that 2 hours of infection led to increased MHCII expression as well as increased expression of co-activation molecules CD80 and CD86 compared to control (Kalupahana *et al.*, 2005). Furthermore, systemic administration with *S. Typhimurium* resulted in increased MHCII and CD86 expression of splenic CD11c<sup>+</sup>MHCII<sup>+</sup> splenic DCs *in vivo* (Yrlid *et al.*, 2000). In contrast, other studies have reported *Salmonella* interferes with HLA-DR (the human equivalent of MHCII) cell surface expression on human APCs (Lapaque *et al.*, 2009; Mitchell *et al.*, 2004). This process has been attributed to a type three secretion system (T3SS)-2-mediated poly-ubiquitination of the HLA-DR molecule, resulting in the degradation of the antigen presenting molecule, thus downregulating HLA-DR on infected cells. Other work in our research group has observed a decrease in MHCII on mucosal-associated DCs following oral *S. Typhimurium* infection (unpublished data). This, combined with the consistency of the data presented herein, provides strong evidence that *S. Typhimurium*-mediated decrease in tumour-associated DC MHCII expression is a true phenomenon. The reduction of MHCII and/or CD80 on DCs would benefit *S. Typhimurium* by reducing the APCs' ability to present antigen, thus delaying or dampening the anti-bacterial T cell response.

To assess the true contribution of the DCs to bacterial-mediated tumour immunity, it would be necessary to either block or deplete DCs. This could be achieved through the employment of  $\alpha$ -CD11c antibody or use of a transgenic

mouse, such as the CD11c-DTR system, which allows expression of the diphtheria toxin receptor (DTR) under control of a CD11c-Cre and can be used to selectively deplete CD11c<sup>+</sup> cells upon diphtheria toxin administration (Jung *et al.*, 2002). With both of these methods, CD11c<sup>+</sup> macrophages and monocytes would also be depleted, so it would be necessary to determine if these cells change functionally or quantitatively in a wild type background in tumour-bearing mice following infection so as to limit the interpretation of the effects in the CD11c-abrogated mice to that of DCs.

#### **4.3.4 Why is it important to understand the type of T cell response in the infected tumour?**

Much of the focus on bacterial cancer therapy and the immune response has focused on the contribution of T<sub>H</sub>1-associated T cell response (Kaimala *et al.*, 2014; Lee *et al.*, 2011; Loeffler *et al.*, 2009; Stern *et al.*, 2015). The data presented herein is in keeping with a possible role for T<sub>H</sub>1 cells with an increase in CD4<sup>+</sup>Tbet<sup>+</sup> cells in the tumour and tdLN. CTLs have also been implicated in mediating the tumour growth inhibition effects of *E. coli* and *Salmonella* (Loeffler *et al.*, 2009; Stern *et al.*, 2015). The data presented in this report is consistent with published data in showing a role for CD8<sup>+</sup> T cells evidenced by the increase in CTLs, CD8<sup>+</sup>IFN- $\gamma$ <sup>+</sup> T cells, in the tumour and tdLN following infection. *S. Typhimurium* is adept at initiating both T<sub>H</sub>1 and T<sub>H</sub>17 responses in the gut (Raffatellu *et al.*, 2008; Ravindran *et al.*, 2005; Ye *et al.*, 2001). Both play important roles in protective immunity to oral *S. Typhimurium* infection. T<sub>H</sub>1 T cells migrate to infected tissue and produce IFN- $\gamma$  which activate macrophages and DCs to carry out their respective anti-microbial functions, as well as inducing oxidative burst of infected macrophages (Kalupahana *et al.*, 2005; MacMicking, 2012). T<sub>H</sub>17 T cells have recently become appreciated as players in T-cell mediated immunity through IL-17 production which stimulates neutrophil recruitment (Ye *et al.*, 2001) and the production of pro-inflammatory cytokines such as TNF- $\alpha$  and IL-1 $\beta$  in macrophages (Jovanovic *et al.*, 1998). Therefore, it was interesting to see an increase in the production of IL-17 in the tumour following infection. To our knowledge, this is the first report to suggest a role for T<sub>H</sub>17 cells in bacterial-mediated tumour therapy. This finding is interesting in the clinical context, as IL-17 is particularly beneficial for mediating tumour growth inhibition in certain cancer cell types such as

melanoma (Martin-Orozco *et al.*, 2010; Muranski *et al.*, 2008). On the contrary, IL-17 is particularly adept at stimulating tumourigenesis on other cancer types such as lymphoma and gastric cancers (He *et al.*, 2011; Liu *et al.*, 2011), suggesting that if T<sub>H</sub>17 cells are critical for the anti-tumour effects of *S. Typhimurium*, these cancer types might be unlikely to respond favourably.

It would be informative to look for CD4<sup>+</sup> T cells which stained positive for the T<sub>H</sub>17-associated transcription factor, ROR $\gamma$ t. However, the staining for ROR $\gamma$ t in the CD3<sup>+</sup>CD4<sup>+</sup> T cell compartment wasn't very strong which made it difficult to assess ROR $\gamma$ t<sup>+</sup> populations. It was possible that this was due to technical issues, but there was evident ROR $\gamma$ t staining within the CD45<sup>+</sup> compartment of the lymph node, which were not CD3<sup>+</sup> T cells.

Interestingly, there was also a decrease in the frequency of CD4<sup>+</sup>Foxp3<sup>+</sup> T cells in the infected tumours compared to the uninfected, which was not reflected in the T cell data from the lymph node. Given the reports regarding the plasticity of Tregs towards T<sub>H</sub>17 cells, it is tempting to speculate that *S. Typhimurium* is mediating the conversion of Tregs into T<sub>H</sub>17 cells. The conversion of Tregs into T<sub>H</sub>17 cells has been reported to be stimulated by IL-6 with the absence of TGF- $\beta$  signalling (Xu *et al.*, 2007). IL-6 is induced following *S. Typhimurium* infection by monocytes (Galdiero *et al.*, 1993) and also by DCs (Valdez *et al.*, 2008). Although TGF- $\beta$  has some pro-inflammatory effects, following on from the initial smouldering inflammation, it is generally an anti-inflammatory cytokine which can be produced by a range of tumour cell types and Tregs (Li *et al.*, 2007). As there is a severe reduction in the number of tumour cells and frequency of CD4<sup>+</sup>Foxp3<sup>+</sup> cells in the tumour following SL7207 infection, it is possible that there is a decrease in TGF- $\beta$  also. It would have been interesting to investigate the change in TGF- $\beta$  in the tumour microenvironment following SL7207 administration as this may have provided more evidence to address the hypothesis of tumour-local Treg to T<sub>H</sub>17 transformation.

However, although it is interesting to find increases in both T<sub>H</sub>1 and T<sub>H</sub>17 T cell responses in the tumour, as well as a decrease in the frequency of CD4<sup>+</sup>FoxP3<sup>+</sup> cells, it is important to point out that the frequency of detected CD4<sup>+</sup> and CD8<sup>+</sup> T cells in the tumour was very low. Although the data was consistent between

samples, the robustness of the data might be called in to question. In an attempt to overcome this limitation, the use of a Percoll density gradient was employed to remove large tumour and immune cells from the T cell compartment, but this was unsuccessful. A more effective approach might be to isolate CD3<sup>+</sup> T cells using MACS<sup>®</sup> Miltenyi Biotech Anti-CD3 $\epsilon$  Microbead magnetic beads, which would be the next logical step in trying to enrich for the CD4<sup>+</sup> and CD8<sup>+</sup> T cells in the tumour preparations.

There was one final interesting observation about the CD3<sup>+</sup> T cells which seemed to be unique to the tumour: the existence of CD4<sup>+</sup>CD8<sup>+</sup> T cells. It is irregular to find such a population in the body except in the thymus during T cell development (Parel & Chizzolini, 2004). This population was found to be present in most, but not all, of the T cell analysis experiments. However, one report demonstrated that this population is overrepresented in human melanoma metastases compared to tissue from healthy controls (Desfrancois *et al.*, 2010). These cells were reported to be as competent as CD4<sup>+</sup> and CD8<sup>+</sup> T cells at producing multiple cytokines but are attenuated in their proliferative capacity compared to the single positive cells *in vitro*. In the present study, these cells were not subjected to investigation due to time constraints, but it might be interesting to retrospectively analyse the transcription factor activation and cytokine production of these cells with the data sets already generated for examining CD4<sup>+</sup> and CD8<sup>+</sup> T cells in the tumour.

#### **4.3.5 Concluding Remarks**

In summary, the tumour-growth inhibitory effect of systemically administered SL7207 in tumour-bearing mice was associated with increased production of pro-inflammatory mediators in the tumour microenvironment and changes in immune cell activation. However, this did not appear to be associated with an infiltration of CD45<sup>+</sup> leukocytes. Neutrophils adopted a pro-inflammatory phenotype following infection and cDC2s possibly increased migration to the tdLN. The most interesting finding was the discovery of a T<sub>H</sub>17 response in the tumour following infection, as well as the concomitant decrease in the frequency of CD4<sup>+</sup>FoxP3<sup>+</sup> T cells in tumour. Given that T<sub>H</sub>17 responses have been demonstrated to be more potentially anti-tumourigenic than T<sub>H</sub>1 cells in some cancer settings, this potential T<sub>H</sub>17 response should be further investigated.

# 5 The role of the monocyte/macrophage compartment in SL7207-mediated tumour growth inhibition

## 5.1 Introduction

Monocytes and macrophages play critical roles in tumourigenesis (Qian & Pollard, 2010). Tumour-associated macrophages (TAMs) have been implicated in promoting an immunosuppressive immune environment, stimulating angiogenesis as well as promoting metastasis at distant sites. It has been reported that in over 80% of clinical studies evaluating multiple tumour types, there was a negative relationship between TAM density and patient prognosis (Bingle *et al.*, 2002).

Monocytes are important components of innate immune defence in *S. Typhimurium* infection (Rydstrom & Wick, 2007). Inflammatory monocytes are rapidly recruited to the Peyer's patches and mesenteric lymph nodes following oral *S. Typhimurium* infection (Rydström & Wick, 2009). Although a subset of monocytes which highly express the monocyte marker Ly6C, termed Ly6C<sup>hi</sup> monocytes, can give rise to tissue-resident macrophages, there are certain physiological conditions where this differentiation process is interfered with, such as during inflammation (Bain *et al.*, 2013; Serbina *et al.*, 2003; Zigmond *et al.*, 2012). Numerous reports have described that following the induction of inflammation, infiltrating monocytes which are recruited to the inflamed tissue, retain their monocyte phenotype and do not differentiate into tissue-resident macrophages (Bain *et al.*, 2013; Zigmond *et al.*, 2012). These monocyte/macrophage intermediates (Ly6C<sup>+</sup>MHCII<sup>+</sup> cells) are highly pro-inflammatory and are critical mediators of inflammation in the tissue. These cells might prove particularly adept at transforming the tumour microenvironment from immunosuppressive to immunostimulatory. However, the role of monocytes in the tumour growth inhibitory effects of *S. Typhimurium* has not been investigated.

TAMs are generally immunosuppressive and, characterised by low expression of MHCII, and PD-1, and the production of TGF- $\beta$  and IL-10 (Gordon *et al.*, 2017; Movahedi *et al.*, 2010; Movahedi & Van Genderachter, 2016). The removal or

ablation of TAMs has resulted in a beneficial outcome in a number of experimental cancer models (Gazzaniga *et al.*, 2007; Kimura *et al.*, 2007; Lin *et al.*, 2001). Macrophages are highly plastic cells and have been reported to change their phenotype depending on environmental signals (Guidicci *et al.*, 2005; Lavin *et al.*, 2014; Saccani *et al.*, 2006). Therefore, it would be beneficial for the purposes of cancer treatment if immunosuppressive TAMs could be stimulated to become pro-inflammatory TAMs, whose secreted cytokines and immune cell recruitment would not be conducive to tumour growth. For this to occur, the TAMs would have to encounter a potent immunostimulatory stimulus capable of modifying their phenotype. Tissue-resident macrophages are reportedly activated following *S. Typhimurium* infection to enhance phagocytosis and produce pro-inflammatory cytokines (Mastroeni *et al.*, 1995; Yrlid *et al.*, 2000). In the present study, it was hypothesised that the systemic administration of *S. Typhimurium* would achieve this, and that this process would be largely responsible for the anti-tumour effects of systemic bacterial administration.

To explore the role of tumour monocyte/macrophages in *S. Typhimurium* mediated tumour inhibition, *Ccr2*<sup>-/-</sup> mice that lack circulating Ly6C<sup>hi</sup> monocytes and liposomes containing clodronate can be employed (Franklin *et al.*, 2014; Gazzaniga *et al.*, 2007). Clodronate is a molecule which can be converted to a non-hydrolysable ATP-analogue in the cytosol of a cell (Rooijen & Sanders, 1994; Weisser *et al.*, 2012). This blocks the ATP translocase in the outer mitochondrial membrane and leads to mitochondrial-mediated cell death within cells that take up the liposomes via phagocytosis, such as monocytes and macrophages.

### 5.1.1 Aims

1. To identify the monocyte and macrophage populations in the B16F10 tumour
2. To understand the changes in tumour monocytes and macrophages following SL7207 infection
3. To investigate the relative contributions of MHCII<sup>lo</sup> TAMs and infiltrating monocytes in the generation of MHCII<sup>+</sup> TAMs following SL7207 infection

4. To investigate the tumour growth inhibitory effects of SL7207 in the absence of monocytes

## 5.2 Results

### 5.2.1 Tumour-associated monocyte/macrophage subsets in the B16F10 tumours in the uninfected state

From the literature, it is apparent that there are multiple gating strategies to look at monocytes and macrophages in a tumour (Franklin *et al.*, 2014; Movahedi *et al.*, 2010). The strategy employed in the present study was adapted from a protocol which is used extensively in our laboratory to look at colonic macrophages (Bain *et al.*, 2014) and was consistent with published reports (Cortez-Retamozo *et al.*, 2012; Movahedi *et al.*, 2010). The gating strategy for the identification of the monocyte and macrophage subsets is presented in Chapter 4, Figure 4.1. The subsets of monocytes and macrophages found to be present in the B16F10 tumour were Ly6C<sup>+</sup>MHCII<sup>-</sup> monocytes (Q1), Ly6C<sup>+</sup>MHCII<sup>+</sup> monocytes (Q2), mature Ly6C<sup>-</sup>MHCII<sup>+</sup> TAMs (Q3) and mature Ly6C<sup>-</sup>MHCII<sup>-</sup> TAMs (Q4) (Figure 5.1A). As well as Ly6C expression, monocytes were distinguishable from TAMs due to lower side scatter and lower expression of the resident macrophage marker F4/80, a marker for macrophage residency (Gundra *et al.*, 2017), which was found at high levels on both TAM populations (Figure 5.1B-D).

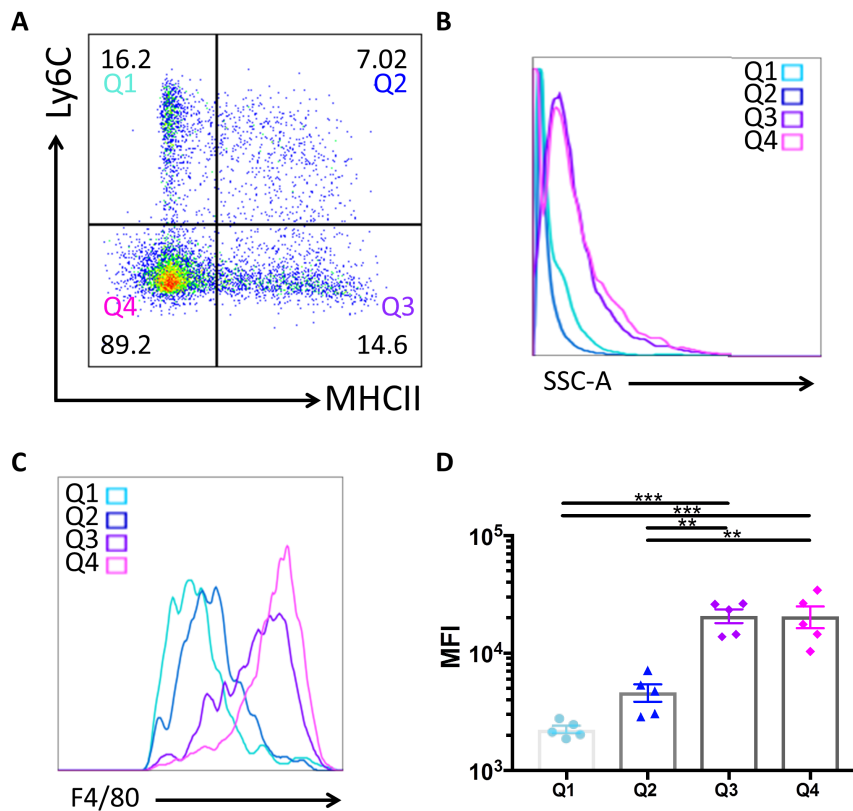


**Figure 5.1 Monocyte/macrophage populations in uninfected B16F10 tumours**

B16F10 tumour cells were seeded in C57BL6 mice and 14 days later, tumours were harvested for flow cytometry analysis of the macrophage/monocyte compartment. **A.** Representative flow cytometry plot of the monocyte/macrophage compartment in B16F10 tumours. Cells were gated as single, live, CD45<sup>+</sup>, CD11b<sup>+</sup>, SiglecF<sup>-</sup>, F4/80<sup>+</sup>, Ly6G<sup>-</sup>. **B.** Representative histogram plot showing side scatter (SSC-A) for the populations shown in A. **C.** Representative histogram plot showing F4/80 expression on each of the populations shown in A. **D.** MFI of F4/80 expression on each of the populations represented in A. Error bars SEM. Statistical analyses performed using One Way Anova; p < 0.05\*, p < 0.01\*\*, p < 0.001\*\*\*.

There appears to a number of different functional characterisations of TAMs based on MHCII expression profiles (Gabrilovich *et al.*, 2012). In one report, TAMs were assigned to be either MHCII<sup>+</sup> or MHCII<sup>lo</sup>, each exhibiting differential tumour-promoting characteristics (Movahedi *et al.*, 2010). Therefore, in the current study, the functional differences in the TAM populations identified, MHCII<sup>-</sup> and MHCII<sup>+</sup> TAMs were investigated in the uninfected state. At 13 days post tumour cell inoculation, the two subsets of MHCII<sup>-</sup> and MHCII<sup>+</sup> mature TAMs had proliferated to the same extent, as evidenced by comparable proportions of cells expressing Ki67 (Figure 5.2A, B). The data are presented as the proportion of cells which were Ki67<sup>+</sup> in the indicated TAM population. In order to assess the functional capacity of TAMs, single cell suspensions of tumour cells were stimulate *in vitro* in the presence of a protein transport inhibitor cocktail before assessing the intracellular expression of cytokines by TAMs using flow cytometry. There was a greater frequency of mature MHCII<sup>+</sup> TAMs which were TNF- $\alpha$ <sup>+</sup>

compared with the MHCII<sup>-</sup> population (Figure 5.2C, D), but there was no statistically significant difference in the expression levels of either IL-12p40 (Figure 5.2E, F) or IL-6 (Figure 5.2G, H) between the populations, although there was a trend towards a decrease in IL-6 expression in the MHCII<sup>+</sup> TAMs ( $p = 0.0506$ ).

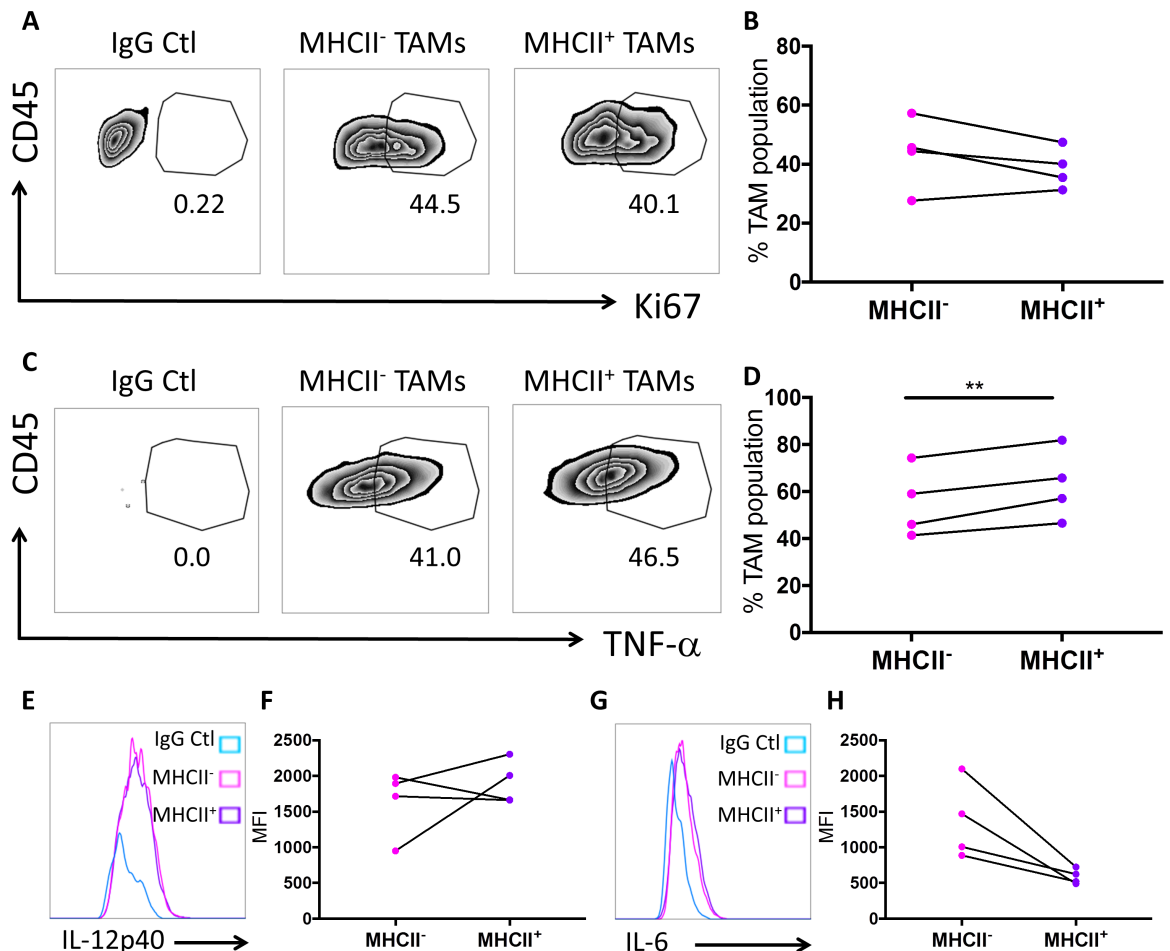


**Figure 5.2 Functional features of MHCII<sup>-</sup> and MHCII<sup>+</sup> TAMs in B16F10 tumours**

B16F10 tumour cells were seeded in C57BL6 mice and 14 days later, tumours were harvested for *in vitro* stimulation and flow cytometry analysis of TAMs. Cells were gated as single, live, CD45<sup>+</sup>, CD11b<sup>+</sup>, SiglecF<sup>-</sup>, F4/80<sup>+</sup>, Ly6G<sup>-</sup>, Ly6C<sup>-</sup>. **A.** Representative flow cytometry plots showing Ki67<sup>+</sup> MHCII<sup>-</sup> and MHCII<sup>+</sup> TAMs, including an IgG isotype control for all TAMs. **B.** Data shown as percentage Ki67<sup>+</sup> cells of total MHCII<sup>-</sup> or MHCII<sup>+</sup> TAMs. **C.** Representative flow cytometry plots showing TNF- $\alpha$ <sup>+</sup> MHCII<sup>-</sup> and MHCII<sup>+</sup> TAMs, including an IgG isotype control for all TAMs. **D.** Data shown as percentage TNF- $\alpha$ <sup>+</sup> cells of total MHCII<sup>-</sup> and MHCII<sup>+</sup> TAMs samples. **E.** Representative histogram plot of MHCII<sup>-</sup> and MHCII<sup>+</sup> TAMs IL-12p40 expression, including an IgG isotype control for all TAMs. **F.** MFI of IL-12p40 expression in MHCII<sup>-</sup> and MHCII<sup>+</sup> TAMs. **G.** Representative histogram plot of MHCII<sup>-</sup> and MHCII<sup>+</sup> TAMs IL-6 expression, including an IgG isotype control for all TAMs. **H.** MFI of IL-6 expression in MHCII<sup>-</sup> and MHCII<sup>+</sup> TAMs. Statistical analyses performed using paired Student's t test where  $p < 0.05^*$ ,  $p < 0.01^{**}$ .

The phagocytic capacity of the TAMs was investigated following the co-incubation of tumour cells with pHrodo<sup>TM</sup> Red *E. coli* Bioparticles<sup>TM</sup>. This

revealed that the MHCII<sup>+</sup> mature TAMs had a significantly greater phagocytic capacity than the MHCII<sup>-</sup> mature TAMs (Figure 5.3).

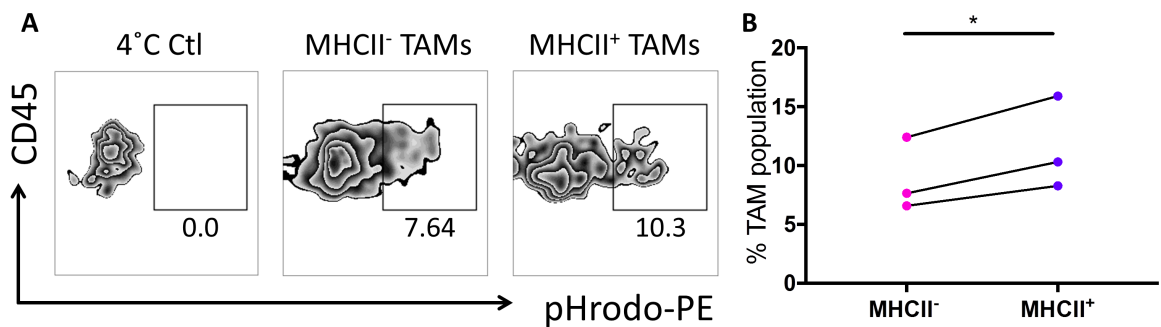


**Figure 5.3 Phagocytic capacities of MHCII<sup>-</sup> and MHCII<sup>+</sup> TAMs**

B16F10 tumour cells were seeded in C57BL/6 mice and 14 days later, tumours were harvested for co-incubation with pHrodo-PE Bioparticles™ to assess phagocytic capacity. **A.** Representative flow cytometry plots showing uptake of pHrodo-PE by MHCII<sup>+</sup> and MHCII<sup>-</sup> TAMs, including a 4°C control. Cells were gated as single, live, CD45<sup>+</sup>, CD11b<sup>+</sup>, SiglecF<sup>-</sup>, F4/80<sup>+</sup>, Ly6G<sup>-</sup>, Ly6C<sup>-</sup>. **B.** Data shown is percentage pHrodo-PE<sup>+</sup> cells among total MHCII<sup>+</sup> and MHCII<sup>-</sup> TAMs. Statistical analysis performed using paired Student's t test where  $p < 0.05^*$ .

### 5.2.2 Effects of systemic SL7207 infection on tumour-associated monocytes

Classical Ly6C<sup>hi</sup> MHCII<sup>-</sup> monocytes are thought to be the precursors of TAMs and accumulation of monocytes and their immediate progeny Ly6C<sup>hi</sup>MHCII<sup>+</sup> cells (Franklin *et al.*, 2014), are a characteristic feature of *S. Typhimurium* infection and other forms of inflammation (Bain *et al.*, 2013; Bain *et al.*, 2014; Rydstrom & Wick, 2007). To examine changes in the monocyte/macrophage populations, tumour-bearing mice were inoculated with SL7207 or PBS and tumours were harvested at multiple time points for flow cytometry analysis.

There were significant decreases in the number of Ly6C<sup>+</sup>MHCII<sup>-</sup> cells following infection at 3 and 7 dpi (Figure 5.4A, B). However, given that the tumours from the infected mice were much smaller than those in the uninfected, absolute numbers might not be reflective of the expansion of a given cell type following infection. Therefore, to establish if there was a reduction of Ly6C<sup>+</sup>MHCII<sup>-</sup> cells within the leukocyte compartment, the number of Ly6C<sup>+</sup>MHCII<sup>-</sup> cells amongst total CD45<sup>+</sup> cells was also evaluated. There was a significant decrease in the Ly6C<sup>+</sup>MHCII<sup>-</sup> cells as a proportion of total CD45<sup>+</sup> cells at 3 dpi (Figure 5.4C).

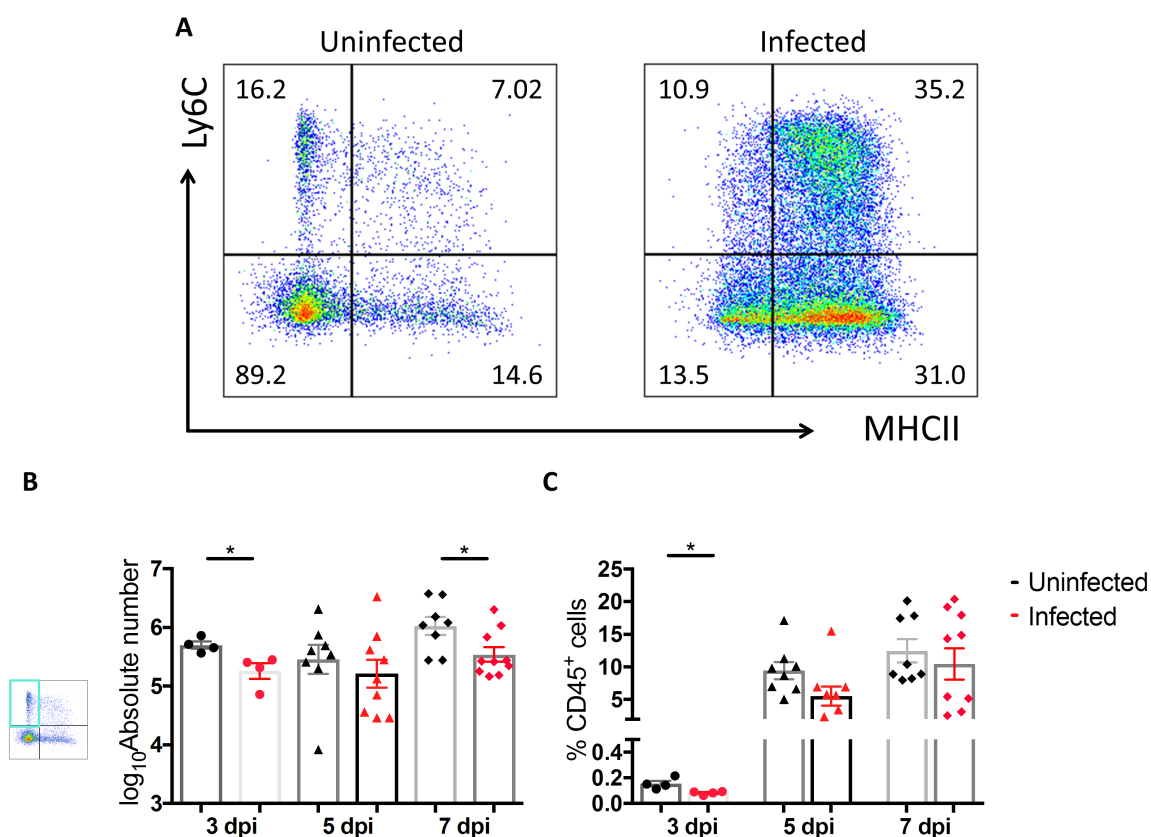


**Figure 5.4 Effects of SL7207 infection on tumour Ly6C<sup>+</sup>MHCII<sup>-</sup> monocyte content**

Tumour-bearing mice were inoculated with SL7207 or PBS and tumours were harvested at 3, 5 and 7 dpi for flow cytometry analysis of tumour immune cell content. **A**. Representative flow cytometry plots of Ly6C<sup>+</sup>MHCII<sup>-</sup> monocytes cells from infected and uninfected tumours at 5 dpi. Cells were gated on single, live, CD45<sup>+</sup>, CD11b<sup>+</sup>, SiglecF<sup>-</sup>, F4/80<sup>+</sup>, Ly6G<sup>-</sup>. **B**. Quantification of absolute number of Ly6C<sup>+</sup>MHCII<sup>-</sup> monocytes from infected and uninfected tumours at the indicated time points. **C**. Data shown as percentage Ly6C<sup>+</sup>MHCII<sup>-</sup> monocytes of total CD45<sup>+</sup> cells from infected and uninfected tumours at the indicated time points. Error bars SEM. Statistical analyses performed using Students t test between infected and uninfected samples at the same time point where  $p < 0.05^*$ .

Within the Ly6C<sup>+</sup>MHCII<sup>-</sup> population, there was an increase in the proportion of cells which were Ki67<sup>+</sup> following infection (Figure 5.5A, B). There was also an increase in the frequency of cells that expressed the pro-inflammatory cytokines TNF- $\alpha$  (Figure 5.5C, D) and pro-IL-1 $\beta$  (Figure 5.5E,F) as well as the population expression of IL-12p40 from infected samples (Figure 5.5G,H). IL-6 expression was unchanged (Figure 5.5I, J). There was no significant difference in the phagocytic capacity of the Ly6C<sup>+</sup>MHCII<sup>-</sup> cells between infected and uninfected samples (Figure 5.6)

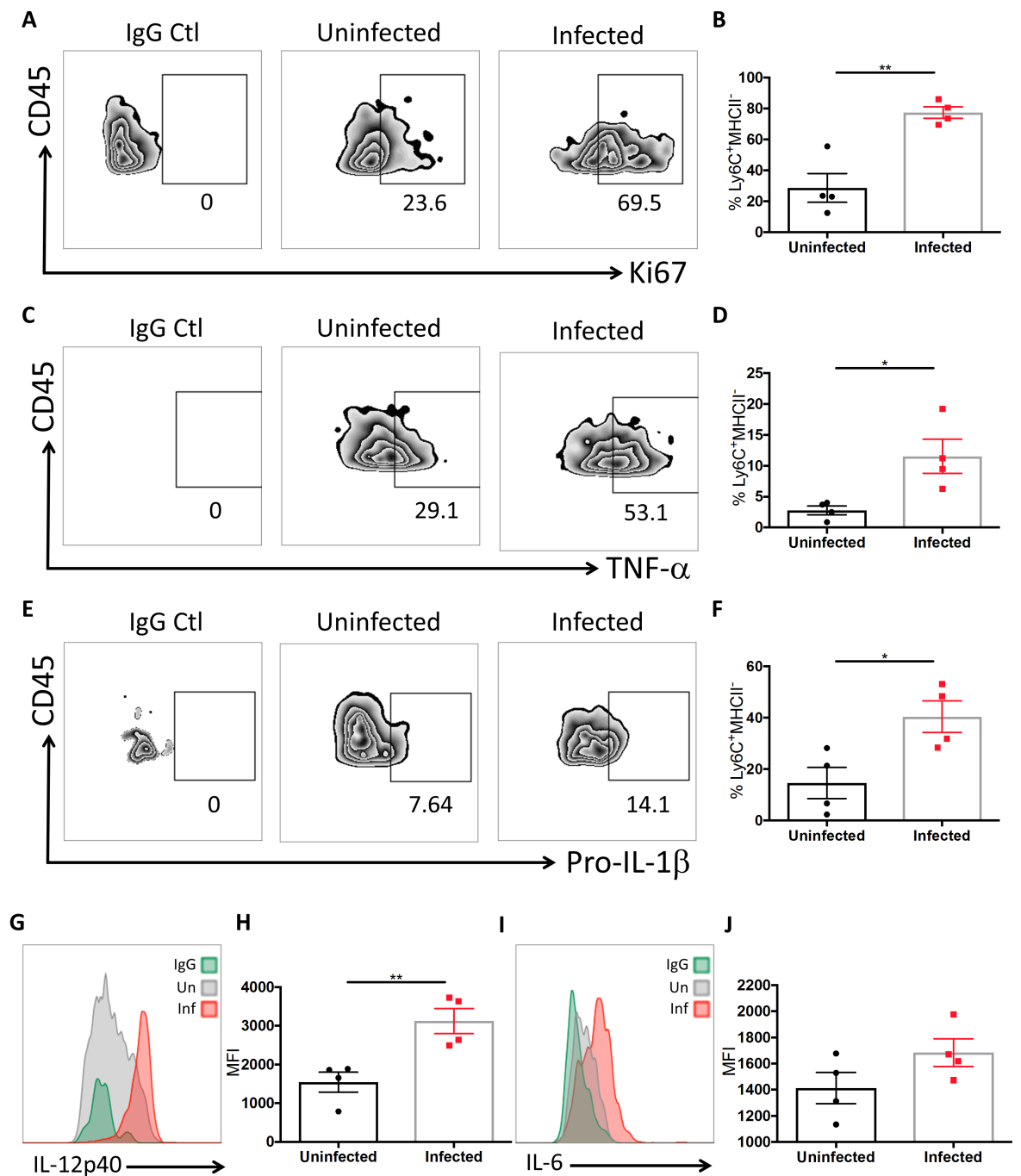


**Figure 5.5 Effects of SL7207 infection on the functional phenotype of tumour Ly6C<sup>+</sup>MHCII<sup>-</sup> monocytes**

Tumour-bearing mice were inoculated with SL7207 or PBS and tumours were harvested at 5 dpi for *in vitro* stimulation and flow cytometry analysis of Ly6C<sup>+</sup>MHCII<sup>-</sup> monocytes. Cells were gated on single, live, CD45<sup>+</sup>, CD11b<sup>+</sup>, SiglecF<sup>-</sup>, F4/80<sup>+</sup>, Ly6G<sup>-</sup>, Ly6C<sup>+</sup>, MHCII<sup>-</sup>. **A**. Representative flow cytometry plots showing Ki67<sup>+</sup> Ly6C<sup>+</sup>MHCII<sup>-</sup> monocytes for infected and uninfected tumours, including an IgG isotype control. **B**. Data shown as percentage Ki67<sup>+</sup> cells of total Ly6C<sup>+</sup>MHCII<sup>-</sup> monocytes from infected and uninfected tumours. **C**. Representative flow cytometry plots showing TNF-α<sup>+</sup> Ly6C<sup>+</sup>MHCII<sup>-</sup> monocytes for infected and uninfected samples including an IgG isotype control. **D**. Data shown as percentage TNF-α<sup>+</sup> cells of total Ly6C<sup>+</sup>MHCII<sup>-</sup> monocytes from infected and uninfected samples. **E**. Representative flow cytometry plots showing pro-IL-1β<sup>+</sup> Ly6C<sup>+</sup>MHCII<sup>-</sup> monocytes for infected and uninfected samples including an IgG isotype control. **F**. Data shown as percentage pro-IL-1β<sup>+</sup> cells of total Ly6C<sup>+</sup>MHCII<sup>-</sup> monocytes from infected and uninfected samples. **G**. Representative histogram plot of Ly6C<sup>+</sup>MHCII<sup>-</sup> monocytes IL-12p40 expression from infected and uninfected samples including an IgG isotype control. **H**. MFI of IL-12p40 expression from Ly6C<sup>+</sup>MHCII<sup>-</sup> monocytes from infected and uninfected samples. **I**. Representative histogram plot of

Ly6C<sup>+</sup>MHCII<sup>-</sup> monocytes IL-6 expression from infected and uninfected samples including an IgG isotype control. **J.** MFI of IL-6 expression from Ly6C<sup>+</sup>MHCII<sup>-</sup> monocytes from infected and uninfected samples. Error bars SEM. Statistical analyses performed using Student's t test between infected and uninfected samples at the same time point where  $p < 0.05^*$ .

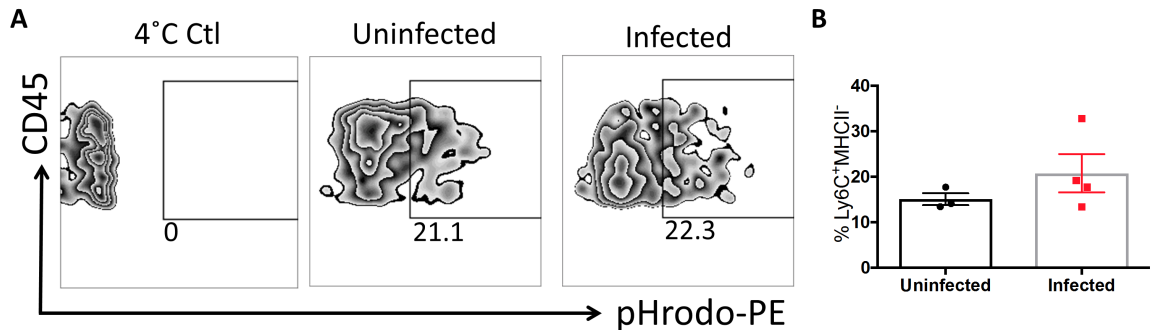


**Figure 5.6 Effect of SL7207 infection on the phagocytic capacity of tumour Ly6C<sup>+</sup>MHCII<sup>+</sup> monocytes**

Tumour-bearing mice were inoculated with SL7207 or PBS and tumours were harvested at 5 dpi for co-incubation with pHrodo-PE Bioparticles<sup>TM</sup> to assess phagocytic capacity. Cells were gated on single, live, CD45<sup>+</sup>, CD11b<sup>+</sup>, SiglecF<sup>-</sup>, F4/80<sup>+</sup>, Ly6G<sup>-</sup>, Ly6C<sup>+</sup>, MHCII<sup>-</sup>. **A.** Representative flow cytometry plots showing uptake of pHrodo-PE by Ly6C<sup>+</sup>MHCII<sup>-</sup> monocytes from infected and uninfected tumours. **B.** Data shown as percentage pHrodo-PE<sup>+</sup> cells among total Ly6C<sup>+</sup>MHCII<sup>-</sup> monocytes from infected and uninfected tumours. Error bars SEM. Statistical analysis performed using Student's t test where  $p < 0.05^*$ .

There was no significant difference in the number of Ly6C<sup>+</sup>MHCII<sup>+</sup> cells between infected and uninfected tumours (Figure 5.7A). However, there were highly significant increases in Ly6C<sup>+</sup>MHCII<sup>+</sup> cells as a proportion of the CD45<sup>+</sup> immune cell compartment at 5 and 7 dpi (Figure 5.7B).

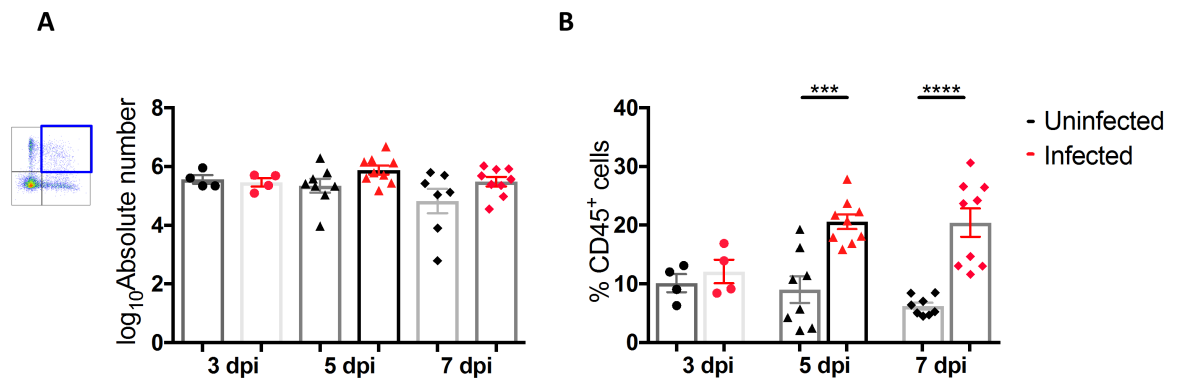


**Figure 5.7 Effects of SL7207 infection on tumour Ly6C<sup>+</sup>MHCII<sup>+</sup> monocyte content**

Tumour-bearing mice were inoculated with SL7207 or PBS and tumours were harvested at 3, 5 and 7 dpi for flow cytometry analysis of tumour immune cell content. Cells were gated on single, live, CD45<sup>+</sup>, CD11b<sup>+</sup>, SiglecF<sup>-</sup>, F4/80<sup>+</sup>, Ly6G<sup>-</sup>, Ly6C<sup>+</sup>, MHCII<sup>-</sup>. **A.** Quantification of absolute number of Ly6C<sup>+</sup>MHCII<sup>+</sup> monocytes from infected and uninfected tumours at the indicated time points. **C.** Data shown as percentage Ly6C<sup>+</sup>MHCII<sup>+</sup> monocytes of total CD45<sup>+</sup> cells from infected and uninfected tumours at the indicated time points. Error bars SEM. Statistical analyses performed using Students t test between infected and uninfected samples at the same time point where  $p < 0.05^*$ ,  $p < 0.01^{**}$ ,  $p < 0.001^{***}$ .

There was an increase in the proportion of Ly6C<sup>+</sup>MHCII<sup>+</sup> cells which expressed Ki67 at 5 dpi (Figure 5.8A, B). Following infection, there were no significant differences in the frequency of Ly6C<sup>+</sup>MHCII<sup>+</sup> cells positive the pro-inflammatory markers, TNF- $\alpha$  (Figure 5.8C, D) or pro-IL-1 $\beta$  (Figure 5.8E,F). There were also no differences in the expression of IL-12p40 (Figure 5.8G,H) between Ly6C<sup>+</sup>MHCII<sup>+</sup> cells from infected and uninfected samples. However, there was a significant increase in the expression of IL-6 in the Ly6C<sup>+</sup>MHCII<sup>-</sup> cells in samples which were infected compared to uninfected controls (Figure 5.8I, J).

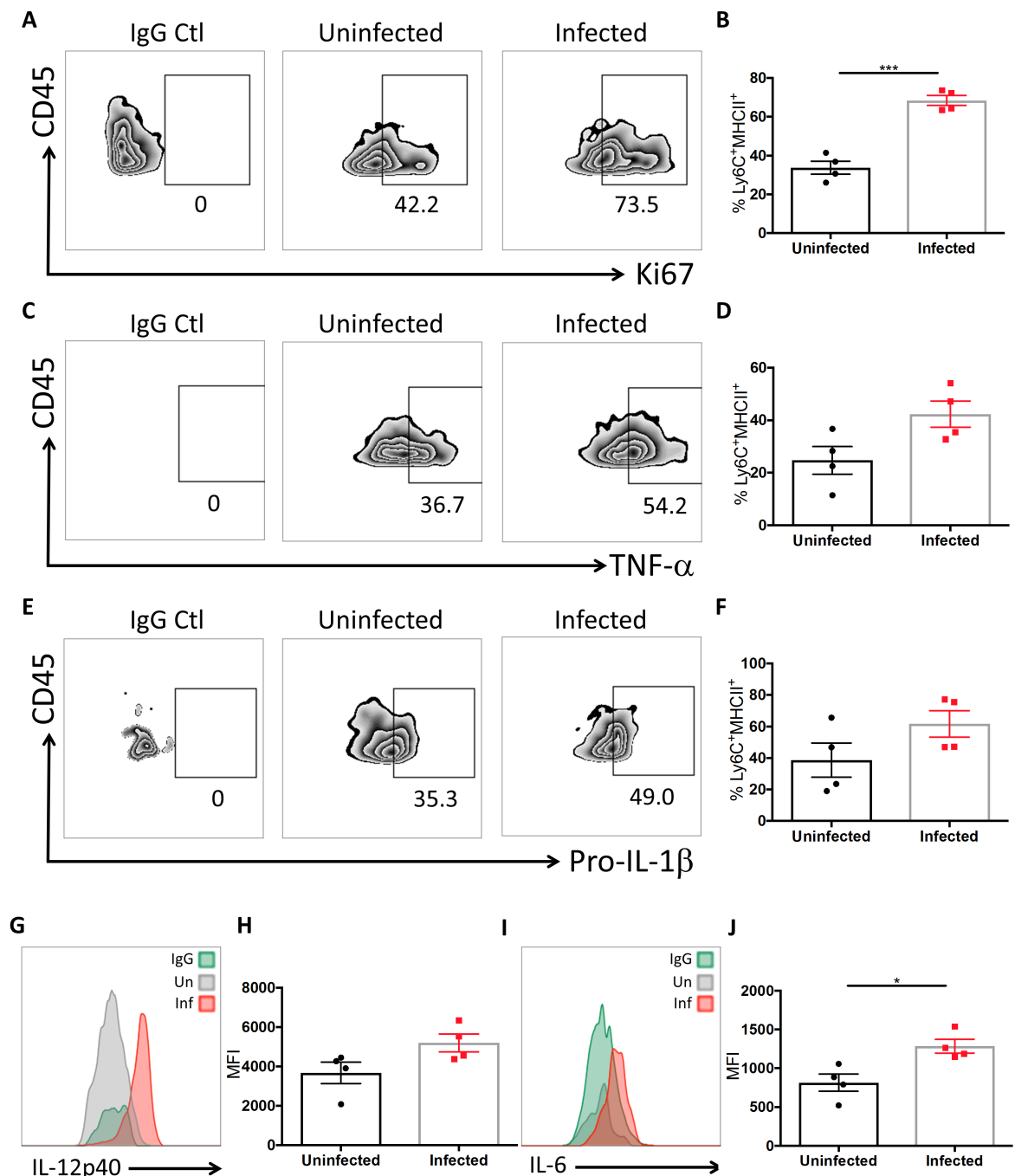


**Figure 5.8 Effects of SL7207 infection functional phenotype of tumour Ly6C<sup>+</sup>MHCII<sup>+</sup> monocytes**

Tumour-bearing mice were inoculated with SL7207 or PBS and tumours were harvested at 5 dpi for *in vitro* stimulation and flow cytometry analysis of Ly6C<sup>+</sup>MHCII<sup>+</sup> monocytes. Cells were gated on single, live, CD45<sup>+</sup>, CD11b<sup>+</sup>, SiglecF<sup>-</sup>, F4/80<sup>+</sup>, Ly6G<sup>-</sup>, Ly6C<sup>+</sup>, MHCII<sup>+</sup>. **A**. Representative flow cytometry plots showing Ki67<sup>+</sup> Ly6C<sup>+</sup>MHCII<sup>+</sup> monocytes for infected and uninfected tumours, including an IgG isotype control. **B**. Data shown as percentage Ki67<sup>+</sup> cells of total Ly6C<sup>+</sup>MHCII<sup>+</sup> monocytes from infected and uninfected tumours. **C**. Representative flow cytometry plots showing TNF-α<sup>+</sup> Ly6C<sup>+</sup>MHCII<sup>+</sup> monocytes for infected and uninfected samples including an IgG isotype control. **D**. Data shown as percentage TNF-α<sup>+</sup> cells of total Ly6C<sup>+</sup>MHCII<sup>+</sup> monocytes from infected and uninfected samples. **E**. Representative flow cytometry plots showing pro-IL-1β<sup>+</sup> Ly6C<sup>+</sup>MHCII<sup>+</sup> monocytes for infected and uninfected samples including an IgG isotype control. **F**. Data shown as percentage pro-IL-1β<sup>+</sup> cells of total Ly6C<sup>+</sup>MHCII<sup>+</sup> monocytes from infected and uninfected samples. **G**. Representative histogram plot of Ly6C<sup>+</sup>MHCII<sup>+</sup> monocytes IL-12p40 expression from infected and uninfected samples including an IgG isotype control. **H**. MFI of IL-12p40 expression from Ly6C<sup>+</sup>MHCII<sup>+</sup> monocytes from infected and uninfected samples. **I**. Representative histogram plot of Ly6C<sup>+</sup>MHCII<sup>+</sup> monocytes IL-6 expression from infected and uninfected samples including an IgG

isotype control. **J.** MFI of IL-6 expression from Ly6C<sup>+</sup>MHCII<sup>+</sup> monocytes from infected and uninfected samples. Error bars SEM. Statistical analyses performed using Students test t between infected and uninfected samples at the same time point where  $p < 0.05^*$ .

There was also a significant increase in the phagocytic capacity of the Ly6C<sup>+</sup>MHCII<sup>+</sup> monocyte cells following infection (Figure 5.9).

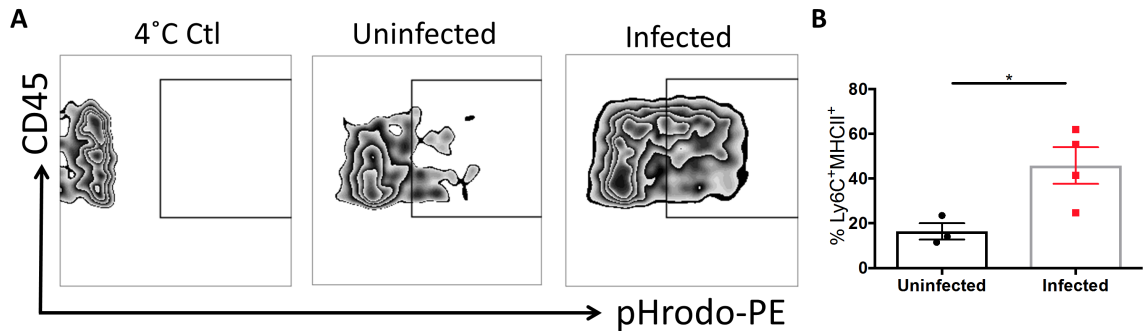


**Figure 5.9 Effect of SL7207 on the phagocytic capacity of tumour Ly6C<sup>+</sup>MHCII<sup>+</sup> monocytes**

Tumour-bearing mice were inoculated with SL7207 or PBS and tumours were harvested at 5 dpi for co-incubation with pHrodo-PE Bioparticles<sup>TM</sup> to assess phagocytic capacity. Cells were gated on single, live, CD45<sup>+</sup>, CD11b<sup>+</sup>, SiglecF<sup>-</sup>, F4/80<sup>+</sup>, Ly6G<sup>-</sup>, Ly6C<sup>+</sup>, MHCII<sup>+</sup>. **A.** Representative flow cytometry plots showing uptake of pHrodo-PE by Ly6C<sup>+</sup>MHCII<sup>+</sup> monocytes from infected and uninfected tumours. **B.** Data shown as percentage pHrodo-PE<sup>+</sup> cells among total Ly6C<sup>+</sup>MHCII<sup>+</sup> monocytes from infected and uninfected tumours. Error bars SEM. Statistical analysis performed using Student's t test where  $p < 0.05^*$ .

These data suggest that the Ly6C<sup>+</sup> tumour monocytes, particularly the Ly6C<sup>+</sup>MHCII<sup>+</sup> cells, become activated following infection and contribute to the inflammatory tumour environment.

### 5.2.3 Effects of systemic SL7207 infection on TAMs

There was no significant difference in the number of MHCII<sup>-</sup> TAMs at any time post infection compared to uninfected controls (Figure 5.10A). There was, however, a significant decrease in these cells as a proportion of CD45<sup>+</sup> leukocytes at 5 and 7 dpi (Figure 5.10B). For the MHCII<sup>+</sup> TAMs, there were no significant differences in the absolute number of cells recovered from infected and uninfected samples (Figure 5.10C), nor was there a difference in these cells as a proportion of CD45<sup>+</sup> cells, although there appeared to be a trend towards an increase in the infected samples, particularly at 5 dpi (Figure 5.10D).

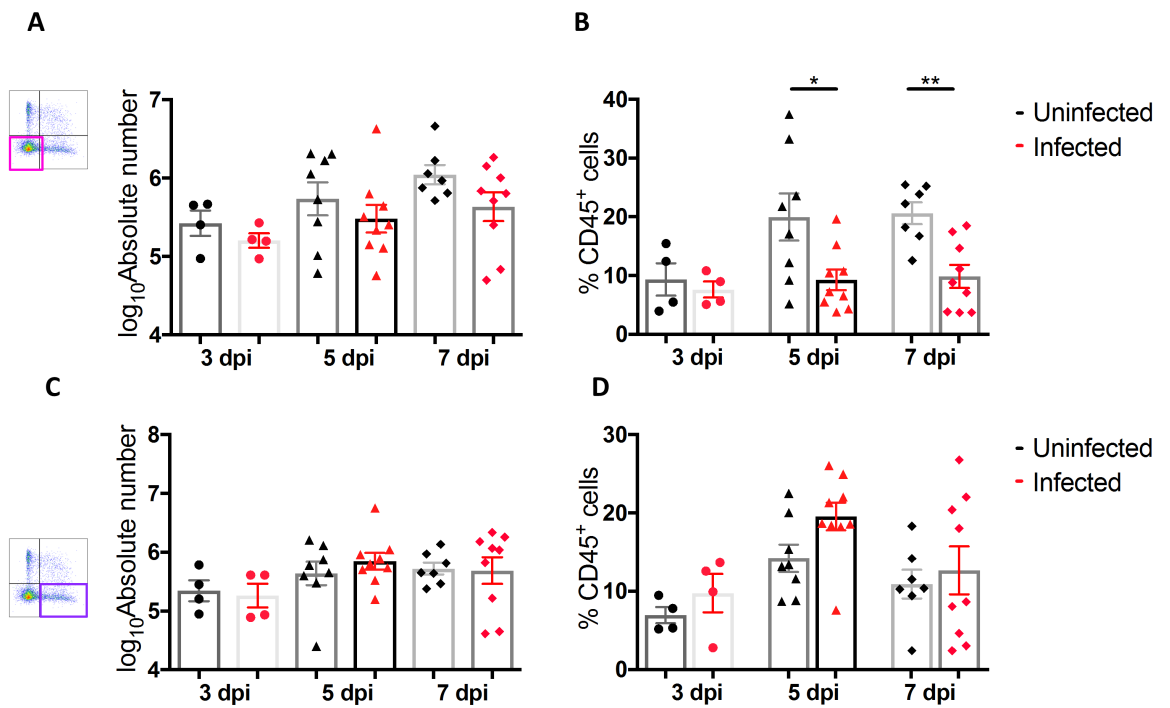


**Figure 5.10 Effects of SL7207 infection on TAM content**

Tumour-bearing mice were inoculated with SL7207 or PBS and tumours were harvested at 3, 5 and 7 dpi for flow cytometry analysis of tumour immune cell content. Cells were gated on single, live, CD45<sup>+</sup>, CD11b<sup>+</sup>, SiglecF<sup>-</sup>, F4/80<sup>+</sup>, Ly6G<sup>-</sup>, Ly6C<sup>-</sup>. **A**. Quantification of absolute number of MHCII<sup>-</sup> TAMs from infected and uninfected tumours at the indicated time points. **B**. Data shown as percentage MHCII<sup>-</sup> TAMs of total CD45<sup>+</sup> cells from infected and uninfected tumours at the indicated time points. **C**. Quantification of absolute number of MHCII<sup>+</sup> TAMs from infected and uninfected tumours at the indicated time points. **D**. Data shown as percentage MHCII<sup>+</sup> TAMs of total CD45<sup>+</sup> cells from infected and uninfected tumours at the indicated time points. Error bars SEM. Statistical analyses performed using Students t test between infected and uninfected samples at the same time point where  $p < 0.05^*$ ,  $p < 0.01^{**}$ .

Despite this, within the TAM population as whole, there was a shift towards increased expression of MHCII following infection (Figure 5.11).

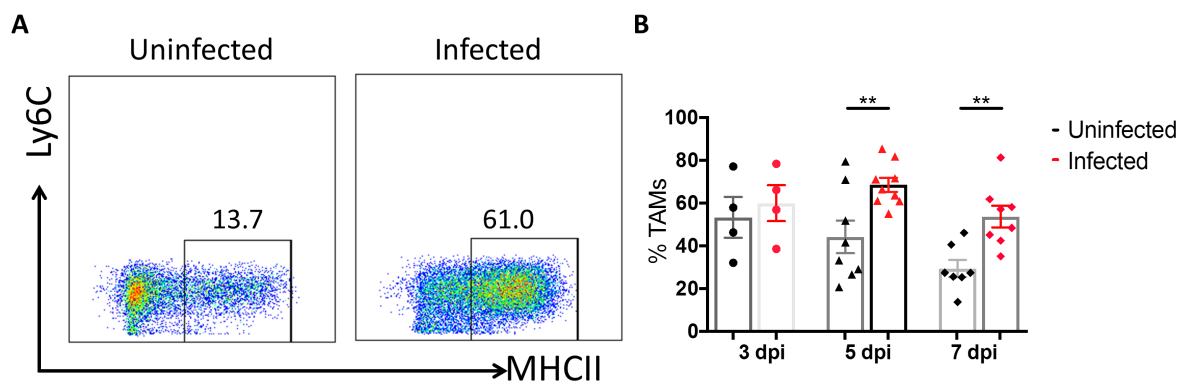


**Figure 5.11 Effect of SL7207 infection on total TAM MHCII expression**

Tumour-bearing mice were inoculated with SL7207 or PBS and tumours were harvested at 3, 5 and 7 dpi for flow cytometry analysis of tumour immune cell content. **A.** Representative flow cytometry plots showing MHCII expression on total TAMs from infected and uninfected tumours at 5 dpi. Cells were gated on single, live, CD45<sup>+</sup>, CD11b<sup>+</sup>, SiglecF<sup>-</sup>, F4/80<sup>+</sup>, Ly6G<sup>-</sup>, Ly6C<sup>-</sup>. **B.** Data shown as percentage MHCII<sup>+</sup> cells of total TAMs from infected and uninfected tumours at the indicated time points. Error bars SEM. Statistical analyses performed using Students t test between infected and uninfected samples at the same time point where  $p < 0.05^*$ ,  $p < 0.01^{**}$ ,  $p < 0.001^{***}$ .

Virtually all MHCII<sup>-</sup> and MHCII<sup>+</sup> TAMs expressed the resident macrophage marker, CD206 in tumours from uninfected mice and this was reduced in both populations after infection, although this was more pronounced in the MHCII<sup>-</sup> population (Figure 5.12).

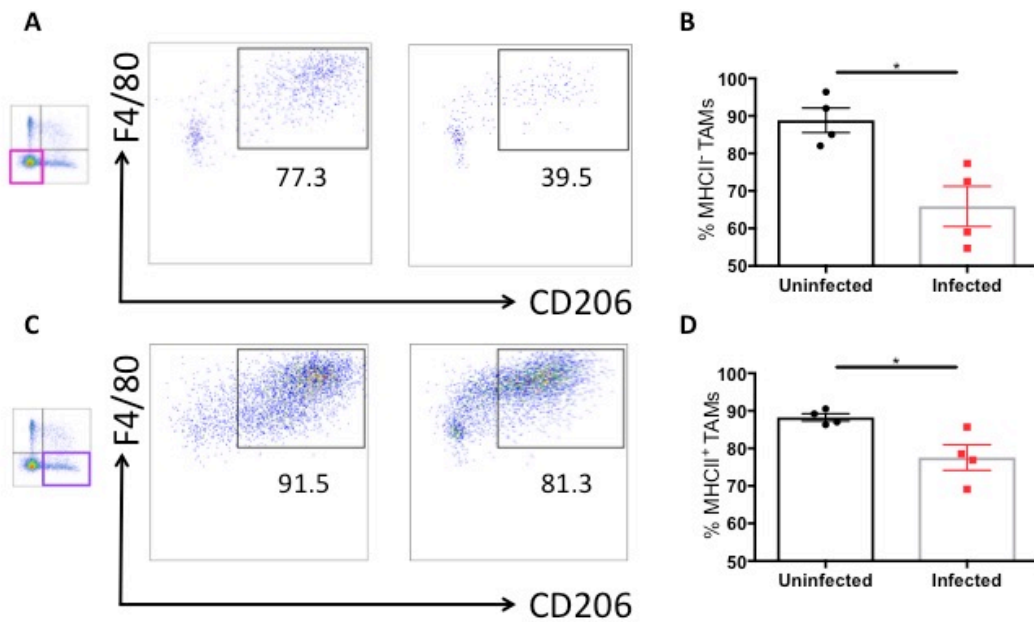


**Figure 5.12 Effects of SL7207 infection on CD206 expression on TAM populations**

Tumour-bearing mice were inoculated with SL7207 or PBS and tumours were harvested at 3 dpi for flow cytometry analysis of tumour immune cell content. Cells were gated on single, live, CD45<sup>+</sup>, CD11b<sup>+</sup>, SiglecF<sup>-</sup>, F4/80<sup>+</sup>, Ly6G<sup>-</sup>, Ly6C<sup>-</sup>. **A.** Representative flow cytometry plots showing CD206 expression on MHCII<sup>-</sup> TAMs from infected and uninfected tumours at 3 dpi. **B.** Data shown as percentage CD206<sup>+</sup> cells of total MHCII<sup>-</sup> TAMs from infected and uninfected tumours. **A.** Representative flow cytometry plots showing CD206 expression on MHCII<sup>+</sup> TAMs from infected and uninfected tumours at 3 dpi. **D.** Data shown as percentage CD206<sup>+</sup> cells of total MHCII<sup>+</sup> TAMs from infected and uninfected tumours. Error bars SEM. Statistical analyses performed using Students t test where  $p < 0.05^*$ ,  $p < 0.01^{**}$ .

Both TAM populations also seemed to increase their proliferative capacity following infection (Figure 5.13).

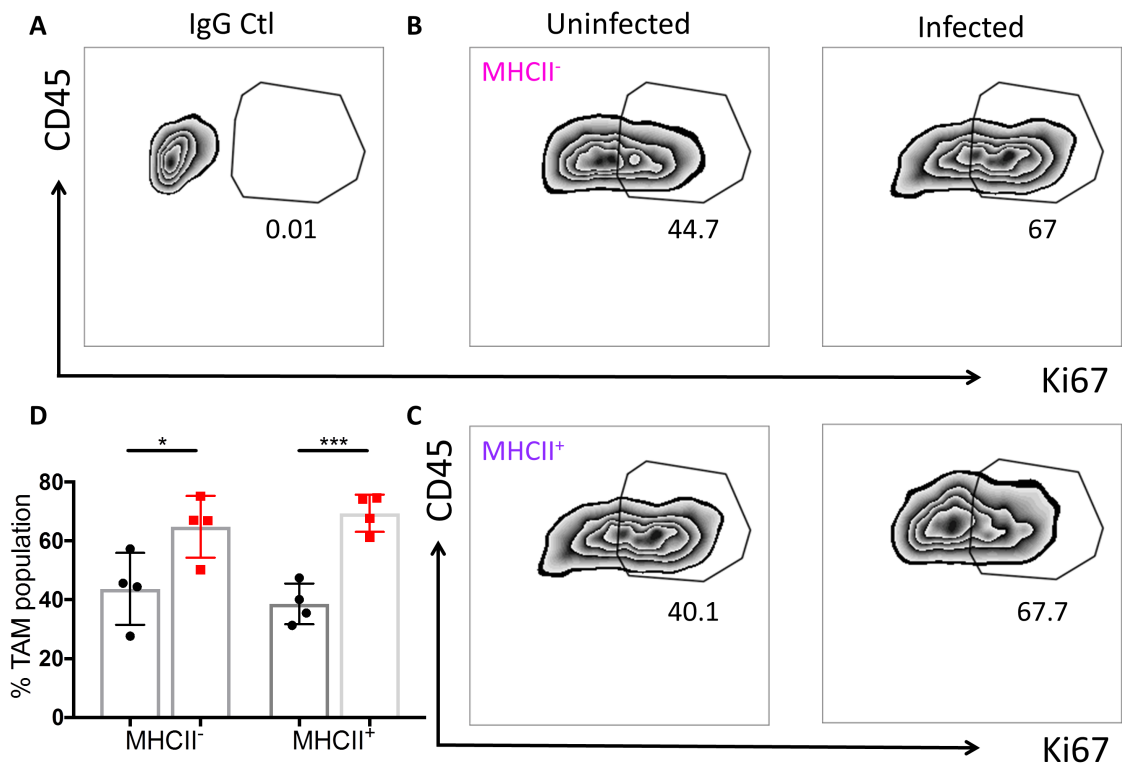


**Figure 5.13 Effects of SL7207 infection on the replicative potential of TAM populations**

Tumour-bearing mice were inoculated with SL7207 or PBS and tumours were harvested at 5 dpi for flow cytometry analysis of TAM populations. Cells were gated on single, live, CD45<sup>+</sup>, CD11b<sup>+</sup>, SiglecF<sup>-</sup>, F4/80<sup>+</sup>, Ly6G<sup>-</sup>, Ly6C<sup>-</sup>. **A.** Representative flow cytometry plot of an IgG isotype control for Ki67 on TAMs. **B.** Representative flow cytometry plots showing Ki67<sup>+</sup> MHCII<sup>-</sup> TAMs for infected and uninfected tumours. **C.** Representative flow cytometry plots showing Ki67<sup>+</sup> MHCII<sup>+</sup> TAMs for infected and uninfected tumours. **D.** Data shown as percentage Ki67<sup>+</sup> cells of total MHCII<sup>-</sup> and MHCII<sup>+</sup> TAMs from infected (red) and uninfected tumours (black). Error bars SEM. Statistical analyses performed using Students t test where  $p < 0.05^*$ ,  $p < 0.01^{**}$ ,  $p < 0.001^{***}$ .

Intracellular cytokine staining revealed that there were no significant changes in the production of the pro-inflammatory mediators TNF- $\alpha$  (Figure 5.14A-D), pro-IL-1 $\beta$  (Figure 5.14E-H), IL-12p40 (Figure 5.14I,J) or IL-6 (Figure 5.14K,L) by either population of mature macrophages following infection.



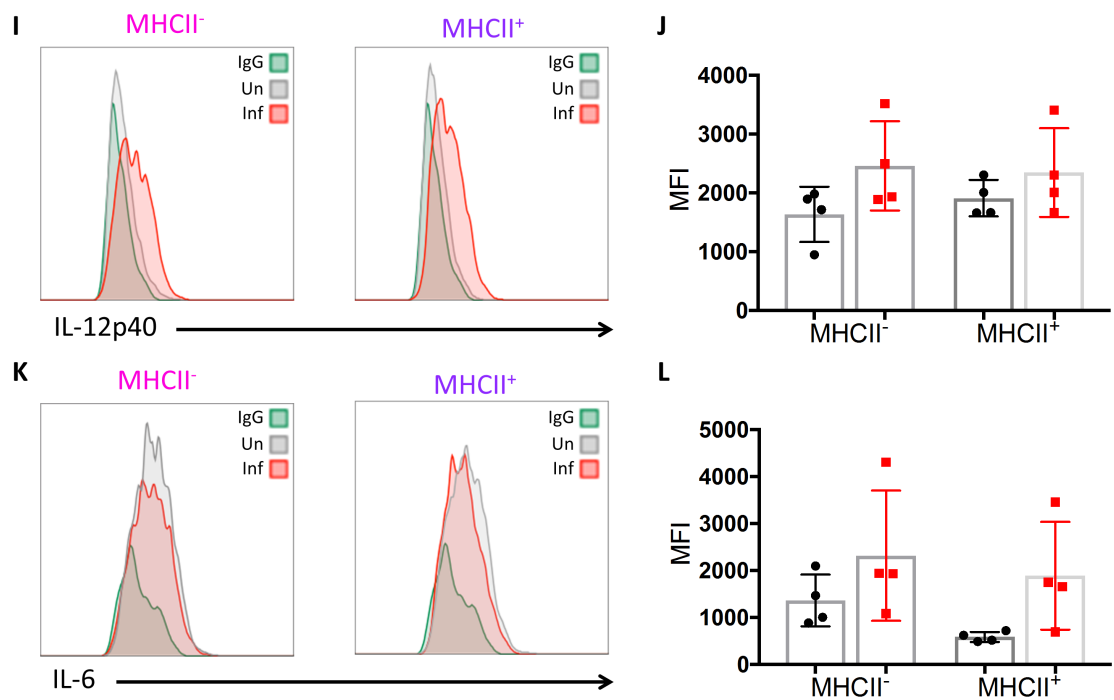


**Figure 5.14 Effects of SL7207 infection on functional phenotype of TAM populations**

Tumour-bearing mice were inoculated with SL7207 or PBS and tumours were harvested at 5 dpi for *in vitro* stimulation and flow cytometry analysis of TAM populations. Cells were gated on single, live, CD45<sup>+</sup>, CD11b<sup>+</sup>, SiglecF<sup>-</sup>, F4/80<sup>+</sup>, Ly6G<sup>-</sup>, Ly6C<sup>-</sup>. **A.** Representative flow cytometry plot of an IgG isotype control for TNF- $\alpha$  on TAMs. **B.** Representative flow cytometry plots showing TNF- $\alpha$ <sup>+</sup> MHCII<sup>-</sup> TAMs for infected and uninfected tumours. **C.** Representative flow cytometry plots showing TNF- $\alpha$ <sup>+</sup> MHCII<sup>+</sup> TAMs for infected and uninfected tumours. **D.** Data shown as percentage TNF- $\alpha$ <sup>+</sup> cells of total MHCII<sup>-</sup> and MHCII<sup>+</sup> TAMs from infected (red) and uninfected tumours (black). **E.** Representative flow cytometry plot of an IgG isotype control for pro-IL-1 $\beta$  on TAMs. **F.** Representative flow cytometry plots showing pro-IL-1 $\beta$ <sup>+</sup> MHCII<sup>-</sup> TAMs for infected and uninfected tumours. **G.** Representative flow cytometry plots showing pro-IL-1 $\beta$ <sup>+</sup> MHCII<sup>+</sup> TAMs for infected (red) and uninfected (black) tumours. **H.** Data shown as percentage pro-IL-1 $\beta$ <sup>+</sup> cells of total MHCII<sup>-</sup> and MHCII<sup>+</sup> TAMs from infected (red) and uninfected tumours (black). **I.** Representative histogram plots of MHCII<sup>-</sup> and MHCII<sup>+</sup> TAM IL-12p40 expression from infected and uninfected samples including an IgG isotype control. **J.** MFI of IL-12p40 expression from MHCII<sup>-</sup> and MHCII<sup>+</sup> TAMs from infected (red) and uninfected (black) samples. **K.** Representative histogram plots of MHCII<sup>-</sup> and MHCII<sup>+</sup> TAM IL-6 expression from infected and uninfected samples including an IgG isotype control. **L.** MFI of IL-6 expression from MHCII<sup>-</sup> and MHCII<sup>+</sup> TAMs from infected (red) and uninfected (black) samples. Error bars SEM. Statistical analyses performed using Students t test where  $p < 0.05^*$ .

There were also no differences between the phagocytic capacity of MHCII<sup>-</sup> TAMs from infected and uninfected tumours, but MHCII<sup>+</sup> TAMs from infected tumours showed a marked increase in phagocytic activity compared with those from uninfected mice (Figure 5.15).

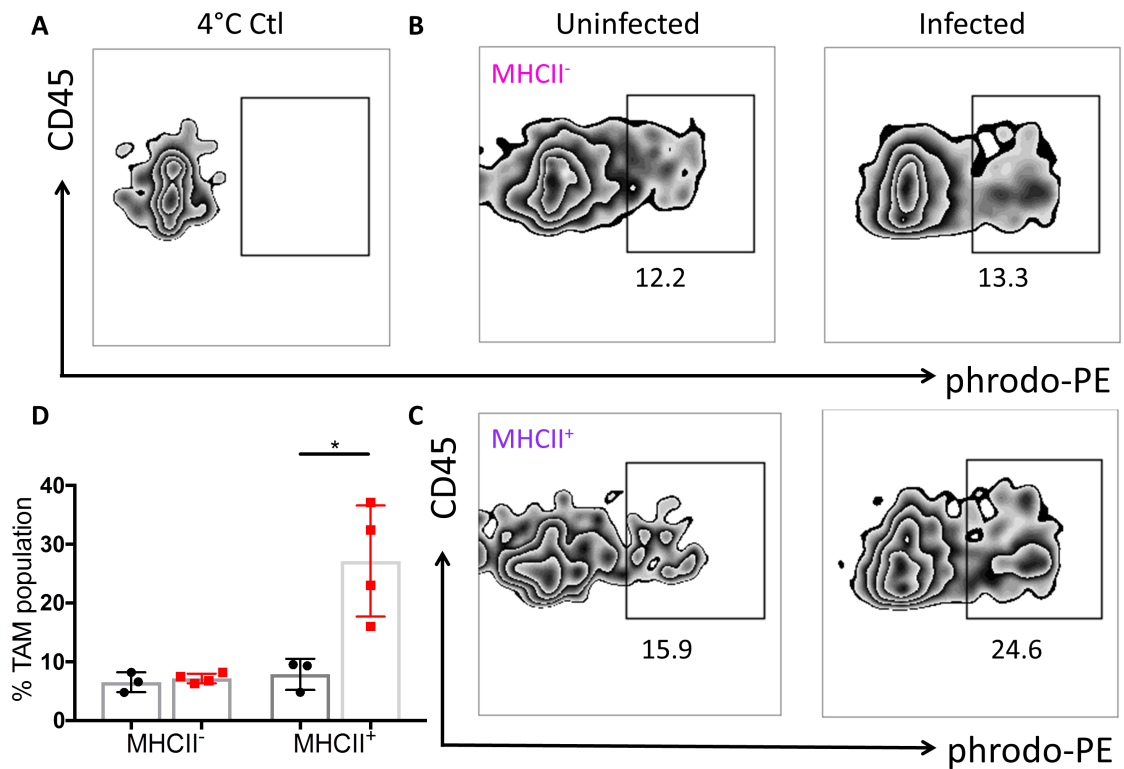


**Figure 5.15 Effects of SL7207 on phagocytic capacities of TAM populations**

Tumour-bearing mice were inoculated with SL7207 or PBS and tumours were harvested at 5 dpi for co-incubation with pHrodo-PE Bioparticles™ to assess phagocytic capacity. Cells were gated on single, live, CD45<sup>+</sup>, CD11b<sup>+</sup>, SiglecF<sup>-</sup>, F4/80<sup>+</sup>, Ly6G<sup>-</sup>, Ly6C<sup>-</sup>. **A.** Representative flow cytometry plot of a 4°C control. **B.** Representative flow cytometry plots showing uptake of pHrodo-PE by MHCII<sup>-</sup> TAMs from infected and uninfected tumours. **C.** Representative flow cytometry plots showing uptake of pHrodo-PE by MHCII<sup>+</sup> TAMs from infected and uninfected tumours. **D.** Data shown as percentage pHrodo-PE<sup>+</sup> cells among total MHCII<sup>-</sup> and MHCII<sup>+</sup> TAMs from infected (red) and uninfected (black) tumours. Error bars SEM. Statistical analysis performed using Student's t test where  $p < 0.05^*$ .

These data suggest that the mature TAMs do not adopt a pro-inflammatory phenotype following systemic SL7207 infection, but may play a role in phagocytosis of cellular debris and bacteria.

#### 5.2.4 Contributions of resident and recruited precursors to MHCII<sup>+</sup> TAMs

Within the TAM population, there was an increase in MHCII expression which conferred to greater phagocytic potential of these cells. It seemed possible that these might be derived either from newly recruited monocytes (Bain *et al.*, 2013) or from local pre-existing MHCII<sup>-</sup> macrophages (Mueller *et al.*, 2005). As there was no increase in the total number of TAMs following infection, it was hypothesised that the Ly6C<sup>+</sup>MHCII<sup>+</sup> cells were not differentiating into MHCII<sup>+</sup> TAMs, but that the MHCII<sup>-</sup> TAMs were instead increasing MHCII expression. To test if this was the case, photoconvertible Kaede transgenic mice were employed

(Ando *et al.*, 2002). In these mice, the cells constitutively express the Kaede green protein, which photoswitches to Kaede red upon stimulation with ultraviolet (UV) light. This allows for the monitoring of cellular movement between organs *in vivo*, as well as local and infiltrating cells to be discriminated in a specific tissue (Mackley *et al.*, 2015; Torcellan *et al.*, 2017). Using this approach, it was hypothesised that photoconversion of the tumour immediately prior to infection would enable the discrimination between cells that were derived from the tumour at the time of photoswitching and so became Kaede red and those which had been recruited after the infection, which would not be photoswitched (Kaede green). We were particularly interested in the monocyte/macrophage (F4/80<sup>+</sup>) cell compartment.

As this system had not been used previously for examination of tumours in the group, it was first necessary to optimise the protocol. The most commonly employed local protocol involves the photoconversion of the ear pinnae (Gibson *et al.*, 2012). This protocol involves the exposure of the tissue to a UV light source for three seconds, three times with five-second breaks between exposures (Protocol 1). The gating strategy for this experiment is depicted in Figure 5.16.

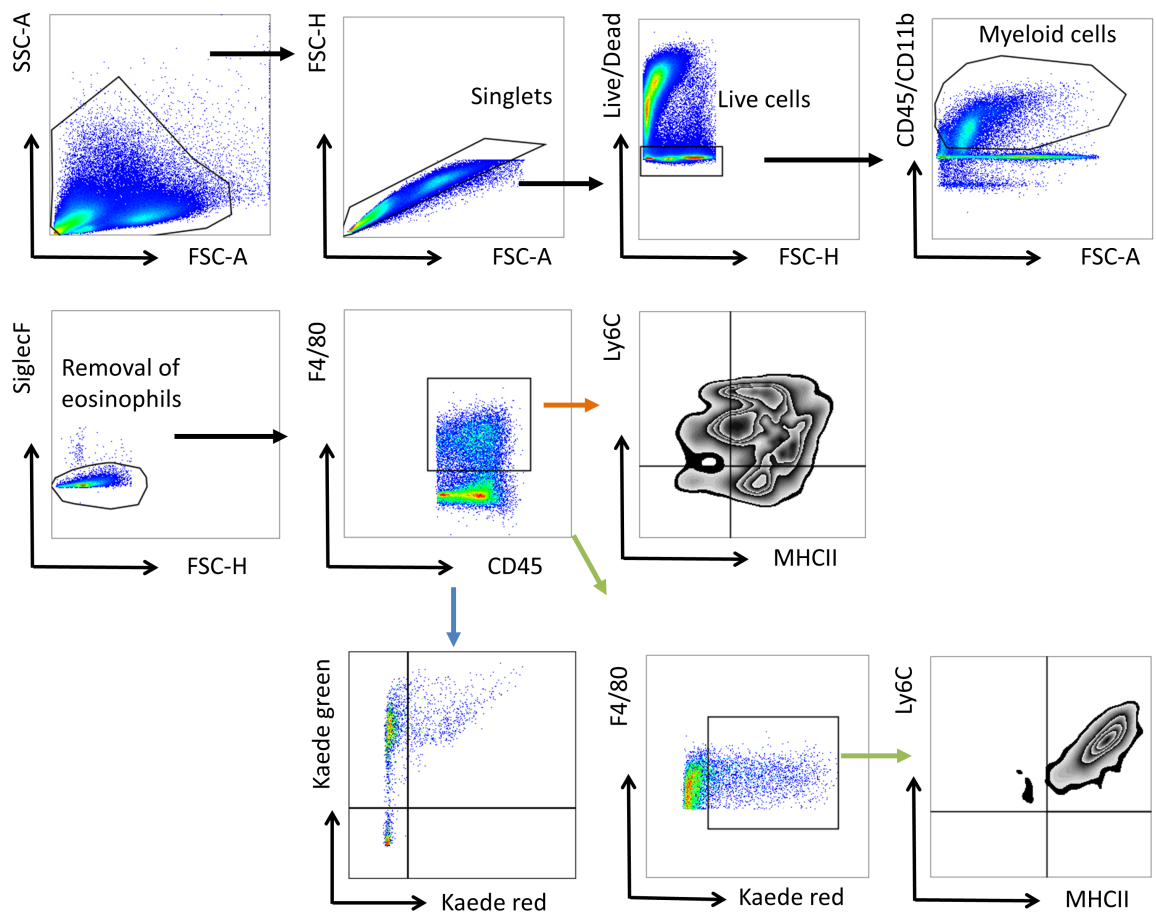


**Figure 5.16 Gating strategy for tumour monocyte/macrophages in tumour-bearing Kaede mice**

The degree of photoconversion amongst the tumour  $F4/80^+$  cell population (black and blue arrows) was assessed by gating on single, live,  $CD45^+CD11b^+$ ,  $SiglecF^-$  (removal of eosinophils),  $F4/80^+$  and then separating the population according to Kaede green or Kaede red expression. To assess the monocyte and macrophage populations in the tumour, (black and orange arrows), cells were gated as single, live,  $CD45^+CD11b^+$ ,  $SiglecF^-$  (removal of eosinophils),  $F4/80^+$  and then separated into monocytes and macrophage populations by Ly6C and MHCII expression. To assess the populations of monocytes and macrophages which were Kaede red<sup>+</sup> (black and green arrows), cells were gated on single, live,  $CD45^+CD11b^+$ ,  $SiglecF^-$  (removal of eosinophils),  $F4/80^+$ , Kaede red<sup>+</sup> and separated into monocytes and macrophage populations by Ly6C and MHCII expression

Kaede mice were seeded with B16F10 cells and tumours were allowed to develop for eight days, at which point the mice were anaesthetised and the tumours were subject to UV exposure according to either Protocol 1 or Protocol 2. The employment of this protocol in the present tumour model allowed for the expression of Kaede red in 22.3% of  $F4/80^+$  cells (Figure 5.17). A second protocol, with one ten second exposure, followed by four five-second exposures with five-second breaks between exposures was employed to try and increase the proportion of Kaede red cells in the tumour (Protocol 2). This resulted in 39.4% of the  $F4/80^+$  cells expressed Kaede red. Although this meant it would not be possible to credit specific function to the infiltrating Kaede green monocytes

(as approximately 60% of the tumour-resident F4/80<sup>+</sup> cells remained Kaede green), the protocol would suffice to ascertain if the tumour-resident MHCII<sup>+</sup> TAMs were increasing MHCII expression following infection.

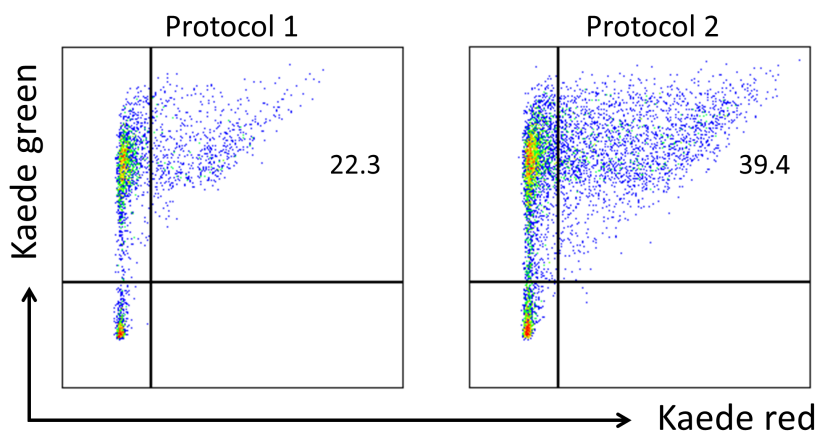


**Figure 5.17 Optimisation of photoconversion protocol**

B16F10 tumours were exposed to UV light using two different protocols, and tumours were harvested for assessment using flow cytometry to determine the proportion of Kaede red<sup>+</sup> cells in the F4/80 compartment. Representative flow cytometry plots from each protocol showing the proportion of total F4/80 cells which expressed Kaede red<sup>+</sup>. Cells were gated on single, live, CD45<sup>+</sup>CD11b<sup>+</sup>, SiglecF<sup>-</sup>, F4/80<sup>+</sup>.

B16F10 tumour cells were injected into Kaede mice and allowed to develop into tumours for nine days before SL7270 was administered intravenously. One day prior to infection, the subcutaneous tumours were exposed to UV light using Protocol 2 (Figure 5.18A; Day 0 is when SL7207 was administered). Three days post infection, mice were culled and their tumours were harvested for flow cytometry analysis of the Kaede green<sup>+</sup> and Kaede red<sup>+</sup> cells. As before, the infected tumours had decreased cellular viability compared with the uninfected tumours (Figure 5.18B,C) and were slightly smaller in size (Figure 5.18D).

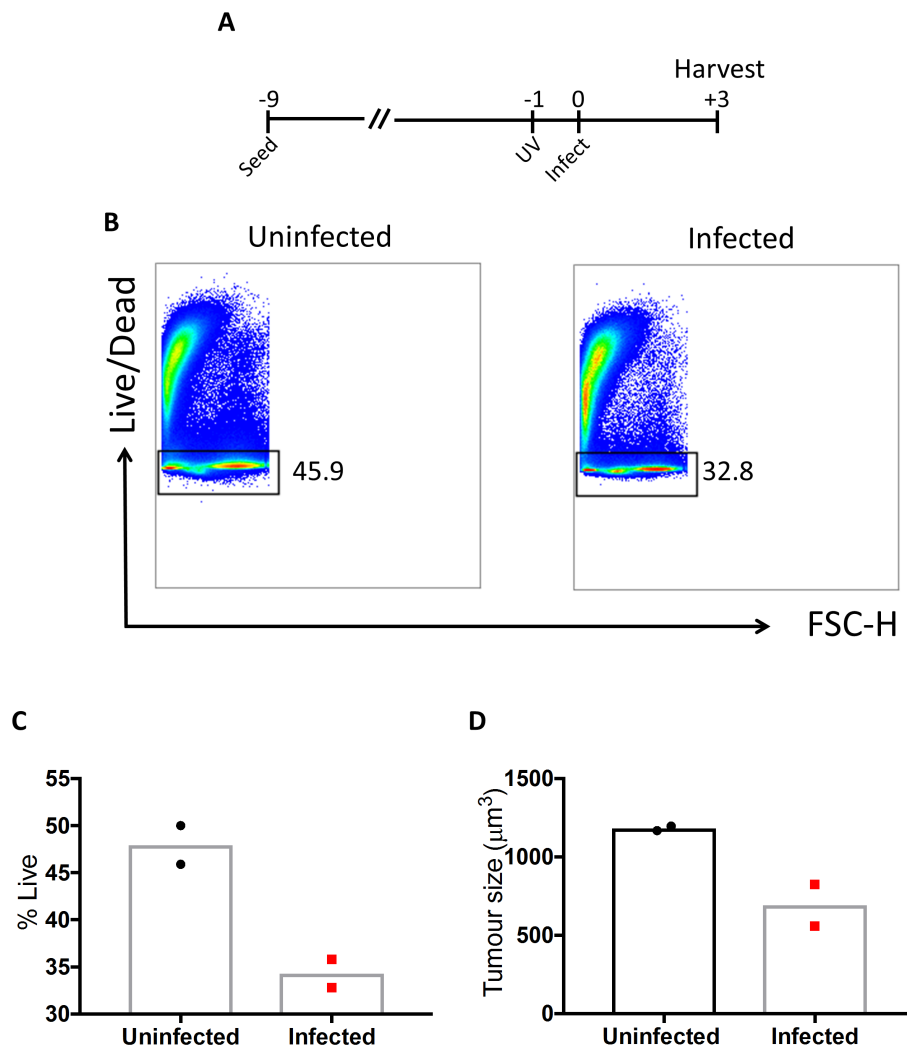


**Figure 5.18 Effects of SL7207 infection on tumour-bearing Kaede mice**

Tumour-bearing Kaede mice were inoculated with SL7207 or PBS and tumours were harvested 3 dpi to assess the effects of SL7207 compared to control mice. **A.** Timeline of experiment. **B.** Representative flow cytometry plots showing viability of whole tumours from infected and uninfected tumours. **C.** Data are shown as percentage of viable (Live/Dead<sup>-</sup>) cells among total cells for infected and uninfected samples. **D.** Tumour size of infected and uninfected tumours at 3 dpi.

Following infection, there was a significant proportion of tumour Ly6C<sup>+</sup>MHCII<sup>+</sup> cells, as expected (Figure 5.19A). Unexpectedly, this pattern was also apparent in the uninfected compartment. There was a greater proportion of F4/80 cells which were Kaede red<sup>+</sup> in the uninfected tumour compared to infected (Figure 5.19B). Surprisingly, the only cells in the monocyte/macrophage compartment that were Kaede red<sup>+</sup> were the Ly6C<sup>+</sup>MHCII<sup>+</sup>. As there was an absence of TAMs which were Kaede red<sup>+</sup>, it was not possible to ascertain if the MHCII<sup>-</sup> TAMs were giving rise to the MHCII<sup>+</sup> TAMs. Therefore, this model was no longer employed as it was apparent that further characterisation and optimisation might be required to address the question we wanted to ask.

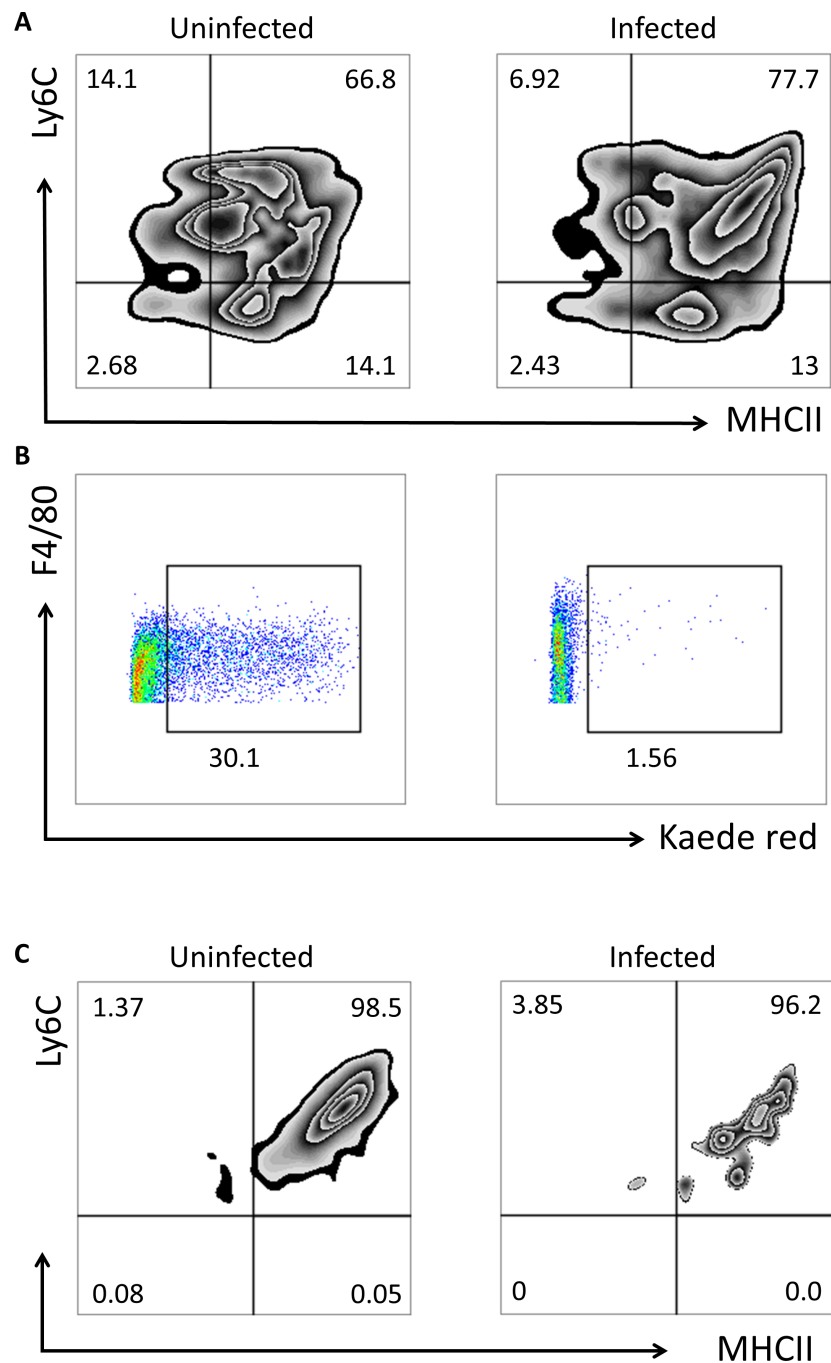


**Figure 5.19 Effects of SL7207 infection on Kaede red<sup>+</sup> monocytes/macrophages in the tumour**

Tumour-bearing Kaede mice were inoculated with SL7207 or and tumours were harvested 3 dpi to assess the effects of SL7207 on the Kaede red<sup>+</sup> cells in the F4/80 compartment. **A.** Representative flow cytometry plots of the monocyte/macrophage compartment of infected and uninfected tumours. Cells were gated on single, live, CD45<sup>+</sup>CD11b<sup>+</sup>, SiglecF<sup>-</sup>, F4/80<sup>+</sup>. **B.** Representative flow cytometry plots showing the proportion of F4/80<sup>+</sup> cells which were Kaede red<sup>+</sup> from infected and uninfected tumours. Cells were gated on single, live, CD45<sup>+</sup>CD11b<sup>+</sup>, SiglecF<sup>-</sup>, F4/80<sup>+</sup>. **C.** Representative flow cytometry plots showing where the Kaede red<sup>+</sup> cells from infected and uninfected tumours lay in the monocyte/macrophage compartment. Cells were gated on single, live, CD45<sup>+</sup>CD11b<sup>+</sup>, SiglecF<sup>-</sup>, F4/80<sup>+</sup>, Kaede red<sup>+</sup>.

### 5.2.5 Effects of SL7207 in monocyte deficient *Ccr2*<sup>-/-</sup> mice

Both the Ly6C<sup>+</sup>MHCII<sup>-</sup> and Ly6C<sup>+</sup>MHCII<sup>+</sup> monocyte populations were activated following infection. Therefore, the role of recruited monocytes in the anti-tumour effects of SL7207 was examined using mice lacking the CCR2 chemokine receptor that have a defect in egress of Ly6C<sup>hi</sup> monocytes from the bone marrow (Serbina & Pamer, 2006).

As this myeloid compartment is known to play a role in mediating tumour growth (Qian & Pollard, 2010) it was first important to establish that the *Ccr2*<sup>-/-</sup> mice did not have significantly different tumour growth dynamics. To investigate this, *Ccr2*<sup>-/-</sup> mice were injected with 2 x 10<sup>5</sup> B16F10 cells and their tumour growth was monitored over time. As a comparison, the growth dynamics of tumours in the wild type mice, as presented in Chapter 3, Figure 3.7, were included to assess any *Ccr2*<sup>-/-</sup>-specific differences. There was no significant difference between the tumour growth dynamics of the *Ccr2*<sup>-/-</sup> tumour-bearing mice compared with wild type (Figure 5.20A). There were also no significant differences in the numbers of total cells in the tumour at 16 days post tumour induction between *Ccr2*<sup>-/-</sup> and wild type tumours (Figure 5.20B).

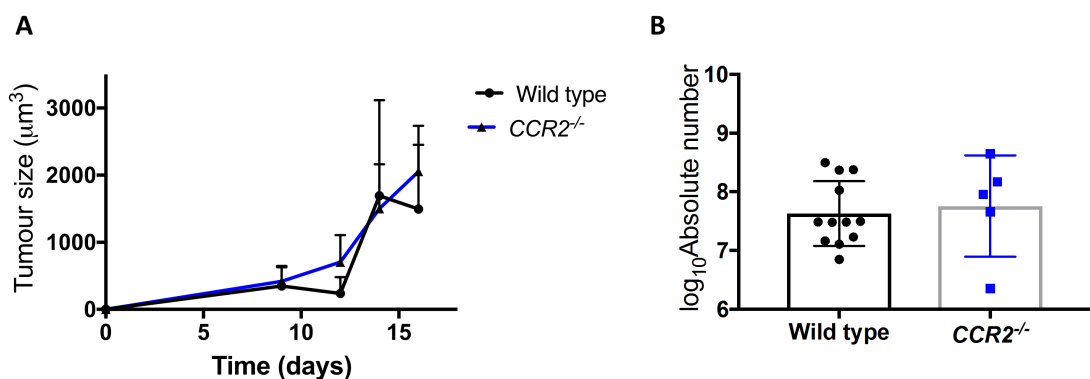


**Figure 5.20 B16F10 tumour growth in *Ccr2*<sup>-/-</sup> mice**

B16F10 tumour cells were seeded in *Ccr2*<sup>-/-</sup> mice and monitored over time, and compared to uninfected wild type mice depicted in Chapter 3, Figure 3.7. **A.** Tumour size of wild type and *Ccr2*<sup>-/-</sup> mice over time, as measured using Vernier calipers. **B.** Quantification of the absolute number of live cells in wild type and *Ccr2*<sup>-/-</sup> tumours. Error bars SEM. Statistical analysis performed using Student's t test where  $p < 0.05^*$ .

Next, it was pertinent to examine the monocyte compartment. As expected, there was a significant decrease in the tumour  $\text{Ly6C}^+\text{MHCII}^-$  monocytes in the  $\text{Ccr2}^{-/-}$  mice compared to wild type (Figure 5.21A-C), which was also the case for the  $\text{Ly6C}^+\text{MHCII}^+$  monocytes (Figure 5.21D, E). As  $\text{Ly6C}^+$  monocytes give rise to mature TAMs (Franklin *et al.*, 2014), the change in the number of TAMs in the  $\text{Ccr2}^{-/-}$  mice was examined in comparison to wild type. There were no significant differences in the numbers of the  $\text{MHCII}^-$  TAMs (Figure 5.21F) or the proportion of  $\text{MHCII}^-$  TAMs amongst total  $\text{CD45}^+$  leukocytes in the  $\text{Ccr2}^{-/-}$  mice compared with wild type (Figure 5.21G) There was also no significant difference in the numbers of  $\text{MHCII}^+$  TAMs between  $\text{Ccr2}^{-/-}$  and wild type mice (Figure 5.21H), but there was a significant decrease in the  $\text{MHCII}^-$  TAMs as a proportion of  $\text{CD45}^+$  cells, suggesting these may derive from  $\text{Ly6C}^+$  monocytes (Figure 5.21I). These results indicated that  $\text{Ccr2}^{-/-}$  mice would be a suitable and specific model for investigating the contribution of monocytes, and their derivatives, to SL7207-mediated tumour growth inhibition.

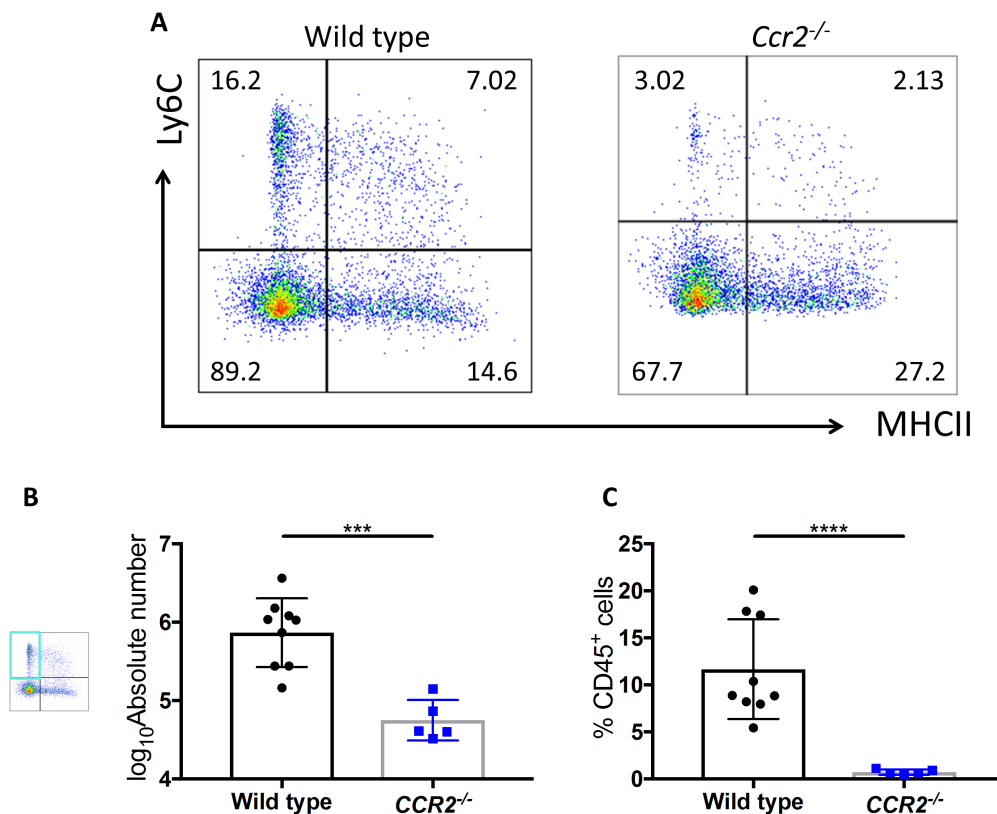
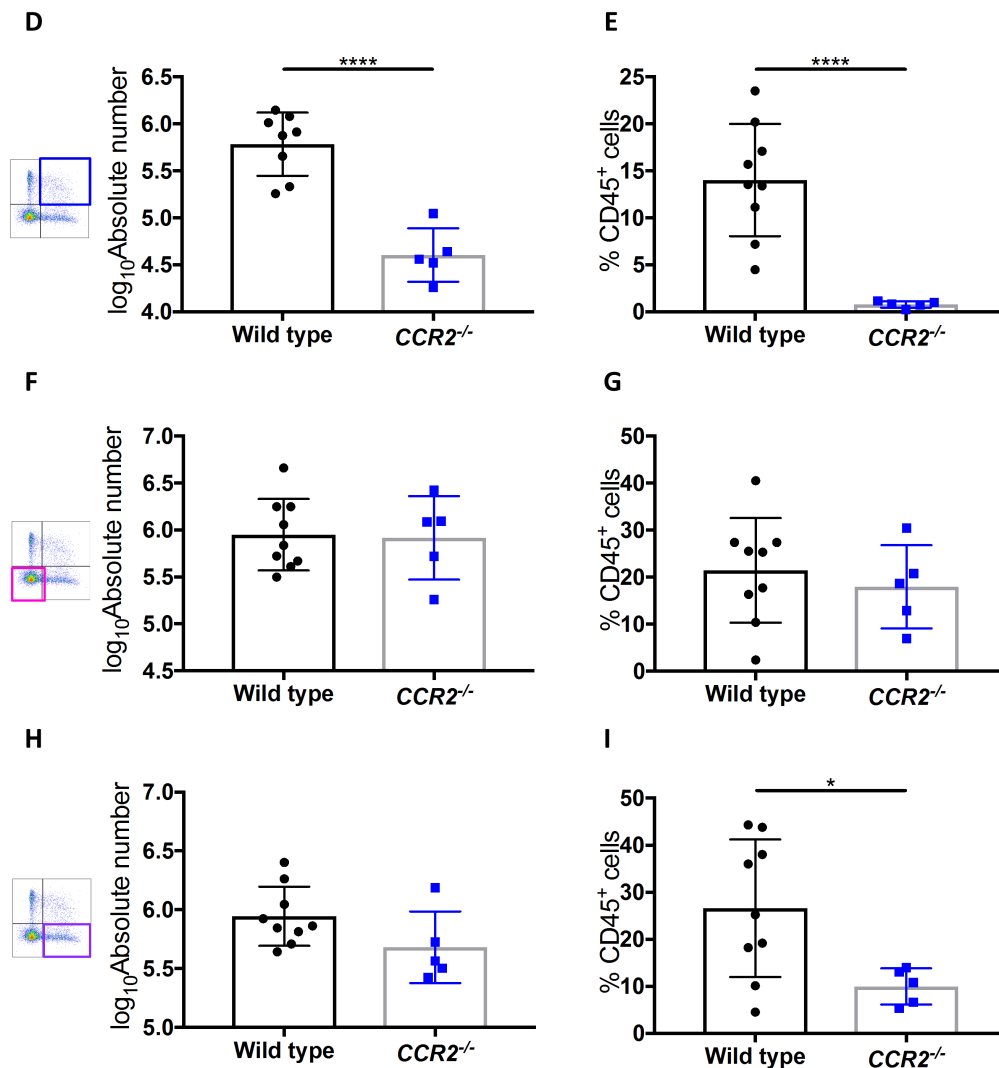


Figure 5.21 continued on the next page



**Figure 5.21 Monocyte and macrophage populations in the *Ccr2*<sup>-/-</sup> mice**

B16F10 tumour cells were seeded in *Ccr2*<sup>-/-</sup> mice and the tumours were harvested at 7 dpi to assess the monocyte and macrophage content, and compared to wild type tumours described in Figures 5.4, 5.7 and 5.10. Cells were gated on single, live, CD45<sup>+</sup>, CD11b<sup>+</sup>, SiglecF<sup>-</sup>, F4/80<sup>+</sup> and Ly6G<sup>-</sup>. **A.** Representative flow cytometry plots showing the monocyte/macrophage compartment of wild type and *Ccr2*<sup>-/-</sup> tumours. **B.** Quantification of absolute number of Ly6C<sup>+</sup>MHCII<sup>-</sup> monocytes in wild type and *Ccr2*<sup>-/-</sup> tumours. **C.** Data shown as percentage Ly6C<sup>+</sup>MHCII<sup>-</sup> monocytes of total CD45<sup>+</sup> cells in wild type and *Ccr2*<sup>-/-</sup> tumours. **D.** Quantification of absolute number of Ly6C<sup>+</sup>MHCII<sup>+</sup> monocytes in wild type and *Ccr2*<sup>-/-</sup> tumours. **E.** Data shown as percentage Ly6C<sup>+</sup>MHCII<sup>+</sup> monocytes of total CD45<sup>+</sup> cells in wild type and *Ccr2*<sup>-/-</sup> tumours. **F.** Quantification of absolute number of MHCII<sup>-</sup> TAMs in wild type and *Ccr2*<sup>-/-</sup> tumours. **G.** Data shown as percentage MHCII<sup>-</sup> TAMs of total CD45<sup>+</sup> cells in wild type and *Ccr2*<sup>-/-</sup> tumours. **H.** Quantification of absolute number of MHCII<sup>+</sup> TAMs in wild type and *Ccr2*<sup>-/-</sup> tumours. **I.** Data shown as percentage MHCII<sup>+</sup> TAMs of total CD45<sup>+</sup> cells in wild type and *Ccr2*<sup>-/-</sup> tumours.

When *Ccr2*<sup>-/-</sup> tumour-bearing mice were infected with 5x10<sup>6</sup> CFU SL7207 intravenously on day nine after tumour induction, they showed the same inhibition of tumour growth as infected wild type mice (Figure 5.22A). Again, the wild type mice used as a comparison come from the data shown in Chapter 3, Figure 3.7. *Ccr2*<sup>-/-</sup> mice also lost body weight in a similar manner to their wild

type counterparts, although this was significantly less from infected *Ccr2*<sup>-/-</sup> mice on 7 dpi (Figure 5.22B).

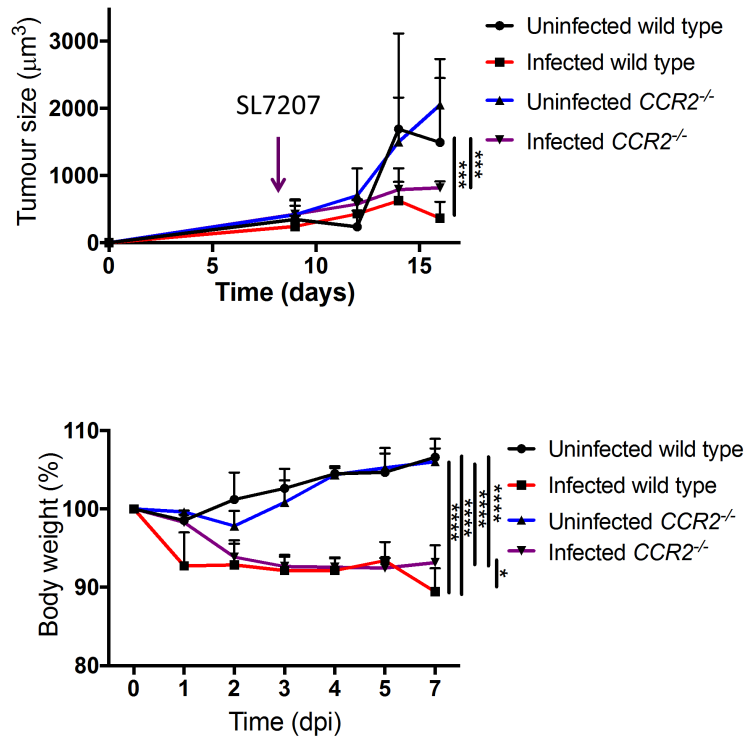


**Figure 5.22 Effects of SL7207 on tumour growth and body weight in tumour-bearing *Ccr2*<sup>-/-</sup> mice**

Tumour-bearing *Ccr2*<sup>-/-</sup> mice were inoculated with SL7207 or PBS control, with tumour growth and weight being measured over time, and compared to wild type tumour-bearing mice depicted in Chapter 3, Figure 3.7. **A.** Tumour sizes of were measured over 7 days using Vernier calipers. **B.** Weight of mice expressed as a percentage of weight at Day 0 of infection. Error bars SEM. Statistical analyses performed using Tukey's multiple comparison test where  $p < 0.05^*$ ,  $p < 0.01^{**}$ ,  $p < 0.001^{***}$ ,  $p < 0.0001^{****}$ .

In parallel with the normal tumour inhibition, there was no significant change in the number of Ly6C<sup>+</sup>MHCII<sup>-</sup> monocytes in the infected *Ccr2*<sup>-/-</sup> mice compared with uninfected, similar to wild type (Figure 5.23A-D). Tumours from infected *Ccr2*<sup>-/-</sup> mice recovered the number of Ly6C<sup>+</sup>MHCII<sup>+</sup> cells comparable to those from the wild type on 7 dpi, with a substantial proportional expansion over the very low numbers of this population in uninfected *Ccr2*<sup>-/-</sup> tumours (Figure 5.23E). There was also an increase in the proportion of Ly6C<sup>+</sup>MHCII<sup>+</sup> amongst CD45<sup>+</sup> cells in the infected *Ccr2*<sup>-/-</sup> mice, in a manner not dissimilar to wild type (Figure 5.23F). As these data indicate that the recruitment of monocytes to the tumour following infection occurs in a CCR2-independent manner, the *Ccr2*<sup>-/-</sup> model was unsuitable to examine the contribution of monocytes to *S. Typhimurium*-mediated tumour growth inhibition.

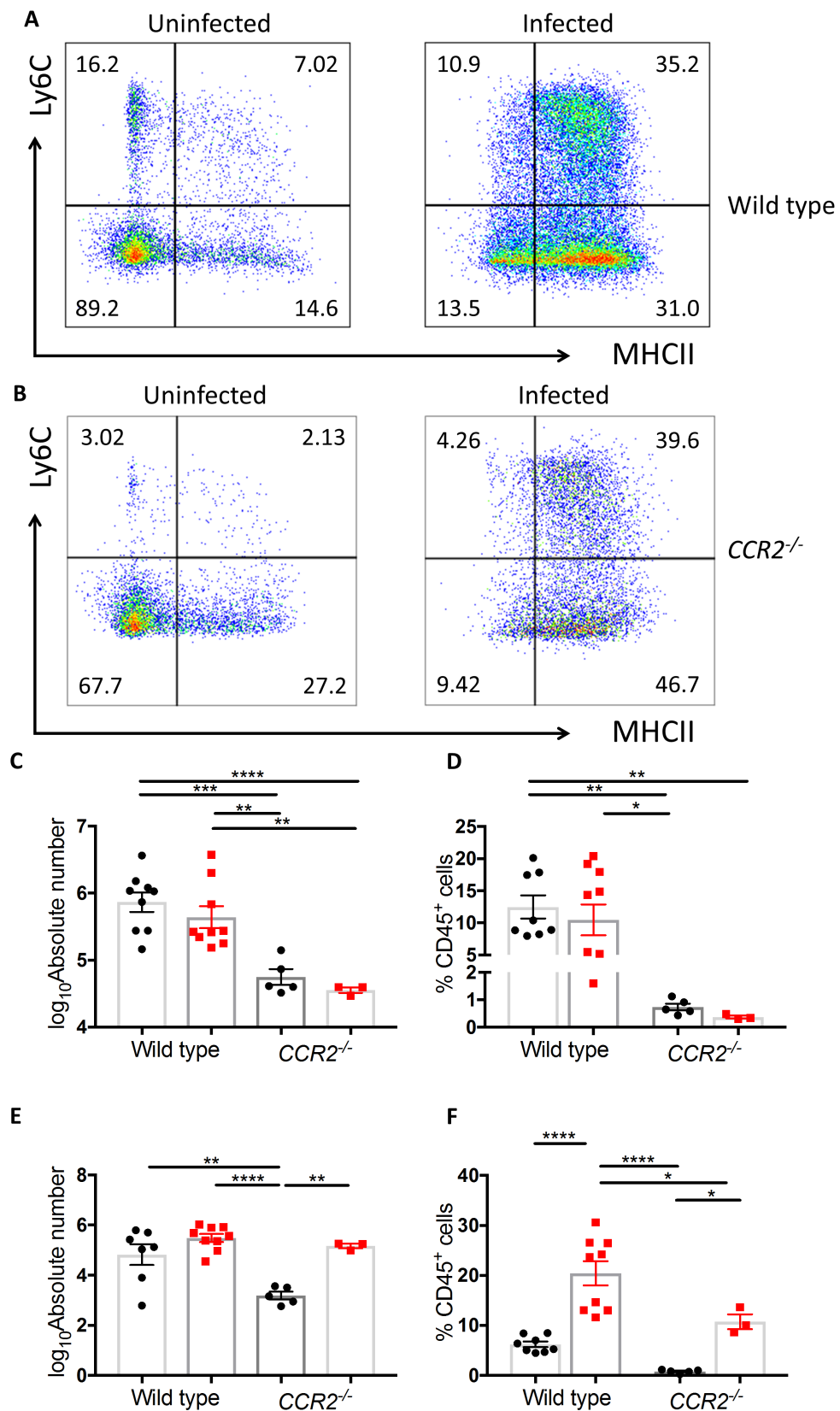


**Figure 5.23 Effects of SL7207 on the tumour monocytes in *Ccr2*<sup>-/-</sup> mice**

Tumour-bearing *Ccr2*<sup>-/-</sup> mice were inoculated with SL7207 or PBS control, and harvested on 7 dpi for flow cytometric analysis of the tumour monocyte/macrophage populations. There were compared to wild type tumour-bearing mice depicted in Figure 5.4 and 5.7. **A**. Representative flow cytometry plots showing the tumour monocyte/macrophage compartment of wild type, *Ccr2*<sup>-/-</sup>, infected and uninfected mice as in Figure 5.2. Cells were gated on single, live, CD45<sup>+</sup>, CD11b<sup>+</sup>, SiglecF<sup>-</sup>, F4/80<sup>+</sup>, Ly6G<sup>-</sup>. **B**. Representative flow cytometry plots showing the tumour

monocyte/macrophage compartment of *Ccr2*<sup>-/-</sup> mice, infected and uninfected. Cells were gated on single, live, CD45<sup>+</sup>, CD11b<sup>+</sup>, SiglecF<sup>-</sup>, F4/80<sup>+</sup>, Ly6G<sup>-</sup>. **C.** Quantification of absolute number of Ly6C<sup>+</sup>MHCII<sup>-</sup> monocytes in wild type and *Ccr2*<sup>-/-</sup> tumour, infected (red) and uninfected (black). **D.** Data shown as percentage Ly6C<sup>+</sup>MHCII<sup>-</sup> monocytes of total CD45<sup>+</sup> cells in wild type and *Ccr2*<sup>-/-</sup> tumour, infected (red) and uninfected (black). **E.** Quantification of absolute number of Ly6C<sup>+</sup>MHCII<sup>+</sup> monocytes in wild type and *Ccr2*<sup>-/-</sup> tumour, infected (red) and uninfected (black). **F.** Data shown as percentage Ly6C<sup>+</sup>MHCII<sup>+</sup> monocytes of total CD45<sup>+</sup> cells in wild type and *Ccr2*<sup>-/-</sup> tumour, infected (red) and uninfected (black). Error bars SEM. Statistical analyses performed using One Way Anova where  $p < 0.05^*$ ,  $p < 0.01^{**}$ ,  $p < 0.001^{***}$ ,  $p < 0.0001^{****}$ .

### **5.2.6 The effects of clodronate liposome-mediated monocyte/macrophage depletion on tumour inhibition by SL7207**

As an alternative strategy for depleting the monocytes/macrophage compartment, clodronate liposomes (Rooijen & Sanders, 1994) were employed to delete monocytes and macrophages (Gazzaniga *et al.*, 2007; Griesmann *et al.*, 2016; Zeisberger *et al.*, 2006). Note that any depletion in the monocyte/macrophage compartments would not be specific to the tumour, but all organs would likely be affected. First, it was important to verify that the clodronate liposomes (Clod Lipo) abrogated the number of monocytes and macrophages compared to the PBS liposome control. To do this, Clod Lipo or PBS liposomes (PBS Lipo) were intravenously injected on days 5 and 8 post tumour cell inoculation (Figure 5.24A). Tumours were harvested on 9 dpi and subjected to flow cytometry analysis for the Ly6C<sup>+</sup> monocyte and macrophage populations. There was a reduction in both the monocytes and Ly6C<sup>-</sup> mature TAMs in the Clod Lipo samples compared to PBS Lipo controls (Figure 5.24B-D). Thus clodronate-containing liposomes depleted tumour infiltrating monocytes and macrophages under normal tumour conditions.

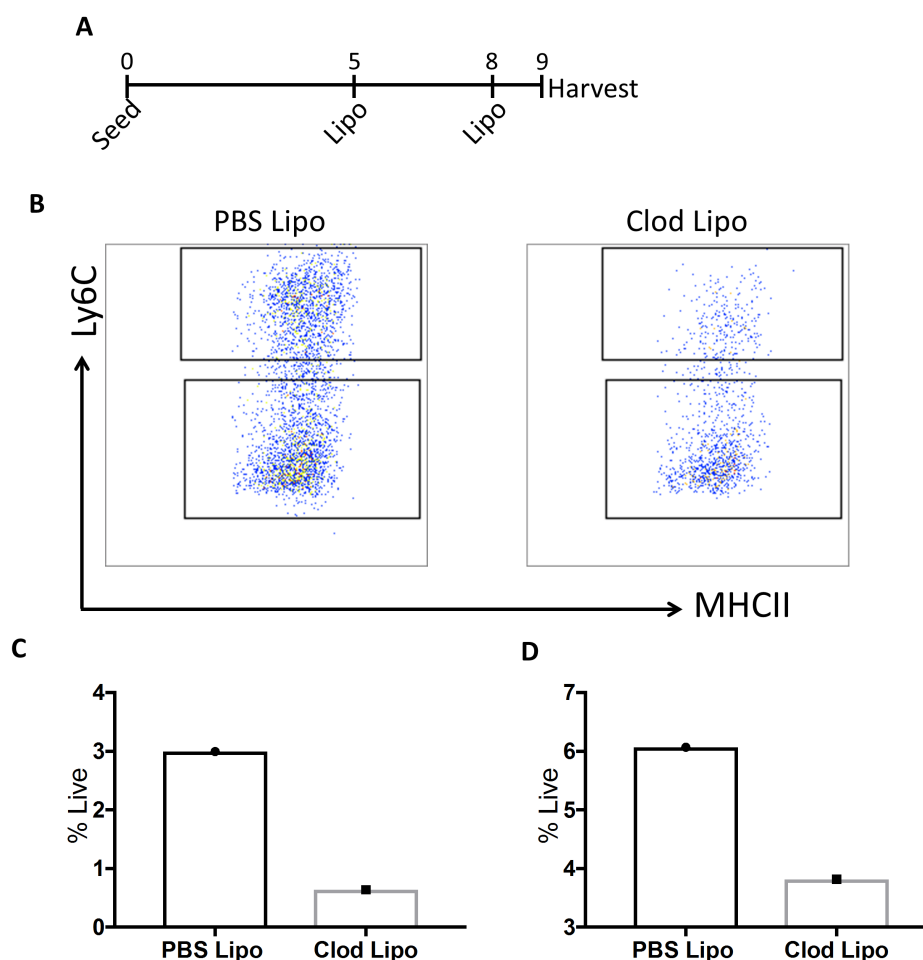


**Figure 5.24 Effects of Clod Lipo on tumour monocyte/macrophage population**

Tumour-bearing mice were intravenously injected with either PBS Liposomes (PBS Lipo) or Clod Liposomes (Clod Lipo) and tumours were harvested for flow cytometry analysis of monocyte and macrophage populations. **A.** Timeline of experiment. **B.** Flow cytometry plots of tumours from PBS Lipo-treated or Clod Lipo-treated tumour-bearing mice. Cells were gated on single, live, CD45<sup>+</sup>, CD11b<sup>+</sup>, SiglecF<sup>-</sup>, F4/80<sup>+</sup>, Ly6G<sup>-</sup>. **C.** Data shown as percentage F4/80<sup>+</sup>Ly6C<sup>+</sup> of total live cells in PBS Lipo and Clod Lipo tumours. **D.** Data shown as percentage F4/80<sup>+</sup>Ly6C<sup>-</sup> of total live cells in PBS Lipo and Clod Lipo tumours.

For the infection study, which would last seven days longer than the pilot, the liposome treatment regime was continued following SL7207 or PBS administration (Figure 5.25A: Day 0 is when SL7207 or PBS was administered). The tumour growth dynamics in mice treated with Clod Lipo or PBS Lipo was compared with untreated mice depicted in Chapter 3, Figure 3.7 (Figure 5.25B). It was not possible to perform statistical analysis on these parameters due to the small sample size of the PBS Lipo group (n=2), but there did not appear to be an obvious difference in the tumour growth dynamics between groups following liposome treatment. Furthermore, there did not appear to be any differences in the weight changes in the PBS Lipo and Clod Lipo-treated mice, except at one time point, but this resolved by the next day (Figure 5.25C).

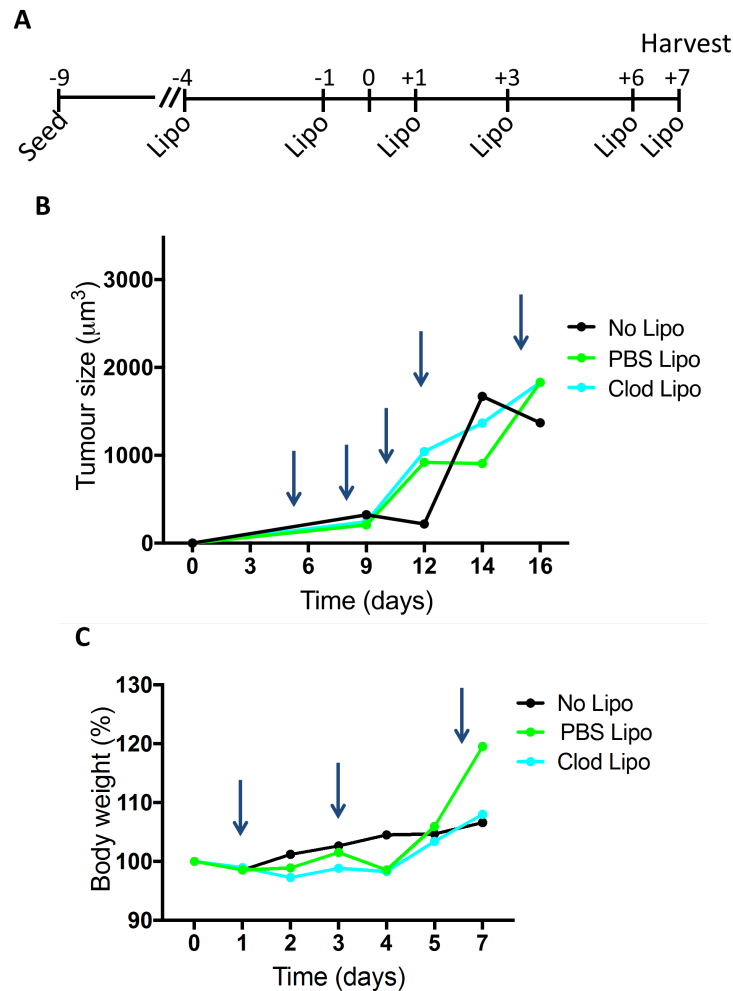


**Figure 5.25 Effects of Clod Lipo on B16F10 tumour growth and body weight**

Tumour-bearing mice were intravenously injected with either PBS Lipo or Clod Lipo with tumour size and body weight tracked over time and compared to no lipo treated samples as depicted in Chapter 3, Figure 3.7. **A.** Timeline of experiment. **B.** Tumour size of wild type and *Ccr2*<sup>-/-</sup> mice over time, as measured using Vernier calipers. Blue arrows indicate time of liposome administration. **C.** Weight of mice expressed as a percentage of weight at Day 0 of infection.

With the PBS Lipo and Clod Lipo treatment deemed to be sufficiently comparable to the No Lipo mice in terms of tumour growth dynamics and host welfare, it was appropriate to compare the infected samples to assess the effects of Clod Lipo treatment on the tumour growth inhibitory effects of SL7207. Infection with SL7207 led to reduced tumour growth compared with PBS Lipo infected mice compared to PBS Lipo uninfected mice (Figure 5.26A). The anti-tumour effects of SL7207 were abrogated by the administration of Clod Lipo and the tumour growth kinetics were more similar to the uninfected samples (Figure 5.26A, B). There was a significant difference in the tumour size of the PBS Lipo infected tumours and Clod Lipo infected tumours at 7 dpi. As in previous experiments, the anti-tumour effect of SL7207 was associated with weight loss in the infected mice, but the Clod Lipo-infected mice were

significantly protected compared to the PBS Lipo infected mice at 7 dpi (Figure 5.26C). There was no difference in the colonisation capacity of SL7207 between the PBS Lipo and Clod Lipo samples in the spleen, liver or tumour (Figure 5.26D).

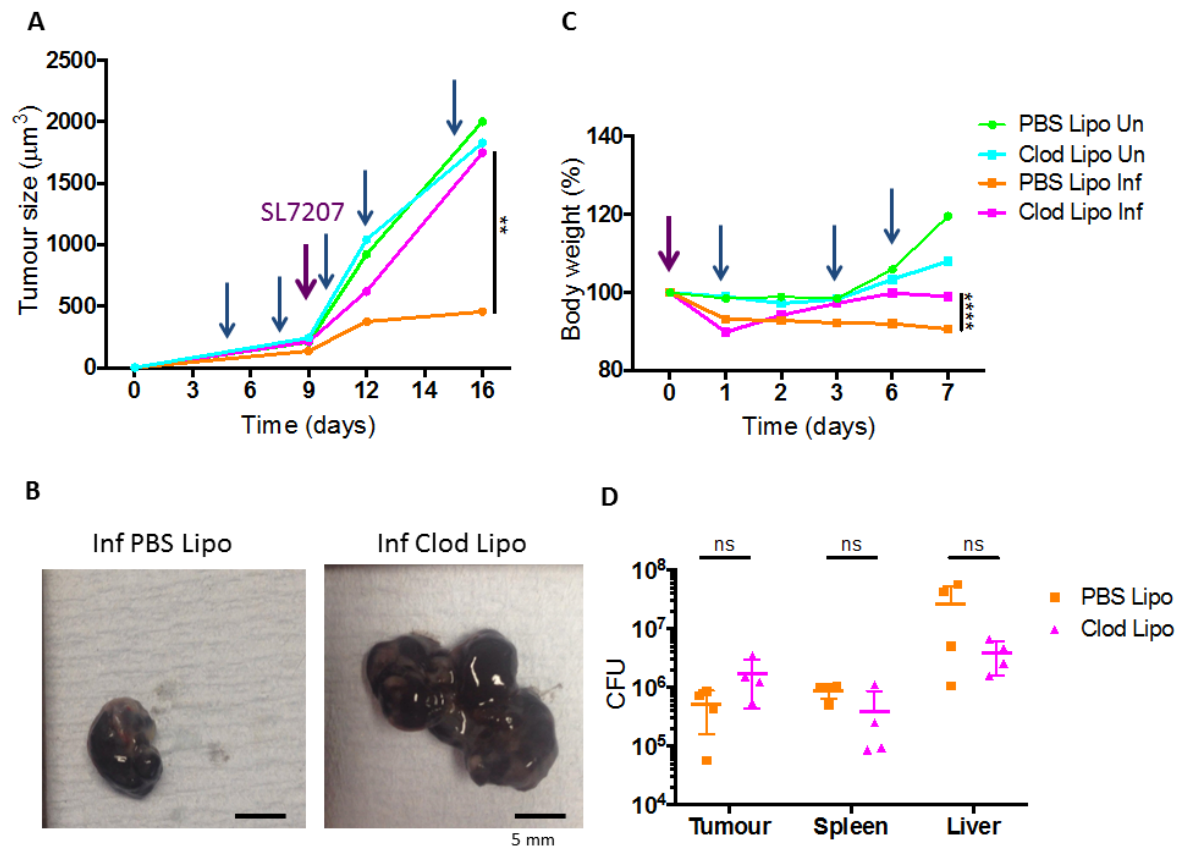
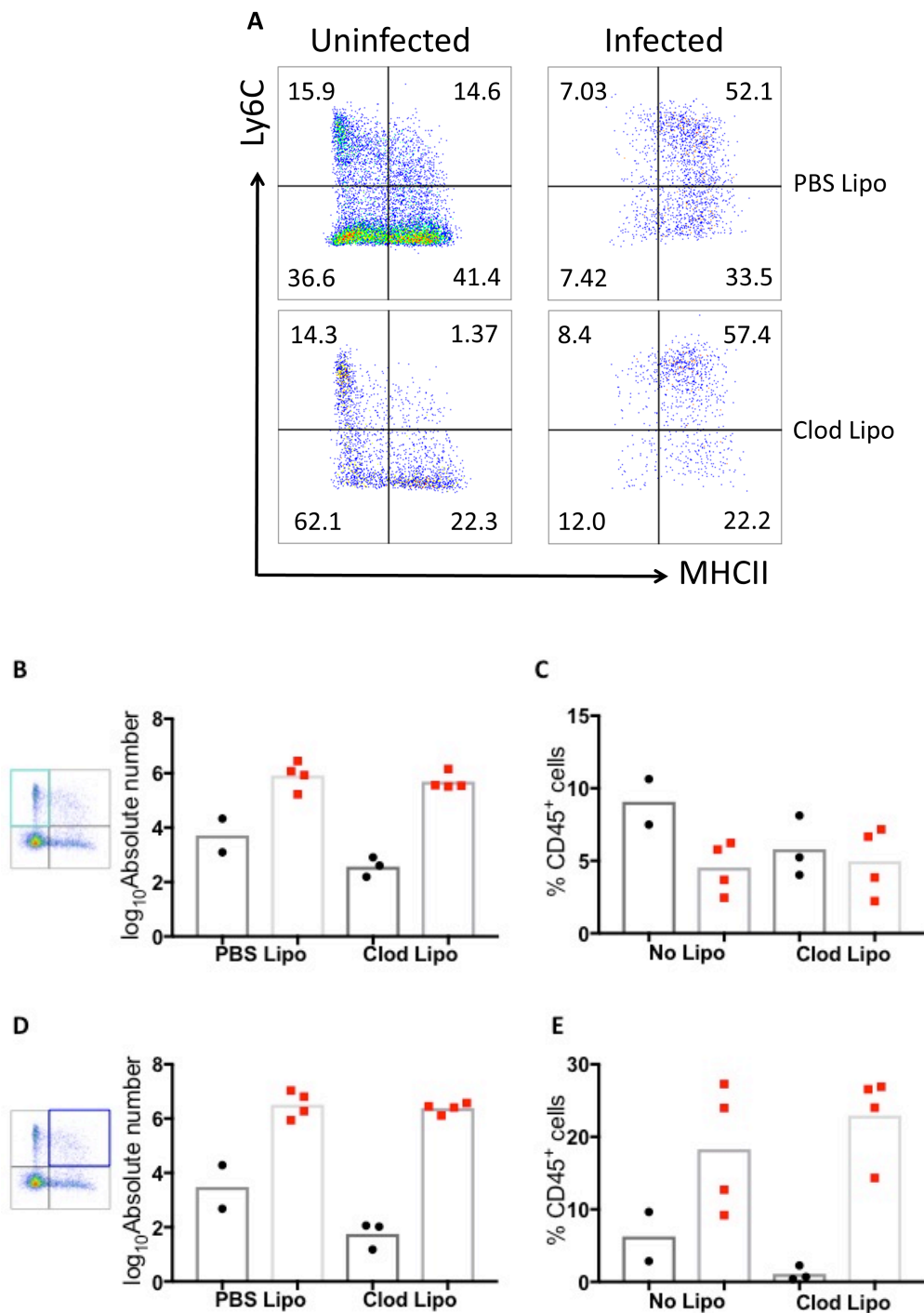


**Figure 5.26 Effects of Clod Lipo on SL7207 infection tumour-bearing mice**

Tumour-bearing mice, intravenously injected with either PBS Lipo or Clod Lipo were also inoculated with SL7207 or PBS control, and tumour size was monitored over time. **A.** Tumour sizes as measured using Vernier calipers. Purple arrow indicates time of SL7207 administration. Blue arrows indicate time of liposome administration. **B.** Infected PBS Lipo and infected Clod Lipo tumours at 7 dpi. Scale bar 5 mm. **C.** Weight of mice expressed as a percentage of weight at Day 0 of infection. **D.** Organs were harvested on 7 dpi and subject to homogenization to generate CFU counts. Statistical analyses performed using Student's t test between tumour sizes body weights and CFU/organ between infected PBS Lipo and infected Clod Lipo samples at 7 dpi where  $p < 0.05^*$ ,  $p < 0.01^{**}$ . NS: not statistically significant.

Tumours were harvested on day 16, 7 dpi, and the infiltrating cells assessed by flow cytometry. In both the PBS Lipo and Clod Lipo, there was an increase in the number of Ly6C<sup>+</sup>MHCII<sup>-</sup> monocytes in the infected samples compared to the uninfected controls but this could not be analysed statistically due to the small size of the uninfected PBS Lipo group (Figure 5.27A, B). There were no real changes in the proportion of these cells amongst the CD45<sup>+</sup> immune cell population (Figure 5.27C). The number and proportion of Ly6C<sup>+</sup>MHCII<sup>+</sup> cells increased following infection in both PBS Lipo and Clod Lipo compared to

uninfected controls (Figure 5.27D, E). For the MHCII<sup>-</sup> TAMs, there appeared to be increases in the number of cells, and a decrease in their proportion amongst CD45<sup>+</sup> leukocytes from infected compared to uninfected samples for both PBS Lipo and Clod Lipo (Figure 5.27F,G). This pattern was also evident in the MHCII<sup>+</sup> TAMs (Figure 5.29H,I). Thus although Clod Lipo treatment inhibited the anti-tumour effects of SL7207, this is not associated with prevention of monocyte-macrophage infiltration into the tumour.



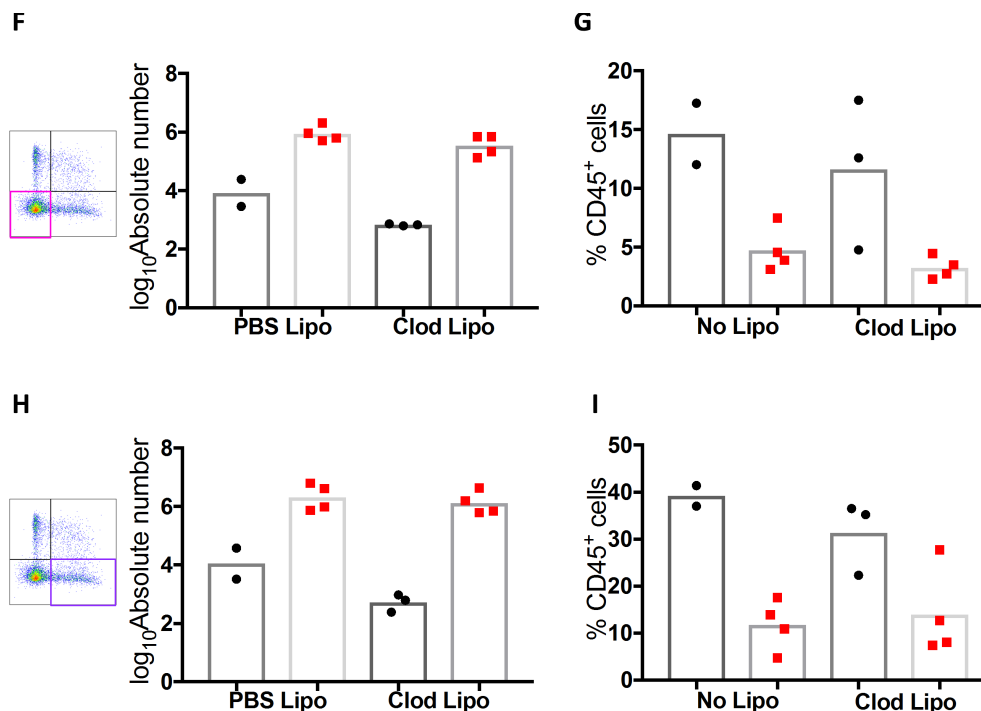


**Figure 5.27 Effects of SL7207 on the tumour monocyte/macrophage compartment in Clod Lipo treated, SL7207-infected mice**

Tumour-bearing mice, intravenously injected with either PBS Lipo or Clod Lipo were also inoculated with SL7207 or PBS control, and tumours were harvested at 7 dpi for flow cytometry analysis of tumour monocyte/macrophage compartment. Cells were gated on single, live, CD45<sup>+</sup>, CD11b<sup>+</sup>, SiglecF<sup>-</sup>, F4/80<sup>+</sup>, Ly6G<sup>-</sup>. **A.** Representative flow cytometry plots of tumour monocyte/macrophage compartment from PBS Lipo and Clod Lipo-treated mice, infected and uninfected. **B.** Quantification of absolute number of Ly6C<sup>+</sup>MHCII<sup>-</sup> monocytes in PBS Lipo and Clod Lipo, infected (red) and uninfected (black). **C.** Data shown as percentage Ly6C<sup>+</sup>MHCII<sup>-</sup> monocytes of total CD45<sup>+</sup> cells in PBS Lipo and Clod Lipo, infected (red) and uninfected (black). **D.** Quantification of absolute number of Ly6C<sup>+</sup>MHCII<sup>+</sup> monocytes in PBS Lipo and Clod Lipo, infected (red) and uninfected (black). **E.** Data shown as percentage Ly6C<sup>+</sup>MHCII<sup>+</sup> monocytes of total CD45<sup>+</sup> cells in PBS Lipo and Clod Lipo, infected (red) and uninfected (black). **F.** Quantification of absolute number MHCII<sup>-</sup> TAMs in PBS Lipo and Clod Lipo, infected (red) and uninfected (black). **G.** Data shown as percentage MHCII<sup>-</sup> TAMs of total CD45<sup>+</sup> cells in PBS Lipo and Clod Lipo, infected (red) and uninfected (black). **H.** Quantification of absolute number MHCII<sup>+</sup> TAMs in PBS Lipo and Clod Lipo, infected (red) and uninfected (black). **I.** Data shown as percentage MHCII<sup>+</sup> TAMs of total CD45<sup>+</sup> cells in PBS Lipo and Clod Lipo, infected (red) and uninfected (black). Statistical analysis performed using Student's t test between infected PBS Lipo and infected Clod Lipo samples where  $p < 0.05^*$ .

## 5.3 Discussion

It has been reported that the monocyte/macrophage compartment plays an important role in stimulating the host pro-inflammatory immune response to *S. Typhimurium* (Wick, 2011). Cancer has also presented a role for the monocytes/macrophages in driving multiple features of tumourigenesis (Qian & Pollard, 2010). Given the dual potential of these cells, it was pertinent to investigate if SL7207 administration could transform the pro-tumour monocyte/macrophages into pro-inflammatory, anti-tumour cells. It was found that the Ly6C<sup>+</sup>MHCII<sup>-</sup> monocytes and Ly6C<sup>+</sup>MHCII<sup>+</sup> monocytes were activated following SL7207 infection, pointing towards the possibility that these were the major anti-tumour effector cell types in the tumour following SL7207 infection. The removal of these cells using clodronate liposomes, reported to selectively target monocytes and macrophages, was investigated. Clodronate liposome treatment abrogated the anti-tumour effects of SL7207 compared to PBS liposome treated and untreated controls, potentially providing a mechanism for *S. Typhimurium*-mediated tumour growth inhibition. However, although the phenotype following Clod Lipo treatment was evident from the experiment, the contribution of the tumour monocyte/macrophage compartment to the anti-tumour effect was not definitive and needs to be repeated to generate informative data pertaining to the changes in immune cell types in the tumours for each condition.

### 5.3.1 Why is it important to define and characterise immune cell subsets in the tumour?

When dealing with any cells, it is imperative to be confident that cell types identified in the study are similarly defined in the literature. This is important as it allows the researcher to draw conclusions about the role of their cell type of interest in their present experimental conditions, as well as others. Immune cell definitions are often attributed to the subset of cell surface markers which they display. As these markers can overlap with other cell types, there is an associated risk of ill-defining an immune cell population, and associating functions to the wrong cell type. The importance of the correct identification of immune cell types for the purposes of cancer therapy lie in the fact that different cancer subtypes often have distinct immune cell signatures (Chifman *et*

*al.*, 2016). This signature might define a patient's suitability to an immunotherapy based on the effector cell type (correctly identified) of the therapy.

For this study, the gating strategy outlined in Chapter 4, Figure 4.1 was concluded to be most suitable. This strategy is used extensively in the laboratory group for the investigation of colonic macrophages, and was also in keeping with previous reports (Bain *et al.*, 2013; Bain *et al.*, 2014; Cortez-Retamozo *et al.*, 2012; Movahedi *et al.*, 2010). However, the present study employs a more rigorous gating strategy than these reports by ensuring the removal of SiglecF<sup>+</sup> eosinophils, CD11c<sup>+</sup>F4/80<sup>-</sup> dendritic cells (DCs) and Ly6G<sup>+</sup> neutrophils. One published gating strategy has defined TAMs from total CD11b<sup>+</sup> cells according to expression of Ly6C and MHCII, in spite of the fact DCs are MHCII<sup>+</sup> (Chapter 4, Figure 4.7) (Movahedi *et al.*, 2010). In a study by Franklin and colleagues, TAMs in a Polyoma Middle-T Oncogene driven mammary tumour model were defined within the total CD11b<sup>+</sup> cell population as CD11b<sup>int</sup>MHCII<sup>hi</sup> and resident mammary tissue macrophages as CD11b<sup>hi</sup>MHCII<sup>hi</sup>. The rationale for this was due to the fact that following transformation of the mammary cells, there was a decrease in the proportion of CD11b<sup>hi</sup>MHCII<sup>hi</sup> and an increase in the proportion of CD11b<sup>int</sup>MHCII<sup>hi</sup> in the tumour myeloid population (Franklin *et al.*, 2014). However, these do not take in to consideration the finding that TAMs are also MHCII<sup>-/lo</sup> (Movahedi *et al.*, 2010). Therefore, it was decided that the gating strategy employed in the present study would be sufficient to rigorously define monocyte and macrophage populations within the tumour.

The given gating strategy produced four populations in the monocyte/macrophage compartment: Ly6C<sup>+</sup>MHCII<sup>-</sup> monocytes Ly6C<sup>+</sup>MHCII<sup>+</sup> monocytes, MHCII<sup>-</sup> TAMs and MHCII<sup>+</sup> TAMs. Ly6C<sup>+</sup>MHCII<sup>-</sup> monocytes are possibly blood-borne cells within the vasculature of the tumour, but likely represent newly arrived tissue monocytes (Bain *et al.*, 2013). With the present gating strategy it is not possible to differentiate the contribution of blood contaminants and tissue-resident cells within the Ly6C<sup>+</sup>MHCII<sup>-</sup> compartment. Furthermore, studies that have investigated the contributions of various immune cells to bacterial-mediated tumour growth inhibition have also failed to control for the possibility that the immune cell population in question was also made up of

blood-borne cells. These considerations are more applicable for some cell types than for others. For example, macrophages do not circulate in the bloodstream so macrophages recovered from a tissue can be thought of as tissue resident. However, neutrophils make up the largest proportion of leukocytes in the circulation, which means it is difficult to discriminate the contribution of blood-borne neutrophils from tissue resident in digested tissue. This is critical, as cells of the immune system continuously recirculate through the vasculature, which permeates every organ, including tumours. These circulatory immune cells exhibit very different phenotypes to tissue-resident cells, and are most often not associated with shaping local immunological responses. Therefore, the contamination of tumour-associated immune cells with blood-borne cells confounds data pertaining to the number and activation of the tissue-resident cells participating in the immune response. This consideration is particularly relevant during systemic inflammation, as there is an increase in the number of circulatory immune cells. This limitation of our study was only made apparent following the conclusion of these experiments. Therefore, a post-hoc examination of the contribution of blood monocytes was performed according to (Anderson *et al.*, 2014). The contribution of blood monocytes was very low, which gave confidence that changes seen in the monocyte populations were due to tissue-resident cells, not blood contaminants (Appendix, Figure 9.3).

In the present study, two populations of monocytes were defined: Ly6C<sup>+</sup>MHCII<sup>-</sup> and Ly6C<sup>+</sup>MHCII<sup>+</sup> cells. However, another population of monocytes, F4/80<sup>+</sup>Ly6C<sup>-</sup>MHCII<sup>-</sup> monocytes have also been reported (Misharin *et al.*, 2014). Ly6C<sup>lo</sup> monocytes in the blood are patrolling monocytes which can crawl along endothelial cells, and thus could possibly be blood contaminants of the tumour preparation (Jakubzick *et al.*, 2017). If this were the case in the present study, these cells would appear in the MHCII<sup>-</sup> TAM population. By analysing the size (side scatter) and F4/80 characteristics of the Ly6C<sup>-</sup>MHCII<sup>-</sup> population within the monocyte/macrophage compartment, these features aligned closely with the MHCII<sup>+</sup> population and not with the Ly6C<sup>+</sup> monocytes providing evidence that these were in fact macrophages as opposed to monocytes. Although these analyses are somewhat definitive, perhaps the most conclusive evidence would be to isolate each cell type for cytospin analysis to enable the morphological characterisation of the different cell types.

### 5.3.2 Why is there an accumulation of Ly6C<sup>+</sup>MHCII<sup>+</sup> cells, and why might this promote anti-tumour effects?

It has been demonstrated that Ly6C<sup>+</sup>MHCII<sup>-</sup> cells can give rise to Ly6C<sup>+</sup>MHCII<sup>+</sup> monocytes which can in turn give rise to tissue-resident Ly6C<sup>+</sup>MHCII<sup>+</sup> macrophages (Bain *et al.*, 2013). This has been demonstrated in both cancer and colonic settings (Bain *et al.*, 2014; Franklin *et al.*, 2014; Movahedi *et al.*, 2010). In the present study, there is an accumulation of the Ly6C<sup>+</sup>MHCII<sup>+</sup> population in the tumour following systemic SL7207 infection. The absence of a statistically significant difference in the number of these cells between infected and uninfected samples is possibly due to the fact that the uninfected tumours are much bigger than the infected tumours as can be seen from Chapter 3, Figure 3.8E. As there does not appear to be an increase in the number of TAMs, it is possible that the differentiation process from Ly6C<sup>+</sup>MHCII<sup>+</sup> to TAM is stalled. This has been reported during inflammatory conditions. It has been demonstrated that in the inflamed colon, a significant proportion of the infiltrating monocytes retain a Ly6C<sup>+</sup>MHCII<sup>+</sup> phenotype (Bain *et al.*, 2013). Furthermore, these cells appear to have greater TNF- $\alpha$  production than resident macrophages and are more responsive to toll like receptor (TLR) stimuli, suggesting that they are the major contributors to inflammation in this setting. The attenuation in this differentiation of Ly6C<sup>hi</sup> monocytes into resident macrophages following DSS-colitis resulted in the accumulation of inflammatory monocytes which had comparatively greater expression for pro-inflammatory mediators such as IL-6, IL-23 $\alpha$ , Nitric Oxide Synthase (NOS) 2 and IL-1 $\beta$  than controls (Zigmond *et al.*, 2012). The removal of these cells using antibody-mediated depletion resulted in the significant decrease in colitis score and weight loss of DSS-induced colitis mice compared to control, further evidencing their role in inducing a pro-inflammatory environment (Shmuel-Galia *et al.*, 2016). We also hypothesise that the differentiation process from Ly6C<sup>+</sup>MHCII<sup>-</sup> monocytes to Ly6C<sup>+</sup>MHCII<sup>+</sup> monocytes is accelerated. The evidence suggesting this comes from a decrease in the number of the former following infection. Although it was interesting to understand the changes in the monocyte to macrophage differentiation process in the tumour following infection, this line of enquiry was not followed up due to time constraints.

The data in the present study also seemed to suggest the monocytes are potent pro-inflammatory mediators which may be responsible for transforming the tumour microenvironment from immunosuppressive to immunostimulatory. Although due to the small sample size, the quantification analysis of the inflammatory mediators was not statistically significant for the Ly6C<sup>+</sup>MHCII<sup>+</sup> monocytes, they all trended towards an increased production of pro-inflammatory mediators following infection. Therefore, these experiments need to be repeated to determine if the Ly6C<sup>+</sup>MHCII<sup>+</sup> monocytes are pro-inflammatory, as they have been credited in other reports. However, this is the first report to suggest tumour monocytes as the effector cells underlying tumour growth inhibition.

There are, however, other reports which demonstrated that Ly6<sup>+</sup>MHCII<sup>+</sup> monocytes can give rise to monocyte-derived DCs under inflammatory conditions (Rivollier *et al.*, 2012; Serbina *et al.*, 2003). In a model of T cell transfer-induced colitis, monocytes digressed from developing into macrophages to developing into two DC populations following inflammation. This was not believed to be the case in the present study as inflammatory monocytes cells were F4/80<sup>+</sup>, which is not expressed on DCs and following infection the proportion of CD11c<sup>+</sup> Ly6C<sup>+</sup>MHCII<sup>+</sup> cells actually decreased (Appendix, Figure 9.4).

These findings have important consequences for the employment of immunotherapies, not just bacterial-mediated therapy, in the clinical context. These data highlight that the monocyte to macrophage differentiation process is a potential node of therapeutic intervention. A recent study demonstrated that Vitamin A is required for the differentiation of monocytes into peritoneal macrophages, but other than this, there is relatively little known about the factors which drive this differentiation process (Gundra *et al.*, 2017). If the factors underlying the differentiation process in the tumour could be interfered with, this would decrease the number of TAMs in the tumour which would subsequently decrease the ability of the TAMs to contribute to tumourigenesis. If it is found to be the case that infiltrating monocytes are critical mediators of bacterial-mediated tumour growth inhibition, this has important ramifications for the use of bacteria in the clinic. Monocytopenia is a clinically-relevant

symptom of myelodysplastic syndromes, which are a group of blood cancers (Gagnat *et al.*, 2015). Therefore, this group of cancers would be unlikely to respond to bacterial-mediated cancer therapy if monocytes were found to be the major effector cell type.

### **5.3.3 What do the changes in TAM phenotype following infection mean, and why is this important?**

MHCII<sup>lo</sup> and MHCII<sup>hi</sup> TAMs have been reported and have gene expression profiles (Movahedi *et al.*, 10). Multiple studies have reported macrophages to be highly plastic cells capable of changing phenotype based on the environment (Guidicci *et al.*, 2005; Lavin *et al.*, 2014; Sacconi *et al.*, 2006). In the present study there was a shift towards MHCII<sup>+</sup> TAMs in the tumour following infection. If these MHCII<sup>+</sup> TAMs exhibited pro-inflammatory properties similar those from *S. Typhimurium* infection studies (Mastroeni *et al.*, 1995; Yrlid *et al.*, 2000), it would suggest that tumours with high densities of MHCII<sup>-</sup> TAMs could be rescued from their anti-inflammatory, pro-tumoural phenotype to a pro-inflammatory, anti-tumourigenic one with SL7207 treatment. However, in the present study, the only cytokine increased in MHCII<sup>+</sup> TAMs in the tumour appeared to be TNF- $\alpha$ , but this was a less than 1.5-fold increase. In fact, the IL-6 expression was actually less in the MHCII<sup>+</sup> TAMs compared to the MHCII<sup>-</sup> TAMs but this was not statistically significant with such low sample size ( $p = 0.0506$ ). Furthermore, following infection there appeared to be no difference in the ability of the MHCII<sup>-</sup> and MHCII<sup>+</sup> TAMs to produce pro-inflammatory mediators following infection. As the data suggests that there is no difference in the ability of either TAM population to generate pro-inflammatory cytokines following infection, it is unlikely that the primary outcome of the increased proportion of MHCII<sup>+</sup> TAMs is increased cytokine production in the tumour. However, it is important to note that there may be other changes in the functional phenotype of the TAMs outwith the parameters investigated in this study, so further characterisation would be necessary before a definitive conclusion can be reached. That being said, a similar phenomenon has been reported in a model of colitis, whereby the resident macrophages did not increase their production of pro-inflammatory mediators compared to control (Bain *et al.*, 2013). In the present study, the MHCII<sup>+</sup> TAMs are more competent at phagocytosis *ex vivo* than the MHCII<sup>-</sup> TAMs in the uninfected state, and this ability was heightened following infection.

Therefore, it is likely that the primary role of the MHCII<sup>+</sup> TAMs in the tumour, particularly following infection, might be phagocytosis of both invading bacteria as well as cellular debris.

The pro-inflammatory effects of TAMs following *Listeria monocytogenes* infection in a murine ovarian carcinoma model were suggested by large increases in pro-inflammatory cytokines in TAMs following infection compared to uninfected controls (Lizotte *et al.*, 2014). However, this study seemed to identify TAMs based solely on CD11b expression, and failed to use macrophage associated markers such as F4/80 or CD64 so it is difficult to assess if these cells were actually macrophages or from another myeloid compartment. Zheng and colleagues asserted an increase in the activation of TAMs following systemic infection with the *S. Typhimurium* strain SHJ2037 (Zheng *et al.*, 2017b). However, the accreditation of macrophages in this study was due to F4/80 expression, which would also include monocytes and possibly F4/80<sup>+</sup> eosinophils (McGarry & Stewart, 1991).

The discrepancy in TAM functions between this study and others could be explained by a number of factors. For (Movahedi *et al.*, 2010), it is possibly explained by contaminating DCs in the MHCII<sup>+</sup> TAM population accounting for the IL-6-producing functions of this population (as cDC2s were not excluded and are similarly LY6C<sup>-</sup>MHCII<sup>+</sup>). Alternatively, the differences might be attributable to the mouse strain. C57BL/6 mice are regarded as a 'T<sub>H</sub>1' type strain whilst BALB/c mice are a 'T<sub>H</sub>2' strain which may result in differing cytokine expression profiles in multiple cell types (Mills *et al.*, 2000; Santos *et al.*, 2006). Furthermore, different tumour cell types have different immunogenic properties (Lechner *et al.*, 2013), so it is likely that there would be differences in the phenotype of the tumour infiltrating immune cells. It is interesting however that such a discrepancy should exist. It might mean that different tumours, such as the model used in (Movahedi *et al.*, 2010), might actually respond better to SL7207 treatment if the shift in MHCII<sup>-</sup> to MHCII<sup>+</sup> is accompanied by increased pro-inflammatory capacities of the latter. However, pinpointing the discrepancies associated with immune cell type function between models was outside the scope of the present study, as the real point of interest was the change in phenotypes following SL7207 administration.

### 5.3.4 Why was the Kaede data not informative and how could this experiment be improved?

The data so far seemed to point to the monocytes as being the primary cell types driving the inflammatory response in the tumour. However, as there were still some changes in the TAMs, and possibly changes we hadn't investigated, it was attractive to investigate the source of these cells. The main focus was to distinguish which of the MHCII<sup>-</sup> TAMs or the Ly6C<sup>+</sup>MHCII<sup>+</sup> monocytes were giving rise to the MHCII<sup>+</sup> TAMs. To do this, the photoconvertible Kaede model was suitable to investigate the changes in the photoswitched TAM populations following infection. Following optimisation of the protocol, it was disappointing that the uninfected photoswitched Kaede tumours seemed to display an inflammatory phenotype, similar to the infected tumours. This was characterised by the accumulation of Ly6C<sup>+</sup>MHCII<sup>+</sup> cells in the tumour. It is unclear why this was the case. It was hypothesised that the UV light might have activated the cells in the tumour. In fact, a recent study has demonstrated that the exposure of THP-1 monocytes to UV light affected the phenotype of these cells (Trotter *et al.*, 2017). Given that the sample size for the present experiment was so small, it might be best to run a pilot experiment to compare UV-treated tumours to untreated to control for the possibility that the UV light might be affecting the phenotype of the immune cells. However, if it was found that the cells were indeed becoming activated by UV light, the Kaede model would be discarded.

It was interesting to see that in all of the tumours, irrespective of infection status, the photoswitched Kaede red F4/80<sup>+</sup> cells mostly appeared in the Ly6C<sup>+</sup>MHCII<sup>+</sup> population. Looking at the pilot experiment, within the F4/80 compartment, the majority of the Kaede red cells were F4/80<sup>lo</sup>, characteristic of Ly6C<sup>+</sup>MHCII<sup>+</sup> cells. It was possible that these cells were activated following UV light exposure and as such, remained in the Ly6C<sup>+</sup>MHCII<sup>+</sup> population, as opposed to differentiating into TAMs. It was unexpected that there were no Kaede red TAMs recovered from either the infected or uninfected samples. It is possible that if they became activated, there may have been increased replication, as shown to occur following infection. There was also far fewer Kaede red<sup>+</sup> cells in the infected tumours in comparison to the uninfected tumours, possibly explained by the fact that there is an increase in Ki67<sup>+</sup> Ly6C<sup>+</sup>MHCII<sup>+</sup> cells in the infected tumour, and cell replication dilutes the intracellular Kaede red protein.

In conclusion, the Kaede transgenic mouse model did not produce informative data about the resident macrophage response to SL7207, but steps have been identified which could optimise the experimental procedure for future work.

### **5.3.5 Why was the *Ccr2*<sup>-/-</sup> murine strain not effective at removing monocytes during SL7207 infection?**

CCR2 is necessary for bone marrow monocytes to egress into the circulation, but not necessarily for uptake into the tissue (Serbina & Pamer, 2006). It was found that there was a decrease in the number of Ly6C<sup>hi</sup> monocytes in the blood of *Ccr2*<sup>-/-</sup> mice compared to wild type, with a concomitant increase in the bone marrow, suggesting these cells were trapped therein (Fujimura *et al.*, 2015; Serbina & Pamer, 2006). However, bone monocytes adoptively transferred from a *Ccr2*<sup>-/-</sup> mouse were capable of migrating out of circulation into tissues in the host in equal measure to bone marrow monocytes from CCR2-competent mice (Serbina & Pamer, 2006). CCL2 has been considered the most important tumour-derived factor to attract circulating monocytes into tumours and metastatic sites in multiple mouse and human models of cancer (Huang *et al.*, 2007; Kitamura *et al.*, 2015; Lin *et al.*, 2006; Qian *et al.*, 2012). As well as tumour cells, CCL2 produced from tumour-associated fibroblasts can recruit monocytes (Silzle *et al.*, 2003). Given that circulating monocytes give rise to TAMs, it was interesting in the present study that there was no difference in the number of TAMs in the wild type and *Ccr2*<sup>-/-</sup> tumour-bearing mice. This was similarly seen by Franklin and colleagues where there was no difference in the proportion of TAMs in tumours derived from *Ccr2*<sup>-/-</sup> mice and wild type mice (Franklin *et al.*, 2014). However, the diphtheria toxin-mediated removal of CCR2<sup>+</sup> cells (CCR2<sup>DTR</sup>) resulted in an approximate 4-fold decrease in TAMs in the tumours of tumour-bearing mice. The discrepancy is likely explained by the increased proliferative capacity of TAMs compared to resident macrophage cells, which compensates for reduced recruitment.

The CCR2-CCL2 axis has also proved important for the recruitment of monocytes to inflamed tissue. This was shown where uptake of *Ccr2*<sup>-/-</sup> monocytes was deficient in comparison to CCR2-competent mice in DSS-induced colitis (Zigmond *et al.*, 2012). Furthermore, a mixed Ly6C<sup>+</sup> monocyte graft consisting of 50:50 *Cx3cr1*<sup>gfp/+</sup>CD45.1 and *Cx3cr1*<sup>gfp/+</sup>*Ccr2*<sup>-/-</sup>CD45.2 demonstrated that there was

almost exclusive recruitment of the CCR2-competent cells in the CX3CR1-GFP compartment in the lamina propria at four days post DSS challenge. However, another study with a conceptually similar experimental protocol and question (is CCR2 required for monocyte recruitment to inflamed tissue?) demonstrated that CCR2<sup>+</sup> monocytes from wild type more readily recruited to inflamed tissue than *Ccr2*<sup>-/-</sup> monocytes when adoptive transfer was carried out at the same time as inflammation, but not when the cells were transferred 60 hours after inflammation (Tsou *et al.*, 2007). Therefore, CCR2-dependent uptake might be time-dependent.

Given that there was a significant decrease in the number of monocytes in the *Ccr2*<sup>-/-</sup> strain compared to wild type, this was seen as an appropriate model to specifically remove the contribution of the infiltrating monocytes to *S. Typhimurium* treated tumours. Therefore, it was surprising that there was a Ly6C<sup>+</sup>MHCII<sup>+</sup> population in the infected *Ccr2*<sup>-/-</sup> tumour-bearing mice, suggesting a CCR2-independent mechanism of monocyte recruitment. In a model of experimental autoimmune uveitis, CCR2 is not required for the recruitment of monocytes in the inflamed retina (Dagkalis *et al.*, 2009). Furthermore, another study has shown that CCR5 depletion can significantly reduce Ly6C<sup>lo</sup> monocytes in atherosclerotic plaques (Tacke *et al.*, 2007). In the present study, the Ly6C<sup>+</sup>MHCII<sup>+</sup> cells in the *Ccr2*<sup>-/-</sup> infected mouse are both Ly6C<sup>lo</sup> and Ly6C<sup>hi</sup>, so CCR5-mediated redundant function does not explain the maintenance of the Ly6C<sup>+</sup>MHCII<sup>+</sup> population in the *Ccr2*<sup>-/-</sup> infected strains.

It has been demonstrated that CCR2-mediated depletion-sensitive cells were highly responsive to LPS (TLR4 ligand), PAM3CSK4 (TLR2 ligand) and MDP (NOD2 ligand) (Zigmond *et al.*, 2012). The severity of colitis was reduced in chimeras where wild type Ly6C<sup>hi</sup> cells were replaced with *TLR2*<sup>-/-</sup>, *NOD2*<sup>-/-</sup> or *MyD88*<sup>-/-</sup> *TICAM1*<sup>-/-</sup> Ly6C<sup>hi</sup> monocytes, suggesting a dependence on MyD88-associate pathways to induce the inflammatory phenotype. In mouse models of infection, *S. Typhimurium* can also activated TLR4 in a MyD88-independent manner (Kawai *et al.*, 2001), proposing there may be alternative pathways activated to attract monocytes independent of the CCR2-CCL2 axis. Investigating the factors responsible for CCR2-independent monocyte recruitment to the *S. Typhimurium*-infected tumour might provide novel insights into mechanisms of monocyte

recruitment in a unique physiological environment. However, although this is interesting, it was outside the remit of the current study.

It has been suggested that during cancer progression, the bone marrow outsources monocyte production to other organs such as the spleen to participate in extra-medullary hemopoiesis. This resulted in increased monocyte-precursors in the spleen of tumour-bearing mice compared to control (Cortez-Retamozo *et al.*, 2012). A splenectomy of the tumour-bearing mice revealed a decreased number of TAMs in lung adenocarcinomas. Furthermore, labelled monocyte-derived splenocytes were recovered with a TAM phenotype in the tumours. The contribution of the CCR2-CCL2 axis to this process is insufficiently understood. CCR2 did not play a role in monocyte egress from the spleen during myocardial infarction (Swirski *et al.*, 2009). In this instance, Angiostatin-II on monocytes was responsible for monocyte egress from the spleen following myocardial infarction. However, in the other study, the silencing of CCR2 using a siRNA (siCCR2) which 'selectively targets' splenic monocytes resulted in decreased TAMs in model of lung adenocarcinoma (Cortez-Retamozo *et al.*, 2012). However, looking at the article which detailed the characteristics and effectiveness on the siCCR2, bone marrow localisation of siCCR2 was reported following systemic administration (Leuschner *et al.*, 2011). Therefore, it is difficult to rule out the possibility of the bone marrow-derived monocytes being responsible for the drop in TAM which Cortez-Retamozo and colleagues credited to the splenic reservoir of monocytes. It is also possible that the decrease in splenic monocytes following siCCR2 administration is because there is a disruption in the trafficking of monocyte precursors from the bone marrow to the spleen, if that is indeed their source.

It would be interesting to assess the contribution of the spleen to the TAM and monocyte populations in the tumour following infection. Such an investigation would further identify patients suitable for certain for this therapeutic strategy as reduced splenic function in cancer models has been reported (Bronte *et al.*, 2000; Marigo *et al.*, 2010). In the first instance, it would be attractive to characterise how the splenic monocyte pool changes between steady state physiological conditions and cancer or infection. Another attractive experimental protocol would be to perform splenectomies on tumour-bearing mice prior to SL7207 or PBS administration to assess the monocyte and

macrophage populations in the infected and uninfected tumours. Unfortunately, the technical assistance for this procedure was not readily available in the local animal facilities and it was not timely to establish this procedure externally.

### **5.3.6 What can be concluded from the clodronate liposome infected mice?**

As the *Ccr2*<sup>-/-</sup> model was insufficient to remove the monocyte populations, an alternative strategy was to employ clodronate liposomes which have been reported to selectively mediate the cell death of monocyte and macrophage populations (Gazzaniga *et al.*, 2007; Griesmann *et al.*, 2016; Zeisberger *et al.*, 2006). The phenotype of the clodronate liposome-treated tumours was very clear: administration of clodronate liposomes abrogated the tumour growth inhibitory effects of SL7207. Unfortunately, the effect of the clodronate liposomes on the monocyte and macrophage populations was not so apparent. It was interesting that there appeared to be an increase in the number of monocytes in the Clod Lipo infected mouse compared to uninfected, potentially demonstrating that the monocytes were not being negatively affected by the clodronate. A likely explanation for this is that the infiltration is so robust, that the Clod Lipo was overwhelmed, in spite of the frequent doses of Clod Lipo which was administered, relative to other studies (Gazzaniga *et al.*, 2007; Griesmann *et al.*, 2016).

However, it is difficult to come to any conclusions when the dynamics of the immune cell infiltrate into the tumour during the course of infection are not known. From the data in the uninfected mice, it is evident that the clodronate is mediating a decrease in the monocyte/macrophage compartment. This is not in keeping with the infected samples, potentially suggesting the bacteria are either interfering with the Clod Lipo, or perhaps the SL7207 cells are adapting to the environment in the absence of monocytes/macrophages. In any case, it casts great doubt on the conclusion that the monocyte/macrophage compartment in the tumour mediates growth inhibition in *S. Typhimurium* treated tumour-bearing mice with the present data. However, it is also important to note that the data displayed herein is representative of 7 dpi, and might not necessarily reflect the distribution of the immune populations throughout the course of infection.

One point of interest is that following Clod Lipo treatment, but not PBS Lipo treatment, there was a drastic decrease in the size of the spleen (Appendix, Figure 9.5). This could be due to monocyte and macrophage depletion in the spleen of Clod Lipo treated mice. Monocytes have been demonstrated to expand in the spleen following systemic infection. Therefore, it is tempting to speculate that the change observed in the spleen following Clod Lipo treatment in the infected mice might be the underlying reason for the abrogation of SL7207-mediated tumour growth inhibition. It is even more tempting to speculate, with the inability of the *Ccr2*<sup>-/-</sup> mice to inhibit monocyte recruitment to the infected cells, and the conjecture of the spleen being the source of these recruited monocytes, that the absence of the splenic monocyte contribution explains how Clod Lipo treatment mitigated the tumour inhibitory effects of SL7207. This would also explain why the Clod Lipo infected mice were protected from excessive weight loss, through the absence of TNF- $\alpha$ -producing splenic macrophages (Di Francia *et al.*, 1994). However, in order to assess this it would first be necessary to confirm that the reduced spleens from the Clod Lipo infected mice indeed lack monocytes, and that these monocytes can play a role in inhibiting tumour growth. The latter could be achieved by adoptively transferring splenic monocytes from an infected tumour-bearing mouse into an uninfected tumour-bearing mouse and investigating the tumour growth inhibitory effects which might accompany this procedure.

In any case, it would be more attractive to employ a system which definitively and selectively depletes tumour monocytes, preferably in an inducible manner. In the first instance, it would be idyllic to repeat the clodronate liposome-mediated depletion study to investigate if the phenotypic readout is reproducible. If this was the case, an expanded antibody staining panel to investigate the effects on other cell types, such as T cell, might enable the identification of the cell type involved. Furthermore, it would be preferable to analyse the immune cell repertoire of the tumour at different time points during the infection. It might also be informative to carry out the liposome-mediated depletion protocol in *Ccr2*<sup>-/-</sup> to enhance the effectiveness of monocyte depletion.

An alternative model to use would be the *Lysm*<sup>Cre/mCherry</sup>*Csf1r*<sup>DTR</sup> strain which

seems to specifically ablate monocytes in the blood and tissue but not other mononuclear phagocytes, when diphtheria toxin is administered (Schreiber *et al.*, 2013). In comparison to the methods employed thus far to remove monocyte/macrophage contributions, this strategy targets only the Ly6C<sup>+</sup>CSF1R<sup>+</sup> double positive cells thus limiting abrogation to the monocyte/macrophage compartment, although it is possible that Ly6C<sup>+</sup> neutrophils would also be affected. Furthermore, the two pronged approach increases the likelihood of successfully removing monocyte/macrophages as it compensates for functional redundancy in removing either Ly6C<sup>+</sup> or CSF1R<sup>+</sup> cells alone. A limitation of this model might be the failure to delineate between the contribution of the monocytes and macrophages to the effects of *S. Typhimurium*-induced tumour growth inhibition. However, this limitation could be overcome by the adoptive transfer of specific monocyte/macrophage populations to tumour-bearing *Lysm<sup>Cre/mCherry</sup>Csf1r<sup>DTR</sup>* mice to assess their specific contribution to *S. Typhimurium*-induced tumour growth inhibition.

### 5.3.7 Concluding remarks

In conclusion, this chapter has suggested a role for tumour monocytes in contributing to the pro-inflammatory phenotype of the tumour microenvironment following infection. We have also shown that TAMs did not drastically change in phenotype following SL7207 infection. Treatment with clodronate liposomes resulted in the abrogation of SL7207-mediated tumour growth inhibition. However, looking at the cell types affected by clodronate treatment in the infected tumours did not demonstrate tumour monocytes and/or TAMs being affected by the clodronate liposomes in comparison to PBS liposome-treated controls. There was, however, a significant difference in the size of the spleen in the clodronate liposome infected mice compared to PBS liposome, highlighting a new avenue of investigation for subsequent experiments; splenic monocytes and their role in mediating tumour growth inhibition following *S. Typhimurium* infection.

## 6 *S. Typhimurium* transformed with an eukaryotic expression plasmid to mediate bactofection in tumour spheroid cells *in vitro*

### 6.1 Introduction

It is apparent, from this report and others, that *S. Typhimurium* is capable of tumour growth arrest in an *in vivo* tumour model (Crull *et al.*, 2011a; Low *et al.*, 1999). However, some research studies have sought to couple this innate anti-tumour behaviour of *S. Typhimurium* to other strategies to enhance the tumouricidal capabilities of the bacteria. This can be achieved in a number of ways. For example, (Ganai *et al.*, 2009) demonstrated that *S. Typhimurium* strain VNP20009 can specifically deliver apoptotic proteins to tumour cells, whilst another report employed a system where the *S. Typhimurium* (SHJ2037) overexpressed plasmid-encoded FlaB from *Vibrio vulnificus* to further slow tumour growth compared to treatment with the bacteria alone (Zheng *et al.*, 2017b). It has also been reported that bacteria can be utilized for the delivery of small hairpin RNA (shRNA) and eukaryotic expression plasmids to cancer cells (Fu *et al.*, 2008; Zheng & Min, 2016). The latter strategy is termed ‘bactofection’.

Bactofection is the utilization of bacteria to deliver genetic material to a target cell or tissue (Powell *et al.*, 1999; Schaffner, 1980). Multiple bacterial strains have been reported to have bactofection capabilities such as *Escherichia*, *Listeria* and also *Salmonella* (Ahmad *et al.*, 2011; Byrne *et al.*, 2014; Paglia *et al.*, 1998; Pijkeren *et al.*, 2010; Pilgrim *et al.*, 2003). Previous studies utilizing *Salmonella* to deliver therapeutic genes to cancer cells have employed host apoptotic, as well as immunogenic, genes to enhance the tumouricidal effects of the bacteria (Fu *et al.*, 2008; Lee *et al.*, 2005; Loeffler *et al.*, 2007; Yuhua *et al.*, 2001). Many cancer cells produce cancer cell-specific *de novo* antigens, and thus act as cancer-specific signals for immune cells to target these cells. For example, both prostate and melanoma cancers have well established tumour-associated antigens which can be detected for diagnostic purposes, as well as being targeted for therapy (Buonaguro *et al.*, 2011). Bacteria can be used to deliver eukaryotic expression vectors encoding tumour antigens to eukaryotic

cells (Dietrich *et al.*, 1998), which has also been employed for the purposes of vaccination against tumour cell challenge (Ahmad *et al.*, 2011).

It was hypothesised that *S. Typhimurium*, transformed with a eukaryotic expression reporter plasmid, pEGFP (Michael *et al.*, 2004), would lead to the production of GFP in the tumour cells. This would be a proof of principle for the ability of the bacteria to bactofect in our *in vitro* model, and would merit the progression of the study to *in vivo* models involving the use therapeutic plasmids encoding apoptotic or immunostimulatory genes.

### 6.1.1 Aims

1. To develop a three-dimensional tumour spheroid model *in vitro* using MDA-MD-231 cells
2. To investigate the invasion properties of *S. Typhimurium* in the tumour spheroid model
3. To investigate if *S. Typhimurium* strains transformed with the eukaryotic expression plasmid pEGFP can mediate the production of GFP in tumour spheroid cells

Furthermore, as it was seen that the *S. Typhimurium* transformed with pEGFP displayed a filamentous phenotype, a subsequent aim included:

4. To identify the feature of the plasmid responsible for inducing filamentation in *S. Typhimurium*-pEGFP

## 6.2 Results

### 6.2.1 The generation of three dimensional tumour spheroids *in vitro*

The ability of MDA-MB-231 cells to form reliable tumour spheroids *in vitro* was investigated to validate the suitability of this model for the subsequent bactofection study. Cells were seeded at multiple cell densities in ultra-low attachment plates in the presence of 2% Matrigel to encourage compact tumour spheroid formation (Ivascu & Kubbies, 2006; Vinci *et al.*, 2015). Tumour growth was observed over a period of 14 days. Light microscopy and scanning electron microscopy (SEM) demonstrated that the tumours which were seeded with  $5 \times 10^6$  MDA-MB-231 cells consistently formed compact structures at 11 days post seeding, with an approximate diameter of 500  $\mu\text{m}$  (Figure 6.1A,B). From histological analysis of tumour slices, it was determined that the tumours displayed similar traits to *in vivo* tumours, particularly with the necrotic core and the viable margin at the circumference of the tumour (Carlsson & Acker, 1998; Sutherland *et al.*, 1986) (Figure 6.1C). The necrotic core was further investigated by scanning electron microscopy (SEM) imaging, with cell debris characteristic of necrosis present in the centre of the spheroids (Figure 6.1D).

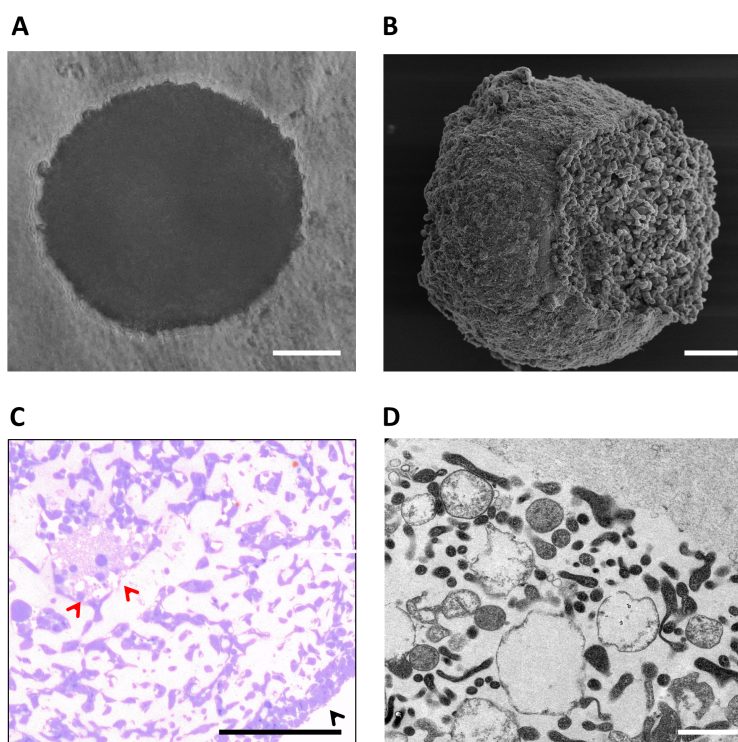


**Figure 6.1** *In vitro* tumour spheroids

MDA-MB-231 tumour cells were seeded at  $5 \times 10^6$  for 11 days in ultralow attachment plates. **A.** Phase contrast image of tumour spheroid in well. Scale bar 100  $\mu\text{m}$ . **B.** Scanning electron microscopy image of a tumour spheroid. Scale bar 100  $\mu\text{m}$ . **C.** Toluidine blue stained section of a 3D tumour spheroid with viable margin (black arrow head) and suspected necrotic core (red arrow heads). Scale bar 100  $\mu\text{m}$ . **D.** High magnification transmission electron microscopy image of the necrotic core of an uninfected tumour spheroid. Scale bar 1  $\mu\text{m}$ .

### 6.2.2 Invasion and biofilm forming capacities of VNP20009 with tumour spheroids

A further step to validate the *in vitro* tumour model for the purposes of bactofection was to verify *S. Typhimurium* could invade tumour cells and penetrate the tumour spheroid as *in vivo*. To do this, tumour spheroids were co-incubated with another cancer therapy *S. Typhimurium* strain VNP20009 (Low *et al.*, 1999) at an approximate multiplicity of infection of 100:1 for 48 hours. After one hour of co-incubation, cultures were treated with gentamycin to kill extracellular bacteria. At 48 hours post infection (hpi), viable bacteria were recovered from the tumour spheroid (Figure 6.2A). From immunofluorescence staining of tumour spheroid slices of tumours infected with VNP20009 carrying pCP25, a prokaryotic GFP-reporter plasmid to enable bacterial visualisation, it was clear that there were bacteria penetrating the outer margin of the tumour up to 150  $\mu\text{m}$  from the periphery (Figure 6.2B, left panel). As a control, wild type VNP20009 infected tumours were also imaged (Figure 6.2B, right panel). However, in the absence of a eukaryotic cell marker, it was not possible to discriminate intracellular bacteria from bacteria present in the interstitial space. Subsequent SEM analysis demonstrated that VNP20009 was capable of invasion of the tumour cells, but the majority localized to the interstitial space (Figure 6.2C, D).

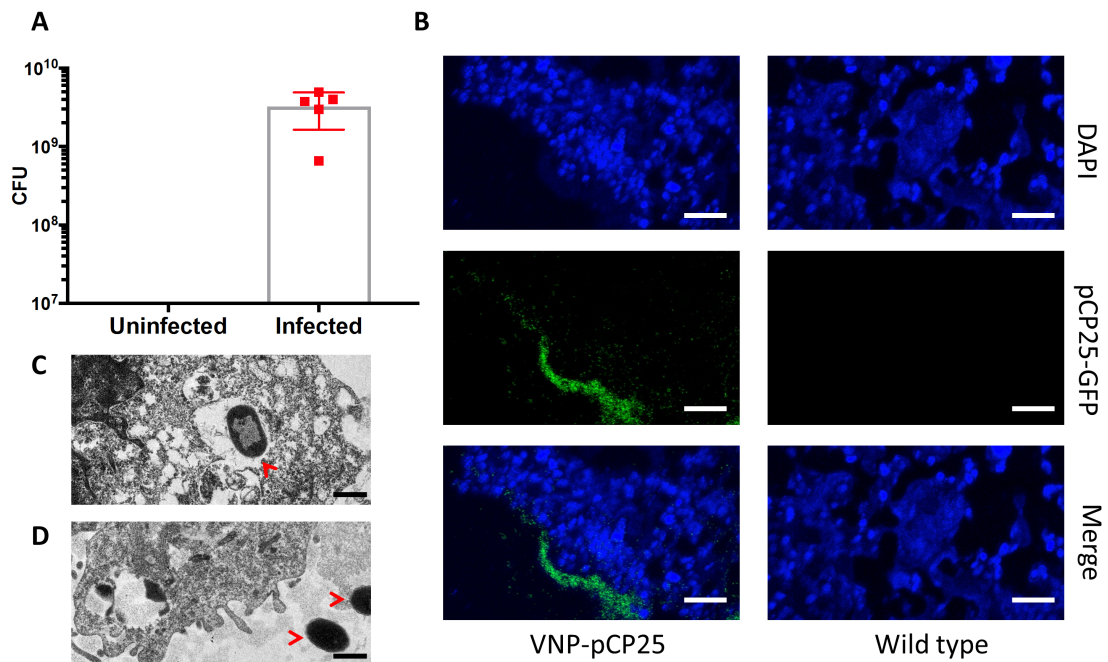


**Figure 6.2 VNP20009 invasion of tumour spheroids**

Tumour spheroids were co-incubated with VNP20009 at an MOI of 100:1 for 48 hours. **A.** Colony forming unit (CFU) counts from MDA-MB-231 tumour spheroids, infected with VNP-pCP25, or uninfected. **B.** Confocal microscopy images of tumour spheroid slices which were infected with either the VNP-pCP25 or wild type VNP20009. Scale bar 50  $\mu\text{m}$ . **C.** Transmission electron microscopy (TEM) image of tumour spheroid slice with VNP20009 localised intracellularly (red arrow; scale bar 1  $\mu\text{m}$ ) **D.** TEM image of tumour spheroid slice with VNP20009 located extracellularly (red arrow, scale bar 1  $\mu\text{m}$ ). Error bars SEM.

From the immunofluorescence images, it appeared as if VNP20009 was forming biofilms on the surface of the tumour, which has also been reported *in vivo* (Crull *et al.*, 2011a). TEM imaging confirmed the presence of an extensive biofilm network on the surface of the tumour spheroid (Figure 6.3). Taken together, these data suggest that *S. Typhimurium* infection in the *in vitro* tumour spheroids model resembles *in vivo* tumour invasion, thus meriting the use of the model for bactofection studies.

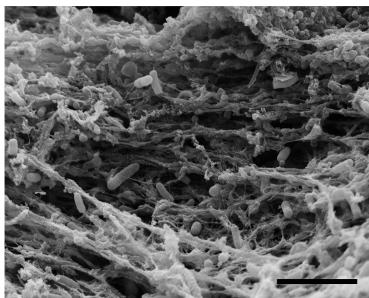


**Figure 6.3 VNP20009 biofilm formation on tumour spheroids**

Tumour spheroids were co-incubated with VNP20009 at an MOI of 100:1 for 48 hours. Scanning electron microscopy image of VNP20009 in a biofilm on the surface of an infected tumour spheroid (scale bar 5  $\mu\text{m}$ ).

### 6.2.3 Selection of VNP20009 through serial reisolations to increase tumour invasion capacity *in vitro*

In order to maximize the potential of the therapeutic effects of *S. Typhimurium*, it was sought to increase the invasion ability of VNP20009 in the *in vitro* models. From the SEM images, it appeared that many of the bacteria resided within the interstitial space. It has been speculated that cellular invasion is a prerequisite for bactofection to take place (Weiss, 2003), so it was pertinent to maximize the cellular invasion capacity of the bacteria in the present study. A previous study demonstrated that the re-isolation of the cancer therapy strain A1 from an *in vivo* tumour resulted in the re-isolated strain, A1-R, exhibited greater tumour-specific localization as well as therapeutic effect than the original A1 strain (Zhao *et al.*, 2006). This principle was applied to the *in vitro* culture by developing a serial screening process to isolate highly infective, intracellular VNP20009. This was achieved by infecting standard monolayer cultures of MDA-MB-231 with the parent stock of VNP20009, followed by reisolating viable bacteria 24 hpi. These reisolated colonies were subsequently used to infect another monolayer. Following multiple reisolations of a given strain, each reisolated strain (Once, Twice, Thrice) was used to infect tumour spheroids at an MOI of 100:1 for 24 hours, with a colony from the parental stock as a baseline control (Zero). It was hypothesized that enriching for highly infective bacteria in the population would lead to greater tumour spheroid infection. For the monolayer-reisolated colonies, there appeared to be a gradual increase in the infection capabilities of the more highly reisolated strains, but this was not statistically significant (Figure 6.4A). With the tumour spheroid-reisolated strain, however, there was a significant increase in the infection competence of the once reisolated colony compared to the parent stock (Figure 6.4B). Therefore, this highly infective strain was used for subsequent experiments.

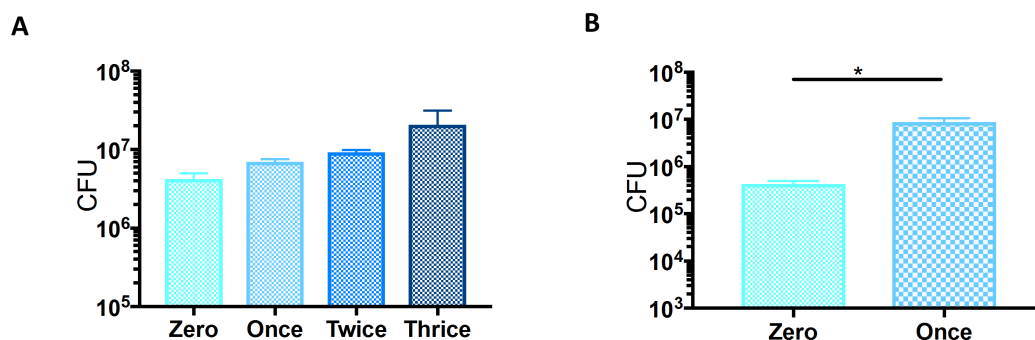


**Figure 6.4 Serial reisolation of infective VNP20009 colonies to increase cumulative infective capacity**

VNP20009 was serially reisolated from 2D monolayer or 3D tumour spheroid *in vitro* cultures before infecting tumor spheroids at equal MOIs for 24 hours. **A.** Colony forming unit (CFU) counts of VNP20009 harvested tumour spheroids infected with the parent stock (Zero), and colonies reisolated from monolayers for Once, Twice and Thrice isolated. **B.** CFU counts of VNP20009 harvested from tumour spheroids from the parent stock (Zero) and colonies reisolated from tumour spheroid (Once). Error bars SEM. Statistical analyses performed using a One Way Anova (A) or a Student's t test (B) where  $p < 0.05^*$ .

### 6.2.4 Bactofection capacities of *S. Typhimurium*-pEGFP

In order to assess if VNP20009 was capable of mediating bactofection, VNP20009 was transformed with a eukaryotic reporter plasmid, pEGFP, which encodes *EGFP* under a eukaryotic promoter, cytomegalovirus (CMV) (Michael *et al.*, 2004). The transcription of the *EGFP* gene is restricted to eukaryotic cells, so the GFP signal should only be evident following bactofection. This protocol was developed during my Masters of Research degree in Dr Wall's group. During the course of the Master's project, many parameters for this protocol were optimised such as infectious dose, density of cells prior to infection, length of incubation etc.

For the present study, cells were infected for 24 hours with VNP20009-pEGFP, with wild type VNP20009 infection serving as a negative control for GFP production in the eukaryotic cells. As a positive control, cell cultures were transfected with pEGFP using Lipofectamine® R 2000. A subpopulation of the cells expressed *EGFP* with GFP signal detected in the cytoplasm (Figure 6.5A). GFP signal was not detected in wild type VNP20009-infected cells as expected (Figure 6.5B), but there was also no clear GFP signal in cells infected with VNP20009-pEGFP (Figure 6.5C). This was also the result when cells were infected with SL7207-pEGFP (Figure 6.5D).

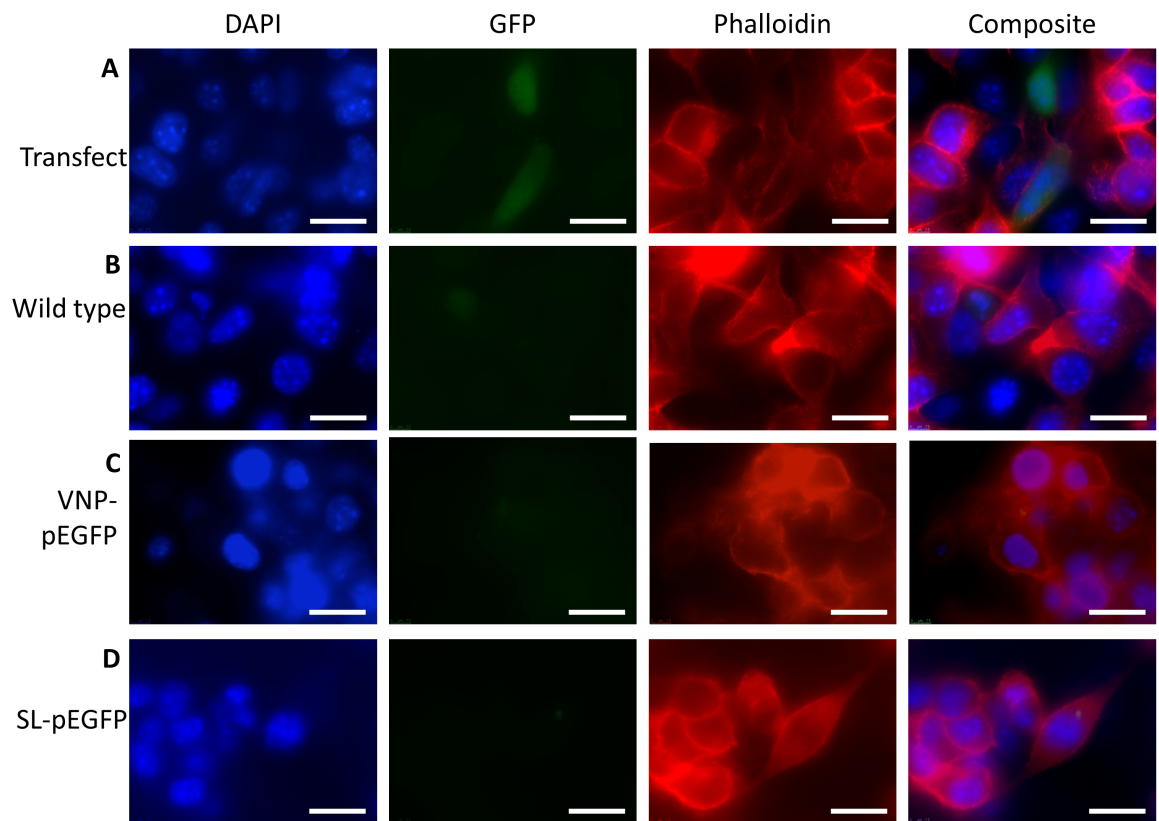


**Figure 6.5 Bactofection capacity of *S. Typhimurium*-pEGFP**

Tumour spheroid cells were co-incubated with *S. Typhimurium* transformed with pEGFP, or wild type at an MOI of 100:1. **A.** Confocal microscopy images of tumour cells transfected with pEGFP for 24 hours as a positive control for GFP production. **B.** Wild-type VNP20009-infected tumour cells. **C.** VNP20009-pEGFP (VNP-pEGFP) infected tumour cells. **D.** SL7207-pEGFP (SL-pEGFP)-infected tumour cells. Scale bars 20  $\mu\text{m}$ .

However, it was possible that the GFP fluorescence was below the threshold of detection on the fluorescence microscope, so cell cultures were infected as above, lysed and subjected to immunoblot analysis for the GFP protein. At this point of the study, the focus was switched to SL7207 as this had been demonstrated to be highly competent of eukaryotic DNA delivery to eukaryotic systems (Berger *et al.*, 2013). The immunoblot analysis again demonstrated that there was no GFP present in the cells infected with SL7207-pEGFP (Figure 6.6A). To control for the possibility that the pEGFP was negatively affecting the bacteria, another reporter plasmid system was employed: a eukaryotic expression plasmid encoding luciferase (Darji *et al.*, 1997) which can be detected using the IVIS. This plasmid is very similar to the pEGFP plasmid except it has *luciferase* in place of *EGFP* and an ampicillin resistance cassette in place of kanamycin. The infection protocol of tumour cells was similar to the pEGFP infection protocol outlined above, except cultures were analysed on the IVIS for

bioluminescence signal (Figure 6.6B, C). The transfected sample exhibited a high bioluminescent signal whereas tumour cells infected with SL7207-pLuc did not have any.

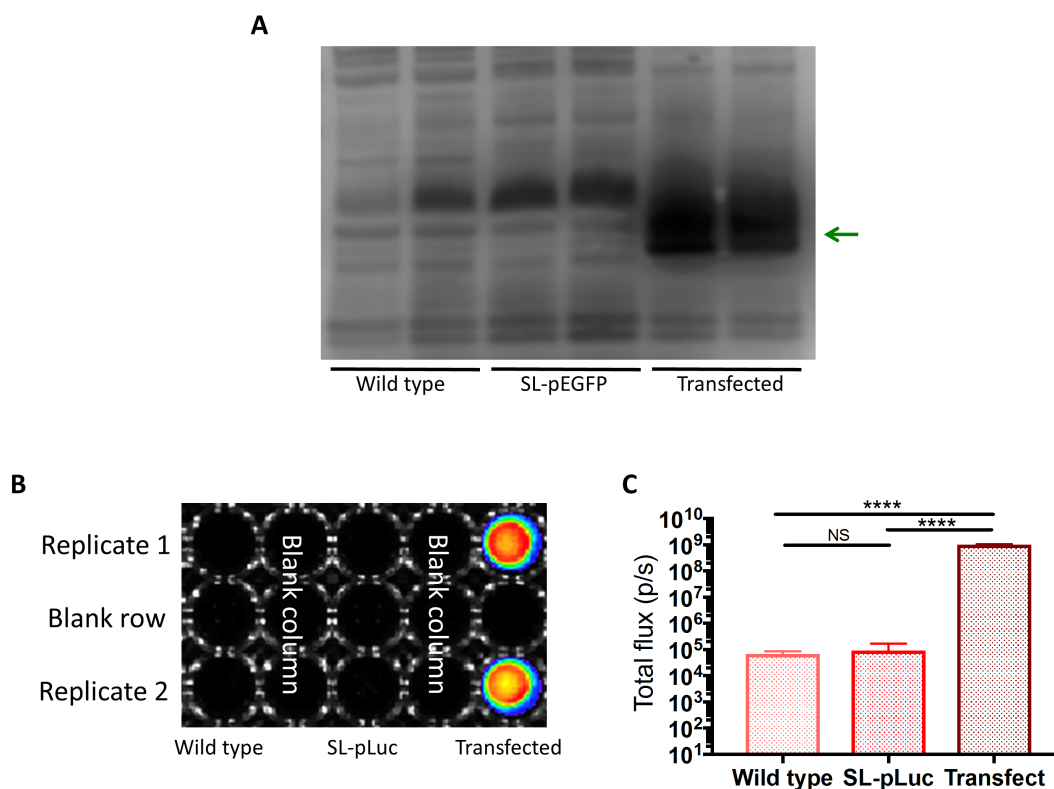


**Figure 6.6 Bactofection capacity of SL7207-pEGFP and SL7207-pLuc**

MDA-MB-231 cells were coincubated with SL-pEGFP or SL-pLuc for 24 hours at an MOI of 100:1. **A.** Immunoblot analysis of wild type SL7207 and SL7207-pEGFP (SL-pEGFP) for GFP protein in tumour cell lysates with pEGFP-transfected tumour cells as a positive control for GFP. Green arrow indicates GFP band. **B.** Bioluminescent signal from wild type SL7207, SL7207-pLuc (SL-pLuc) and pLuc-transfected tumour cells as a positive control for bioluminescence. **C.** Quantification of the bioluminescent signal from the samples in (B). Error bars SEM. Statistical analyses performed using a One Way Anova where  $p < 0.05^*$ ,  $p < 0.01^{**}$ ,  $p < 0.001^{***}$ ,  $p < 0.0001^{****}$ .

### 6.2.5 Morphological characterisation of *S. Typhimurium* transformed with pEGFP

Bactofection into multiple tissues has been reported, which was frustrating for the current study in which neither VNP2009 nor SL7207 were able to replicate the data produced in these reports (Ahmad *et al.*, 2011; Berger *et al.*, 2013; Darji *et al.*, 1997). The absence of bactofection warranted greater investigation into the phenotype of the pEGFP-transformed bacteria. High magnification light microscopy of Gram stained SL7207-pEGFP demonstrated that these cultures displayed a filamentous phenotype compared to the untransformed, wild type cultures (Figure 6.7A). Quantification of the cell lengths of the bacteria revealed that the mean cell length of SL7207-pEGFP was significantly greater than the

wild type cultures (Figure 6.7B). Interestingly, only some of the cells of the culture displayed a filamentous phenotype, which was defined as a cell length of more than 6  $\mu\text{m}$  (Humphrey *et al.*, 2011). The proportion of cells in a transformed culture which was filamentous was 39.58% ( $\pm 10.82\%$ ), whereas there was less than 0.01% of untransformed cells which were filamentous (Figure 6.7C).

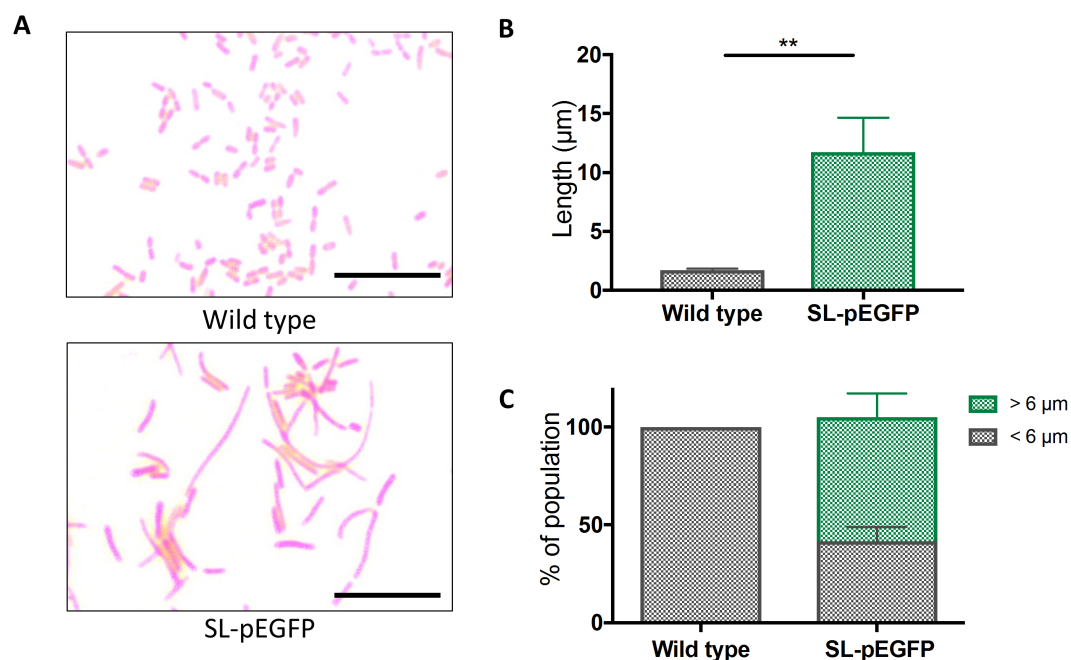


#### Figure 6.7 Morphology of SL7207-pEGFP

Wild type SL7207 and SL-pEGFP were grown in culture to mid-log phase and subject to Gram staining and light microscopy. **A.** Representative light microscopy images of Gram stained SL7207 cultures, wild type and SL-pEGFP. Scale bars 10  $\mu\text{m}$ . **B.** The mean length of individual SL7207 bacteria, wild type and -pEGFP. **C.** Quantification of the proportion of SL7207 in culture which were filamentous ( $> 6 \mu\text{m}$ ) for wild type and -pEGFP. Error bars SEM. Statistical analyses performed using a Students t test where  $p < 0.05^*$ ,  $p < 0.01^{**}$ .

The filamentous phenotype induced by the transformation of pEGFP into *S. Typhimurium* was not restricted to SL7207, but multiple *S. Typhimurium* strains tested also displayed filamentous phenotypes following transformation with pEGFP such as the original preferred strain, VNP20009 (Figure 6.8A, B) and the common lab strain LT2 (Figure 6.8C, D). The differences between pEGFP-transformed *S. Typhimurium* strains and their wild type counterparts were comparable to that seen with the SL7207 cultures.

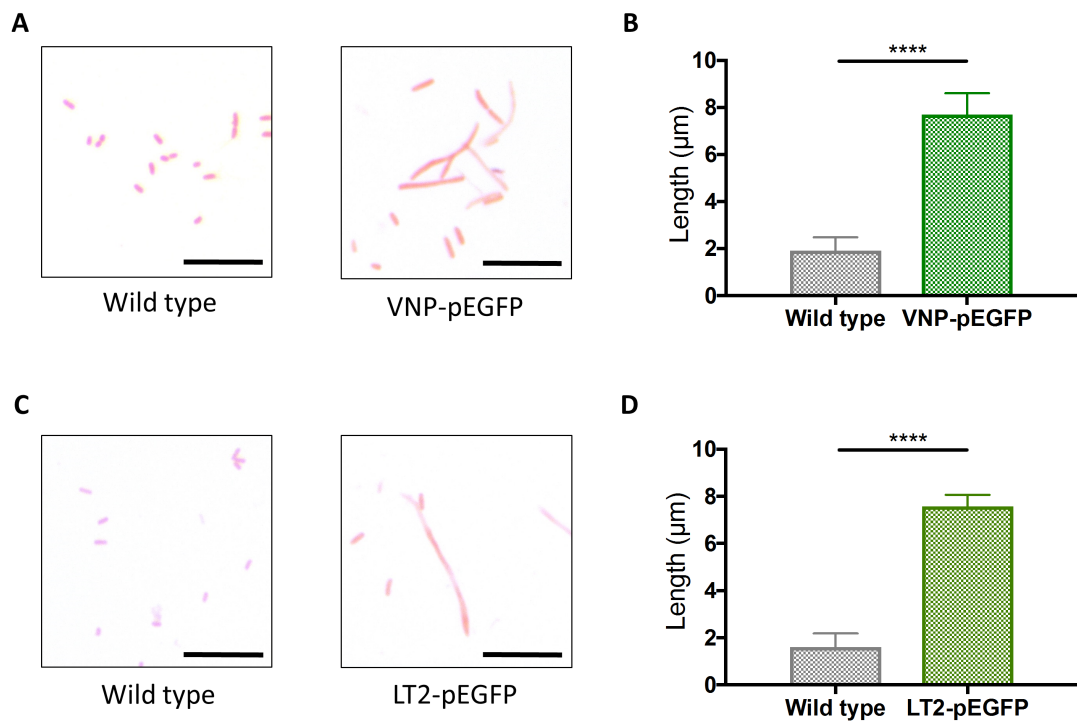


**Figure 6.8 Morphology of other *S. Typhimurium* strains transformed with pEGFP**

VNP2009 and LT2 strains were transformed with pEGFP and subject to analysis as in Figure 6.7. **A.** Representative light microscopy images of Gram stained VNP2009, wild type and transformed with pEGFP (VNP-pEGFP). **B.** Quantification of the mean cell lengths of cultures represented in (A). **C.** Representative light microscopy images of Gram stained LT2, wild type and transformed with pEGFP (LT2-pEGFP). **D.** Quantification of the mean cell lengths of cultures represented in (C). Scale bars 10 μm. Error bars SEM. Statistical analyses performed using a Students t test where  $p < 0.05^*$ ,  $p < 0.01^{**}$ ,  $p < 0.001^{***}$ ,  $p < 0.0001^{****}$ .

### 6.2.6 Effects of pEGFP transformation on *E. coli* strains

It was questioned whether this was a *S. Typhimurium*-specific phenomenon. To investigate this, *E. coli* strains were transformed with pEGFP and the mean cell lengths were compared to untransformed, wild type cultures as before. Although there was a slight increase in the average mean cell lengths of the transformed cultures, there was no statistically significant difference between pEGFP-transformed cultures and non-transformed wild-type cultures for K12 (Figure 6.9A, B;  $p = 0.2269$ ), F18 (Figure 6.9C, D;  $p = 0.2070$ ) or LF82 (Figure 6.9 E, F;  $p = 0.2715$ ) (Figure 6.9). This data suggested that pEGFP-induced filamentation was *S. Typhimurium*-specific.

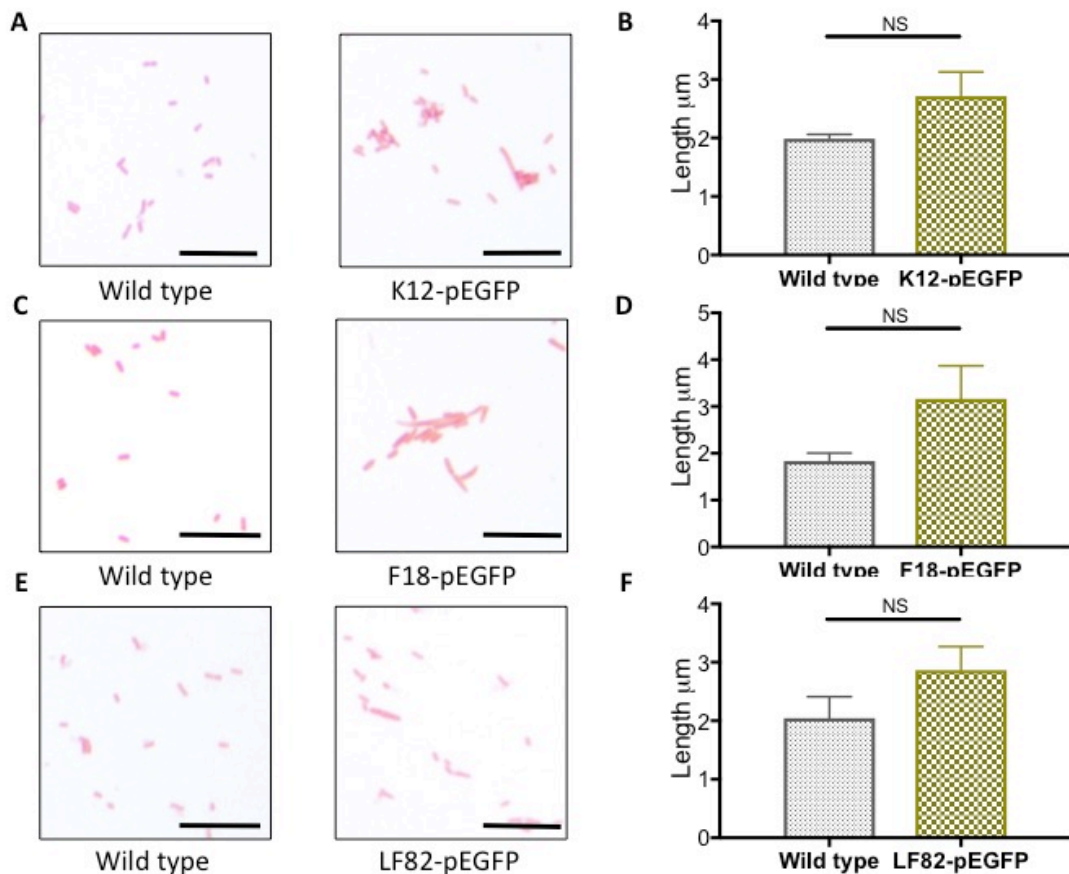


**Figure 6.9 Morphology of *E. coli* strains transformed with pEGFP**

Multiple *E. coli* strains were transformed with pEGFP and subject to analysis as in 6.7. **A.** Representative light microscopy images of Gram stained K12, wild type and transformed with pEGFP (K12-pEGFP). **B.** Quantification of the mean cell lengths of cultures represented in (A). **C.** Representative light microscopy images of Gram stained F18, wild type and transformed with pEGFP (F18-pEGFP). **D.** Quantification of the mean cell lengths of cultures represented in (C). **E.** Representative light microscopy images of Gram stained LF82, wild type and transformed with pEGFP (LF82-pEGFP). **F.** Quantification of the mean cell lengths of cultures represented in (E). Scale bars 10 μm Error bars SEM. Statistical analyses performed using a Student's *t* test where  $p < 0.05^*$ .

There was a great degree of variation in the cell lengths of individuals within a given SL7207-pEGFP culture samples. This was evidenced by the large spread in the standard deviation values of the mean cell lengths in SL-pEGFP cultures (Figure 6.10A). The high standard deviation values and the spread were not present in wild type, untransformed cultures. The cell size variation within a culture was also apparent in the distribution of individual cells between different cell size categories for SL7207-pEGFP but not for wild type SL7207 (Figure 6.10B). The degree of variation was a concern as it highlighted the difficulty in controlling for the proportion of cells in the culture which were filamentous. This could prove challenging in a given experimental setting if there were phenotypic changes associated with the filamentous cultures.

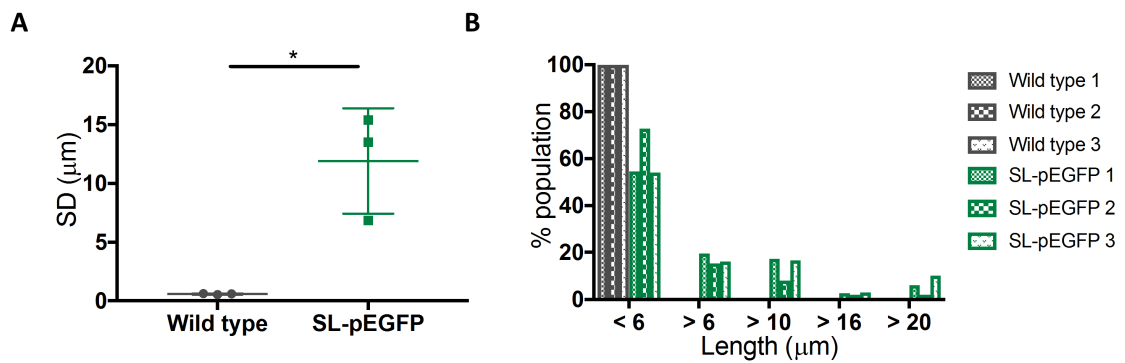


**Figure 6.10 Variability in cell length of SL-pEGFP compared to wild type**

The mean cell length data from wild type and SL-pEGFP cultures were compared for differences in standard deviation and size distribution. **A.** Standard deviations of cell length in individual experiments for wild type and SL-pEGFP cultures. **B.** Distribution of wild type and SL-pEGFP cultures between multiple size categories. Statistical analysis was performed using a Student's *t* test where  $p < 0.05^*$ .

### 6.2.7 Effects of filamentation on growth and invasion of SL-pEGFP

In order to assess the effects that pEGFP-induced filamentation had on the behaviour of *S. Typhimurium*, multiple phenotypic characteristics of SL7207 transformed with pEGFP were compared to wild type. SL7207-pEGFP displayed slowed cell growth *in vitro* compared to wild type (Figure 6.11A). Furthermore, SL7207-pEGFP had decreased *in vitro* intracellular replication when invading MDA-MB-231 cells, compared to wild type (Figure 6.11B) as well as a decreased capacity to invade cancer cells (Figure 6.11C).

The decreased infection capacity of SL7207-pEGFP was further investigated by investigating the degree of SPI-1 activation in these cells compared to control. SPI-1 activation is critical for mediating invasion of eukaryotic epithelial cells, and *prgH* encodes a type III needle apparatus protein required for this process. JH3010 is a derivative of *S. Typhimurium* strain SL1344 (the ancestral strain of SL7207), with a *Salmonella* pathogenicity island-1 (SPI-1) green fluorescent reporter (*prgH-gfp*<sup>+</sup>) (Hautefort *et al.*, 2003). These cells fluoresce green when *prgH* is switched on and the cells are capable of invading epithelial cells. This therefore acts as a surrogate readout for SPI-1 activation. SL1344-pEGFP was used as a negative control for green fluorescent signal to control for the possibility of bactofected GFP creating a background signal. It was found that JH3010-pEGFP had decreased *prgH-gfp* expression compared to wild type JH3010, as evidenced by a greater proportion of bacteria fluorescing green

(Figure 6.11D, E). Decreased SPI-1 expression may account for the attenuated invasion capacity of *S. Typhimurium*-pEGFP (Figure 6.11D, E). Note that the GFP signal in this experiment is from *prgH-gfp*, and not from the pEGFP eukaryotic expression plasmid.

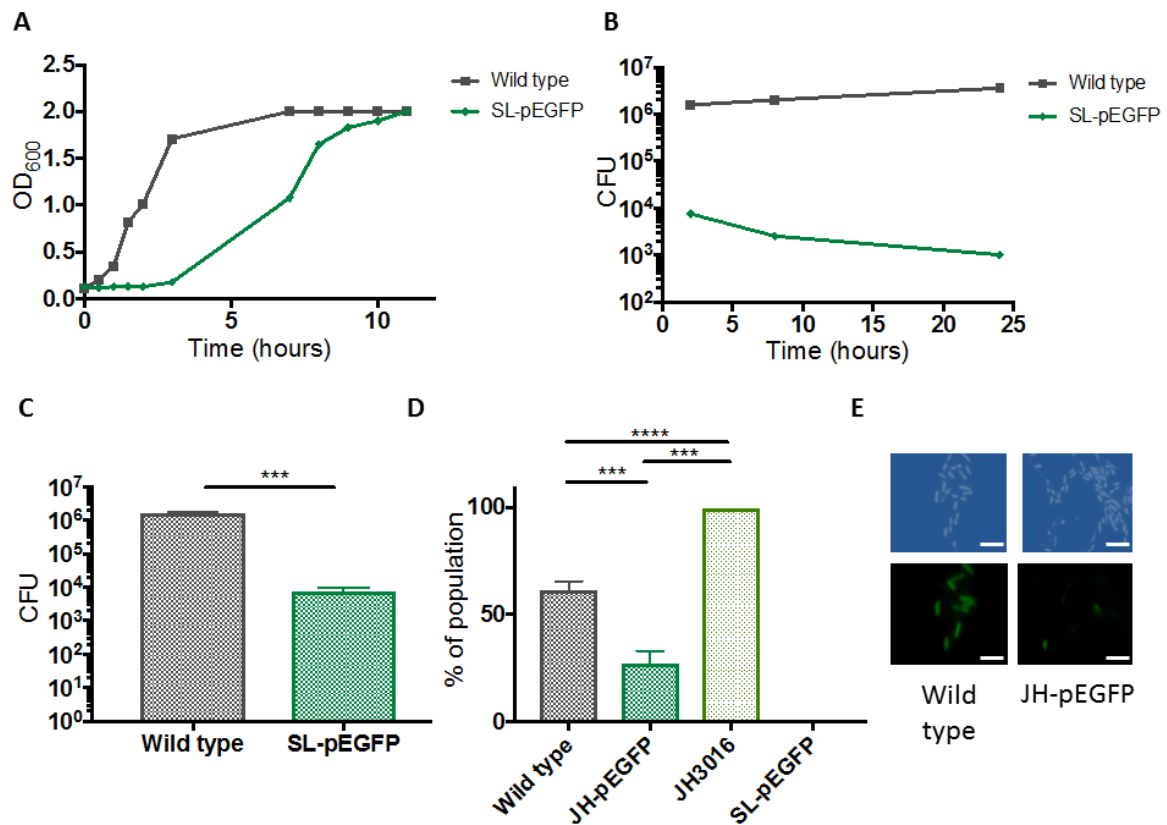


**Figure 6.11 Growth and invasion characteristics of SL-pEGFP**

Wild type and SL-pEGFP cultures were compared for multiple growth and invasion characteristics. **A.** Representative growth curves of wild-type and SL-pEGFP. **B.** Colony forming unit (CFU) counts of wild type and SL-pEGFP recovered from MDA-MB-231 cells at 2, 8 and 24 hours post infection. **C.** CFU counts of wild type and pEGFP-transformed SL7207 recovered from MDA-MB-231 2 hours post infection. **D.** Quantification of the proportion of bacteria in culture expressing SPI-1 at mid-log phase using a SPI-1 reporter SL1344 strain, JH3010. JH3016 served as a positive control as it is a constitutively expressing GFP strain. SL-pEGFP served as a negative control for GFP expression. **E.** Representative images of JH3010 wildtype and transformed with pEGFP (JH-pEGFP). Top row are DAPI-stained images pseudocoloured to aid visualization. Bottom row shows green fluorescence is from *prgH-gfp* expression. Scale bars 5 μm. Error bars SEM. Statistical analyses performed using a Student's t test (C) or One Way Anova (D) where  $p < 0.05^*$ ,  $p < 0.01^{**}$ ,  $p < 0.001^{***}$ ,  $p < 0.0001^{****}$ .

## 6.2.8 Stress responses induced in pEGFP-transformed *S. Typhimurium* cultures

As filamentation has been associated with cell stress, it was investigated which stress response, if any, was upregulated in the filamentous cultures (Humphrey *et al.*, 2011; Mattick *et al.*, 2000; Stackhouse *et al.*, 2012). Both the general stress response and the SOS DNA damage stress response have been investigated

in filamentation studies. RpoS, the ribosomal sigma factor whose upregulation is indicative of general stress response activation, was found to be unchanged in expression levels between multiple pEGFP-transformed *S. Typhimurium* strains and wild type (Figure 6.12A). However, the SOS stress response protein, RecA was seen to be upregulated in SL7207 cultures transformed with pEGFP, suggesting that the SOS response is increased in SL7207-pEGFP cultures (Figure 6.12B).

The induction of the SOS response inhibits septation of replicating bacteria (Justice *et al.*, 2008; Justice *et al.*, 2000). This phenotype was investigated in the filamentous cultures by staining fixed cultures with the nuclear stain DAPI. Fluorescence microscopy images of filamentous bacteria demonstrated multiple nuclei aligned along a filamentous bacterium, which was not evident in the wild type cultures. This data further suggested a role for the SOS response in the SL-pEGFP cultures, which may be driving the filamentous phenotype (Figure 6.12C).

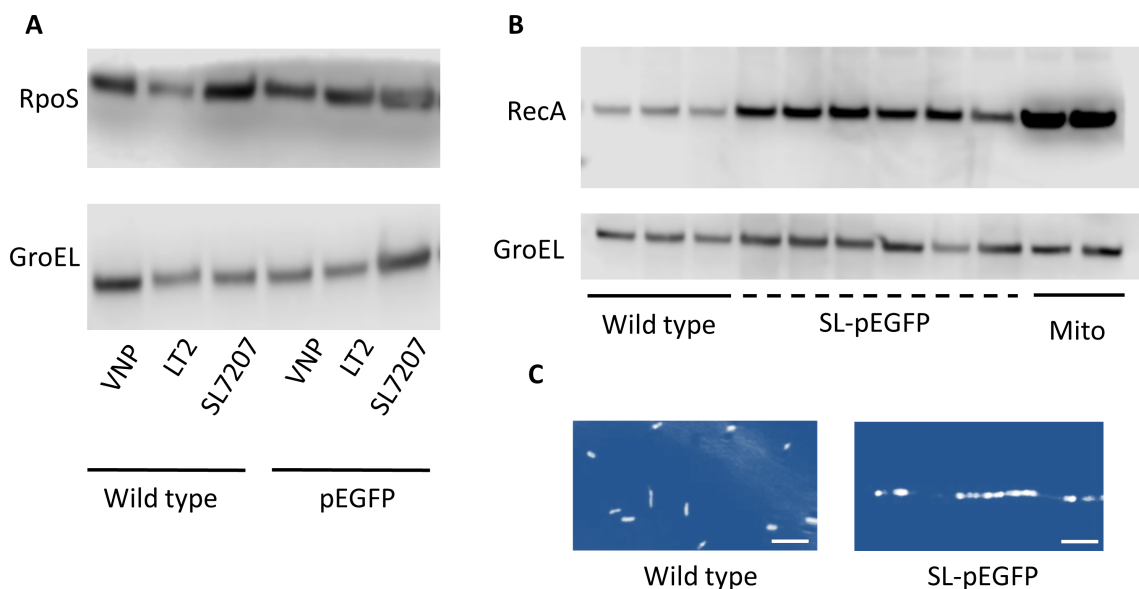


**Figure 6.12 Stress response activation in *S. Typhimurium*-pEGFP**

Cultures were grown to mid-log phase and harvested for western blot analysis for stress response proteins or immunofluorescence staining. **A.** Immunoblot analysis for RpoS, of different *S. Typhimurium* strains, wild type or transformed with pEGFP. GroEL served as a loading control. **B.** Immunoblot analysis for RecA, of multiple wildtype of pEGFP-transformed SL7207 colonies with Mitomycin C-treated (Mito) untransformed cultures serving as a positive control for RecA production. **C.** Representative DAPI-stained wild type and SL-pEGFP cultures. Images were pseudo-coloured to aid visualization of segmented phenotype of SL-pEGFP. Scale bars 5  $\mu$ m.

### 6.2.9 The contribution of the *f1 ori* in pEGFP to the filamentous phenotype of SL-pEGFP

As multiple *S. Typhimurium* strains were induced to become filamentous when transformed with pEGFP, it was hypothesized that there was a feature of pEGFP which was responsible for inducing the filamentous phenotype (Figure 6.13A). The SOS response is triggered in *S. Typhimurium* in response to the presence of single stranded DNA (ssDNA) in the bacterium. Investigation of the pEGFP plasmid revealed that the filamentous phage 1 origin of replication (*f1 ori*), a phagemid capable of phage-directed ssDNA production (Russel & Model, 1989). Furthermore, other phages have been reported to induce the SOS response in *Salmonella enterica* (Campoy *et al.*, 2006). Therefore, it was hypothesized that the *f1 ori* may be responsible for inducing the filamentous phenotype in *S. Typhimurium*-pEGFP. To test this hypothesis, the *f1 ori* sequence in pEGFP was replaced with *lacZ* from pUC19 to give rise to pEGFPLacZ, which no longer contained the *f1 ori* but contains the functional elements to enable bactofection. This plasmid was then transformed into SL7207 and the morphology of the bacteria was assessed. Light microscopy imaging of Gram stained SL7207-pEGFPLacZ demonstrated that this plasmid did not induce a filamentous phenotype in the bacteria (Figure 6.13B, bottom panel). The mean cell lengths of the wild type and SL-pEGFPLacZ cultures were not significantly different from each other, but both were significantly different from the mean cell length of SL-pEGFP cultures (Figure 6.13C). This data suggested that the *f1 ori* was responsible for inducing the filamentous phenotype in the *S. Typhimurium* cultures.

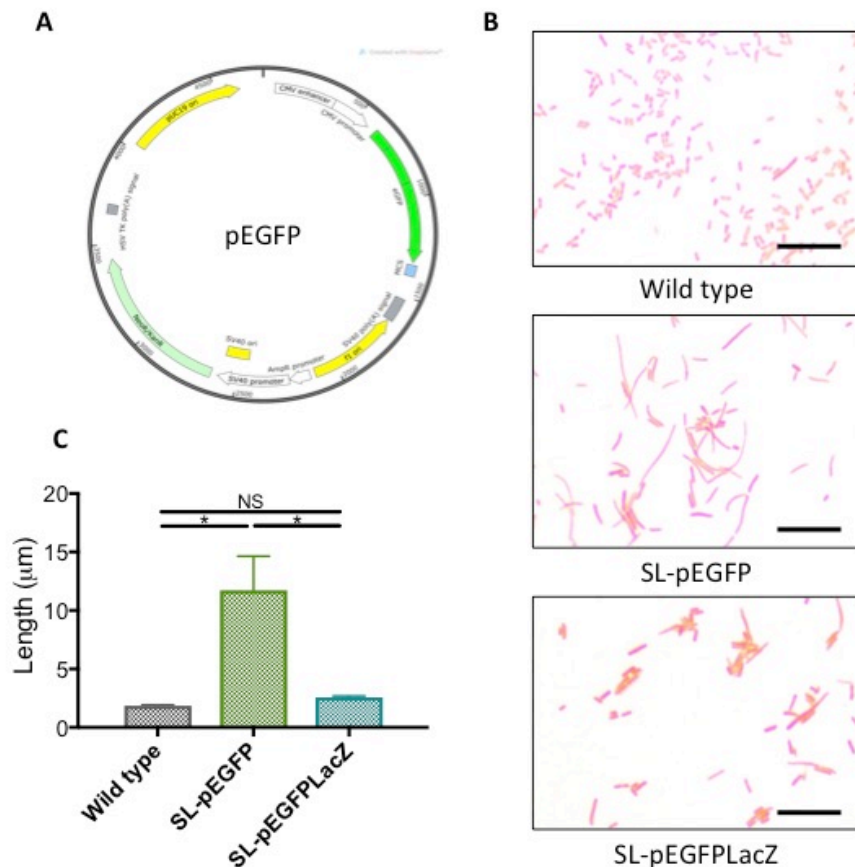


**Figure 6.13 Effect of the removal of f1 from pEGFP on cell length with resultant plasmid, pEGFPΔLacZ**

Cultures were transformed with the indicated plasmid, grown to mid log phase and Gram stained. **A.** Plasmid map of pEGFP. **B.** Representative light microscopy images of Gram stained SL7207, wild type, or transformed with pEGFP or pEGFPΔLacZ. **C.** Quantification of the mean cell lengths of the cultures in (B). Scale bars 10 μm. Statistical analysis was performed using a One Way ANOVA with  $p < 0.05^*$ .

However, other features of the plasmid were also investigated to ensure that the f1 ori was the only feature driving filamentation. Three additional features were examined: the EGFP transgene, the plasmid ori and the antibiotic resistance cassette.

There has been a report which suggested that there were prokaryotic promoters and promoter elements located within the CMV promoter (Goussard *et al.*, 2003). Therefore it was possible that the bacteria transformed with pEGFP were producing the EGFP protein, which could be inducing stress. To investigate this, fluorescence readings of *S. Typhimurium* strains transformed with pEGFP were taken, with wild type VNP20009 and VNP20009 transformed with a prokaryotic GFP reporter plasmid, *rpsM*-GFP, serving as negative and positive controls for GFP signal respectively (Figure 6.14A). According to this data, the levels of GFP fluorescence in transformed cultures was no different to untransformed, wild

type VNP2009, suggesting there was no GFP protein produced in the bacteria. To definitively rule out the possibility that the transgene may be having a filamentation-inducing effect on the bacteria, the portion of the pEGFP plasmid containing the CMV promoter and the *EGFP* transgene was cloned into the pACYC184 backbone, which itself does not drive filamentation in *S. Typhimurium* cultures. When this plasmid, pACYC-EGFP, was transformed into SL7207, the bacteria did not display a filamentous phenotype, further providing evidence that the transgene was not driving the filamentous phenotype (Figure 6.14B). In fact, the mean length of the cultures transformed with pACYC-EGFP were not significantly different from wild type SL7207 (Figure 6.14C).

pEGFP has a high copy number origin of replication, pUC19 *ori*, so it was questioned if a high copy number plasmid might lend to stress, as discussed in the literature (Wegrzyn & Wegrzyn, 2002). However, transformation of SL7207 with a commercially available pUC19 plasmid failed to induce a filamentous phenotype compared to the wild type control (Figure 6.14.B). The mean cell length of SL-pUC19 was not significantly different from wild type SL7207 (Figure 6.14C).

The choice of antibiotic resistance cassette has also been associated with inducing a filamentous phenotype in *S. Typhimurium* (Clark *et al.*, 2009). To investigate the possibility that the kanamycin cassette was playing a role in mediating the filamentous phenotype, a similar plasmid to pEGFP, pLuc was employed. This plasmid has an ampicillin cassette but also differs from pEGFP in its transgene, which is the *luciferase* gene. It has already been demonstrated that the *EGFP* transgene was not responsible for inducing the filamentous phenotype observed in the *S. Typhimurium* cultures, so there was confidence that the pLuc plasmid could isolate the possible effects of the antibiotic resistance cassette on filamentation. pLuc was transformed into SL7207 and light microscopy was employed to investigate the morphology of SL7207-pLuc. The presence of this plasmid was sufficient to induce filamentation similar to pEGFP, suggesting that the kanamycin cassette in pEGFP was not driving the filamentous phenotype. Of course, it was possible that luciferase was inducing filamentation, but this would not explain the filamentous phenotype in pEGFP-transformed cultures.

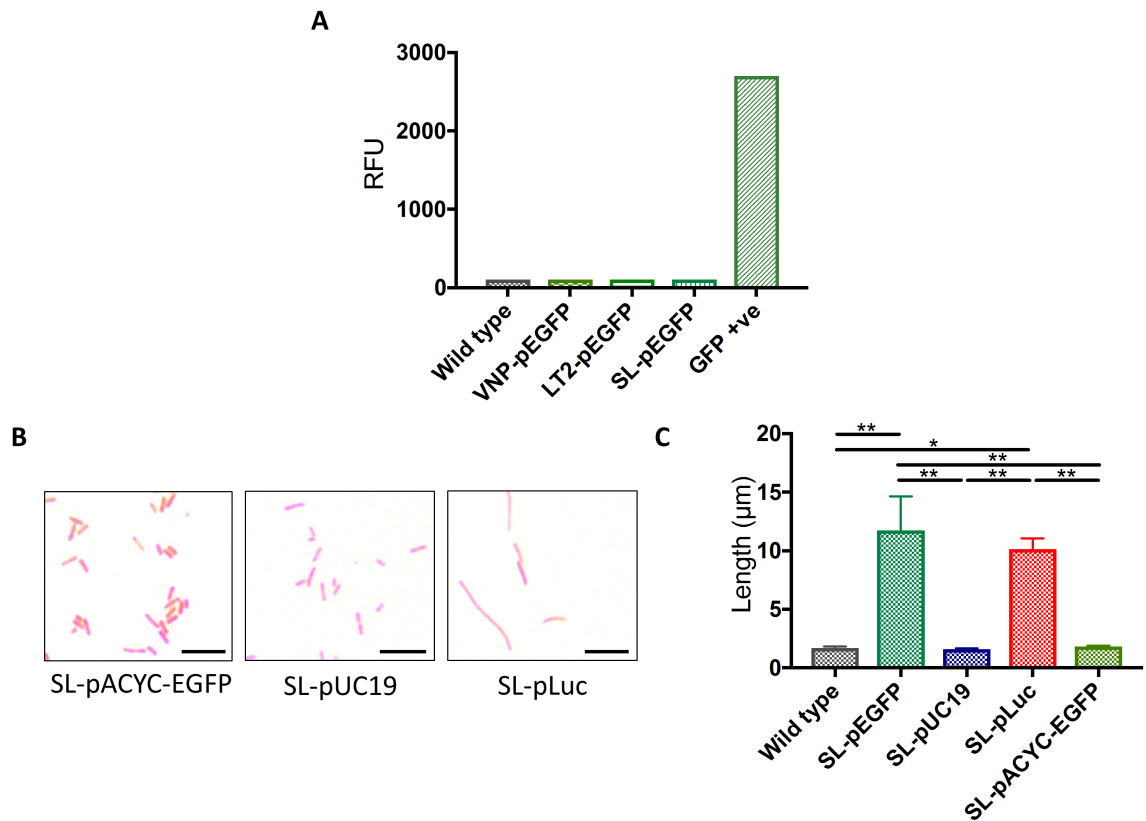


**Figure 6.14 Effects of other plasmid features on the pEGFP-induced filamentous phenotype**  
 Multiple features of pEGFP were investigated for their ability to induce filamentation in pEGFP-transformed *S. Typhimurium*. **A.** Relative fluorescence units (RFU) readings of *S. Typhimurium* cultures transformed with pEGFP. Wild type VNP20009 served as a negative control for GFP signal and SL7207-rpsmGFP served as a positive control (GFP +ve). **B.** Representative light microscopy images of Gram stained SL7207, transformed with pACYC-EGFP, pUC19 or pLuc. **C.** Quantification of the mean cell lengths of the cultures in plus wild type SL7207 and SL-pEGFP. Scale bars 10 µm. Statistical analysis was performed using a One Way ANOVA with  $p < 0.05^*$ ,  $p < 0.01^{**}$ ,  $P < 0.001^{***}$ ,  $p < 0.0001^{****}$ .

## 6.3 Discussion

The use of bacteria as a vehicle for gene delivery is an ever-growing field, with the number of publications pertaining to this topic increasing, with *Salmonella* as a delivery vector driving this upward trend (Forbes, 2010). The utilization of bacteria to deliver genetic material to eukaryotic systems has been demonstrated *in vivo* in multiple pathologies including cystic fibrosis and cancer. Of all of the bacterial species reported in the literature, *Salmonella* is arguably the most studied and well characterized. *Salmonella* has been employed to deliver multiple eukaryotic genes to cancer cells *in vivo* including apoptosis-associated genes Smac and TNF- $\alpha$  related apoptosis inducing ligand (TRAIL) as well as for cytokine gene therapy in subcutaneous tumour mouse models (Fu *et al.*, 2008; Loeffler *et al.*, 2007; Yuhua *et al.*, 2001). However, before undertaking *in vivo* work, it was necessary to investigate the bactofection capacity of *S. Typhimurium in vitro*. Here, an *in vitro* tumour spheroid culture system which recapitulates many features of the *in vivo* tumour architecture was developed. It was determined that *S. Typhimurium* transformed with a eukaryotic expression plasmid, pEGFP, induced a filamentous phenotype and was associated with the induction of the bacterial SOS DNA damage response and as a consequence of the f1 *ori* present on the plasmid. This phenotype may explain why there was no detectable bactofection carried out in our culture system, contrary to published reports.

### 6.3.1 Why employ tumour spheroids for the preliminary *in vitro* study?

It is well known that bacteria behave differently in various environments. The tumour microenvironment is distinct from other non-tumorous tissues in the body with heterogeneous cell populations distributed throughout and gradients of nutrients present in distinct regions of the tumours. It has been demonstrated that within distinct regions, bacteria behave differently (Kasinskas & Forbes, 2006, 2007). Therefore, in designing the bactofection experiment, it was important to employ an *in vitro* system that best represented the dynamics of bacterial tumour invasion and behaviour *in vivo*. A three dimensional (3D) tumour spheroid system was employed, which had been reported to mimic the *in*

*vivo* environment with a necrotic core, nutrient gradients and an outer viable rim being some of the most prominent features (Freyer, 1988; Sutherland *et al.*, 1986). Of particular interest to us was the presence of the necrotic core has been demonstrated to be a region of hypoxia *in vitro* (Carlsson & Acker, 1998). *S. Typhimurium* is a facultative anaerobe, so it can survive in both oxygenated and hypoxic environments. This is an important consideration for downstream refinement of a bactofection protocol as limiting the production of the transgene to a tumour-specific location would allow for maximal anti-tumour result with minimal off-target effects. In the case of the hypoxic environment, this could be achieved with a hypoxia-associated promoter, such as the *pepT* promoter (Yu *et al.*, 2012). First, however, it would be important to determine whether the tumour spheroids contained hypoxic regions. This could have been achieved by immunofluorescence staining of tumour spheroid section using Hypoxyprobe<sup>TM</sup>-1 antibody as performed by Yu and colleagues. However, in light of the filamentous phenotype of the pEGFP-transformed bacteria, further experiments to characterise the tumour spheroids were abandoned to focus on elucidating the underlying mechanism of filamentation in the transformed cultures.

### **6.3.2 Why were there still VNP20009 cells on the surface of the tumour spheroid following gentamycin treatment, and why is this a concern?**

From the confocal microscopy images of VNP20009 infecting the tumour spheroids, it appeared that there was *S. Typhimurium* surrounding the tumour spheroid following gentamycin antibiotic treatment. This suggested that the bacteria were resistant to the antibiotic. Closer inspection with TEM confirmed the existence of a biofilm surrounding the tumour spheroid, which might account for the antibiotic resistant cells.

Biofilm formation on tumours by *S. Typhimurium* has been reported *in vivo*, which is interesting as *S. Typhimurium* is not normally associated with being a potent biofilm former (Crull *et al.*, 2011b). It would be interesting to generate mutant strains incapable of forming biofilms to see if this would abrogate the antibiotic-resistant cells, however this has been shown to reduce tumour colonisation (Crull *et al.*, 2011b). Although the bacteria may be beneficial for

tumour growth inhibition, antibiotic-resistant bacteria are a major safety concern, particularly in cancer patients who are often immunocompromised (Hübel *et al.*, 1999; Viscoli *et al.*, 2005). In a subsequent study, Crull and colleagues demonstrated that systemically administered bacteria in tumour-bearing mice were almost completely cleared from the liver, spleen and tumour 14 days post ciprofloxacin treatment (Crull & Weiss, 2011). However, it is difficult to be satisfied with this as the outcome in a clinical setting, as complete bacterial clearance was not achieved. Furthermore, there is the ever-present concern of antibiotic resistance, which was discussed in Chapter 3.

### **6.3.3 Why increase the tumour cell invasion potential of *S. Typhimurium*?**

At present, it is unknown if the anti-tumour effects of bacterial-mediated cancer therapy is primarily due to tumour-specific bacterial localization or to the systemic inflammation associated with intravenous bacterial administration. Numerous reports, although focused on other research questions, have inadvertently provided evidence for one phenomenon or the other (Binder *et al.*, 2013; Kocijancic *et al.*, 2017; Thornlow *et al.*, 2015; Zhao *et al.*, 2006). One such study has suggested that increased tumour specific bacterial localization improves the anti-tumour effects of the bacteria when administered systemically (Zhao *et al.*, 2006). This data points towards bacterial colonization of the tumour being an important factor for a successful bacterial cancer therapy.

In the present study, scanning electron microscopy demonstrated that bacteria which had penetrated the tumour spheroid were present both within the tumour cells, as well as in the interstitial space. From these images, it was observed that there was a greater proportion in the interstitial space. For bacteria to mediate bactofection, it is believed to be necessary to gain entry to the cytosol so as to transfer the plasmid to the eukaryotic cell (Weiss, 2003). Therefore, it was pertinent to increase the cell invasion capacity of the bacteria to maximize both colonization as well as bactofection rates. The aforementioned study by Zhao and colleagues intensified the tumour invasion capacity of the cancer therapy strain A1 by reisolating the bacteria from tumours in an *in vivo* tumour model, termed A1-R, therefore selecting the colonies most capable of tumour colonization (Zhao *et al.*, 2006). Herein, this phenomenon was recapitulated *in*

*vitro*, using both monolayers and tumour spheroid cultures as instruments to select for the most infective individuals in the population. Even after three serial reisolations, the colonies reisolated for a third time from the monolayers were not significantly more infective than the parent stock. The tumour spheroid reisolation process was more selective, as the colonies isolated for the first time were significantly more infective than the parent stock. However, with the knowledge of the biofilm formation ability of the VNP20009 on the surface of the tumour, this data must be interpreted with caution as it is possible that the selection process is actually selecting for biofilm formers, as opposed to bacteria more able to invade and penetrate the tumour.

It is interesting to speculate what may be accountable for the differences in infection ability between individuals in a population. Previous reports have demonstrated that only a proportion of *Salmonella* in a population activate SPI-1, even in SPI-1 priming conditions (Humphrey *et al.*, 2011). It is possible that the serial reisolation protocol was selecting SPI-1-expressing individuals in this category. However, as there was a linear relationship between the number of reisolations and the number of bacteria infecting the tumour spheroids, this suggests that there is a permanency in the features which enabled these bacteria to invade. This could be loss-of-function gene mutations in genes which should turn off SPI-1, or alternatively could be gain-of-function mutations which amplify or sustain SPI-1 activation. One report sequentially selected for hypermotile bacteria in a bacterial cultures subjected to *in vitro* swarm plate assay (Thornlow *et al.*, 2015). By doing so, they increased the cumulative swimming velocity of a given population within a tumour-on-chip *in vitro*. They also demonstrated that this phenotype was maintained for over 30 passages, suggesting that these bacteria have a genetic, or epigenetic advantage over their former colony colleagues. Therefore, it is possible that the changes in the cumulative invasion capacity of the bacteria reisolated in the present study are due to permanent changes pertaining to epigenetic or genetic factors. RNA sequencing, genomic sequencing and bisulfite sequencing analyses would help discriminate which factors are playing a role, but these technologies are expensive and were outside the remit of the present study.

Obtaining information pertaining to the factors dictating tumour-specific colonization would illuminate strategies that could further promote therapeutic effect. This is very much dependent on dissecting the contributions of systemic inflammation and bacterial localization in the tumour to the anti-tumour effects of the bacteria. It has been suggested that the requirement for bacterial tumour localization for anti-tumour efficacy is tumour type-specific (Kocijancic *et al.*, 2017). In the instances where bacterial localization is important to the anti-tumour effects, strategies such as the one described herein for increasing tumour cell invasion, may be critical for maximizing the potential of bacterial mediated tumour therapy.

#### **6.3.4 What is the relevance of the attenuated replication and invasion features of the filamentous cultures?**

In order to enable the bacteria to bactofect, they must first be transformed with a eukaryotic expression vector. For this study, *S. Typhimurium* strains were transformed with the eukaryotic expression vector, pEGFP. This plasmid was chosen as it can be transferred to eukaryotic cells from *S. Typhimurium* (Michael *et al.*, 2004). Furthermore, this plasmid, and its derivatives, have been employed in mammalian expression studies (Song *et al.*, 2015; Ying *et al.*, 2012). Using multiple experimental platforms, it was found that the bacteria were incapable of bactofection which is contrary to numerous reports in the literature. It was at this point a closer look at the phenotype of the *S. Typhimurium* transformed with pEGFP revealed that these cultures displayed a filamentous phenotype that was only really apparent at high magnification. To my knowledge, there are no reports of a eukaryotic expression vector inducing filamentation in bacteria, in the bactofection literature or elsewhere. It has been reported that certain mutations in a pBR332 plasmid can induce invasion defects in *S. Typhimurium*, but this was attributed to plasmid architecture (Clark *et al.*, 2009). The degree of filamentation was quite striking; the mean length of the transformed SL7207 cultures was more than three times that of the wild type and 39.58% ( $\pm 10.82\%$  standard deviation) of each culture was classed as filamentous. The classification of 'filamentous' was based on a previous study attributing bacteria greater than three cell lengths (6  $\mu\text{m}$ ) as being filamentous (Humphrey *et al.*, 2011).

The filamentous cultures had significantly decreased propensities to replicate and invade eukaryotic cells. One of the striking features of these cultures was that there were both filamentous and non-filamentous cells in the same culture. A previous study elegantly demonstrated a correlation between the increased length and decreased propensity to invade epithelial cells (Humphrey *et al.*, 2011). There was a great degree of variation between SL-pEGFP cultures in terms of the mean cell length of the culture, as well as the distribution of cells in a given cell size category. This demonstrates the difficulty in controlling for the variation between cultures, thus making the variability between experiments more challenging. Such variability can mask true experimental results, and lead to incorrect conclusions being drawn from a given experiment. To our knowledge, this phenotype has not been reported in f1 *ori*-containing plasmids, which also include commonly employed plasmids such as pBluescript- and pcDNA3.1. Therefore, it is possible that researches employing the use of these plasmids (or their derivatives) in *S. Typhimurium* strains are unaware of the potentially confounding factor that is the filamentous phenotype. Upon the discovery of the f1 *ori* as being the factor in pEGFP driving the filamentous phenotype, it would have been interesting to see if the SL-pEGFPLacZ (the plasmid which lacks f1 *ori*) could mediate bactofection. Unfortunately, time constraints did not allow for this investigation.

### **6.3.5 What is the role of the f1 *ori* in eukaryotic expression plasmids and how might it be inducing filamentation?**

The data presented herein suggests that the f1 origin of replication is capable of inducing filamentation in *S. Typhimurium*. The purpose of the f1 *ori* in the pEGFP plasmid is uncertain and unreported. The f1 *ori* is capable of ssDNA replication and phage packaging (Horiuchi, 1980; Russel & Model, 1989). It is speculated that the f1 *ori* was previously employed in eukaryotic expression vectors to introduce mutations into genes on the plasmid when induced with the appropriate phage (José Penades, personal communication). To activate the f1 *ori*, it must first be nicked by an endonuclease, Gp2 protein of the filamentous phage which recognizes a consensus sequence in the origin sequence and cleaves a single strand to allow the initiation of ssDNA packaging by the phage (Higashitani *et al.*, 1992). The presence of the f1 *ori* may lead to the generation of ssDNA by the Gp2 protein associated with the filamentous phage elements in

*S. Typhimurium*, or some other mechanism. The production of ssDNA is sufficient to activate the SOS stress response. This stress response involved the cleavage of the LexA repressor, which then allows for the SOS transcriptional programme to be activated (Little, 1984). The culmination of this transcriptional programme is the Sula-mediated arrest of FtsZ oligomerisation, the protein responsible for daughter cell septation during replication (Trusca *et al.*, 1998). Septational arrest subsequently results in filamentation, with nuclear staining clearly depicting multiple nuclei along a single filamentous bacterium, as seen in the present study.

However, to definitively appoint the *f1 ori* as feature inducing filamentation, it is necessary to clone the *f1 ori* into another plasmid backbone which does not induce filamentation in *S. Typhimurium*, such as pACYC184. The ability of this plasmid to induce filamentation in transformed *S. Typhimurium* would provide definitive that it is indeed the *f1 ori* which is responsible for the filamentous phenotype.

### 6.3.6 Concluding remarks

The data presented herein provides evidence for the *f1 ori* inducing a filamentous phenotype in pEGFP-transformed *S. Typhimurium* cultures. The model we propose is one in which the *f1 ori* of the pEGFP plasmid induces ssDNA production in the cell, activating the SOS response and inducing filamentation. The induction of filamentation attenuates invasion and intracellular replication, which we believe affects the bactofection capacity of *S. Typhimurium*.

These findings are relevant as the *f1 ori* is present in commonly employed plasmids such as pcDNA3.1 and pBluescript. This information is important for researchers employing these plasmids in studies involving *S. Typhimurium* as the filamentation may confound the experimental readout. This is particularly pertinent given the decreased growth and invasion characteristics exhibited by the pEGFP-transformed cultures, and the variation between cultures. However, the effects of the *f1 ori* on other bacterial species, *Escherichia coli* excepted, and how it might affect experimental readouts is still unknown and requires further investigation. Therefore, those coupling *f1 ori*-containing plasmids to *S.*

Typhimurium for the purposes of scientific investigation should exhibit extreme caution.

## 7 Conclusions and future perspectives

The outstanding aim of this thesis was to examine changes in the tumour immune environment following infection, with a particular interest in the contribution of the monocyte/macrophage compartment to mediating bacterial-mediated tumour growth inhibition.

The tumour model that was developed, the B16F10 melanoma model, was found to be highly reproducible and time-efficient, so was considered suitable to investigate changes in the tumour milieu following infection. However, it is critical to bear in mind the  $T_H1$  response-bias of this mouse strain (Mills *et al.*, 2000; Santos *et al.*, 2006) before generating definitive conclusions on any aspects of the changes in immune cell repertoire and function. In order to definitively ascertain the contribution of a given immune cell type to *S. Typhimurium*-induced tumour growth inhibition, it would be important to repeat these experiments in a different mouse strain, such as BALB/c. However, such a line of enquiry would not address the outstanding limitation of transplantable tumour models which is the absence of tumour cell selection through early tumour development, resulting in clonogenic cells making up the tumour mass (Zitvogel *et al.*, 2016). Therefore, it would be optimal to repeat these studies in a spontaneous tumour model, which although time-consuming and expensive, provides a more human-like tumour environment than transplantable models. However, in the present study, we were primarily interested in the *change* in tumour immune-phenotype following infection, so the transplantable tumour model sufficed.

It was hypothesised that there would be change in the tumour immune cell composition and phenotype following infection. Evidence in favour of this hypothesis comes from the fact that there were increased levels of multiple pro-inflammatory cytokines, IFN- $\gamma$ , TNF- $\alpha$ , IL-6, and IL-12p40 in the tumour following infection. These cytokines are associated with a non-permissive environment to tumourigenesis (Bromberg *et al.*, 1996; Burke *et al.*, 1999; Wall *et al.*, 2003). Neutrophils, monocytes and T cells were, in part, responsible for the production of these cytokines and possibly DCs, although the latter was not investigated in detail. It was very interesting that there was not a mass influx of immune cells into the tumour following *S. Typhimurium* infection as is seen in the mucosa

(Barthel *et al.*, 2003; Rydström & Wick, 2009) and spleen (Johansson *et al.*, 2006). Therefore, one might conclude that the pro-inflammatory environment was achieved without a notable leukocyte influx, providing evidence for the tumour-resident immune cells being sufficient to propagate this phenotype. There are many caveats to this conclusion though: macrophages undergo pyroptosis following *S. Typhimurium* infection (Monack *et al.*, 1996), so the degree of cell death might just equal the degree of infiltration masking the true dynamics of leukocyte influx into the tumour following infection. Furthermore, looking at the flow cytometry plots alone, there is obvious recruitment of monocytes to the tumour, in spite of the fact that this is not reflected in the absolute number of Ly6C<sup>+</sup>MHCII<sup>+</sup> monocytes in the infected tumour compared to uninfected. The most likely explanation for this is the size difference between the large uninfected tumour and the much smaller infected tumours. This would mean there was a greater density of Ly6C<sup>+</sup>MHCII<sup>+</sup> monocytes in the tumour in the infected compared to the uninfected samples, which may be an important factor. Another piece of evidence which might suggest leukocyte recruitment is the fact that all of the myeloid cell types investigated exhibited increased expression of Ki67, a marker for replication, which might be reflective of inflammation-induced myeloid progenitor growth in the bone marrow or spleen, as opposed to tissue-resident proliferation (Ueda *et al.*, 2009; Zhang *et al.*, 2010).

This study also focused on the T cell repertoire in the tumour following infection. There was an increase in the frequency of T<sub>H</sub>1 cells and CTLs corresponding to bacterial-mediated tumour growth inhibition, but it was exciting to see changes in the frequency of T<sub>H</sub>17 and Treg cells. To our knowledge, this is the first report to suggest a link between bacterial-mediated cancer therapy and T<sub>H</sub>17 or Treg cells. T<sub>H</sub>17 cells are particularly adept at mediating tumour immunity in melanomas (Martin-Orozco *et al.*, 2010; Muranski *et al.*, 2008), so we would be interested to investigate the contribution of T<sub>H</sub>17 cells to bacterial-mediated tumour growth inhibition, through the antibody blockage of IL-17. We would also like to investigate the possibility that Tregs are induced to adopt a T<sub>H</sub>17-phenotype. This would involve the adoptive transfer of CD4<sup>+</sup>FoxP3<sup>+/gfp</sup> Tregs into tumour-bearing mice prior to systemic *S. Typhimurium* infection and subsequent phenotypic analysis of the CD4<sup>+</sup>GFP<sup>+</sup> cells from infected

tumours. This line of inquiry could reveal a role for Treg-T<sub>H</sub>17 cells in mediating the anti-tumour effects of *S. Typhimurium*. This would be important, as IL-17 is associated with tumour-promoting activities in certain cancer types, such as lymphoma and gastric cancers (He *et al.*, 2011; Liu *et al.*, 2011). Therefore these cancer types might not be suitable for the application of *S. Typhimurium* as a cancer therapy.

At the outset of this study, we were particularly interested in the phenotypic changes afforded by the resident TAMs in response to *S. Typhimurium* infection. However, in this study, we report that the only differences in the TAM functional phenotype following infection were an up-regulation of MHCII within the entire TAM population and an increased phagocytic capacity of MHCII<sup>+</sup> TAMs. Of note, there were no statistically significant changes in the cytokine production following infection, which we hypothesised would be a reliable readout to assess changes in the functional phenotype of these cells (Bain *et al.*, 2013; Yrlid *et al.*, 2000). Of course, it is possible that there were other changes in the TAM populations following infection that our study did not investigate, so it is remiss to suggest that the TAMs do not change in phenotype following infection.

In contrast, the tumour monocyte population was highly responsive to systemic *S. Typhimurium* infection. The Ly6C<sup>+</sup>MHCII<sup>-</sup> monocytes increased the expression of many inflammatory mediators. To our knowledge, this is the first report to specifically indicate a role for monocytes in playing a role in bacterial-mediated tumour growth inhibition. The reason for this is most likely due to the fact that many studies do not differentiate monocytes and designate all F4/80 cells as 'TAMs' (Lee *et al.*, 2011, 2008; Zheng *et al.*, 2017b), which is reductionist given the emerging roles of monocytes in multiple physiological settings, particularly inflammation (Bain *et al.*, 2013; Jakubzick *et al.*, 2017). We hypothesised that these monocytes were mediating the anti-tumoural effects of SL7207. We tried to test this hypothesis through the use of *Ccr2*<sup>-/-</sup> mice, but these were insufficient to reduce monocyte infiltration into the tumour following infection. However, the employment of clodronate liposomes (Clod Lipo), which can reduce the monocyte and macrophage tumour content (Gazzaniga *et al.*, 2007; Griesmann *et al.*, 2016), resulted in an abrogation in the anti-tumour effects of SL7207. Upon investigation of the tumour monocyte/macrophage compartment

following infection, it was clear that Clod Lipo treatment, similar to the *Ccr2*<sup>-/-</sup> mice, was an insufficient experimental approach to deplete tumour monocytes and macrophages following infection. It was, however, of great interest that the spleens of the infected Clod Lipo-treated mice were much smaller than the infected PBS Lipo mice. This finding was made subsequent to the discovery that there was no significant change in the number of tumour-associated monocytes and macrophages between infected PBS Lipo and Clod Lipo tumours, and there was insufficient time to carry out further experiments to investigate this outcome. Splenic monocytic cells are an important site for pro-inflammatory cytokine production following infection (Serbina *et al.*, 2003; Serbina & Pamer, 2006), and splenic monocytes can be directed to tumour mass (Cortez-Retamozo *et al.*, 2012). Whether these monocytes are bone-marrow derived or propagated exclusively from splenic progenitors is unclear.

This information contributes to the formation of our current hypothesis: the pro-inflammatory splenic monocytes from infected tumour-bearing mice are responsible for driving the anti-tumour effects of *S. Typhimurium*. We propose that the abrogation of tumour growth inhibition following SL7207 infection following Clod Lipo administration was due to the absence of splenic-derived pro-inflammatory monocytes (Figure 7.1). Evidence in favour of this hypothesis from this study comes from the protective effects of Clod Lipo treatment on the body weight of the mice, which were likely lacking systemic TNF- $\alpha$  due to the (presumed) abrogation of splenic monocytes. Current efforts in the group are focused on testing this hypothesis. This will involve the characterisation of the splenic monocyte pool in tumour-bearing mice, both infected and uninfected as well as following treatment with either PBS Lipo and Clod Lipo. The identification of pro-inflammatory monocytes in the infected spleens, but not in the uninfected or infected Clod Lipo spleen would provide evidence in favour of the current hypothesis. It would have been highly informative to administer the bacteria intra-tumourally, as this would largely reduce the systemic response, and allowed us to examine the role tumour-specific colonisation plays in the anti-tumour effects of the bacteria in isolation from the systemic immune response. It would also be informative to perform splenectomies on tumour-bearing mice, and assess the subsequent tumour response to systemic *S. Typhimurium* infection. Finally, it would be pertinent to perform adoptive

transfer experiments with splenic monocytes isolated from infected and uninfected tumour-bearing mice to untreated tumour-bearing mice to assess the changes in tumour growth dynamics in the latter. Throughout these experiments, it would also be informative to investigate the functional phenotype of the monocytes recruited to the tumour, as the absence of pro-inflammatory monocytes from infected tumour from Clod Lipo-treated and splenectomised mice would provide evidence in favour of pro-inflammatory monocytes of splenic origin contributing to bacterial-mediated tumour growth inhibition. These findings would provide evidence for the mechanism to describe how systemically administered bacteria can mediate anti-tumour effects, and as such would inform future studies, both in this lab group and others.

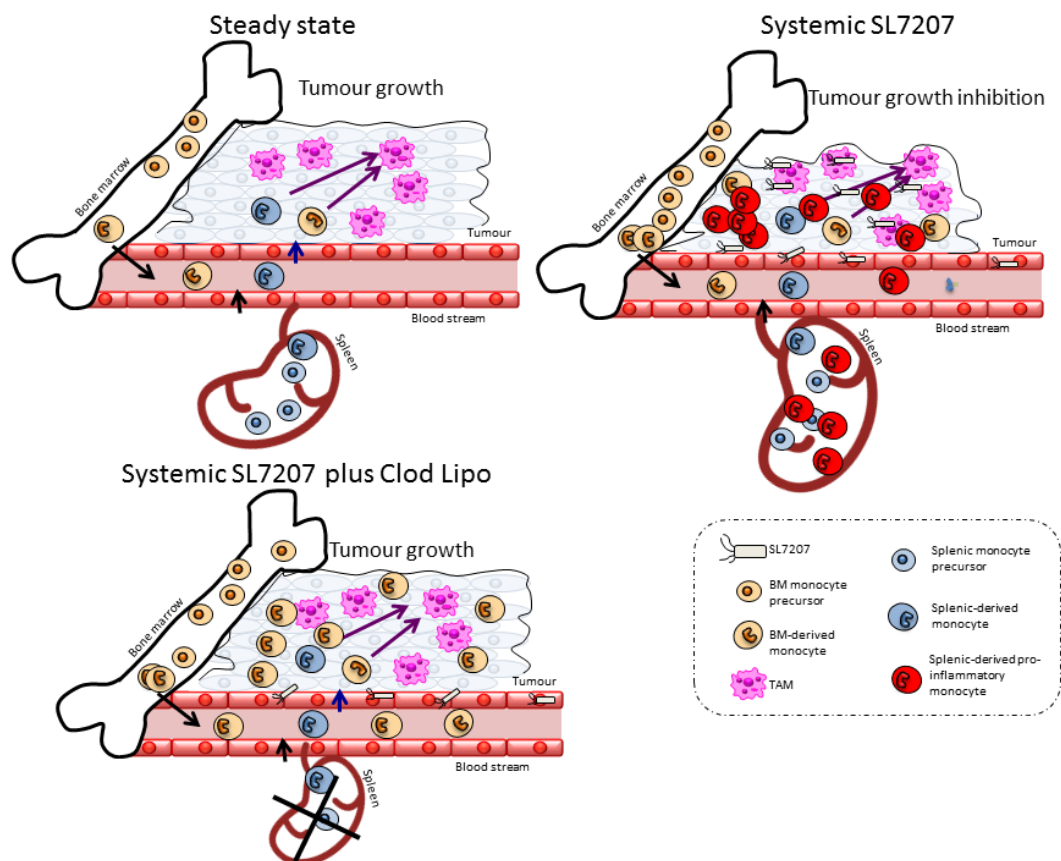


**Figure 7.1 Proposed mechanism for Clod Lipo abrogating SL7207 tumour growth inhibition**  
In steady state, tumour associated macrophages (TAMs) are derived from both splenic and bone marrow (BM) monocytes. Following systemic SL7207 infection, there is an expansion of pro-inflammatory monocytes in the spleen, which are subsequently recruited to the tumour and mediate tumour growth inhibition. Following Clod Lipo treatment, these cells are depleted and tumour growth is unaffected by SL7207.

A final line of investigation from this report was to enhance the anti-tumour effects of SL7207 by bactofection. Although we were unable to recapitulate

bactofection as reported in the literature (Berger *et al.*, 2013; Byrne *et al.*, 2014; Michael *et al.*, 2004), we believe that we identified a feature of eukaryotic expression vectors, the f1 *ori*, which might be antagonising the bactofection potential of *S. Typhimurium* strains. This information is important to bear in mind when designing bactofection studies, as coupling *S. Typhimurium* f1 *ori*-containing plasmids would induce filamentation undermining the invasion and probably bactofection of the bacteria.

## 8 References

- Abel, E. L., Angel, J. M., Kiguchi, K., & DiGiovanni, J. (2009). Multi-stage chemical carcinogenesis in mouse skin: Fundamentals and applications. *Nature Protocols*, 4(9), 1350-1362.
- Agrawal, N., Bettegowda, C., Cheong, I., Geschwind, J.-F., Drake, C. G., Hipkiss, E. L., ... Vogelstein, B. (2004). Bacteriolytic therapy can generate a potent immune response against experimental tumors. *Proceedings of the National Academy of Sciences of the United States of America*, 101(42), 15172-7.
- Ahmad, S., Casey, G., Cronin, M., Rajendran, S., Sweeney, P., Tangney, M., & O'Sullivan, G. C. (2011). Induction of effective antitumor response after mucosal bacterial vector mediated DNA vaccination with endogenous prostate cancer specific antigen. *Journal of Urology*, 186(2), 687-693.
- Anderson, K. G., Mayer-Barber, K., Sung, H., Beura, L., James, B. R., Taylor, J. J., ... Masopust, D. (2014). Intravascular staining for discrimination of vascular and tissue leukocytes. *Nature Protocols*, 9(1), 209-222.
- Ando, R., Hama, H., Yamamoto-Hino, M., Mizuno, H., & Miyawaki, A. (2002). An optical marker based on the UV-induced green-to-red photoconversion of a fluorescent protein. *Proceedings of the National Academy of Sciences*, 99(20), 12651-12656.
- Andzinski, L., Kasnitz, N., Stahnke, S., Wu, C. F., Gereke, M., Von Köckritz-Blickwede, M., ... Jablonska, J. (2016). Type I IFNs induce anti-tumor polarization of tumor associated neutrophils in mice and human. *International Journal of Cancer*, 138(8), 1982-1993.
- Apostolou, I., & von Boehmer, H. (2004). *In vivo* Instruction of Suppressor Commitment in Naive T Cells. *The Journal of Experimental Medicine*, 199(10), 1401-1408.
- Arpaia, N., Godec, J., Lau, L., Sivick, K. E., Mclaughlin, L. M., Jones, M. B., ... Barton, G. M. (2011). TLR signaling is required for virulence of an intracellular pathogen. *Cell*, 144(5), 675-688.
- Asano, M. (1996). Autoimmune disease as a consequence of developmental abnormality of a T cell subpopulation. *Journal of Experimental Medicine*, 184(2), 387-396.
- Atarashi, K., Tanoue, T., Shima, T., Imaoka, A., Kuwahara, T., Momose, Y., ... Honda, K. (2011). Induction of colonic regulatory T cells by indigenous *Clostridium* species. *Science*, 331(6015), 337-341.
- Avogadri, F., Martinoli, C., Petrovska, L., Chiodoni, C., Transidico, P., Bronte, V., ... Rescigno, M. (2005). Cancer immunotherapy based on killing of

- Salmonella* -infected tumor cells. *Cancer Research*, 10(9), 3920-3927.
- Avogadri, F., Mittal, D., Saccheri, F., Sarrafiore, M., Ciocca, M., Larghi, P., ... Rescigno, M. (2008). Intra-tumoral *Salmonella* Typhimurium induces a systemic anti-tumor immune response that is directed by low-dose radiation to treat distal disease. *European Journal of Immunology*, 38(7), 1937-1947.
- Azzi, S., Hebda, J. K., & Gavard, J. (2013). Vascular Permeability and Drug Delivery in Cancers. *Frontiers in Oncology*, 3(2), 1-14.
- Baban, C. K., Cronin, M., Akin, A. R., O'Brien, A., Gao, X., Tabirca, S., ... Tangney, M. (2012). Bioluminescent Bacterial Imaging *In vivo*. *Journal of Visualized Experiments*, (69), 1-6.
- Babjuk, M., Oosterlinck, W., Sylvester, R., Kaasinen, E., Böhle, A., Palou-Redorta, J., & Rouprêt, M. (2011). EAU guidelines on non-muscle-invasive urothelial carcinoma of the bladder, the 2011 update. *European Urology*, 59(6), 997-1008.
- Bain, C. C., Bravo-Blas, A., Scott, C. L., & Perdiguero, E. G. (2014). Constant replenishment from circulating monocytes maintains the macrophage pool in adult intestine. *Nature Immunology*, 15(10), 929-937.
- Bain, C. C., Scott, C. L., Uronen-Hansson, H., Gudjonsson, S., Jansson, O., Grip, O., ... Mowat, A. M. (2013). Resident and pro-inflammatory macrophages in the colon represent alternative context-dependent fates of the same Ly6Chi monocyte precursors. *Mucosal Immunology*, 6(3), 498-510.
- Bak, S. P., Alonso, A., Turk, M. J., & Berwin, B. (2008). Murine ovarian cancer vascular leukocytes require arginase-1 activity for T cell suppression. *Molecular Immunology*, 46(2), 258-268.
- Balkwill, F., & Mantanovi, A. (2001). Inflammation and cancer: back to Virchow? *Lancet*, 357(9255) 539-545.
- Banchereau, J., & Steinman, R. M. (1998). Dendritic cells and the control of immunity. *Nature*, 392(6673), 245-252.
- Bao, S., Beagley, K. W., France, M. P., Shen, J., & Husband, A. J. (2000). Interferon- $\gamma$  plays a critical role in intestinal immunity against *Salmonella* Typhimurium infection. *Immunology*, 99(3), 464-472.
- Barthel, M., Hapfelmeier, S., Quintanilla-Martínez, L., Kremer, M., Rohde, M., Hogardt, M., ... Hardt, W. D. (2003). Pretreatment of mice with streptomycin provides a *Salmonella enterica* serovar Typhimurium colitis model that allows analysis of both pathogen and host. *Infection and Immunity*, 71(5), 2839-2858.
- Bates, G. J., Fox, S. B., Han, C., Leek, R. D., Garcia, J. F., Harris, A. L., &

- Banham, A. H. (2006). Quantification of regulatory T cells enables the identification of high-risk breast cancer patients and those at risk of late relapse. *Journal of Clinical Oncology*, 24(34), 5373-5380.
- Beck, K. E., Blansfield, J. A., Tran, K. Q., Feldman, A. L., Hughes, M. S., Royal, R. E., ... Yang, J. C. (2006). Enterocolitis in patients with cancer after antibody blockade of cytotoxic T-lymphocyte-associated antigen 4. *Journal of Clinical Oncology*, 24(15), 2283-2289.
- Belai, E. B., de Oliveira, C. E., Gasparoto, T. H., Ramos, R. N., Torres, S. A., Garlet, G. P., ... Campanelli, A. P. (2014). PD-1 blockage delays murine squamous cell carcinoma development. *Carcinogenesis*, 35(2), 424-431.
- Benoist, C., & Mathis, D. (2012). Treg cells, life history, and diversity. *Cold Spring Harbor Perspectives in Biology*, 4(9), 1-14.
- Berger, E., Soldati, R., Huebener, N., Hohn, O., Stermann, A., Durmus, T., ... Fest, S. (2013). *Salmonella* SL7207 application is the most effective DNA vaccine delivery method for successful tumor eradication in a murine model for neuroblastoma. *Cancer Letters*, 331(2), 167-173.
- Bettelli, E., Carrier, Y., Gao, W., Korn, T., Strom, T. B., Oukka, M., ... Kuchroo, V. K. (2006). Reciprocal developmental pathways for the generation of pathogenic effector T<sub>H</sub>17 and regulatory T cells. *Nature*, 441(7090),
- Beuzón, C. R., Meresse, S., Unsworth, K. E., Ruiz-Albert, J., Garvis, S., Waterman, S. R., ... Holden, D. W. (2000). *Salmonella* maintains the integrity of its intracellular vacuole through the action of SifA. *Embo J.*, 19(13), 3235-3249.
- Beuzón, C. R., Salcedo, S. P., & Holden, D. W. (2002). Growth and killing of a *Salmonella enterica* serovar Typhimurium *sifA* mutant strain in the cytosol of different host cell lines. *Microbiology*, 148(9), 2705-2715.
- Binder, D. C., Arina, A., Wen, F., Tu, T., Zhao, M., Hoffman, R. M., ... Schreiber, H. (2016). Tumor relapse prevented by combining adoptive T cell therapy with *Salmonella typhimurium*. *Oncolmmunology*, 5(6), e1130207.
- Binder, D. C., Engels, B., Arina, A., Yu, P., Slauch, J. M., Fu, Y.-X., ... Schreiber, H. (2013). Antigen-Specific Bacterial Vaccine Combined with Anti-PD-L1 Rescues Dysfunctional Endogenous T Cells to Reject Long-Established Cancer. *Cancer Immunology Research*, 1(2), 123-133.
- Bingle, L., Brown, N. J., & Lewis, C. E. (2002). The role of tumour-associated macrophages in tumour progression: Implications for new anticancer therapies. *Journal of Pathology*, 196(3), 254-265.
- Bisiaux, A., Thiounn, N., Timsit, M. O., Eladaoui, A., Chang, H. H., Mapes, J., ... Albert, M. L. (2009). Molecular Analyte Profiling of the Early Events and

- Tissue Conditioning Following Intravesical Bacillus Calmette-Guerin Therapy in Patients With Superficial Bladder Cancer. *Journal of Urology*, 181(4),
- Blank, C., Brown, I., Peterson, A. C., Transgenic, T. C. R., Cells, C. D. T., Spiotto, M., ... Gajewski, T. F. (2004). PD-L1 / B7H-1 Inhibits the Effector Phase of Tumor Rejection by T Cell Receptor ( TCR ) Transgenic CD8 + T Cells PD-L1 / B7H-1 Inhibits the Effector Phase of Tumor Rejection by T Cell Receptor. *Cancer Research*, (11), 1140-1145.
- Bloom, M. B., Perry-Lalley, D., Robbins, P. F., Li, Y., el-Gamil, M., Rosenberg, S. A., & Yang, J. C. (1997). Identification of tyrosinase-related protein 2 as a tumor rejection antigen for the B16 melanoma. *The Journal of Experimental Medicine*, 185(3), 453-9.
- Bonnetblanc, J., & Bédane, C. (2003). Erysipelas: recognition and management. *American Journal of Clinical Dermatology*, 4(3), 157-163.
- Bouso, P. (2008). T-cell activation by dendritic cells in the lymph node: lessons from the movies. *Nat Rev Immunol*, 8(9), 675-684.
- Brahmer, J., Reckamp, K. L., Baas, P., Crinò, L., Eberhardt, W. E. E., Poddubskaya, E., ... Spigel, D. R. (2015). Nivolumab versus Docetaxel in Advanced Squamous-Cell Non-Small-Cell Lung Cancer. *New England Journal of Medicine*, 373(2), 123-135.
- Bredel-Geissler, A., Karbach, U., Walenta, S., Vollrath, L., & Mueller-Klieser, W. (1992). Proliferation-associated oxygen consumption and morphology of tumor cells in monolayer and spheroid culture. *Journal of Cellular Physiology*, 153(1), 44-52.
- Brennan, M. A., & Cookson, B. T. (2000). *Salmonella* induces macrophage death by caspase-1-dependent necrosis. *Molecular Microbiology*, 38(1), 31-40.
- Brent, R., & Ptashne, M. (1981). Mechanism of action of the *lexA* gene product. *Proceedings of the National Academy of Sciences of the United States of America*, 78(7), 4204-8.
- Brinkmann, V., Reichard, U., Goosmann, C., Fauler, B., Uhlemann, Y., Weiss, D. S., ... Zychlinsky, A. (2004). Neutrophil Extracellular Traps Kill Bacteria. *Science*, 303(5663), 1532-1535.
- Bromberg, J. F., Horvath, C. M., Wen, Z., Schreiber, R. D., & Darnell, J. E. (1996). Transcriptionally active Stat1 is required for the antiproliferative effects of both interferon alpha and interferon gamma. *Proceedings of the National Academy of Sciences of the United States of America*, 93(15), 7673-7678.
- Bronte, V., Apolloni, E., Cabrelle, A., Ronca, R., Serafini, P., Zamboni, P., ... Zanovello, P. (2000). Identification of a CD11b(+)/Gr-1(+)/CD31(+) myeloid

- progenitor capable of activating or suppressing CD8(+) T cells. *Blood*, 96(12), 3838-46.
- Brown, J. A., Dorfman, D. M., Ma, F.-R., Sullivan, E. L., Munoz, O., Wood, C. R., ... Freeman, G. J. (2003). Blockade of Programmed Death-1 Ligands on Dendritic Cells Enhances T Cell Activation and Cytokine Production. *The Journal of Immunology*, 170(3), 1257-1266.
- Broz, P., Newton, K., Lamkanfi, M., Mariathasan, S., Dixit, V. M., & Monack, D. M. (2010). Redundant roles for inflammasome receptors NLRP3 and NLRC4 in host defence against *Salmonella*. *The Journal of Experimental Medicine*, 207(8), 1745-1755.
- Buongoro, L., Petrizzo, A., Tornesollo, M. L. & Buonguro, F. M. (2011). Translating Tumor Antigens into Cancer Vaccines. *Clinical and Vaccine Immunology*, 18(1), 23-34.
- Burke, F., Smith, P. D., Crompton, M. R., Upton, C., & Balkwill, F. R. (1999). Cytotoxic response of ovarian cancer cell lines to IFN- $\gamma$  is associated with sustained induction of IRF-1 and p21 mRNA. *British Journal of Cancer*, 80(8), 1236-1244.
- Burnet, F. (1957). Cancer - a biological approach. *British Medical Journal*, 1,(5023), 841-847.
- Byrne, W. L., Murphy, C. T., Cronin, M., Wirth, T., & Tangney, M. (2014). Bacterial-mediated DNA delivery to tumour associated phagocytic cells. *Journal of Controlled Release*, 196, 384-393.
- Campoy, S., Hervàs, A., Busquets, N., Erill, I., Teixidó, L., & Barbé, J. (2006). Induction of the SOS response by bacteriophage lytic development in *Salmonella enterica*. *Virology*, 351(2), 360-367.
- Carlsson, J., & Acker, H. (1998). Relations between pH, oxygen partial pressure and growth in cultured cell spheroids. *International Journal of Cancer*, 42(5), 715-720.
- Cederbom, L., Hall, H., & Ivars, F. (2000). CD4+CD25+ regulatory T cells down-regulate co-stimulatory molecules on antigen-presenting cells. *European Journal of Immunology*, 30, 1538-1543.
- Cella, M., Engering, A., Pinet, V., Pieters, J., & Lanzavecchia, A. (1997). Inflammatory stimuli induce accumulation of MHC class II complexes on dendritic cells. *Nature*, 388(6644), 782-727.
- Cheminay, C., Chakravorty, D., & Hensel, M. (2004). Role of Neutrophils in Murine Salmonellosis. *Infection and Immunity*, 72(1), 468-477.
- Chen, C., Qu, Q. X., Shen, Y., Mu, C. Y., Zhu, Y. B., Zhang, X. G., & Huang, J. A.

- (2012). Induced expression of B7-H4 on the surface of lung cancer cell by the tumor-associated macrophages: A potential mechanism of immune escape. *Cancer Letters*, 317(1), 99-105.
- Chen, J., Yang, B., Cheng, X., Qiao, Y., Tang, B., Chen, G., ... Hua, Z. C. (2012). *Salmonella*-mediated tumor-targeting TRAIL gene therapy significantly suppresses melanoma growth in mouse model. *Cancer Science*, 103(2), 325-333.
- Chen, M. Wang, Y. H., Wang, Y., Huang, L., Sandovi, H., Liu, Y. J. & Wang, J. (2006). Dendritic cell apoptosis in the maintenance of immune tolerance. *Science*, 311(5764), 1160-1164.
- Chen, M.-L., Pittet, M. J., Gorelik, L., Flavell, R. A., Weissleder, R., von Boehmer, H., & Khazaie, K. (2005). Regulatory T cells suppress tumor-specific CD8 T cell cytotoxicity through TGF-beta signals *in vivo*. *Proceedings of the National Academy of Sciences of the United States of America*, 102(2), 419-24.
- Chen, W., Jin, W., Hardegen, N., Lei, K., Li, L., Marinos, N., ... Wahl, S. M. (2003). Conversion of Peripheral CD4<sup>+</sup> CD25<sup>-</sup> Naïve T Cells to CD4<sup>+</sup> CD25<sup>+</sup> Regulatory T Cells by TGF- $\beta$  Induction of Transcription Factor Foxp3. *Journal of Experimental Medicine*, 198(12), 1875-1886.
- Chifman, J., Pullikuth, A., Chou, J. W., Bedognetti, D., & Miller, L. D. (2016). Conservation of immune gene signatures in solid tumors and prognostic implications. *BMC Cancer*, 16(1), 911.
- Chopra, D., Rehan, H., Sharma, V., & Mishra, R. (2016). Chemotherapy-induced adverse drug reactions in oncology patients: A prospective observational survey. *Indian Journal of Medical and Paediatric Oncology*, 37(1), 42-46.
- Chow, J. C., Young, D. W., Golenbock, D. T., Christ, W. J., & Gusovsky, F. (1999). Toll-like receptor-4 mediates lipopolysaccharide-induced signal transduction. *Journal of Biological Chemistry*, 274(16), 10689-10692.
- Chuang, T.-H., Lee, J., Kline, L., Mathison, J. C., & Ulevitch, R. J. (2002). Toll-like receptor 9 mediates CpG-DNA signaling. *Journal of Leukocyte Biology*, 71(3), 538-544.
- Chung, T. C., Jones, C. H., Gollakota, A., Kamal Ahmadi, M., Rane, S., Zhang, G., & Pfeifer, B. A. (2015). Improved *Escherichia coli* bacterofection and cytotoxicity by heterologous expression of bacteriophage  $\phi$ x174 lysis gene e. *Molecular Pharmaceutics*, 12(5), 1691-1700.
- Clairmont, C., Lee, K. C., Pike, J., Ittensohn, M., Low, K. B., Pawelek, J., ... King, I. (2000). Biodistribution and genetic stability of the novel antitumor agent VNP20009, a genetically modified strain of *Salmonella* Typhimurium. *The Journal of Infectious Diseases*, 181, 1996-2002.

- Clark, L., Martinez-Argudo, I., Humphrey, T. J., & Jepson, M. A. (2009). GFP plasmid-induced defects in *Salmonella* invasion depend on plasmid architecture, not protein expression. *Microbiology*, *155*(2), 461-467.
- Clark, M. A., Reed, K. A., Lodge, J., Stephen, J., Hirst, B. H., & Jepson, M. A. (1996). Invasion of murine intestinal M cells by *Salmonella* typhimurium inv mutants severely deficient for invasion of cultured cells. *Infection and Immunity*, *64*(10), 4363-4368.
- Coffelt, S. B., Chen, Y.-Y., Muthana, M., Welford, A. F., Tal, A. O., Scholz, A., ... Lewis, C. E. (2011). Angiopoietin 2 stimulates TIE2-expressing monocytes to suppress T cell activation and to promote regulatory T cell expansion. *Journal of Immunology*, *186*(7), 4183-90.
- Coffelt, S. B., Kersten, K., Doornebal, C. W., Weiden, J., Vrijland, K., Hau, C.-S., ... de Visser, K. E. (2015). IL-17-producing  $\gamma\delta$  T cells and neutrophils conspire to promote breast cancer metastasis. *Nature*, *522*(7556), 345-348.
- Coffelt, S. B., Tal, A. O., Scholz, A., De Palma, M., Patel, S., Urbich, C., ... Lewis, C. E. (2010). Angiopoietin-2 regulates gene expression in TIE2-expressing monocytes and augments their inherent proangiogenic functions. *Cancer Research*, *70*(13), 5270-5280.
- Coffelt, S. B., Wellenstein, M. D., & de Visser, K. E. (2016). Neutrophils in cancer: neutral no more. *Nature Reviews Cancer*, *16*(7), 431-446.
- Coley, W. B. (1883). The treatment of malignant tumours by repeated inoculations of erysipelas: with a brief report of ten original cases. *The American Journal of the Medical Sciences*, *105*(5), 487-511.
- Coley Nauts, H., Swift, W. E., & Coley, B. L. (1946). The Treatment of Malignant Tumors by Bacterial Toxins as Developed by the Late William B. Coley, M.D., Reviewed in the Light of Modern Research. *Cancer Research*, *6*(4), 205-216.
- Collier-Hyams, L. S., Zeng, H., Sun, J., Tomlinson, A. D., Bao, Z. Q., Chen, H., ... Neish, A. S. (2002). Cutting Edge: *Salmonella* AvrA Effector Inhibits the Key Proinflammatory, Anti-Apoptotic NF- $\kappa$ B Pathway. *The Journal of Immunology*, *169*(6), 2846-2850.
- Cordell, S. C., Robinson, E. J. H., & Lowe, J. (2003). Crystal structure of the SOS cell division inhibitor Sula and in complex with FtsZ. *Proceedings of the National Academy of Sciences of the United States of America*, *100*(13), 7889-94.
- Cortez-Retamozo, V., Etzrodt, M., Newton, a., Rauch, P. J., Chudnovskiy, a., Berger, C., ... Pittet, M. J. (2012). Origins of tumor-associated macrophages and neutrophils. *Proceedings of the National Academy of Sciences*, *109*(7), 2491-2496.

- Cronin, M., Akin, A. R., Collins, S. A., Meganck, J., Kim, J., Baban, C. K., ... Tangney, M. (2012). High Resolution *In vivo* Bioluminescent Imaging for the Study of Bacterial Tumour Targeting, *7*(1).
- Cronin, M., Morrissey, D., Rajendran, S., El Mashad, S. M., van Sinderen, D., O'Sullivan, G. C., & Tangney, M. (2010). Orally Administered *Bifidobacteria* as Vehicles for Delivery of Agents to Systemic Tumors. *Molecular Therapy*, *18*(7), 1397-1407.
- Crull, K., Bumann, D., & Weiss, S. (2011)a. Influence of infection route and virulence factors on colonization of solid tumors by *Salmonella enterica* serovar Typhimurium. *FEMS Immunology and Medical Microbiology*, *62*(1), 75-83.
- Crull, K., Rohde, M., Westphal, K., Loessner, H., Wolf, K., Felipe-lópez, A., ... Weiss, S. (2011)b. Biofilm formation by *Salmonella enterica* serovar Typhimurium colonizing solid tumours. *Cell Microbiology*, *13*(8), 1223-1233.
- Crull, K., & Weiss, S. (2011). Antibiotic control of tumor-colonizing *Salmonella enterica* serovar Typhimurium. *Experimental Biology and Medicine*, *236*, 1282-1290.
- Cunningham, C., & Nemunaitis, J. (2001). A phase I trial of genetically modified *Salmonella typhimurium* expressing cytosine deaminase (TAPET-CD, VNP20029) administered by intratumoral injection in combination with 5-fluorocytosine for patients with advanced or metastatic cancer. Protocol no: CL-. *Human Gene Therapy*, *12*(12), 1594-6.
- Curiel, T. J., Coukos, G., Zou, L., Alvarez, X., Cheng, P., Mottram, P., ... Zou, W. (2004). Specific recruitment of regulatory T cells in ovarian carcinoma fosters immune privilege and predicts reduced survival. *Nature Medicine*, *10*(9), 942-949.
- Dagkalis, A., Wallace, C., Xu, H., Liebau, S., Manivannan, A., Stone, M. A., ... Crane, I. J. (2009). Development of experimental autoimmune uveitis: Efficient recruitment of monocytes is independent of CCR2. *Investigative Ophthalmology and Visual Science*, *50*(9), 4288-4294.
- Dang, L. H., Bettegowda, C., Huso, D. L., Kinzler, K. W., & Vogelstein, B. (2001). Combination bacteriolytic therapy for the treatment of experimental tumors. *Proceedings of the National Academy of Sciences*, *98*(26), 15155-15160.
- Darji, A., Guzmán, C. A., Gerstel, B., Wachholz, P., Timmis, K. N., Wehland, J., ... Weiss, S. (1997). Oral somatic transgene vaccination using attenuated *S. typhimurium*. *Cell*, *91*(6), 765-775.
- De Boer, E. C., De Jong, W. H., Van Der Meijden, A. P. M., Steerenberg, P. A., Witjes, J. A., Vegt, P. D. J., ... Ruitenbergh, E. J. (1991). Presence of

- activated lymphocytes in the urine of patients with superficial bladder cancer after intravesical immunotherapy with *Bacillus Calmette-Guérin*. *Cancer Immunology Immunotherapy*, 33(6), 411-416.
- de la Roche, M., Asano, Y., & Griffiths, G. M. (2016). Origins of the cytolytic synapse. *Nature Reviews Immunology*, 16(7), 421-432.
- De Monte, L., Reni, M., Tassi, E., Clavenna, D., Papa, I., Recalde, H., ... Protti, M. P. (2011). Intratumor T helper type 2 cell infiltrate correlates with cancer-associated fibroblast thymic stromal lymphopoietin production and reduced survival in pancreatic cancer. *The Journal of Experimental Medicine*, 208(3), 469-478.
- Dean, D. A. (1997). Import of plasmid DNA into the nucleus is sequence specific. *Experimental Cell Research*, 302(230), 293-302.
- Dean, D. A., Dean, B. S., Muller, S., & Smith, L. C. (1999). Sequence requirements for plasmid nuclear import. *Experimental Cell Research*, 253(2), 713-22.
- De Palma, M., Mazzieri, R., Politi, L. S., Pucci, F., Zonari, E., Sitia, G., ... Naldini, L. (2008). Tumor-Targeted Interferon- $\alpha$  Delivery by Tie2-Expressing Monocytes Inhibits Tumor Growth and Metastasis. *Cancer Cell*, 14(4), 299-311.
- De Palma, M., Venneri, M. A., Galli, R., Sergi, L. S., Politi, L. S., Sampaolesi, M., & Naldini, L. (2005). Tie2 identifies a hematopoietic lineage of proangiogenic monocytes required for tumor vessel formation and a mesenchymal population of pericyte progenitors. *Cancer Cell*, 8(3), 211-226.
- de Vooght, V., Vanoirbeek, J. A. J., Luyts, K., Haenen, S., Nemery, B., & Hoet, P. H. M. (2010). Choice of mouse strain influences the outcome in a mouse model of chemical-induced asthma. *PLoS ONE*, 5(9), 1-9.
- Del Prete, G., De Carli, M., Almerigogna, F., Giudizi, M. G., Biagiotti, R., & Romagnani, S. (1993). Human IL-10 is produced by both type 1 helper (Th1) and type 2 helper (Th2) T cell clones and inhibits their antigen-specific proliferation and cytokine production. *Journal of Immunology*, 150(2), 353-360.
- del Rio, M.-L., Bernhardt, G., Rodriguez-Barbosa, J.-I., & Förster, R. (2010). Development and functional specialization of CD103<sup>+</sup> dendritic cells. *Immunological Reviews*, 234(1), 268-281.
- Delgado-Rizo, V., Martínez-Guzmán, M. A., Iñiguez-Gutierrez, L., García-Orozco, A., Alvarado-Navarro, A., & Fafutis-Morris, M. (2017). Neutrophil extracellular traps and its implications in inflammation: An overview. *Frontiers in Immunology*, 8(FEB).

- den Haan, J. M., Lehar, S. M., & Bevan, M. J. (2000). CD8(+) but not CD8(-) dendritic cells cross-prime cytotoxic T cells *in vivo*. *The Journal of Experimental Medicine*, 192(12), 1685-96.
- Deryugina, E. I., Zajac, E., Juncker-Jensen, A., Kupriyanova, T. A., Welter, L., & Quigley, J. P. (2014). Tissue-Infiltrating Neutrophils Constitute the Major *In vivo* Source of Angiogenesis-Inducing MMP-9 in the Tumor Microenvironment. *Neoplasia*, 16(10), 771-788.
- Desfrancois, J., Moreau-Aubry, A., Vignard, V., Godet, Y., Khammari, A., Dréno, B., ... Gervois, N. (2010). Double positive CD4CD8  $\alpha\beta$  T cells: A new tumor-reactive population in human melanomas. *PLoS ONE*, 5(1).
- Di Francia, M., Barbier, D., Mege, J. L., & Orehek, J. (1994). Tumor necrosis factor-alpha levels and weight loss in chronic obstructive pulmonary disease. *American Journal of Respiratory and Critical Care Medicine*, 150(5 Pt 1), 1453-1455.
- Dietrich, G., Bubert, A., Gentschev, I., Sokolovic, Z., Simm, A., Catic, A., ... Goebel, W. (1998). Delivery of antigen-encoding plasmid DNA into the cytosol of macrophages by attenuated suicide *Listeria monocytogenes*. *Nature Biotechnology*, 16(2), 181-185.
- Din, M. O., Danino, T., Prindle, A., Skalak, M., Selimkhanov, J., Allen, K., ... Hasty, J. (2016). Synchronized cycles of bacterial lysis for *in vivo* delivery. *Nature*, 536(7614), 81-85.
- Doedens, A. L., Stockmann, C., Rubinstein, M. P., Liao, D., Zhang, N., DeNardo, D. G., ... Johnson, R. S. (2010). Macrophage expression of HIF-1 $\alpha$  suppresses T cell function and promotes tumor progression. *Cancer Research*, 70(19), 7465-75.
- Dong, H., Strome, S., Salomao, D., Tamura, H., Hirano, F., Flies, D., ... Chen, L. (2002). Tumor-associated B7-H1 promotes T-cell apoptosis: a potential mechanism of immune evasion. *Nature Medicine*, 8, 792-800.
- Dovas, A., Patsialou, A., Harney, A. S., Condeelis, J., & Cox, D. (2013). Imaging interactions between macrophages and tumour cells that are involved in metastasis *in vivo* and *in vitro*. *Journal of Microscopy*, 251(3), 261-269.
- Dudziak, D., Kamphorst, A. O., Heidkamp, G. F., Buchholz, V. R., Trumfheller, C., Yamazaki, S., ... Nussenzweig, M. C. (2007). Differential Antigen Processing by Dendritic Cell Subsets *in vivo*. *Science*, 315(5808), 107-111.
- Dunn, G. P., Old, L. J., & Schreiber, R. D. (2004). The Three Es of Cancer Immunoediting. *Annual Review of Immunology*, 22(1), 329-360.
- DuPage, M., & Bluestone, J. A. (2016). Harnessing the plasticity of CD4+ T cells to treat immune-mediated disease. *Nature Reviews Immunology*, 16(3), 149-

163.

- Edwards, J. G., Swinson, D. E. B., Jones, J. L., Muller, S., Waller, D. A., & O'Byrne, K. J. (2003). Tumor Necrosis Correlates with Angiogenesis and Is a Predictor of Poor Prognosis in Malignant Mesothelioma. *Chest*, *124*(5), 1916-1923.
- Endo, Y., Marusawa, H., Kou, T., Nakase, H., Fujii, S., Fujimori, T., ... Chiba, T. (2008). Activation-Induced Cytidine Deaminase Links Between Inflammation and the Development of Colitis-Associated Colorectal Cancers. *Gastroenterology*, *135*(3).
- Epelman, S., Lavine, K. J., Randolph, G. J., A-Gonzalez, N., Guillen, J. A., Gallardo, G., ... Kolattukudy, P. E. (2014). Origin and functions of tissue macrophages. *Immunity*, *41*(1), 21-35.
- Erickson, J. W., & Gross, C. A. (1989). Identification of the  $\sigma^E$  subunit of Escherichia coli RNA polymerase: a second alternate sigma factor involved in high-temperature gene expression. *Genes & Development*, *3*, 1462-1471.
- Eriksson, S., Lucchini, S., Thompson, A., Rhen, M., & Hinton, J. C. D. (2003). Unravelling the biology of macrophage infection by gene expression profiling of intracellular *Salmonella enterica*. *Molecular Microbiology*, *47*(1), 103-118.
- Ernst, W. A., Thoma-Uszynski, S., Teitelbaum, R., Ko, C., Hanson, D. A., Clayberger, C., ... Modlin, R. L. (2000). Granulysin, a T Cell Product, Kills Bacteria by Altering Membrane Permeability. *Journal of Immunology*, *165*, 7102-7108.
- Escobar, Y., Cajaraville, G., Virizuela, J. A., Álvarez, R., Muñoz, A., Olariaga, O., ... Tornamira, M. V. (2015). Incidence of chemotherapy-induced nausea and vomiting with moderately emetogenic chemotherapy: ADVICE (Actual Data of Vomiting Incidence by Chemotherapy Evaluation) study. *Supportive Care in Cancer*, *23*(9), 2833-2840.
- Facciabene, A., Peng, X., Hagemann, I. S., Balint, K., Barchetti, A., Wang, L.-P., ... Coukos, G. (2011). Tumour hypoxia promotes tolerance and angiogenesis via CCL28 and Treg cells. *Nature*, *475*(7355), 226-230.
- Felgner, S., Frahm, M., Kocijancic, D., Rohde, M., Eckweiler, D., Bielecka, A., ... Weiss, S. (2016). *aroA* -Deficient *Salmonella enterica* Serovar Typhimurium Is More Than a Metabolically Attenuated Mutant. *mBio*, *7*(5), e01220-16.
- Fesnak, A. D., June, C. H., & Levine, B. L. (2016). Engineered T cells: the promise and challenges of cancer immunotherapy. *Nature Reviews Cancer*, *16*(9), 566-581.
- Feuillet, V., Medjane, S., Mondor, I., Demaria, O., Pagni, P. P., Galan, J. E., ...

- Alexopoulou, L. (2006). Involvement of Toll-like receptor 5 in the recognition of flagellated bacteria. *Proceedings of the National Academy of Sciences*, 103(33), 12487-12492. h
- Fidler, I. J. (1973). Selection of Successive Tumour Lines for Metastasis. *Nature*, 242(118), 148-149.
- Fidler, I., & Nicolson, G. L. (1976). Organ selectivity for implantation survival and growth of b16 melanoma variant tumor lines. *Journal of the National Cancer Institute*, 57(5), 1199-1202.
- Figueira, R., & Holden, D. W. (2012). Functions of the *Salmonella* pathogenicity island 2 (SPI-2) type III secretion system effectors. *Microbiology*, 158(5), 1147-1161.
- Fink, S. L., & Cookson, B. T. (2006). Caspase-1-dependent pore formation during pyroptosis leads to osmotic lysis of infected host macrophages. *Cellular Microbiology*, 8(11), 1812-1825.
- Fiorentino, D. F., Bond, M. W., & Mosmann, T. R. (1989). Two types of mouse T helper cell. IV. Th2 clones secrete a factor that inhibits cytokine production by Th1 clones. *The Journal of Experimental Medicine*, 170(6), 2081-95.
- Fiorentino, D. F., Zlotnik, A., Vieira, P., Mosmann, T. R., Howard, M., Moore, K. W., & O'Garra, A. (1991). IL-10 acts on the antigen-presenting cell to inhibit cytokine production by T<sub>H</sub>1 cells. *Journal of Immunology*, 146(10), 3444-51.
- Flies, D. B., Higuchi, T., Harris, J. C., Jha, V., Gimotty, P. A., & Adams, S. F. (2016). Immune checkpoint blockade reveals the stimulatory capacity of tumor-associated CD103<sup>+</sup> dendritic cells in late-stage ovarian cancer. *Oncotarget*, 5(8), 00-00.
- Fontenot, J. D., Gavin, M. A., & Rudensky, A. Y. (2003). Foxp3 programs the development and function of CD4<sup>+</sup>CD25<sup>+</sup> regulatory T cells. *Nature Immunology*, 4(4), 330-336.
- Forbes, N. S. (2010). Engineering the perfect (bacterial) cancer therapy. *Nature Reviews Cancer*, 10(11), 785-794.
- Forbes, N. S., Munn, L. L., Fukumura, D., & Jain, R. K. (2003). Sparse initial entrapment of systemically injected *Salmonella typhimurium* leads to heterogeneous accumulation within tumors. *Cancer Research*, 63(17), 5188-5193.
- Franchi, L., Amer, A., Body-Malapel, M., Kanneganti, T.-D., Özören, N., Jagirdar, R., ... Núñez, G. (2006). Cytosolic flagellin requires Ipaf for activation of caspase-1 and interleukin 1 $\beta$  in *Salmonella*-infected macrophages. *Nature Immunology*, 7(6), 576-582.

- Franchi, L., Eigenbrod, T., Muñoz-Planillo, R., & Nuñez, G. (2009). The Inflammasome: A Caspase-1 Activation Platform Regulating Immune Responses and Disease Pathogenesis. *Nature Immunology*, 10(3), 241.
- Franklin, R. a, Liao, W., Sarkar, A., Kim, M. V, Bivona, M. R., Liu, K., ... Li, M. O. (2014). The cellular and molecular origin of tumor-associated macrophages. *Science*, 344(6186), 921-5.
- Freeman, G. J., Long, A. J., Iwai, Y., Bourque, K., Chernova, T., Nishimura, H., ... Honjo, T. (2000). Engagement of the Pd-1 Immunoinhibitory Receptor by a Novel B7 Family Member Leads to Negative Regulation of Lymphocyte Activation. *The Journal of Experimental Medicine*, 192(7), 1027-1034.
- Freyer, J. P. (1988). Role of Necrosis in Regulating the Growth Saturation of Multicellular Spheroids. *Cancer Research*, 48(9), 2432-2439.
- Friebel, A., Ilchmann, H., Aepfelbacher, M., Ehrbar, K., Machleidt, W., & Hardt, W. D. (2001). SopE and SopE2 from *Salmonella typhimurium* Activate Different Sets of RhoGTPases of the Host Cell. *Journal of Biological Chemistry*, 276(36), 34035-34040.
- Fritz, J., Ferrero, R., Philpott, D., & Girardin, S. (2006). Nod-like proteins in immunity, inflammation and disease. *Nature Immunology*, 7(12), 1250-1257.
- Fu, W., Liang, C., Xinwei, H., Xinyuan, L., & Daming, R. (2008). Synergistic antitumoral effects of human telomerase reverse transcriptase-mediated dual-apoptosis-related gene vector delivered by orally attenuated *Salmonella enterica* Serovar Typhimurium in murine tumor models. *The Journal of Gene Medicine*, 10(6), 690-701.
- Fu, Y., & Galán, J. E. (1998). The *Salmonella typhimurium* tyrosine phosphatase SptP is translocated into host cells and disrupts the actin cytoskeleton. *Molecular Microbiology*, 27(2), 359-368.
- Fuertes, M. B., Kacha, A. K., Kline, J., Woo, S.-R., Kranz, D. M., Murphy, K. M., & Gajewski, T. F. (2011). Host type I IFN signals are required for antitumor CD8<sup>+</sup> T cell responses through CD8α<sup>+</sup> dendritic cells. *The Journal of Experimental Medicine*, 208(10), 2005-2016.
- Fujimura, N., Xu, B., Dalman, J., Deng, H., Aoyama, K., & Dalman, R. L. (2015). CCR2 inhibition sequesters multiple subsets of leukocytes in the bone marrow. *Scientific Reports*, 5(1), 11664.
- Gabrilovich, D. I., Chen, H. L., Girgis, K. R., Cunningham, H. T., Meny, G. M., Nadaf, S., ... Carbone, D. P. (1996). Production of vascular endothelial growth factor by human tumors inhibits the functional maturation of dendritic cells. *Nature Medicine*, 2(10), 1096-103.
- Gabrilovich, D. I., Ostrand-Rosenberg, S., & Bronte, V. (2012). Coordinated

- regulation of myeloid cells by tumours. *Nature Reviews Immunology*, 12(4), 253-268.
- Gabrilovich, D., Ishida, T., Oyama, T., Ran, S., Kravtsov, V., Nadaf, S., & Carbone, D. P. (1998). Vascular endothelial growth factor inhibits the development of dendritic cells and dramatically affects the differentiation of multiple hematopoietic lineages *in vivo*. *Blood*, 92(11), 4150-66.
- Gagnat, N., Ptnaik, M. M., Begna, K., Kourelis, T., Al-Kali, A., Elliot, M. A., Hogan, W. J., ... Tefferi, A. (2015). Primary myelodysplastic syndromes: the Mayo Clinic experience with 1,000 patients. *Mayo Clinical Proceedings*, 90(12), 1623-1638.
- Galán, J. E., & Curtiss, R. (1989). Cloning and molecular characterization of genes whose products allow *Salmonella typhimurium* to penetrate tissue culture cells. *Proceedings of the National Academy of Sciences of the United States of America*, 86(16), 6383-7.
- Galán, J. E., & Ginocchio, C. (1994). The molecular genetic bases of *Salmonella* entry into mammalian cells. *Biochemical Society Transactions*, 22(2), 301-316.
- Galdiero, F., De L'Ero, G. C., Benedetto, N., Galdiero, M., & Tufano, M. A. (1993). Release of cytokines induced by *Salmonella typhimurium* porins. *Infection and Immunity*, 61(1), 155-161.
- Ganai, S., Arenas, R. B., & Forbes, N. S. (2009). Tumour-targeted delivery of TRAIL using *Salmonella Typhimurium* enhances breast cancer survival in mice. *British Journal of Cancer*, 101(10), 1683-1691.
- Gardner, A., & Ruffell, B. (2016). Dendritic Cells and Cancer Immunity. *Trends in Immunology*, 37(12), 855-865.
- Gavin, M. A., Rasmussen, J. P., Fontenot, J. D., Vasta, V., Manganiello, V. C., Beavo, J. A., & Rudensky, A. Y. (2007). Foxp3-dependent programme of regulatory T-cell differentiation. *Nature*, 445(7129), 771-775.
- Gazzaniga, S., Bravo, A. I., Guglielmotti, A., van Rooijen, N., Maschi, F., Vecchi, A., ... Wainstok, R. (2007). Targeting Tumor-Associated Macrophages and Inhibition of MCP-1 Reduce Angiogenesis and Tumor Growth in a Human Melanoma Xenograft. *Journal of Investigative Dermatology*, 127(8), 2031-2041.
- Geddes, K., Rubino, S., Streutker, C., Cho, J. H., Magalhaes, J. G., Bourhis, L. Le, ... Philpott, D. J. (2010). Nod1 and Nod2 regulation of inflammation in the *Salmonella colitis* model. *Infection and Immunity*, 78(12), 5107-5115.
- Ghoreschi, K., Laurence, A., Yang, X.-P., Tato, C. M., McGeachy, M. J., Konkel, J. E., ... O'Shea, J. J. (2010). Generation of pathogenic T<sub>H</sub>17 cells in the

- absence of TGF- $\beta$  signalling. *Nature*, 467(7318), 967-971.
- Gibson, V. B., Benson, R. A., Bryson, K. J., McInnes, I. B., Rush, C. M., Grassia, G., ... Garside, P. (2012). A novel method to allow noninvasive, longitudinal imaging of the murine immune system *in vivo*. *Blood*, 119(11), 2545-2551.
- Ginocchio, C. C., Olmsted, S. B., Wells, C. L., & Galan, J. E. (1994). Contact with epithelial cells induces the formation of surface appendages on *Salmonella typhimurium*. *Cell*, 76(4), 717-724.
- Girardin, S., Boneca, I., Carneiro, L., Antignac, A., Jéhanho, M., Viala, J., ... Philpott, D. (2003). Nod1 detects a unique muropeptide from Gram-negative bacterial peptidoglycan. *Science*, 300, 1584-1587.
- Gobert, M., Treilleux, I., Bendriss-Vermare, N., Bachelot, T., Goddard-Leon, S., Arfl, V., ... Ménétrier-Caux, C. (2009). Regulatory T cells recruited through CCL22/CCR4 are selectively activated in lymphoid infiltrates surrounding primary breast tumors and lead to an adverse clinical outcome. *Cancer Research*, 69(5), 2000-2009.
- Gordon, S. R., Maute, R. L., Dulken, B. W., Hutter, G., George, B. M., McCracken, M. N., ... Weissman, I. L. (2017). PD-1 expression by tumour-associated macrophages inhibits phagocytosis and tumour immunity. *Nature*, 545(7655), 495-499.
- Gorelik, L. *et al.* (2002). Mechanism of Transforming Growth Factor beta-induced Inhibition of T Helper Type 1 Differentiation. *Journal of Experimental Medicine*, 195(11), 1499-1505.
- Gottfried, E., Kunz-schughart, L. a, Ebner, S., Mueller-klieser, W., Hoves, S., Andreesen, R., ... Kreutz, M. (2013). Tumor-derived lactic acid modulates dendritic cell activation and antigen expression. *Differentiation*, 107(5), 2013-2021.
- Goussard, S., Grillot-Courvalin, C., & Courvalin, P. (2003). Eukaryotic promoters can direct protein synthesis in gram-negative bacteria. *Journal of Molecular Microbiology and Biotechnology*, 6(3-4), 211-218.
- Greten, F. R., Eckmann, L., Greten, T. F., Park, J. M., Li, Z. W., Egan, L. J., ... Karin, M. (2004). IKK $\beta$  links inflammation and tumorigenesis in a mouse model of colitis-associated cancer. *Cell*, 118(3), 285-296.
- Griesmann, H., Drexel, C., Milosevic, N., Sipos, B., Rosendahl, J., Gress, T. M., & Michl, P. (2016). Pharmacological macrophage inhibition decreases metastasis formation in a genetic model of pancreatic cancer. *Gut*, 66(7), 1278-1285..
- Griffioen, A., Damen, C., Blijham, G., & Groenewegen, G. (1996). Tumor angiogenesis is accompanied by a decreased inflammatory response of

- tumor-associated endothelium. *Blood*, 88(2), 667-673.
- Griffioen, A., Damen, C., Martinotti, S., Blijham, G., & Groenewegen, G. (1996). Endothelial Intercellular Adhesion Molecule-1 Expression Is Suppressed in Human. *Cancer Research*, 1(56), 1111-1117.
- Guan, G. Fang, Zhao, M., Liu, L. M., Jin, C. S., Sun, K., Zhang, D. J., ... Wen, L. J. (2013). *Salmonella typhimurium* mediated delivery of apoptin in human laryngeal cancer. *International Journal of Medical Sciences*, 10(12), 1639-1648.
- Guiducci, A., Sangaletti, S., Trinchieri, G., Colombo, M., & Christiana, V. (2005). Redirecting *in vivo* elicited tumor infiltrating macrophages and dendritic cells towards tumor rejection. *Cancer Research*, 65(8), 3437-3446.
- Guiducci, C., Vicari, A., Sangaletti, S., Trinchieri, G., & Colombo, M. (2005). Redirecting *in vivo* elicited tumor infiltrating macrophages and dendritic cells towards tumor rejection. *Cancer Research*, 65(8), 3437-3446.
- Gundra, U. M., Girgis, N. M., Gonzalez, M. A., San Tang, M., Van Der Zande, H. J. P., Lin, J.-D., ... Loke, P. (2017). Vitamin A mediates conversion of monocyte-derived macrophages into tissue-resident macrophages during alternative activation. *Nature Immunology*, 18(6), 642-653.
- Guy, C. T., Cardiff, R. D., & Muller, W. J. (1992). Induction of mammary tumors by expression of polyomavirus middle T oncogene: a transgenic mouse model for metastatic disease. *Molecular and Cellular Biology*, 12(3), 954-961.
- Haabeth, O. A. W., Lorvik, K. B., Hammarström, C., Donaldson, I. M., Haraldsen, G., Bogen, B., & Corthay, A. (2011). Inflammation driven by tumour-specific T<sub>H</sub>1 cells protects against B-cell cancer. *Nature Communications*, 2, 240.
- Halle, S., Halle, O., & Förster, R. (2017). Mechanisms and Dynamics of T Cell-Mediated Cytotoxicity *In vivo*. *Trends in Immunology*, 38(6), 432-443.
- Han, Y., Yang, Y., Chen, Z., Jiang, Z., Gu, Y., Liu, Y., ... Cao, X. (2014). Human hepatocellular carcinoma-infiltrating CD4<sup>+</sup>CD69<sup>+</sup>Foxp3<sup>-</sup> regulatory T cell suppresses T cell response via membrane-bound TGF-β1. *Journal of Molecular Medicine*, 92(5), 539-550.
- Hanahan, D., & Weinberg, R. A. (2011). Hallmarks of cancer: The next generation. *Cell*, 144(5), 646-674.
- Haraga, A., & Miller, S. I. (2003). A *Salmonella enterica* serovar Typhimurium translocated leucine-rich repeat effector protein inhibits NF-κB-dependent gene expression. *Infection and Immunity*, 71(7), 4052-4058.
- Harbour, S. N., Maynard, C. L., Zindl, C. L., Schoeb, T. R., & Weaver, C. T.

- (2015). T<sub>H</sub>17 cells give rise to Th1 cells that are required for the pathogenesis of colitis. *Proceedings of the National Academy of Sciences*, 112(22), 7061-7066.
- Harimoto, H., Shimizu, M., Nakagawa, Y., Nakatsuka, K., Wakabayashi, A., Sakamoto, C., & Takahashi, H. (2013). Inactivation of tumor-specific CD8+ CTLs by tumor-infiltrating tolerogenic dendritic cells. *Immunology and Cell Biology*, 91(9), 545-555.
- Harris, J., Dupont, H., & Hornick, R. (1972). Fecal leukocytes in diarrheal illness. *Annals of International Medicine*, 76(5), 697-703.
- Hautefort, I., Jose, M., & Hinton, J. C. D. (2003). Single-copy green fluorescent protein gene fusions allow accurate measurement of *Salmonella* gene expression *in vitro* and during infection of mammalian cells. *Applied and Environmental Microbiology*, 69(12), 7480-7491.
- Hayashi, B. A. (1998). Immuno-friendly the use remarkably patients improves survival. *Proceedings of the Japanese Academy*, 74(B), 50-55.
- Hayashi F, (2001). The innate immune response to bacterial flagellin is mediated by Toll-like receptor 5. *Nature*, 410(6832), 1099-1103.
- He, D., Hui, L., Yusuf, N., Elmets, C., Li, J., Mountz, J., & Xu, H. (2011). IL-17 promotes tumour development through the induction of tumour promoting microenvironments at tumour sites and myeloid-derived suppressor cells. *Journal of Immunology*, 184(5), 2281-2288.
- Hegazy, A. N., Peine, M., Helmstetter, C., Panse, I., Fröhlich, A., Bergthaler, A., ... Löhning, M. (2010). Interferons Direct T<sub>H</sub>2 Cell Reprogramming to Generate a Stable GATA-3+T-bet+ Cell Subset with Combined T<sub>H</sub>2 and T<sub>H</sub>1 Cell Functions. *Immunity*, 32(1), 116-128.
- Heimann, D. M., & Rosenberg, S. a. (2003). Continuous intravenous administration of live genetically modified *Salmonella typhimurium* in patients with metastatic melanoma. *Journal of Immunotherapy*, 26(2), 179-180.
- Helft, J., Ginhoux, F., Bogunovic, M., & Merad, M. (2010). Origin and functional heterogeneity of non-lymphoid tissue dendritic cells in mice. *Immunological Reviews*, 234(1), 55-75.
- Henry, T., Couillault, C., Rockenfeller, P., Boucrot, E., Dumont, A., Schroeder, N., ... Méresse, S. (2006). The *Salmonella* effector protein PipB2 is a linker for kinesin-1. *Proceedings of the National Academy of Sciences of the United States of America*, 103(36), 13497-502.
- Hense, M., Domann, E., Krusch, S., Wachholz, P., Dittmar, K. E., Rohde, M., ... Weiss, S. (2001). Eukaryotic expression plasmid transfer from the

- intracellular bacterium *Listeria monocytogenes* to host cells. *Cellular Microbiology*, 3, 599-609.
- Hersh, D., Monack, D. M., Smith, M. R., Ghori, N., Falkow, S., & Zychlinsky, A. (1999). The *Salmonella* invasin SipB induces macrophage apoptosis by binding to caspase-1. *Proceedings of the National Academy of Sciences of the United States of America*, 96(5), 2396-401.
- Higashitani, N., Higashitani, A., & Horiuchi, K. (1995). SOS induction in *Escherichia coli* by single-stranded DNA of mutant filamentous phage: Monitoring by cleavage of LexA repressor. *Journal of Bacteriology*, 177(12), 3610-3612.
- Higashitani, N., Higashitani, A., Roth, A., & Horiuchi, K. (1992). SOS induction in *Escherichia coli* by infection with mutant filamentous phage that are defective in initiation of complementary-strand DNA synthesis. *Journal of Bacteriology*, 174(5), 1612-1618.
- Hirota, K., Duarte, J. H., Veldhoen, M., Hornsby, E., Li, Y., Cua, D. J., ... Stockinger, B. (2011). Fate mapping of IL-17-producing T cells in inflammatory responses. *Nature Immunology*, 12(3), 255-263.
- Hockel, M., & Vaupel, P. (2001). Tumor Hypoxia: Definitions and Current Clinical, Biologic, and Molecular Aspects. *JNCI Journal of the National Cancer Institute*, 93(4), 266-276.
- Hohl, T. M., Rivera, A., Lipuma, L., Gallegos, A., Shi, C., Mack, M., & Pamer, E. G. (2010). Responses during Respiratory Fungal Infection, 6(5), 470-481.
- Hoiseth, S. K., & Stocker, B. A. D. (1981). Aromatic-dependent *Salmonella typhimurium* are non-virulent and effective as live vaccines. *Nature*, 291(5812), 238-9.
- Horiuchi, K. (1980). Origin of DNA replication of bacteriophage f1 as the signal for termination. *Proceedings of the National Academy of Sciences*, 77(9), 5226-5229.
- Houghton, A. M., Rzymkiewicz, D. M., Ji, H., Gregory, A. D., Egea, E. E., Metz, H. E., ... Shapiro, S. D. (2010). Neutrophil elastase-mediated degradation of IRS-1 accelerates lung tumor growth. *Nature Medicine*, 16(2), 219-223.
- Huang, B., Lei, Z., Zhao, J., Gong, W., Liu, J., Chen, Z., ... Feng, Z. (2007). CCL2/CCR2 pathway mediates recruitment of myeloid suppressor cells to cancers.
- Hübel, K., Hegener, K., Schnell, R., Mansmann, G., Oberhäuser, F., Staib, P., ... Engert, A. (1999). Suppressed neutrophil function as a risk factor for severe infection after cytotoxic chemotherapy in patients with acute nonlymphocytic leukemia. *Annals of Hematology*, 78(2), 73-77.

- Humphrey, S., Macvicar, T., Stevenson, A., Roberts, M., Humphrey, T. J., & Jepson, M. A. (2011). SulA-induced filamentation in *Salmonella enterica* serovar Typhimurium: effects on SPI-1 expression and epithelial infection. *Journal of Applied Microbiology*, *111*, 185-196.
- Humphrey, T. (2004). *Salmonella*, stress responses and food safety. *Nature Reviews Microbiology*, *2*(6), 504-509.
- Humphreys, S., Stevenson, A., Bacon, A., Weinhardt, A. B., & Roberts, M. (1999). The alternative sigma factor,  $\sigma(E)$ , is critically important for the virulence of *Salmonella typhimurium*. *Infection and Immunity*, *67*(4), 1560-1568.
- Infante-Duarte, C., Horton, H. F., Byrne, M. C., & Kamradt, T. (2000). Microbial Lipopeptides Induce the Production of IL-17 in Th Cells. *The Journal of Immunology*, *165*(11), 6107-6115.
- Ingersoll, M. A., & Albert, M. L. (2013). From infection to immunotherapy: host immune responses to bacteria at the bladder mucosa. *Mucosal Immunology*, *6*(6), 1041-1053.
- Inohara, N., Ogura, Y., Fontalba, A., Gutierrez, O., Pons, F., Crespo, J., ... Nuñez, G. (2003). Host recognition of bacterial muramyl dipeptide mediated through NOD2: Implications for Crohn's disease. *Journal of Biological Chemistry*, *278*(8), 5509-5512.
- Ishi, Y., Sonezaki, S., Iwasaki, Y., Miyata, Y., Kato, Y., & Amano, F. (2000). Regulatory role of C-terminal residues of SulA in its degradation by Lon protease in *Escherichia coli*. *Journal of Biochemistry*, *127*(5), 837-844.
- Ito, T., Wang, Y. H., & Liu, Y. J. (2005). Plasmacytoid dendritic cell precursors/type I interferon-producing cells sense viral infection by Toll-like receptor (TLR) 7 and TLR9. *Springer Seminars in Immunopathology*, *26*(3), 221-229.
- Ivanov, I. I., McKenzie, B. S., Zhou, L., Tadokoro, C. E., Lepelley, A., Lafaille, J. J., ... Flavell, R. A. (2006). The orphan nuclear receptor ROR $\gamma$  directs the differentiation program of proinflammatory IL-17<sup>+</sup> T helper cells. *Cell*, *126*(6), 1121-33.
- Ivascu, A., & Kubbies, M. (2006). Rapid Generation of Single-Tumor Spheroids for High-Throughput Cell Function and Toxicity Analysis. *Journal of Biomolecular Screening*, *11*(8), 922-932.
- Iwai, Y., Ishida, M., Tanaka, Y., Okazaki, T., Honjo, T., & Minato, N. (2002). Involvement of PD-L1 on tumor cells in the escape from host immune system and tumor immunotherapy by PD-L1 blockade. *Proceedings of the National Academy of Sciences*, *99*(19), 12293-12297.

- Jago, C. B., Yates, J., Câmara, N. O. S., & Lechler, R. I. (2004). Differential expression of CTLA-4 among T cell subsets. *Clinical Experimental Immunology*, 136(3), 436-471.
- Jakubzick, C. V., Randolph, G. J., & Henson, P. M. (2017). Monocyte differentiation and antigen-presenting functions. *Nature Reviews Immunology*, 17(6), 349-362.
- Jang, M. H., Sougawa, N., Tanaka, T., Hirata, T., Hiroi, T., Tohya, K., ... Miyasaka, M. (2006). CCR7 Is Critically Important for Migration of Dendritic Cells in Intestinal Lamina Propria to Mesenteric Lymph Nodes. *The Journal of Immunology*, 176(2), 803-810.
- Jensen, P. R., & Hammer, K. (1998). The sequence of spacers between the consensus sequences modulates the strength of prokaryotic promoters. *Applied and Environmental Microbiology*, 64(1), 82-87.
- Jeong, J. H., Kim, K., Lim, D., Jeong, K., Hong, Y., Nguyen, V. H., ... Choy, H. E. (2014). Anti-tumoral effect of the mitochondrial target domain of Noxa delivered by an engineered *Salmonella Typhimurium*. *PLoS ONE*, 9(1), 1-11.
- Jesenberger, V., Procyk, K. J., Yuan, J., Reipert, S., & Baccharini, M. (2000). *Salmonella*-induced caspase-2 activation in macrophages: a novel mechanism in pathogen-mediated apoptosis. *The Journal of Experimental Medicine*, 192(7), 1035-46.
- Jia, L., Wei, D., Sun, Q., Huang, Y., Wu, Q., & Hua, Z. (2007). Oral delivery of tumor-targeting *Salmonella* for cancer therapy in murine tumor models. *Cancer Science*, 98(7), 1107-1112.
- Johanns, T. M., Ertelt, J. M., Rowe, J. H., & Way, S. S. (2010). Regulatory t cell suppressive potency dictates the balance between bacterial proliferation and clearance during persistent *Salmonella* infection. *PLoS Pathogens*, 6(8), 31-32.
- Johansson, C., Ingman, M., & MJ, W. (2006). Elevated neutrophil, macrophage and dendritic cell numbers characterize immune cell populations in mice chronically infected with *Salmonella*. *Microbial Pathogenesis*, 41(2), 49-58.
- Johnson, S. A., Ormsby, M. J., & Wall, D. M. (2017). Draft Genome Sequence of the Tumor-Targeting *Salmonella enterica* Serovar Typhimurium Strain SL7207. *Genome Announcements*, 5(5), e01591-16.
- Joly, E., & Hudrisier, D. (2003). What is trogocytosis and what is its purpose? *Nature Immunology*, 4(9), 815.
- Jones, B. D., Ghori, N., & Falkow, S. (1994). *Salmonella typhimurium* initiates murine infection by penetrating and destroying the specialized epithelial M cells of the Peyer's patches. *The Journal of Experimental Medicine*, 180(1),

15-23.

- Jones, C. H., Rane, S., Patt, E., Ravikrishnan, A., Chen, C. K., Cheng, C., & Pfeifer, B. A. (2013). Polymyxin B treatment improves bactofection efficacy and reduces cytotoxicity. *Molecular Pharmaceutics*, *10*(11), 4301-4308.
- Jorgensen, I., Zhang, Y., Krantz, B. A., & Miao, E. A. (2016). Pyroptosis triggers pore-induced intracellular traps (PITs) that capture bacteria and lead to their clearance by efferocytosis. *The Journal of Experimental Medicine*, *213*(10), 2113-2128.
- Jovanovic, D. V, Di Battista, J. A., Martel-Pelletier, J., Jolicoeur, F. C., He, Y., Zhang, M., ... Pelletier, J. P. (1998). IL-17 stimulates the production and expression of proinflammatory cytokines, IL-beta and TNF-alpha, by human macrophages. *Journal of Immunology*, *160*(7), 3513-21.
- Jung, S., Unutmaz, D., Wong, P., Sano, G. I., De Los Santos, K., Sparwasser, T., ... Lang, R. A. (2002). *In vivo* depletion of CD11c+ dendritic cells abrogates priming of CD8+ T cells by exogenous cell-associated antigens. *Immunity*, *17*(2), 211-220.
- Justice, S., Hundstad, D., Cegelski, L., & Hultgren, S. (2008). Morphological plasticity as a bacterial survival strategy. *Nature Reviews Microbiology*, *6*(2), 162-168.
- Justice, S. S., García-Lara, J., & Rothfield, L. I. (2000). Cell division inhibitors SulA and MinC/MinD block septum formation at different steps in the assembly of the Escherichia coli division machinery. *Molecular Microbiology*, *37*(2), 410-423.
- Kaimala, S., Mohamed, Y. A., Nader, N., Issac, J., Elkord, E., Chouaib, S., ... Al-Ramadi, B. K. (2014). *Salmonella*-mediated tumor regression involves targeting of tumor myeloid suppressor cells causing a shift to M1-like phenotype and reduction in suppressive capacity. *Cancer Immunology, Immunotherapy*, *63*(6), 587-599.
- Kalupahana, R. S., Mastroeni, P., Maskell, D., & Blacklaws, B. A. (2005). Activation of murine dendritic cells and macrophages induced by *Salmonella* enterica serovar Typhimurium, 462-472.
- Kaniga, K., Trollinger, D., & Galan, J. E. (1995). Identification of two targets of the type III protein secretion system encoded by the *inv* and *spa* loci of *Salmonella* typhimurium that have homology to the Shigella IpaD and IpaA proteins. *Journal of Bacteriology*, *177*(24), 7078-7085.
- Kaplan, D. H., Shankaran, V., Dighe, A. S., Stockert, E., Aguet, M., Old, L. J., & Schreiber, R. D. (1998). Demonstration of an interferon  $\gamma$ -dependent tumor surveillance system in immunocompetent mice. *Immunology*, *95*(June), 7556-7561.

- Kasinskas, R. W., & Forbes, N. S. (2006). *Salmonella typhimurium* specifically chemotax and proliferate in heterogeneous tumor tissue *in vitro*. *Biotechnology and Bioengineering*, 94(4), 710-721.
- Kasinskas, R. W., & Forbes, N. S. (2007). *Salmonella Typhimurium* lacking ribose chemoreceptors localize in tumor quiescence and induce apoptosis. *Cancer Research*, 67(7), 3201-3209.
- Kato, H., Sato, S., Yoneyama, M., Yamamoto, M., Uematsu, S., Matsui, K., ... Akira, S. (2005). Cell type-specific involvement of RIG-I in antiviral response. *Immunity*, 23(1), 19-28.
- Kaufmann, S.H.E. and Dorhoi. (2016). Molecular determinants in phagocyte-bacteria interactions. *Immunity*, 44, 476-491.
- Kawai, T., Takeuchi, O., Fujita, T., Inoue, J. -i., Muhlradt, P. F., Sato, S., ... Akira, S. (2001). Lipopolysaccharide Stimulates the MyD88-Independent Pathway and Results in Activation of IFN-Regulatory Factor 3 and the Expression of a Subset of Lipopolysaccharide-Inducible Genes. *The Journal of Immunology*, 167(10), 5887-5894.
- Keefe, D., Shi, L., Feske, S., Massol, R., Navarro, F., Kirchhausen, T., & Lieberman, J. (2005). Perforin triggers a plasma membrane-repair response that facilitates CTL induction of apoptosis. *Immunity*, 23(3), 249-262.
- Keir, M. E., Liang, S. C., Guleria, I., Latchman, Y. E., Qipo, A., Albacker, L. A., ... Sharpe, A. H. (2006). Tissue expression of PD-L1 mediates peripheral T cell tolerance. *The Journal of Experimental Medicine*, 203(4), 883-895.
- Kel, J. M., Girard-Madoux, M. J. H., Reizis, B., & Clausen, B. E. (2010). TGF- Is Required To Maintain the Pool of Immature Langerhans Cells in the Epidermis. *The Journal of Immunology*, 185(6), 3248-3255.
- Kim, B.-H., Shenoy, A. R., Kumar, P., Das, R., Tiwari, S., MacMicking, J. D., ... Fujita, N. (2011). A family of IFN- $\gamma$ -inducible 65-kD GTPases protects against bacterial infection. *Science*, 332(6030), 717-21.
- Kim, N., Piatyszek, M., Prowse, K., Harley, C., West, M., Ho, P., ... Shay, J. (1994). Specific association of human telomerase activity with immortal cells and cancer. *Science*, 266(5193), 2011-2015.
- Kimura, Y. N., Watari, K., Fotovati, A., Hosoi, F., Yasumoto, K., Izumi, H., ... Ono, M. (2007). Inflammatory stimuli from macrophages and cancer cells synergistically promote tumor growth and angiogenesis. *Cancer Science*, 98(12), 2009-2018.
- King, I., Bermudes, D., Lin, S., Belcourt, M., Pike, J., Troy, K., ... Zheng, L.-M. (2002). Tumor-targeted *Salmonella* expressing cytosine deaminase as an anticancer agent. *Human Gene Therapy*, 13, 1225-1233.

- Kitamura, T., Qian, B.-Z., Soong, D., Cassetta, L., Noy, R., Sugano, G., ... Pollard, J. W. (2015). CCL2-induced chemokine cascade promotes breast cancer metastasis by enhancing retention of metastasis-associated macrophages. *The Journal of Experimental Medicine*, 212(7), 1043-1059.
- Klastersky, J., & Aoun, M. (2004). Opportunistic infections in patients with cancer. *Annals of Oncology: Official Journal of the European Society for Medical Oncology / ESMO*, 15 Suppl 4(Supplement 4), iv329-35.
- Kobayashi, T., Hamaguchi, Y., Hasegawa, M., Fujimoto, M., Takehara, K., & Matsushita, T. (2014). B cells promote tumor immunity against B16F10 melanoma. *Am J Pathol*, 184(11), 3120-3129.
- Kocijancic, D., Leschner, S., Felgner, S., Komoll, R.-M., Frahm, M., Pawar, V., & Weiss, S. (2017a). Therapeutic benefit of *Salmonella* attributed to LPS and TNF- $\alpha$  is exhaustible and dictated by tumor susceptibility. *Oncotarget*, 6-9.
- Koenen, H. J. P. M., Smeets, R. L., Vink, P. M., Rijssen, E. Van, Boots, A. M. H., & Joosten, I. (2008). Human CD25 high Foxp3 pos regulatory T cells differentiate into IL-17 - producing cells. *Blood*, 112(6), 2340-2352.
- Konishi, J., Yamazaki, K., Azuma, M., Kinoshita, I., Dosaka-Akita, H., & Nishimura, M. (2004). B7-H1 expression on non-small cell lung cancer cells and its relationship with tumor-infiltrating lymphocytes and their PD-1 expression. *Clinical Cancer Research: An Official Journal of the American Association for Cancer Research*, 10(15), 5094-5100.
- Kraman, M., Bambrough, P., Arnold, J., Roberts, E., Magiera, L., Jones, J., ... Fearon, D. (2010). Suppression of antitumor immunity by stromal cells expressing fibroblast activation protein- $\alpha$ . *Science*, 330(6005), 827-830.
- Krempski, J., Karyampudi, L., Behrens, M. D., Erskine, C. L., Hartmann, L., Dong, H., ... Knutson, K. L. (2011). Tumor-Infiltrating Programmed Death Receptor-1+ Dendritic Cells Mediate Immune Suppression in Ovarian Cancer. *The Journal of Immunology*, 186(12), 6905-6913.
- Krusch, S., Domann, E., Frings, M., Zelmer, A., Diener, M., Chakraborty, T., & Weiss, S. (2002). *Listeria monocytogenes* mediated CFTR transgene transfer to mammalian cells. *Journal of Gene Medicine*, 4(6), 655-667.
- Kryczek, I., Zou, L., Rodriguez, P., Zhu, G., Wei, S., Mottram, P., ... Zou, W. (2006). B7-H4 expression identifies a novel suppressive macrophage population in human ovarian carcinoma. *J Exp Med*, 203(4), 871-881.
- Kuan, Y.-D., & Lee, C.-H. (2016). *Salmonella* overcomes tumor immune tolerance by inhibition of tumor indoleamine 2, 3-dioxygenase 1 expression. *Oncotarget*, 7(1), 374-85.

- Kuang, D.-M., Zhao, Q., Peng, C., Xu, J., Zhang, J.-P., Wu, C., & Zheng, L. (2009). Activated monocytes in peritumoral stroma of hepatocellular carcinoma foster immune privilege and disease progression through PD-L1. *The Journal of Experimental Medicine*, 206(6), 1327-1337.
- Kunik, T., Tzfira, T., Kapulnik, Y., Gafni, Y., Dingwall, C., & Citovsky, V. (2001). Genetic transformation of HeLa cells by Agrobacterium. *Proceedings of the National Academy of Sciences*, 98(4), 1871-1876.
- Kusuda, T., Shigemasa, K., Arihiro, K., Fujii, T., Nagai, N., & Ohama, K. (2005). Relative expression levels of Th1 and Th2 cytokine mRNA are independent prognostic factors in patients with ovarian cancer. *Oncology Reports*, 13(6), 1153-1158.
- Lampe, M. F., Wilson, C. B., Bevan, M. J., & Starnbach, M. N. (1998). Gamma interferon production by cytotoxic T lymphocytes is required for resolution of Chlamydia trachomatis infection. *Infection and Immunity*, 66(11), 5457-61.
- Laoui, D., Keirse, J., Morias, Y., Van Overmeire, E., Geeraerts, X., Elkrim, Y., ... Van Ginderachter, J. A. (2016). The tumour microenvironment harbours ontogenically distinct dendritic cell populations with opposing effects on tumour immunity. *Nature Communications*, 7, 13720.
- Lapaque, N., Hutchinson, J. L., Jones, D. C., Meresse, S., Holden, D. W., Trowsdale, J., & Kelly, A. P. (2009). Salmonella regulates polyubiquitination and surface expression of MHC class II antigens. *Proceedings of the National Academy of Sciences*, 106(33), 14052-14057.
- Lara-Tejero, M., Sutterwala, F. S., Ogura, Y., Grant, E. P., Bertin, J., Coyle, A. J., ... Galán, J. E. (2006). Role of the caspase-1 inflammasome in Salmonella typhimurium pathogenesis. *The Journal of Experimental Medicine*, 203(6), 1407-1412.
- Larsen, M., Griesenbach, U., Goussard, S., Gruenert, D., Feddes, D., Scheule, R., ... Alton, E. (2013). Bactofection of lung epithelial cells *in vitro* and *in vivo* using a genetically modified Escherichia coli. *Gene Therapy*, 15(6), 434-442.
- Lathrop, S. K., Bloom, S. M., Rao, S. M., Nutsch, K., Chang-Lio, W., Santacruz, N., ... Stappenbeck, T. S. (2011). Peripheral education of the immune system by colonic commensal microbiota. *Nature*, 478(7368), 250-254.
- Lavin, Y., Winter, D., Blecher-Gonen, R., David, E., Keren-Shaul, H., Merad, M., ... Amit, I. (2014). Tissue-resident macrophage enhancer landscapes are shaped by the local microenvironment. *Cell*, 159(6), 1312-1326.
- Lechner, M. G., Karimi, S. S., Barry-Holson, K., Angell, T. E., Murphy, K. A., Church, C. H., ... Epstein, A. L. (2013). Immunogenicity of Murine Solid

- Tumor Models as a Defining Feature of *In vivo* Behavior and Response to Immunotherapy. *Journal of Immunotherapy*, 36(9), 477-489.
- Lee, C. A., Silva, M., Siber, A. M., Kelly, A. J., Galyov, E., & McCormick, B. A. (2000). A secreted *Salmonella* protein induces a proinflammatory response in epithelial cells, which promotes neutrophil migration. *Proceedings of the National Academy of Sciences of the United States of America*, 97(22), 12283-12288.
- Lee, C. H., Hsieh, J. L., Wu, C. L., Hsu, P. Y., & Shiau, A. L. (2011). T cell augments the antitumor activity of tumor-targeting *Salmonella*. *Applied Microbiology and Biotechnology*, 90(4), 1381-1388.
- Lee, C. H., Wu, C. L., & Shiau, A. L. (2008). Toll-like receptor 4 mediates an antitumor host response induced by *Salmonella choleraesuis*. *Clinical Cancer Research*, 14(6), 1905-1912.
- Lee, C. H., Wu, C. L., Tai, Y. S., & Shiau, A. L. (2005). Systemic administration of attenuated *Salmonella choleraesuis* in combination with cisplatin for cancer therapy. *Molecular Therapy*, 11(5), 707-716.
- Lee, C., Wu, C., & Shiau, A. (2005). Systemic administration of attenuated *Salmonella choleraesuis* survival in the murine melanoma model. *Cancer Gene Therapy*, 12(2), 175-184.
- Lee, I. S., Lin, J., Hall, H. K., & Foster, J. W. (1995). The stationary-phase sigma factor sigma S (RpoS) is required for a sustained acid tolerance response in virulent *Salmonella typhimurium*. *Molecular Microbiology*, 17(1), 155-167.
- Lee, S.-J., Dunmire, S., & McSorley, S. J. (2012). MHC class-I-restricted CD8 T cells play a protective role during primary *Salmonella* infection. *Immunology Letters*, 148(2), 138-143. h
- Lehouritis, P., Cummins, J., Stanton, M., Murphy, C. T., McCarthy, F. O., Reid, G., ... Tangney, M. (2015). Local bacteria affect the efficacy of chemotherapeutic drugs. *Scientific Reports*, 5, 14554.
- Leschner, S., Deyneko, I. V., Lienenklaus, S., Wolf, K., Bloecker, H., Bumann, D., ... Weiss, S. (2012). Identification of tumor-specific *Salmonella* Typhimurium promoters and their regulatory logic. *Nucleic Acids Research*, 40(7), 2984-2994.
- Leschner, S., Westphal, K., Dietrich, N., Viegas, N., Jablonska, J., Lienenklaus, S., ... Weiss, S. (2009). Tumor invasion of *Salmonella enterica* serovar Typhimurium is accompanied by strong hemorrhage promoted by TNF- $\alpha$ . *PLoS ONE*, 4(8).
- Leuschner, F., Dutta, P., Gorbatov, R., Novobrantseva, T. I., Donahoe, J. S., Courties, G., ... Nahrendorf, M. (2011). Therapeutic siRNA silencing in

- inflammatory monocytes in mice. *Nature Biotechnology*, 29(11), 1005-1010.
- Li, B., He, H., Zhang, S., Zhao, W., & Li, N. (2012). *Salmonella* Typhimurium strain SL7207 induces apoptosis and inhibits the growth of HepG2 hepatoma cells *in vitro* and *in vivo*. *Acta Pharmaceutica Sinica B*, 2(6), 562-568.
- Li, B., Smith, P., Horvath, D. J., Romesberg, F. E., & Justice, S. S. (2010). SOS regulatory elements are essential for UPEC pathogenesis. *Microbes and Infection*, 12(8-9), 662-668.
- Li, M. O., Wan, Y. Y., & Flavell, R. A. (2007). T Cell-Produced Transforming Growth Factor- $\beta$ 1 Controls T Cell Tolerance and Regulates Th1- and Th17-Cell Differentiation. *Immunity*, 26(5), 579-591.
- Liang, S., Alard, P., Zhao, Y., Parnell, S., Clark, S. L., & Kosiewicz, M. M. (2005). Conversion of CD4<sup>+</sup> CD25<sup>-</sup> cells into CD4<sup>+</sup> CD25<sup>+</sup> regulatory T cells *in vivo* requires B7 costimulation, but not the thymus. *The Journal of Experimental Medicine*, 201(1), 127-37.
- Lievens, D., Habets, K. L., Robertson, A. K., Laouar, Y., Winkels, H., Rademakers, T., ... Lutgens, E. (2013). Abrogated transforming growth factor beta receptor II (TGFBR2) signalling in dendritic cells promotes immune reactivity of T cells resulting in enhanced atherosclerosis. *European Heart Journal*, 34(48), 3717-3727.
- Lin, E. Y., Li, J. F., Gnatovskiy, L., Deng, Y., Zhu, L., Grzesik, D. A., ... Pollard, J. W. (2006). Macrophages regulate the angiogenic switch in a mouse model of breast cancer. *Cancer Research*, 66(23), 11238-11246.
- Lin, E. Y., Nguyen, A. V, Russell, R. G., & Pollard, J. W. (2001). Colony-stimulating factor 1 promotes progression of mammary tumors to malignancy. *The Journal of Experimental Medicine*, 193(6), 727-40.
- Linsley, P. S., Brady, W., Urnes, M., Grosmaire, L. S., Damle, N. K., & Ledbetter, J. a. (1991). CTLA-4 is a second receptor for the B cell activation antigen B7. *The Journal of Experimental Medicine*, 174(3), 561-569.
- Linsley, P. S., Nadler, S. G., Bajorath, J., Peach, R., Leung, H. T., Rogers, J., ... Shaw, S. Y. (1995). Binding stoichiometry of the cytotoxic T lymphocyte-associated molecule-4 (CTLA-4): A disulfide-linked homodimer binds two CD86 molecules. *Journal of Biological Chemistry*, 270(25), 15417-15424.
- Little, J. W. (1984). Autodigestion of lexA and phage lambda repressors. *Proceedings of the National Academy of Sciences*, 81(5), 1375-1379.
- Liu, H., Wu, X., Wand, D., Deng, W., Zan, L. and Yu, S. (2013). *In vitro* repolarized tumour macrophages inhibit gastric tumor growth. *Oncology Research*, 20(7), 275-280.

- Liu, J., Duan, Y., Cheng, X., Chen, X., Xie, W., Long, H., ... Zhu, B. (2011). IL-17 is associated with poor prognosis and promotes angiogenesis via stimulating VEGF productions in cancer cells in colorectal cancer. *Biochemical and Biophysical Research Communications*, 407(2), 348-354.
- Liu, Y., & Cao, X. (2015). Intratumoral dendritic cells in the anti-tumor immune response. *Cellular and Molecular Immunology*, 12(4), 387-390.
- Lizotte, P. H., Baird, J. R., Stevens, C. A., Lauer, P., Green, W. R., Brockstedt, D. G., & Fiering, S. N. (2014). Attenuated *Listeria monocytogenes* reprograms M2-polarized tumor-associated macrophages in ovarian cancer leading to iNOS-mediated tumor cell lysis. *Oncotarget*, 3(5), e28926.
- Llopiz, D., Ruiz, M., Infante, S., Villanueva, L., Silva, L., Hervas-Stubbs, S., ... Sarobe, P. (2016). IL-10 expression defines an immunosuppressive dendritic cell population induced by antitumor therapeutic vaccination. *Oncotarget*, 8(2), 2659-2671.
- Loeffler, M., Le'Negrate, G., Krajewska, M., & Reed, J. C. (2007). Attenuated *Salmonella* engineered to produce human cytokine LIGHT inhibit tumor growth. *Proceedings of the National Academy of Sciences of the United States of America*, 104(31), 12879-83.
- Loeffler, M., Le'Negrate, G., Krajewska, M., & Reed, J. C. (2009). *Salmonella* Typhimurium engineered to produce CCL21 inhibit tumor growth. *Cancer Immunology, Immunotherapy*, 58(5), 769-775.
- Loke, P., & Allison, J. P. (2003). PD-L1 and PD-L2 are differentially regulated by Th1 and Th2 cells. *Proceedings of the National Academy of Sciences*, 100(9), 5336-5341.
- Lord, B. I., Bronchud, M. H., Owens, S., Chang, J., Howell, A., Souza, L., & Dexter, T. M. (1989). The kinetics of human granulopoiesis following treatment with granulocyte colony-stimulating factor *in vivo*. *Proceedings of the National Academy of Sciences*, 86(23), 9499-9503.
- Low, K. B., Ittensohn, M., Le, T., Platt, J., Sodi, S., Amoss, M., ... Bermudes, D. (1999). Lipid A mutant *Salmonella* with suppressed virulence and TNFalpha induction retain tumor-targeting *in vivo*. *Nature Biotechnology*, 17, 37-41.
- Lu, B., Makhija, S. K., Nettelbeck, D. M., Rivera, A. A., Wang, M., Komarova, S., ... Zhu, Z. B. (2005). Evaluation of tumor-specific promoter activities in melanoma. *Gene Therapy*, 12(4), 330-338.
- Luo, X., Li, Z., Lin, S., Ittensohn, M., Bermudes, D., Runyab, J. D., ... Lm, Z. (2001). Antitumor effect of VNP20009, an attenuated *Salmonella*, in murine tumor models. *Oncology Research Featuring Preclinical and Clinical Cancer Therapeutics*, 12(11-12), 11-12.

- Lv, L., Pan, K., Li, X. dong, She, K. lin, Zhao, J. jing, Wang, W., ... Xia, J. chuan. (2011). The accumulation and prognosis value of tumor infiltrating IL-17 producing cells in esophageal squamous cell carcinoma. *PLoS ONE*, 6(3), 20-26.
- Macatonia, S. E., Hosken, N. A., Litton, M., Vieira, P., Hsieh, C. S., Culpepper, J. A., ... O'Garra, A. (1995). Dendritic cells produce IL-12 and direct the development of Th1 cells from naive CD4<sup>+</sup> T cells. *Journal of Immunology*, 154(10), 5071-9.
- Mackley, E. C., Houston, S., Marriott, C. L., Halford, E. E., Lucas, B., Cerovic, V., ... Withers, D. R. (2015). CCR7-dependent trafficking of ROR $\gamma$ <sup>+</sup> ILCs creates a unique microenvironment within mucosal draining lymph nodes. *Nature Communications*, 6, 5862.
- MacMicking, J. D. (2012). Interferon-inducible effector mechanisms in cell-autonomous immunity. *Nature Reviews Immunology*, 12(5), 367-382.
- MacPherson, G. G., Jenkins, C. D., Stein, M. J., & Edwards, C. (1995). Endotoxin-mediated dendritic cell release from the intestine. Characterization of released dendritic cells and TNF dependence. *Journal of Immunology*, 154(3), 1317-1322.
- Majowicz, S., Musto, J., Scallan, E., Angulo, F., Kirk, M., O'Brien, S., ... Hoekstra, R. (2010). The global burden of non-typhoidal *Salmonella* gastroenteritis. *Clinical Infectious Diseases*, 50(6), 882-889.
- Maletzki, C., Linnebacher, M., Kreikemeyer, B., & Emmrich, J. (2008). Pancreatic cancer regression by intratumoural injection of live *Streptococcus pyogenes* in a syngeneic mouse model. *Gut*, 57(4), 483-491.
- Mantovani, A., Allavena, P., Sica, A., & Balkwil, F. (2008). Cancer-related inflammation. *Nature*, 454(7203), 436-444.
- Mantovani, A., Sozzani, S., Locati, M., Allavena, P., & Sica, A. (2002). Macrophage polarization: Tumor-associated macrophages as a paradigm for polarized M2 mononuclear phagocytes. *Trends in Immunology*, 23(11), 549-555.
- Marigo, I., Bosio, E., Solito, S., Mesa, C., Fernandez, A., Dolcetti, L., ... Bronte, V. (2010). Tumor-induced tolerance and immune suppression depend on the C/EBP $\beta$  transcription factor. *Immunity*, 32(6), 790-802.
- Marth, C., Fiegl, H., Zeimet, A. G., Müller-Holzner, E., Deibl, M., Doppler, W., & Daxenbichler, G. (2004). Interferon- $\gamma$  expression is an independent prognostic factor in ovarian cancer. *American Journal of Obstetrics and Gynecology*, 191(5), 1598-1605.
- Martin-Orozco, N., Muranski, P., Chung, Y., Yang, X. O., Lu, S., Hwu, P., ...

- Dong, C. (2010). Th17 cells promote cytotoxic T cell activation in tumor immunity. *Immunity*, 31(5), 787-798.
- Mashayekhi, M., Sandau, M., Dunay, I., Frickel, E., Khan, A., Goldszmid, R., ... Murphy, K. (2011). CD8alpha<sup>+</sup> Dendritic Cells Are the Critical Source of Interleukin-12 that Controls Acute Infection by *Toxoplasma gondii* Tachyzoites. *Immunity*, 35(2), 249-259.
- Mastroeni, P., Skepper, J. N., & Hormaeche, C. E. (1995). Effect of anti-tumor necrosis factor alpha antibodies on histopathology of primary *Salmonella* infections. *Infection and Immunity*, 63(9), 3674-3682.
- Mathé, G., Florentin, I., Bruley-Rosset, M., Hayat, M., & Bourot, C. (1977). Heat-killed *Pseudomonas aeruginosa* as a systemic adjuvant in cancer immunotherapy. *Biomedicine*, 27(910), 368-373.
- Matsunaga, T., Saito, H., & Ikeguchi, M. (2011). Increased B7-H1 and B7-H4 expressions on circulating monocytes and tumor-associated macrophages are involved in immune evasion in patients with gastric cancer. *Yonago Acta Medica*, 54(1), 1-10.
- Mattick, K. L., Jørgensen, F., Legan, J. D., Cole, M. B., & Porter, J. (2000). Survival and filamentation of *Salmonella enterica* Serovar Enteritidis PT4 and *Salmonella enterica* serovar Typhimurium DT104 at low water activity. *Applied and Environmental Microbiology*, 66(4), 1274-1279.
- Mazzieri, R., Pucci, F., Moi, D., Zonari, E., Raghetti, A., Berti, A., ... De Palma, M. (2011). Targeting the ANG2/TIE2 Axis Inhibits Tumor Growth and Metastasis by Impairing Angiogenesis and Disabling Rebounds of Proangiogenic Myeloid Cells. *Cancer Cell*, 19(4), 512-526.
- McCarthy, E. F. (2006). The toxins of William B. Coley and the treatment of bone and soft-tissue sarcomas. *The Iowa Orthopaedic Journal*, 26, 154-8.
- McCormick, B. A., Hofman, P. M., Kim, J., Carnes, D. K., Miller, S. I., & Madara, J. L. (1995). Surface attachment of *Salmonella typhimurium* to intestinal epithelia imprints the subepithelial matrix with gradients chemotactic for neutrophils. *Journal of Cell Biology*, 131(6 I), 1599-1608.
- McDonald, B., Urrutia, R., Yipp, B. G., Jenne, C. N., & Kubes, P. (2012). Intravascular neutrophil extracellular traps capture bacteria from the bloodstream during sepsis. *Cell Host and Microbe*, 12(3), 324-333.
- McGarry, M. P., & Stewart, C. C. (1991). Murine eosinophil granulocytes bind the murine macrophage-monocyte specific monoclonal antibody F4/80. *Journal of Leukocyte Biology*, 50(5), 471-478.
- McGhie, E. J., Hayward, R. D., & Koronakis, V. (2001). Cooperation between actin-binding proteins of invasive *Salmonella*: SipA potentiates SipC

nucleation and bundling of actin. *EMBO Journal*, 20(9), 2131-2139.

- McIntosh, A., Meikle, L. M., Ormsby, M., McCormick, B. A., Christie, J. M., Brewer, J. M., ... Wall, D. M. (2017). SipA activation of caspase-3 is a decisive mediator of host cell survival at early stages of *Salmonella* Typhimurium infection. *Infection and Immunity*, (June), IAI.00393-17.
- McMeechan, A., Roberts, M., Cogan, T. A., Jørgensen, F., Stevenson, A., Lewis, C., ... Humphrey, T. J. (2007). Role of the alternative sigma factors  $\sigma E$  and  $\sigma S$  in survival of *Salmonella* enterica serovar Typhimurium during starvation, refrigeration and osmotic shock. *Microbiology*, 153(1), 263-269.
- McSorley, H. J., & Maizels, R. M. (2012). Helminth infections and host immune regulation. *Clinical Microbiology Reviews*, 25(1098-6618 (Electronic)), 585-608.
- Mempel, T. R., Henrickson, S.E. and von Andrian, U. H. (2004). T cell priming by dendritic cells in lymph nodes occurs in three distinct phases. *Nature*, 427 (6970), 154-159.
- Merad, M., Sathe, P., Helft, J., Miller, J., & Mortha, A. (2013). The Dendritic Cell Lineage: Ontogeny and Function of Dendritic Cells and Their Subsets in the Steady State and the Inflamed Setting. *Annual Review of Immunology*, 31(1), 563-604.
- Mercado-Lubo, R., Zhang, Y., Zhao, L., Rossi, K., Wu, X., Zou, Y., ... McCormick, B. A. (2016). A *Salmonella* nanoparticle mimic overcomes multidrug resistance in tumours. *Nature Communications*, 7, 12225.
- Mesika, A., Grigoreva, I., Zohar, M., & Reich, Z. (2001). A Regulated, NF $\kappa$ B-Assisted Import of Plasmid DNA into Mammalian Cell Nuclei. *Molecular Therapy*, 3(5), 653-657.
- Miao, E. A., & Warren, S. E. (2010). Innate immune detection of bacterial virulence factors via the NLRC4 inflammasome. *Journal of Clinical Immunology*, 30(4), 502-506.
- Michael, A., Stratford, R., Khan, S., Dalgleish, A., & Pandha, H. (2004). Novel strains of *Salmonella* typhimurium as potential vectors for gene delivery, 238, 345-351.
- Miller, A. M., & Dean, D. A. (2009). Tissue-specific and transcription factor-mediated nuclear entry of DNA. *Advanced Drug Delivery Reviews*, 61(7-8), 603-613.
- Miller, A. M., Munkonge, F. M., Alton, E. W. F. W., & Dean, D. a. (2009). Identification of protein cofactors necessary for sequence-specific plasmid DNA nuclear import. *Molecular Therapy: The Journal of the American Society of Gene Therapy*, 17(11), 1897-1903.

- Mills, C. D., Kincaid, K., Alt, J. M., Heilman, M. J., & Hill, A. M. (2000). M-1/M-2 Macrophages and the Th1/Th2 Paradigm. *The Journal of Immunology*, *164*(12), 6166-6173.
- Mills, D. M., Bajaj, V., & Lee, C. A. (1995). A 40 kb chromosomal fragment encoding *Salmonella* typhimurium invasion genes is absent from the corresponding region of the *Escherichia coli* K-12 chromosome. *Molecular Microbiology*, *15*(4), 749-759.
- Misharin, A. V., Cuda, C. M., Saber, R., Turner, J. D., Gierut, A. K., Kenneth Haines, G. K., ... Perlman, H. (2014). Nonclassical Ly6C- monocytes drive the development of inflammatory arthritis in mice. *Cell Reports*, *9*(2), 591-604.
- Mitchell, E. K., Mastroeni, P., Kelly, A. P., & Trowsdale, J. (2004). Inhibition of cell surface MHC class II expression by *Salmonella*. *European Journal of Immunology*, *34*(9), 2559-2567.
- Mizusawa, S., & Gottesman, S. (1983). Protein degradation in *Escherichia coli*: the lon gene controls the stability of sulA protein. *Proceedings of the National Academy of Sciences of the United States of America*, *80*(2), 358-362.
- Monack, D. M., Raupach, B., Hromockyj, A. E., & Falkow, S. (1996). *Salmonella* typhimurium invasion induces apoptosis from infected macrophages. *Proceedings of the National Academy of Sciences*, *93*(18), 9833-9838.
- Morales, A., Eidinger, D., & Bruce, A. (1992). Intracavitary Bacillus Calmette-Guerin in the treatment of superficial bladder tumors. *Journal of Urology*, *116*, 180-183.
- Morel, Y., Truneh, a, Sweet, R. W., Olive, D., & Costello, R. T. (2001). The TNF superfamily members LIGHT and CD154 (CD40 ligand) costimulate induction of dendritic cell maturation and elicit specific CTL activity. *Journal of Immunology*, *167*, 2479-2486.
- Mosser, D. M., & Edwards, J. P. (2008). Exploring the full spectrum of macrophage activation. *Nature Reviews Immunology*, *8*(12), 958-969.
- Movahedi, K., Laoui, D., Gysemans, C., Baeten, M., Stangé, G., Van Bossche, J. Den, ... Van Ginderachter, J. A. (2010). Different tumor microenvironments contain functionally distinct subsets of macrophages derived from Ly6C(high) monocytes. *Cancer Research*, *70*(14), 5728-5739.
- Movahedi, K., & Van Ginderachter, J. A. (2016). The ontogeny and microenvironmental regulation of tumor-associated macrophages. *Antioxidants and Redox Signaling*, *0*(0), 1-17.
- Mrsny, R., Gewirtz, A., Siccardi, D., Savidge, T., Hurley, B., Madara, J., & McCormick, B. (2004). Identification of hepoxilin A3 in inflammatory events:

- A required role in neutrophil migration across intestinal epithelia. *Proceedings of the National Academy of Sciences*, 101(19), 7421-7426.
- Mueller, R. B., Skapenko, A., Grunke, M., Wendler, J., Stuhlmüller, B., Kalden, J. R., & Schulze-Koops, H. (2005). Regulation of myeloid cell function and major histocompatibility complex class II expression by tumor necrosis factor. *Arthritis and Rheumatism*, 52(2), 451-460.
- Müller, A. J., Hoffmann, C., Galle, M., Van Den Broeke, A., Heikenwalder, M., Falter, L., ... Hardt, W. D. (2009). The *S. Typhimurium* Effector SopE Induces Caspase-1 Activation in Stromal Cells to Initiate Gut Inflammation. *Cell Host and Microbe*, 6(2), 125-136.
- Muller, W. J., Sinn, E., Pattengale, P. K., Wallace, R., & Leder, P. (1988). Single-step induction of mammary adenocarcinoma in transgenic mice bearing the activated c-neu oncogene. *Cell*, 54(1), 105-115.
- Munkonge, F. M., Amin, V., Hyde, S. C., Green, A. M., Pringle, I. A., Gill, D. R., ... Alton, E. W. F. W. (2009). Identification and functional characterization of cytoplasmic determinants of plasmid DNA nuclear import. *Journal of Biological Chemistry*, 284(39), 26978-26987.
- Murai, M., Turovskaya, O., Kim, G., Madan, R., Karp, C. L., Cheroutre, H., & Kronenberg, M. (2009). Interleukin 10 acts on regulatory T cells to maintain expression of the transcription factor Foxp3 and suppressive function in mice with colitis. *Nature Immunology* 10(11), 1178-1184.
- Muranski, P., Boni, A., Antony, P., Cassard, L., Irvine, K., Kaiser, A., ... Restifo, N. (2008). Tumor-specific T<sub>H</sub>17-polarized cells eradicate large established melanoma. *Blood*, 112(2), 362-373.
- Murray, P. J., Allen, J. E., Biswas, S. K., Fisher, E. A., Gilroy, D. W., Goerdts, S., ... Wynn, T. A. (2014). Macrophage Activation and Polarization: Nomenclature and Experimental Guidelines. *Immunity*, 41(1), 14-20.
- Nakahara, T., Oba, J., Shimomura, C., Kido-Nakahara, M., & Furue, M. (2016). Early Tumor-Infiltrating Dendritic Cells Change their Characteristics Drastically in Association with Murine Melanoma Progression. *Journal of Investigative Dermatology*, 136(1), 146-153.
- Nakanishi, J., Wada, Y., Matsumoto, K., Azuma, M., Kikuchi, K., & Ueda, S. (2007). Overexpression of B7-H1 (PD-L1) significantly associates with tumor grade and postoperative prognosis in human urothelial cancers. *Cancer Immunology, Immunotherapy*, 56(8), 1173-1182.
- Nardi, R. M., Vieira, E. C., Crocco-Afonso, L. C., Silva, M. E., Bamber, E. A., Andrade, A. M., & Nicoli, J. R. (1991). Bacteriological and immunological aspects of conventional and germfree mice infected with *Salmonella typhimurium*. *Revista Latinoamericana de Microbiologia*, 33(4), 239-243.

- Nazareth, M. R., Broderick, L., Simpson-Abelson, M. R., Kelleher, R. J., Yokota, S. J., & Bankert, R. B. (2007). Characterization of Human Lung Tumor-Associated Fibroblasts and Their Ability to Modulate the Activation of Tumor-Associated T Cells. *Journal of Immunology*, 178,(9) 5552-5562.
- Ngiow, S. F., Loi, S., Thomas, D., & Smyth, M. J. (2016). *Mouse Models of Tumor Immunotherapy. Advances in Immunology* (1st ed., Vol. 130). Elsevier Inc.
- Niess, J. H. (2005). CX3CR1-Mediated Dendritic Cell Access to the Intestinal Lumen and Bacterial Clearance. *Science*, 307(5707), 254-258.
- Noman, M. Z., Desantis, G., Janji, B., Hasmim, M., Karray, S., Dessen, P., ... Chouaib, S. (2014). PD-L1 is a novel direct target of HIF-1 $\alpha$ , and its blockade under hypoxia enhanced MDSC-mediated T cell activation. *The Journal of Experimental Medicine*, 211(5), 781-790. h
- Nomi, T., Sho, M., Akahori, T., Hamada, K., Kubo, A., Kanehiro, H., ... Nakajima, Y. (2007). Clinical significance and therapeutic potential of the programmed death-1 ligand/programmed death-1 pathway in human pancreatic cancer. *Clinical Cancer Research*, 13(7), 2151-2157.
- O'Sullivan, C., Lewis, C., Harris, A., & McGee, J. (1993). Secretion of epidermal growth factor by macrophages associated with breast carcinoma. *Lancet*, 342(8864), 148-149.
- O'Sullivan, G. C., & Lewis, C. E. (1994). Tumour associated leukocytes: friends or foes in breast carcinoma. *Journal of Pathology*, 172(3), 229-235.
- Ogura, Y., Inohara, N., Benito, A., Chen, F. F., Yamaoka, S., & Núñez, G. (2001). Nod2, a Nod1/Apaf-1 Family Member That Is Restricted to Monocytes and Activates NF- $\kappa$ B. *Journal of Biological Chemistry*, 276(7), 4812-4818.
- Ohigashi, Y., Sho, M., Yamada, Y., Tsurui, Y., Hamada, K., Ikeda, N., ... Nakajima, Y. (2005). Clinical Significance of Programmed Death-1Ligand-1 and Programmed Death-1Ligand-2 Expression in Human Esophageal Cancer. *Clinical Cancer Research*, 11(17), 2947-2953.
- Ohkuri, T., Ghosh, A., Kosaka, A., Zhu, J., Ikeura, M., David, M., ... Okada, H. (2014). STING contributes to antiglioma immunity via triggering type I IFN signals in the tumor microenvironment. *Cancer Immunology Research*, 2(12), 1199-1208.
- Ohl, L., Mohaupt, M., Czeloth, N., Hintzen, G., Kiafard, Z., Zwirner, J., ... Förster, R. (2004). CCR7 governs skin dendritic cell migration under inflammatory and steady-state conditions. *Immunity*, 21(2), 279-288.
- Ojalvo, L. S., King, W., Cox, D., & Pollard, J. W. (2009). High-density gene expression analysis of tumor-associated macrophages from mouse mammary tumors. *The American Journal of Pathology*, 174(3), 1048-1064.

- Ormsby, M. J., Johnson, S. A., & Wall, D. M. (2016). Draft Genome Sequence of the Commensal *Escherichia coli* Strain F-18. *Genome Announc*, 4.
- Padua, D., Zhang, X. H. F., Wang, Q., Nadal, C., Gerald, W. L., Gomis, R. R., & Massagué, J. (2008). TGF $\beta$  Primes Breast Tumors for Lung Metastasis Seeding through Angiopoietin-like 4. *Cell*, 133(1), 66-77.
- Paglia, P., Medina, E., Arioli, I., Guzman, C. a, & Colombo, M. P. (1998). Gene transfer in dendritic cells, induced by oral DNA vaccination with *Salmonella typhimurium*, results in protective immunity against a murine fibrosarcoma. *Blood*, 92(9), 3172-6.
- Palucka, K., & Banchereau, J. (2013). Dendritic-Cell-Based Therapeutic Cancer Vaccines. *Immunity*, 39(1), 38-48.
- Panteli, J. T., Forkus, B. a., Van Dessel, N., & Forbes, N. S. (2015). Genetically modified bacteria as a tool to detect microscopic solid tumor masses with triggered release of a recombinant biomarker. *Integrative Biology*, 7, 423-434.
- Panzer, M., Sitte, S., Wirth, S., Drexler, I., Sparwasser, T., & Voehringer, D. (2012). Rapid *In vivo* Conversion of Effector T Cells into Th2 Cells during Helminth Infection. *The Journal of Immunology*, 188(2), 615-623.
- Pardoll, D. M. (2012). The blockade of immune checkpoints in cancer immunotherapy. *Nature Reviews Cancer*, 12(4), 252-264.
- Parel, Y., & Chizzolini, C. (2004). CD4<sup>+</sup> CD8<sup>+</sup> double positive (DP) T cells in health and disease. *Autoimmunity Reviews*, 3(3), 215-220.
- Parikh, P., Palazzo, J. P., Rose, L. J., Daskalakis, C., & Weigel, R. J. (2005). GATA-3 expression as a predictor of hormone response in breast cancer. *Journal of the American College of Surgeons*, 200(5), 705-710.
- Peggs, K. S., Quezada, S. A., Chambers, C. A., Korman, A. J., & Allison, J. P. (2009). Blockade of CTLA-4 on both effector and regulatory T cell compartments contributes to the antitumor activity of anti-CTLA-4 antibodies. *The Journal of Experimental Medicine*, 206(8), 1717-1725.
- Pejcic-Karapetrovic, B., Gurnani, K., Russell, M. S., Finlay, B. B., Sad, S., & Krishnan, L. (2007). Pregnancy impairs the innate immune resistance to *Salmonella typhimurium* leading to rapid fatal infection. *J Immunol*, 179(9), 6088-6096.
- Perry, L., Feilzer, K., & Caldwell, H. (1997). Immunity to *Chlamydia trachomatis* is mediated by T helper 1 cells through IFN-gamma-dependent and -independent pathways.
- Phan, G. Q., Yang, J. C., Sherry, R. M., Hwu, P., Topalian, S. L.,

- Schwartzentruber, D. J., ... Rosenberg, S. A. (2003). Cancer regression and autoimmunity induced by cytotoxic T lymphocyte-associated antigen 4 blockade in patients with metastatic melanoma. *Proceedings of the National Academy of Sciences of the United States of America*, 100(14), 8372-7.
- Pijkereen, J. P. Van, Morrissey, D., Monk, I. R., Cronin, M., Rajendran, S., Sullivan, G. C. O., ... Tangney, M. (2010). A Novel *Listeria monocytogenes* - Based DNA Delivery System for Cancer Gene Therapy. *Human Gene Therapy*, 416(4), 405-416.
- Pilgrim, S., Stritzker, J., Schoen, C., Kolb-Mäurer, A., Geginat, G., Loessner, M. J., ... Goebel, W. (2003). Bactofection of mammalian cells by *Listeria monocytogenes*: improvement and mechanism of DNA delivery. *Gene Therapy*, 10(24), 2036-2045.
- Pinkoski, M. J., Waterhouse, N. J., Heibein, J. A., Wolf, B. B., Kuwana, T., Goldstein, J. C., ... Green, D. R. (2001). Granzyme B-mediated Apoptosis Proceeds Predominantly through a Bcl-2-inhibitable Mitochondrial Pathway. *Journal of Biological Chemistry*, 276(15), 12060-12067.
- Platt, C. D., Ma, J. K., Chalouni, C., Ebersold, M., Bou-Reslan, H., Carano, R. A. D., ... Delamarre, L. (2010). Mature dendritic cells use endocytic receptors to capture and present antigens. *Proceedings of the National Academy of Sciences of the United States of America*, 107(9), 4287-92.
- Popivanova, B. K., Kitamura, K., Wu, Y., Kondo, T., Kagaya, T., Kaneko, S., ... Mukaida, N. (2008). Blocking TNF-alpha in mice reduces colorectal carcinogenesis associated with chronic colitis. *The Journal of Clinical Investigation*, 118(2), 560-70.
- Powell, R., GK, L., & Hone, D. (1999). Method for introducing and expressing genes in animal cells and live invasive bacterial vectors for use in the same. Patent US6150170.
- Pugh, C. W., MacPherson, G. G., & Steer, H. W. (1983). Characterization of nonlymphoid cells derived from rat peripheral lymph. *The Journal of Experimental Medicine*, 157(6), 1758-79.
- Qian, B.-Z., & Pollard, J. W. J. W. (2010). Macrophage diversity enhances tumor progression and metastasis. *Cell*, 141(1), 39-51.
- Qian, B.-Z., Zhang, H., Li, J., He, T., Yeo, E.-J., Soong, D. Y. H., ... Pollard, J. W. (2015). FLT1 signaling in metastasis-associated macrophages activates an inflammatory signature that promotes breast cancer metastasis. *The Journal of Experimental Medicine*, 212(9), 1433-48.
- Qian, B., Li, J., Zhang, H., Kitamura, T., Zhang, J., Liang, R., ... Pollard, J. W. (2012). CCL2 recruits inflammatory monocytes to facilitate breast tumour

- metastasis. *Nature*, 475(7355), 222-225.
- Quillardet, P., Rouffaud, M.-A., & Bouige, P. (2003). DNA array analysis of gene expression in response to UV irradiation in *Escherichia coli*. *Research in Microbiology*, 154(8), 559-572.
- Rabsch, W., Tshape, H., & Baumler, A. (2001). Non-typhoidal salmonellosis: emerging problems. *Microbes and Infection*, 3(3), 237-247.
- Raffatellu, M., Santos, R. L., Verhoeven, D. E., George, M. D., Wilson, R. P., Winter, S. E., ... Bäumlner, A. J. (2008). Simian immunodeficiency virus-induced mucosal interleukin-17 deficiency promotes *Salmonella* dissemination from the gut. *Nature Medicine*, 14(4), 421-428.
- Raupach, B., Peuschel, S. K., Monack, D. M., & Zychlinsky, A. (2006). Caspase-1-mediated activation of interleukin-1 $\beta$  (IL-1 $\beta$ ) and IL-18 contributes to innate immune defenses against *Salmonella* enterica serovar typhimurium infection. *Infection and Immunity*, 74(8), 4922-4926.
- Ravindran, R., Foley, J., Stoklasek, T., Glimcher, L. H., & McSorley, S. J. (2005). Expression of T-bet by CD4 T cells is essential for resistance to *Salmonella* infection. *Journal of Immunology*, 175(7), 4603-4610.
- Reis e Sousa, C., Hieny, S., Scharon-Kersten, T., Jankovic, D., Charest, H., Germain, R. N., & Sher, A. (1997). *In vivo* microbial stimulation induces rapid CD40 ligand-independent production of interleukin 12 by dendritic cells and their redistribution to T cell areas. *The Journal of Experimental Medicine*, 186(11), 1819-1829.
- Richter-Dahlfors, a, Buchan, a M., & Finlay, B. B. (1997). Murine salmonellosis studied by confocal microscopy: *Salmonella* typhimurium resides intracellularly inside macrophages and exerts a cytotoxic effect on phagocytes *in vivo*. *The Journal of Experimental Medicine*, 186(4), 569-580.
- Riedel, C. U., Casey, P. G., Mulcahy, H., O'Gara, F., Gahan, C. G. M., & Hill, C. (2007). Construction of p16Slux, a novel vector for improved bioluminescent labeling of gram-negative bacteria. *Applied and Environmental Microbiology*, 73(21), 7092-7095.
- Riemensberger, J., Böhle, A., & Brandau, S. (2002). IFN-gamma and IL-12 but not IL-10 are required for local tumour surveillance in a syngeneic model of orthotopic bladder cancer. *Clinical and Experimental Immunology*, 127(1), 20-26.
- Rivollier, A., He, J., Kole, A., Valatas, V., & Kelsall, B. L. (2012). Inflammation switches the differentiation program of Ly6C<sup>hi</sup> monocytes from antiinflammatory macrophages to inflammatory dendritic cells in the colon. *The Journal of Experimental Medicine*, 209(1), 139-155.

- Roberts, E. W., Broz, M. L., Binnewies, M., Headley, M. B., Nelson, A. E., Wolf, D. M., ... Krummel, M. F. (2016). Critical Role for CD103 + /CD141 + Dendritic Cells Bearing CCR7 for Tumor Antigen Trafficking and Priming of T Cell Immunity in Melanoma HHS Public Access. *Cancer Cell*, 30(2), 324-336.
- Roberts, N. J., Zhang, L., Janku, F., Collins, A., Bai, R.-Y., Staedtke, V., ... Zhou, S. (2014). Intratumoral injection of Clostridium novyi-NT spores induces antitumor responses. *Science Translational Medicine*, 6(249), 249ra111-249ra111.
- Roca, A., & Singleton, S. (2003). Direct evaluation of a mechanism for activation of the RecA nucleoprotein filament. *Journal of the American Chemical Society*, 125(50), 15366-15375.
- Roca, H., Craig, M. J., Ying, C., Varsos, Z. S., Czarnieski, P., Alva, A. S., ... Pienta, K. J. (2012). IL-4 induces proliferation in prostate cancer PC3 cells under nutrient-depletion stress through the activation of the JNK-pathway and survivin up-regulation. *Journal of Cellular Biochemistry*, 113(5), 1569-1580.
- Rodriguez, P., Quiceno, D., Zabaleta, J., Ortiz, B., Zea, A., Piazuelo, M., ... Ochoa, A. (2004). Arginase I production in the tumor microenvironment by mature myeloid cells inhibits T-cell receptor expression and antigen-specific T-cell responses. *Cancer Research*, 64(16), 5839-5849.
- Roe, A. J., Naylor, S. W., Spears, K. J., Yull, H. M., Dransfield, T. A., Oxford, M., ... Gally, D. L. (2004). Co-ordinate single-cell expression of LEE4- and LEE5-encoded proteins of Escherichia coli O157:H7. *Molecular Microbiology*, 54(2), 337-352.
- Roland, C. L., Lynn, K. D., Toombs, J. E., Dineen, S. P., Udugamasooriya, D. G., & Brekken, R. A. (2009). Cytokine levels correlate with immune cell infiltration after anti-VEGF therapy in preclinical mouse models of breast cancer. *PLoS ONE*, 4(11), 1-13.
- Rooijen, N. Van, & Sanders, A. (1994). Liposome mediated depletion of macrophages: mechanism of action, preparation of liposomes and applications. *Journal of Immunological Methods*, 174(1-2), 83-93.
- Rossini, V., Zhurina, D., Radulovic, K., Manta, C., Walther, P., Riedel, C., & JH, N. (2014). CX3CR1(+) cells facilitate the activation of CD4 T cells in the colonic lamina propria during antigen-driven colitis. *Mucosal Immunology*, 7(3), 553-548.
- Rothstein, T., Mage, M., Jones, G., & McHugh, L. (1978). Cytotoxic T lymphocyte sequential killing of immobilized allogeneic tumor target cells measured by time-lapse microcinematography. *Journal of Immunology*, 121(5), 1652-1656.

- Rowe, J. H., Ertelt, J. M., Aguilera, M. N., Farrar, M. A., & Way, S. S. (2011). Foxp3 + regulatory T cell expansion required for sustaining pregnancy compromises host defense against prenatal bacterial pathogens. *Cell Host and Microbe*, 10(1), 54-64.
- Ruffell, B., Chang-Strachan, D., Chan, V., Rosenbusch, A., Ho, C. M. T., Pryer, N., ... Coussens, L. M. (2014). Macrophage IL-10 Blocks CD8+ T Cell-Dependent Responses to Chemotherapy by Suppressing IL-12 Expression in Intratumoral Dendritic Cells. *Cancer Cell*, 26(5), 623-637.
- Russel, M., & Model, P. (1989). Genetic analysis of the filamentous bacteriophage packaging signal and of the proteins that interact with it. *Journal of Virology*, 63(8), 3284-95.
- Rydstrom, A., & Wick, M. J. (2007). Monocyte Recruitment, Activation, and Function in the Gut-Associated Lymphoid Tissue during Oral *Salmonella* Infection. *The Journal of Immunology*, 178(9), 5789-5801.
- Rydström, A., & Wick, M. J. (2009). Monocyte and neutrophil recruitment during oral *Salmonella* infection is driven by MyD88-derived chemokines. *European Journal of Immunology*, 39(11), 3019-3030.
- Rytkönen, A., Poh, J., Garmendia, J., Boyle, C., Thompson, A., Liu, M., ... Holden, D. W. (2007). SseL, a *Salmonella* deubiquitinase required for macrophage killing and virulence. *Proceedings of the National Academy of Sciences of the United States of America*, 104(9), 3502-7.
- Saccani, A., Schioppa, T., Porta, C., Biswas, S. K., Nebuloni, M., Vago, L., ... Sica, A. (2006). p50 nuclear factor- $\kappa$ B overexpression in tumor-associated macrophages inhibits M1 inflammatory responses and antitumor resistance. *Cancer Research*, 66(23), 11432-11440.
- Saccheri, F., Pozzi, C., Avogadri, F., Barozzi, S., Faretta, M., Fusi, P., & Rescigno, M. (2010). Bacteria-Induced Gap Junctions in Tumors Favor Antigen Cross-Presentation and Antitumor Immunity. *Science Translational Medicine*, 2(44), 44ra57-44ra57.
- Sakaguchi, S., Miyara, M., Costantino, C. M., & Hafler, D. A. (2010). FOXP3+ regulatory T cells in the human immune system. *Nature Reviews Immunology*, 10(7), 490-500.
- Sakaguchi, S., Sakaguchi, N., Asano, M., Itoh, M., & Toda, M. (1995). Immunologic Self-Tolerance Maintained by Activated T Cells Expressing 11-2 Receptor  $\alpha$ -Chains (CD25). Breakdown of a single mechanism of self-tolerance causes various autoimmune diseases.. *J. Immunol*, 155(3), 1152-1164.
- Salcedo, S. P., Noursadeghi, M., Cohen, J., & Holden, D. W. (2001). Intracellular replication of *Salmonella typhimurium* strains in specific subsets of splenic

- macrophages *in vivo*. *Cellular Microbiology*, 3(9), 587-597.
- Sansonetti, P. (2001). Phagocytosis of bacterial pathogens: implications in the host response. *Seminars in Immunology*, 13(6), 381-390.
- Santos, J. L., Andrade, A. a, Dias, A. a M., Bonjardim, C. a, Reis, L. F. L., Teixeira, S. M. R., & Horta, M. F. (2006). Differential sensitivity of C57BL/6 (M-1) and BALB/c (M-2) macrophages to the stimuli of IFN-gamma/LPS for the production of NO: correlation with iNOS mRNA and protein expression. *Journal of Interferon & Cytokine Research: The Official Journal of the International Society for Interferon and Cytokine Research*, 26(9), 682-688.
- Scallan, E., Hoekstra, R. M., Angulo, F. J., Tauxe, R. V., Widdowson, M. A., Roy, S. L., ... Griffin, P. M. (2011). Foodborne illness acquired in the United States-Major pathogens. *Emerging Infectious Diseases*, 17(1), 7-15.
- Schaffner, W. (1980). Direct transfer of cloned genes from bacteria to mammalian cells. *Proceedings of the National Academy of Sciences of the United States of America*, 77(4), 2163-2167.
- Schlitzer, A., McGovern, N., Teo, P., Zelante, T., Atarashi, K., Low, D., ... Ginhoux, F. (2013). IRF4 Transcription Factor-Dependent CD11b+ Dendritic Cells in Human and Mouse Control Mucosal IL-17 Cytokine Responses. *Immunity*, 38(5), 970-983.
- Schmidt, A., Eriksson, M., Shang, M. M., Weyd, H., & Tegnér, J. (2016). Comparative analysis of protocols to induce human CD4+Foxp3+ regulatory T cells by combinations of IL-2, TGF-beta, retinoic acid, rapamycin and butyrate. *PLoS ONE*, 11(2).
- Schneider, K., Potter, K. G., & Ware, C. F. (2004). Lymphotoxin and LIGHT signaling pathways and target genes. *Immunological Reviews*, 202, 49-66.
- Schreiber, H. A., Loschko, J., Karssemeijer, R. A., Escolano, A., Meredith, M. M., Mucida, D., ... Nussenzweig, M. C. (2013). Intestinal monocytes and macrophages are required for T cell polarization in response to *Citrobacter rodentium*. *The Journal of Experimental Medicine*, 210(10), 2025-2039.
- Schwartz, R. (1992). Costimulation of T lymphocytes: the role of CD28, CTLA-4, and B7/BB1 in interleukin-2 production and immunotherapy. *Cell*, 71(7), 1065-1068.
- Segal, A. W. (2005). How Neutrophils Kill Microbes. *Annual Review of Immunology*, 23(1), 197-223.
- Serbina, N. V., Salazar-Mather, T. P., Biron, C. A., Kuziel, W. A., & Pamer, E. G. (2003). TNF/iNOS-producing dendritic cells mediate innate immune defense against bacterial infection. *Immunity*, 19(1), 59-70.

- Serbina, N. V., & Pamer, E. G. (2006). Monocyte emigration from bone marrow during bacterial infection requires signals mediated by chemokine receptor CCR2. *Nature Immunology*, 7(3), 311-317.
- Shankaran, V., Ikeda, H., Bruce, a T., White, J. M., Swanson, P. E., Old, L. J., & Schreiber, R. D. (2001). IFN $\gamma$  and lymphocytes prevent primary tumour development and shape tumour immunogenicity. *Nature*, 410(6832), 1107-1111.
- Sharma, A., Kuzu, O. F., Nguyen, F. D., Sharma, A., & Noory, M. (2015). Current State of Animal (Mouse) Modeling in Melanoma Research. *Cancer Growth and Metastasis*, 81.
- Shi, L., Keefe, D., Durand, E., Feng, H., Zhang, D., & Lieberman, J. (2005). Granzyme B binds to target cells mostly by charge and must be added at the same time as perforin to trigger apoptosis. *Journal of Immunology*, 174(9), 5456-5461.
- Shimizu, J., Yamazaki, S., & Sakaguchi, S. (1999). Induction of tumor immunity by removing CD25+CD4+ T cells: a common basis between tumor immunity and autoimmunity. *Journal of Immunology*, 163(10), 5211-8.
- Shmuel-Galia, L., Aychek, T., Fink, A., Porat, Z., Zarmi, B., Bernshtein, B., ... Shai, Y. (2016). Neutralization of pro-inflammatory monocytes by targeting TLR2 dimerization ameliorates colitis. *The EMBO Journal*, 35(6), 685-698.
- Shurin, M. R., Yurkovetsky, Z. R., Tourkova, I. L., Balkir, L., & Shurin, G. V. (2002). Inhibition of CD40 expression and CD40-mediated dendritic cell function by tumor-derived IL-10. *International Journal of Cancer*, 101(1), 61-68.
- Sica, A., Larghi, P., Mancino, A., Rubino, L., Porta, C., Totaro, M. G., ... Mantovani, A. (2008). Macrophage polarization in tumour progression. *Seminars in Cancer Biology*, 18(5), 349-355.
- Siccardi, D., Mummy, K. L., Wall, D. M., Bien, J. D., & McCormick, B. A. (2008). *Salmonella* enterica serovar Typhimurium modulates P-glycoprotein in the intestinal epithelium. *American Journal of Physiology. Gastrointestinal and Liver Physiology*, 294(6), G1392-400.
- Silzle, T., Kreutz, M., Dobler, M. A., Brockhoff, G., Knuechel, R., & Kunz-Schughart, L. A. (2003). Tumor-associated fibroblasts recruit blood monocytes into tumor tissue. *European Journal of Immunology*, 33(5), 1311-1320.
- Sizemore, D. R., Branstrom, a a, & Sadoff, J. C. (1995). Attenuated Shigella as a DNA delivery vehicle for DNA-mediated immunization. *Science*, 270(5234), 299-302.

- Smith, E., Zarbock, A., Stark, M. a, Burcin, T. L., Bruce, A. C., Foley, P., & Ley, K. (2007). IL-23 Is Required for Neutrophil Homeostasis in Normal and Neutrophilic Mice. *The Journal of Immunology*, 179(12), 8274-8279.
- Smyth, M. J., Thia, K. Y., Street, S. E., MacGregor, D., Godfrey, D. I., & Trapani, J. A. (2000). Perforin-mediated cytotoxicity is critical for surveillance of spontaneous lymphoma. *J Exp Med*, 192(5), 755-760.
- Song, Z., Li, Z. H., Lei, X. Q., Xu, T. S., Zhang, X. H., Li, Y. J., ... Wei, Z. G. (2015). Construction of the mammalian expressing vector pEGFP-N1-P53 and its expression successful in chicken fibroblast cells and blastoderm. *Genetics and Molecular Research*, 14(1), 931-939.
- Sonnenberg, G. F., Fouser, L. A., & Artis, D. (2010). Functional biology of the IL-22-IL-22R pathway in regulating immunity and inflammation at barrier surfaces. *Advances in Immunology*, 107(C), 1-29.
- Srikanth, C. V., Wall, D. M., Maldonado-Contreras, A., Shi, H. N., Zhou, D., Demma, Z., ... McCormick, B. A. (2010). *Salmonella* Pathogenesis and Processing of Secreted Effectors by Caspase-3. *Science*, 330(6002), 390-393.
- Stackhouse, R. R., Faith, N. G., Kaspar, C. W., Czuprynski, C. J., & Wong, A. C. L. (2012). Survival and virulence of *Salmonella* enterica serovar enteritidis filaments induced by reduced water activity. *Applied and Environmental Microbiology*, 78(7), 2213-2220.
- Starnes, C. O. (1992). Coley's toxins in perspective. *Nature*, 357(6373), 11-2.
- Stender, S., Friebel, A., Linder, S., Rohde, M., Miold, S., & Hardt, W. D. (2000). Identification of SopE2 from *Salmonella typhimurium*, a conserved guanine nucleotide exchange factor for Cdc42 of the host cell. *Molecular Microbiology*, 36(6), 1206-21.
- Stern, C., Kasnitz, N., Kocijancic, D., Trittel, S., Riese, P., Guzman, C. a, ... Weiss, S. (2015). Induction of CD4(+) and CD8(+) anti-tumor effector T cell responses by bacteria mediated tumor therapy. *International Journal of Cancer*, 2028, 2019-2028.
- Stoitzner, P., Green, L. ., Jung, J., Price, K., Atarea, H., Kivell, B., & Ronchese, F. (2008). Inefficient presentation of tumor-derived antigen by tumor-infiltrating dendritic cells. *Cancer Immunology, Immunotherapy*, 57, 1665-1673.
- Strauss, L., Bergmann, C., Szczepanski, M., Gooding, W., Johnson, J. T., & Whiteside, T. L. (2007). A unique subset of CD4+CD25highFoxp3+ T cells secreting interleukin-10 and transforming growth factor-B1 mediates suppression in the tumor microenvironment. *Clinical Cancer Research*, 13(15), 4345-4354.

- Streilein, J. W. (1995). Unraveling immune privilege. *Science*, 270(November), 2-3.
- Stritesky, G. L., Yeh, N., & Kaplan, M. H. (2008). IL-23 Promotes Maintenance but Not Commitment to the. *The Journal of Immunology*, 181(9), 5948-5955.
- Suggit, M., & Bibby, M. (2005). 50 years of preclinical anticancer drug screening: empirical to target-driven approaches. *Clinical Cancer Research*, 11(3), 971-981.
- Sutherland, R. M., Sordat, B., Bamat, J., Gabbert, H., & Bourrā, B. (1986). Oxygenation and Differentiation in Multicellular Colon Carcinoma Spheroids of Human. *Regulation*, (10), 5320-5329.
- Suttman, H., Riemensberger, J., Bentien, G., Schmaltz, D., Stöckle, M., Jocham, D., ... Brandau, S. (2006a). Neutrophil Granulocytes Are Required for Effective Bacillus Calmette-Guéri Immunotherapy of Bladder Cancer and Orchestrate Local Immune Responses. *Cancer Research*, 66(16), 8250-8257.
- Suttman, H., Riemensberger, J., Bentien, G., Schmaltz, D., Stöckle, M., Jocham, D., ... Brandau, S. (2006b). Neutrophil granulocytes are required for effective Bacillus Calmette-Guérin immunotherapy of bladder cancer and orchestrate local immune responses. *Cancer Research*, 66(16), 8250-8257.
- Swirski, F. K., Nahrendorf, M., Etzrodt, M., Wildgruber, M., Panizzi, P., Figueiredo, J., ... Pittet, J. (2009). Identification Monocytes Inflammatory of Splenic Reservoir and Their Deployment Sites. *Science*, 325(5940), 612-616.
- Symonds, E. L., Riedel, C. U., O'Mahony, D., Laphorne, S., O'Mahony, L., & Shanahan, F. (2009). Involvement of T helper type 17 and regulatory T cell activity in *Citrobacter rodentium* invasion and inflammatory damage. *Clinical and Experimental Immunology*, 157(1), 148-154.
- Szabo, S. J., Kim, S. T., Costa, G. L., Zhang, X., Fathman, C. G., & Glimcher, L. H. (2000). A novel transcription factor, T-bet, directs Th1 lineage commitment. *Cell*, 100(6), 655-669. h
- Tacke, F., Alvarez, D., Kaplan, T. J., Jakubzick, C., Spanbroek, R., Llodra, J., ... Randolph, G. J. (2007). Monocyte subsets differentially employ CCR2, CCR5, and CX3CR1 to accumulate within atherosclerotic plaques. *Journal of Clinical Investigation*, 117(1), 185-194.
- Tam, M. A., Rydström, A., Sundquist, M., & Wick, M. J. (2008). Early cellular responses to *Salmonella* infection: Dendritic cells, monocytes, and more. *Immunological Reviews*, 225(1), 140-162.
- Tan, M. C. B., Goedegebuure, P. S., Belt, B. a, Flaherty, B., Sankpal, N., Gillanders, W. E., ... Linehan, D. C. (2009). Disruption of CCR5-dependent

- homing of regulatory T cells inhibits tumor growth in a murine model of pancreatic cancer. *Journal of Immunology*, 182, 1746-1755.
- Tassi, E., Gavazzi, F., Albarello, L., Senyukov, V., Longhi, R., Dellabona, P., ... Protti, M. P. (2008). Carcinoembryonic Antigen-Specific but Not Antiviral CD4+ T Cell Immunity Is Impaired in Pancreatic Carcinoma Patients. *The Journal of Immunology*, 181(9), 6595-6603.
- Terme, M., Ullrich, E., Aymeric, L., Meinhardt, K., Desbois, M., Delahaye, N., ... Zitvogel, L. (2011). IL-18 induces PD-1-dependent immunosuppression in cancer. *Cancer Research*, 71(16), 5393-5399.
- Thomas, D. a, & Massagué, J. (2005). TGF-beta directly targets cytotoxic T cell functions during tumor evasion of immune surveillance. *Cancer Cell*, 8(5), 369-80.
- Thomas, D. L., Kim, M., Bowerman, N. A., Narayanan, S., Kranz, D. M., Schreiber, H., & Roy, E. J. (2009). Recurrence of intracranial tumors following adoptive T cell therapy can be prevented by direct and indirect killing aided by high levels of tumor antigen cross-presented on stromal cells. *Journal of Immunology*, 183(3), 1828-1837.
- Thompson, R. H., Gillett, M. D., Cheville, J. C., Lohse, C. M., Dong, H., Webster, W. S., ... Kwon, E. D. (2004). Costimulatory B7-H1 in renal cell carcinoma patients: Indicator of tumor aggressiveness and potential therapeutic target. *Proceedings of the National Academy of Sciences of the United States of America*, 101(49), 17174-9.
- Thornlow, D. N., Brackett, E. L., Gigas, J. M., Van Dessel, N., & Forbes, N. S. (2015). Persistent enhancement of bacterial motility increases tumor penetration. *Biotechnology and Bioengineering*, 112(11), 2397-2405.
- Topalian, S. L., Hodi, F. S., Brahmer, J. R., Gettinger, S. N., Smith, D. C., McDermott, D. F., ... Sznol, M. (2012). Safety, Activity, and Immune Correlates of Anti-PD-1 Antibody in Cancer. *New England Journal of Medicine*, 366(26), 2443-2454.
- Torcellan, T., Hampton, H. R., Bailey, J., Tomura, M., Brink, R., & Chtanova, T. (2017). *In vivo* photolabeling of tumor-infiltrating cells reveals highly regulated egress of T-cell subsets from tumors. *Proceedings of the National Academy of Sciences*, 114(22), 5677-5682.
- Toso, B. J. F., Gill, V. J., Hwu, P., Marincola, F. M., Restifo, N. P., Schwartzentruber, D. J., ... Rosenberg, S. A. (2002). Phase I Study of the Intravenous Administration of Attenuated *Salmonella typhimurium* to Patients With Metastatic Melanoma. *Journal of Clinical Oncology*, 20(1), 142-152.
- Tosolini, M., Kirilovsky, A., Mlecnik, B., Fredriksen, T., Mauger, S., Bindea, G., ...

- Galon, J. (2011). Clinical impact of different classes of infiltrating T cytotoxic and helper cells (Th1, Th2, Treg, Th17) in patients with colorectal cancer. *Cancer Research*, 71(4), 1263-1271.
- Trotter, L. A., Patel, D., Dubin, S., Guerra, C., McCloud, V., Lockwood, P., ... Nabeshima, Y. (2017). Violet/blue light activates Nrf2 signaling and modulates the inflammatory response of THP-1 monocytes. *Photochemical and Photobiological Sciences*, 16(6), 883-889.
- Trusca, D., Scott, S., & Thompson, C. (1998). Bacterial SOS Checkpoint Protein Sula Inhibits Polymerization of Purified FtsZ Cell Division Protein. *Journal of Bacteriology*, 180(15), 3946-3953.
- Tsou, C. L., Peters, W., Si, Y., Slaymaker, S., Aslanian, A. M., Weisberg, S. P., ... Charo, I. F. (2007). Critical roles for CCR2 and MCP-3 in monocyte mobilization from bone marrow and recruitment to inflammatory sites. *Journal of Clinical Investigation*, 117(4), 902-909.
- Tsuji, S., Matsumoto, M., Takeuchi, O., Akira, S., Azuma, I., Hayashi, A., ... Seya, T. (2000). Maturation of human dendritic cells by cell wall skeleton of *Mycobacterium bovis bacillus Calmette-Guérin*: involvement of toll-like receptors. *Infection and Immunity*, 68(12), 6883-6890.
- Turnbull, E. L., Yrlid, U., Jenkins, C. D., & Macpherson, G. G. (2005). Intestinal dendritic cell subsets: differential effects of systemic TLR4 stimulation on migratory fate and activation *in vivo*. *Journal of Immunology*, 174, 1374-1384.
- Ueda, Y., Cain, D., Kuraoka, M., Kondo, M., & Kelsoe, G. (2009). IL-1RI dependent HSC proliferation is necessary for Inflammatory granulopoiesis and reactive neutrophils. *Journal of Immunology*, 182(10), 6477-6484.
- Uhlig, H. H., Coombes, J., Mottet, C., Izcue, A., Thompson, C., Fanger, A., ... Powrie, F. (2006). Characterization of Foxp3+CD4+CD25+ and IL-10-Secreting CD4+CD25+ T Cells during Cure of Colitis. *The Journal of Immunology*, 177(9), 5852-5860.
- Vacik, J., Dean, B. S., Zimmer, W. E., & Dean, D. A. (1999). Cell-specific nuclear import of plasmid DNA. *Gene Therapy*, 6(6), 1006-1014.
- Valdez, Y., Diehl, G. E., Vallance, B. A., Grassl, G. A., Guttman, J. A., Brown, N. F., ... Finlay, B. B. (2008). Nramp1 expression by dendritic cells modulates inflammatory responses during *Salmonella* Typhimurium infection. *Cellular Microbiology*, 10(8), 1646-1661.
- Van der Velden, A., Tam, J., & Bliska, J. (2015). Essential role for CCR2+ inflammatory monocytes in early and late control of persistent *Salmonella* infection. *Journal of Immunology*, 194(1), 120-124.

- van Elsas, A., Hurwitz, a a, & Allison, J. P. (1999). Combination immunotherapy of B16 melanoma using anti-cytotoxic T lymphocyte-associated antigen 4 (CTLA-4) and granulocyte/macrophage colony-stimulating factor (GM-CSF)-producing vaccines induces rejection of subcutaneous and metastatic tumors accompanied . *The Journal of Experimental Medicine*, 190(3), 355-366.
- Vance, R. E., Isberg, R. R., & Portnoy, D. A. (2010). Pathogenic Microbes By the Innate Immune System. *Cell*, 6(1), 10-21.
- Vaughan, E. E., & Dean, D. A. (2006). Intracellular trafficking of plasmids during transfection is mediated by microtubules. *Molecular Therapy*, 13(2), 422-428.
- Veldhoen, M., Hocking, R. J., Atkins, C. J., Locksley, R. M., & Stockinger, B. (2006). TGF $\beta$  in the context of an inflammatory cytokine milieu supports de novo differentiation of IL-17-producing T cells. *Immunity*, 24(2), 179-189.
- Vicari, A. P., Chiodoni, C., Vaure, C., Ait-Yahia, S., Dercamp, C., Matsos, F., ... Caux, C. (2002). Reversal of tumor-induced dendritic cell paralysis by CpG immunostimulatory oligonucleotide and anti-interleukin 10 receptor antibody. *The Journal of Experimental Medicine*, 196(4), 541-549.
- Vinci, M., Box, C., & Eccles, S. A. (2015). Three-Dimensional (3D) Tumor Spheroid Invasion Assay. *Journal of Visualized Experiments*, (99).
- Viscoli, C., Varnier, O., & Machetti, M. (2005). Infections in Patients with Febrile Neutropenia: Epidemiology, Microbiology, and Risk Stratification. *Clinical Infectious Diseases*, 40(Supplement 4), S240-S245.
- Wada, Y., Yoshida, K., Hihara, J., Konishi, K., Tanabe, K., Ukon, K., ... Mizuiri, H. (2006). Sivelestat, a specific neutrophil elastase inhibitor, suppresses the growth of gastric carcinoma cells by preventing the release of transforming growth factor- $\alpha$ . *Cancer Science*, 97(10), 1037-1043.
- Wada, Y., Yoshida, K., Tsutani, Y., Shigematsu, H., Oeda, M., Sanada, Y., ... Hihara, J. (2007). Neutrophil elastase induces cell proliferation and migration by the release of TGF- $\alpha$ , PDGF and VEGF in esophageal cell lines. *Oncology Reports*, 17(1), 161-7.
- Wall, D. M., Nadeau, W. J., Pazos, M. A., Shi, H. N., Galyov, E. E., & McCormick, B. A. (2007). Identification of the *Salmonella* enterica serotype Typhimurium SipA domain responsible for inducing neutrophil recruitment across the intestinal epithelium. *Cellular Microbiology*, 9(9), 2299-2313.
- Wall, L., Burke, F., Barton, C., Smyth, J., & Balkwill, F. (2003). IFN-gamma induces apoptosis in ovarian cancer cells *in vivo* and *in vitro*. *Clinical Cancer Research*. 9(1078), 2487-2496.
- Wall, L., Burke, F., Barton, C., Smyth, J., & Balkwill, F. (2003). IFN-gamma

- induces apoptosis in ovarian cancer cells *in vivo* and *in vitro*. *Clinical Cancer Research: An Official Journal of the American Association for Cancer Research*, 9(7), 2487-2496.
- Wang, C. Z., Kazmierczak, R. A., & Eisenstark, A. (2016). Strains, mechanism, and perspective: *Salmonella* -based cancer therapy: *Salmonella* -based cancer therapy. *International Journal of Microbiology*, 2016.
- Wang, W., Lau, R., Yu, D., Zhu, W., Korman, A., & Weber, J. (2009). PD1 blockade reverses the suppression of melanoma antigen-specific CTL by CD4 1 CD25 Hi regulatory T cells. *International Immunology*, 21(9), 1065-1077.
- Watanabe, H., Numata, K., Ito, T., Takagi, K., & Matsukawa, A. (2004). Innate immune response in Th1- and Th2-dominant mouse strains. *Shock*, 22(5), 460-466.
- Wegrzyn, G., & Wegrzyn, A. (2002). Stress responses and replication of plasmids in bacterial cells. *Microbial Cell Factories*, 1(1), 2.
- Weiss, S. (2003). Transfer of eukaryotic expression plasmids to mammalian hosts by attenuated *Salmonella* spp. *International Journal of Medical Microbiology: IJMM*, 293(1), 95-106.
- Weisser, S. B., van Rooijen, N., & Sly, L. M. (2012). Depletion and Reconstitution of Macrophages in Mice. *Journal of Visualized Experiments*, (66).
- Westphal, K., Leschner, S., Jablonska, J., Loessner, H., & Weiss, S. (2008). Containment of tumor-colonizing bacteria by host neutrophils. *Cancer Research*, 68(8), 2952-2960.
- Wick, M. J. (2011). Innate immune control of *Salmonella* enterica serovar typhimurium: Mechanisms contributing to combating systemic *Salmonella* infection. *Journal of Innate Immunity*, 3(6), 543-549.
- Williams, C., Yeh, E., & Soloff, A. (2016). Tumour-associated macrophages: unwitting accomplices in breast cancer malignancy. *Breast Cancer*, 2, 15025-15034.
- Williams, L. M., & Rudensky, A. Y. (2007). Maintenance of the Foxp3-dependent developmental program in mature regulatory T cells requires continued expression of Foxp3. *Nature Immunology*, 8(3), 277-284.
- Wu, Q., Martin, R. J., Rino, J. G., Breed, R., Torres, R. M., & Chu, H. W. (2007). IL-23-dependent IL-17 production is essential in neutrophil recruitment and activity in mouse lung defense against respiratory *Mycoplasma pneumoniae* infection. *Microbes and Infection*, 9(1), 78-86.
- Xu, L., Kitani, A., Fuss, I., & Strober, W. (2007). Cutting Edge: Regulatory T Cells Induce T Cells or Are Self-Induced to Become Th17 Cells in the Absence of

- Exogenous TGF-beta. *The Journal of Immunology*, 178(8), 6725-6729.
- Yamamoto, M., Sato, S., Hemmi, H., Hoshino, K., Kaisho, T., Sanjo, H., ... Akira, S. (2003). Role of Adaptor TRIF in the MyD88-Independent Toll-Like Receptor Signaling Pathway. *Science*, 301(5633), 640-643.
- Yamamura, Y., Sakatani, M., Ogura, T., & Azuma, I. (1979). Adjuvant immunotherapy of lung cancer with BCG cell wall skeleton (BCG-CWS). *Cancer*, 43(4), 1314-1319.
- Yang, X. O., Nurieva, R., Martinez, G. J., Kang, H. S., Chung, Y., Pappu, B. P., ... Dong, C. (2008). Molecular Antagonism and Plasticity of Regulatory and Inflammatory T Cell Programs. *Immunity*, 29(1), 44-56.
- Yano, S., Zhang, Y., Zhao, M., Hiroshima, Y., Miwa, S., Uehara, F., ... Hoffman, R. (2014). Tumor-targeting *Salmonella* typhimurium A1-R decoys quiescent cancer cells to cycle as visualized by FUCCI imaging and become sensitive to chemotherapy. *Cell Cycle*, 13(24), 3958-3963.
- Ye, P., Rodriguez, F. H., Kanaly, S., Stocking, K. L., Schurr, J., Schwarzenberger, P., ... Kolls, J. K. (2001). Requirement of Interleukin 17 Receptor Signaling for Lung Cxc Chemokine and Granulocyte Colony-Stimulating Factor Expression, Neutrophil Recruitment, and Host Defense. *The Journal of Experimental Medicine*, 194(4), 519-528.
- Ying, L., Aifeng, Z., Wenqi, H., Guoliang, L., Junbo, Z., Jie, G., ... Chaofeng, S. (2012). Construction of recombinant plasmid pEGFP-C2-L539fs/47 and its expression in HEK293 cells. *Journal of Medical Colleges of PLA*, 27(3), 125-133.
- Yoon, W. S., Chae, Y. S., Hong, J., Park, Y. K. (2001). Antitumor therapeutic effects of a genetically engineered *Salmonella* typhimurium harboring TNF $\alpha$  in mice. *Applied Microbiology and Biotechnology*, 89, 1807-1819.
- Yrlid, U., Cerovic, V., Milling, S., Jenkins, C. D., Klavinskis, L. S., & MacPherson, G. G. (2006). A distinct subset of intestinal dendritic cells responds selectively to oral TLR7/8 stimulation. *European Journal of Immunology*, 36(10), 2639-2648.
- Yrlid, U., Svensson, M., Johansson, C., & Wick, M. J. (2000). *Salmonella* infection of bone marrow-derived macrophages and dendritic cells: influence on antigen presentation and initiating an immune response. *FEMS Immunology and Medical Microbiology*, 27(4), 313-20.
- Yu, B., Yang, M., Shi, L., Yao, Y., Jiang, Q., Li, X., ... Huang, J.-D. (2012). Explicit hypoxia targeting with tumor suppression by creating an "obligate" anaerobic *Salmonella* Typhimurium strain. *Scientific Reports*, 2.
- Yuhua, L., Kunyuan, G., Hui, C., Yongmei, X., Chaoyang, S., Xun, T., & Daming,

- R. (2001). Oral cytokine gene therapy against murine tumor using attenuated *Salmonella typhimurium*. *International Journal of Cancer*, *94*(3), 438-443.
- Zea, A. H., Rodriguez, P. C., Culotta, K. S., Hernandez, C. P., DeSalvo, J., Ochoa, J. B., ... Ochoa, A. C. (2004). L-Arginine modulates CD3zeta expression and T cell function in activated human T lymphocytes. *Cellular Immunology*, *232*(1-2), 21-31.
- Zeisberger, S. M., Odermatt, B., Marty, C., Zehnder-Fjällman, A. H. M., Ballmer-Hofer, K., & Schwendener, R. A. (2006). Clodronate-liposome-mediated depletion of tumour-associated macrophages: a new and highly effective antiangiogenic therapy approach. *British Journal of Cancer*, *95*(3), 272-281.
- Zhang, J., Nguyen-Jackson, H., Panopoulos, A., Li, H., Murray, P., & Watowich, S. (2010). STAT3 controls myeloid progenitor growth during emergency granulopoiesis. *Blood*, *115*(14), 2462-2471.
- Zhang, Q. J., Li, X. L., Wang, D., Huang, X. C., Mathis, J. M., Duan, W. M., ... Jefferies, W. A. (2008). Trogocytosis of MHC-I/Peptide Complexes Derived from Tumors and Infected Cells Enhances Dendritic Cell Cross-Priming and Promotes Adaptive T Cell Responses. *PLoS ONE*, *3*(8).
- Zhang, Y., Zhang, N., Zhao, M., & Hoffman, R. M. (2015). Comparison of the selective targeting efficacy of *Salmonella typhimurium* A1-R and VNP20009 on the Lewis lung carcinoma in nude mice. *Oncotarget*, *6*(16), 14625-14631.
- Zhao, M., Yang, M., Li, X. M., Jiang, P., Baranov, E., Li, S., ... Trump, D. L. (2005). Tumor-targeting bacterial therapy with amino acid auxotrophs of GFP-expressing *Salmonella typhimurium*. *Urologic Oncology: Seminars and Original Investigations*, *23*(5), 380.
- Zhao, M., Yang, M., Ma, H., Li, X., Tan, X., Li, S., ... Hoffman, R. M. (2006). Targeted therapy with a *Salmonella typhimurium* leucine-arginine auxotroph cures orthotopic human breast tumors in nude mice. *Cancer Research*, *66*(15), 7647-7652.
- Zheng, J. H., & Min, J.-J. (2016). Targeted Cancer Therapy Using Engineered *Salmonella typhimurium*. *Chonnam Medical Journal*, *52*(3), 173-84.
- Zheng, J. H., Nguyen, V. H., Jiang, S.-N., Park, S.-H., Tan, W., Hong, S. H., ... Min, J. (2017a). Molecular Profiling Reveals a Tumor-Promoting Phenotype of Monocytes and Macrophages in Human Cancer Progression. *Science Translational Medicine*, *9*(eaak9537), 815-829.
- Zheng, J. H., Nguyen, V. H., Jiang, S.-N., Park, S.-H., Tan, W., Hong, S. H., ... Min, J. (2017b). Two-step enhanced cancer immunotherapy with engineered *Salmonella typhimurium* secreting heterologous flagellin. *Science Translational Medicine*, *9*(eaak9537), 1-11.

- Zheng, W., & Flavell, R. A. (1997). The Transcription Factor GATA-3 Is Necessary and Sufficient for Th2 Cytokine Gene Expression in CD4 T Cells. *Cell*, *89*(4), 587-596.
- Zheng, Y., Valdez, P. A., Danilenko, D. M., Hu, Y., Sa, S. M., Gong, Q., ... Ouyang, W. (2008). Interleukin-22 mediates early host defense against attaching and effacing bacterial pathogens. *Nature Medicine*, *14*(3), 282-289.
- Zhou, X., Bailey-bucktrout, S., Jeker, L. T., Penaranda, C., Ashby, M., Nakayama, M., ... Jeffrey, A. (2010). Foxp3 instability leads to the generation of pathogenic memory T cells *in vivo*. *Nature Immunology*, *10*(9), 1000-1007.
- Zigmond, E., Varol, C., Farache, J., Elmaliah, E., Satpathy, A. T., Friedlander, G., ... Jung, S. (2012). Ly6Chi Monocytes in the Inflamed Colon Give Rise to Proinflammatory Effector Cells and Migratory Antigen-Presenting Cells. *Immunity*, *37*(6),
- Zitvogel, L., Pitt, J. M., Daillère, R., Smyth, M. J., & Kroemer, G. (2016). Mouse models in oncoimmunology. *Nature Reviews Cancer*, *16*(12), 759-773.
- Zou, W. (2005). Immunosuppressive networks in the tumour environment and their therapeutic relevance. *Nature Reviews Cancer*, *5*(4), 263-274.

## 9 Appendix

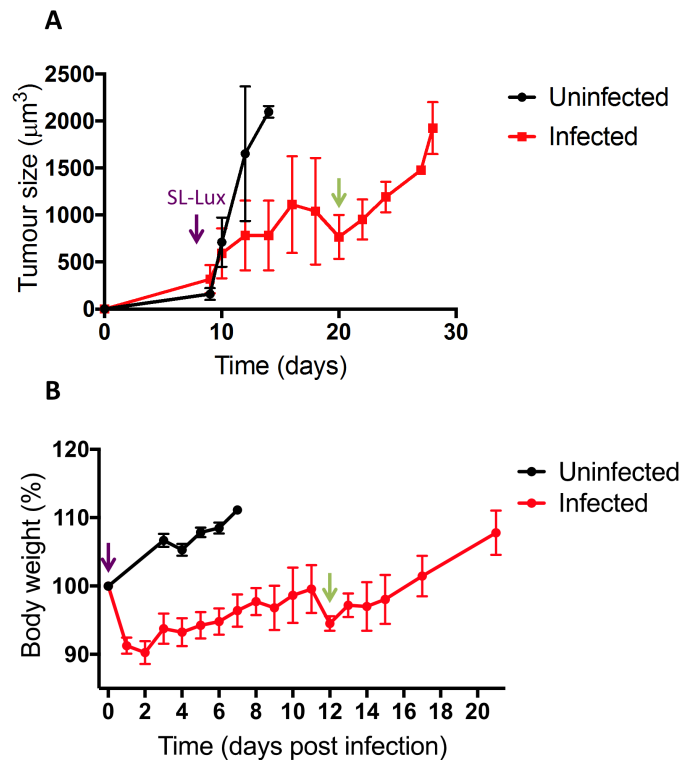


**Figure 9.1 Long term SL7207 infection in tumour-bearing mice**

Tumour-bearing mice were infected with SL7207 or PBS, and tumour size and body weights were measured over time. **A.** Tumour size of infected and uninfected mice as measured by Vernier calipers. **B.** Weight of mice expressed as a percentage of weight at Day 0 of infection. Purple arrows indicate time point at which SL7207 was administered. Green arrows indicate time point from which tumour size (top, 20 days post tumour cell inoculation, 11 dpi) and body weight (bottom, 12 dpi) started to increase.

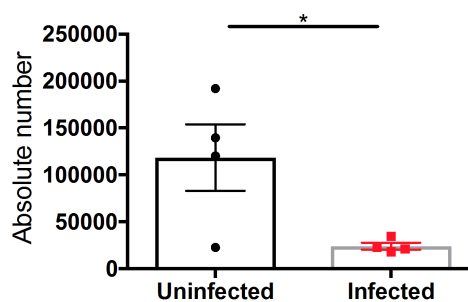


**Figure 9.2 Effects of SL7207 infection on size of tdLN**

Tumour-bearing mice were infected with SL7207 or PBS, and tdLNs were harvested 5 dpi for flow cytometry analysis of cell populations. Absolute cell number recovered from infected and uninfected tdLNs. Error bars SEM. Statistical analysis performed using Student's t test where  $p < 0.05^*$ .

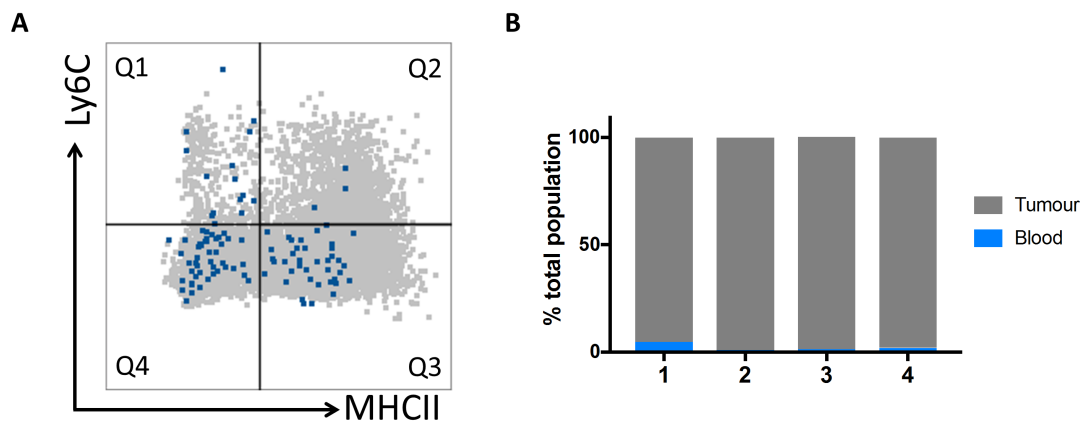


**Figure 9.3 Contribution of blood-borne monocyte/macrophages to total monocyte/macrophage population in tumour preparation**

Tumour-bearing mice were infected with SL7207. At 7 dpi, mice were intravenously injected with 6  $\mu\text{g}$   $\alpha\text{-CD45}$  FITC to assess the contribution of blood-borne cells to the populations designated as tumour resident cells. **A.** Representative flow cytometry plot with total monocyte/macrophage cells (grey) overlaid with  $\text{CD45FITC}^+$  monocyte/macrophages. Cells were gated on single, live,  $\text{CD45}^+$ ,  $\text{CD11b}^+$ ,  $\text{SiglecF}^-$ ,  $\text{F4/80}^+$ ,  $\text{Ly6G}^-$ . **B.** Data shown as the percentage of blood borne cells of total cells in a given population.

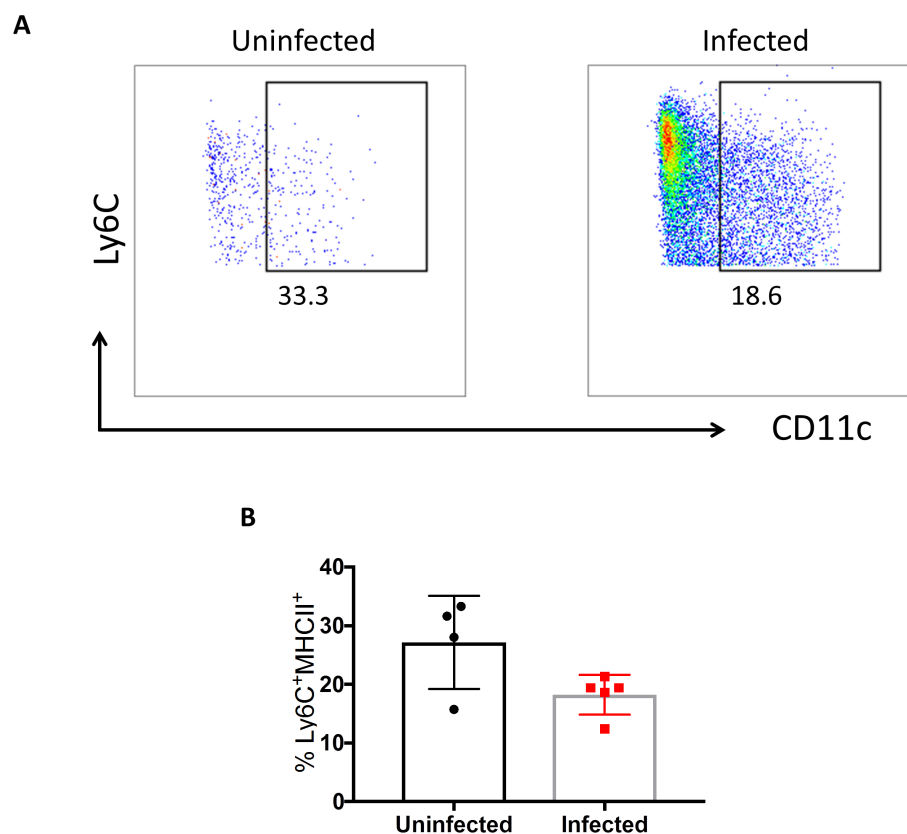


**Figure 9.4 CD11c expression in the  $\text{Ly6C}^+\text{MHCII}^+$  monocyte population following SL7207 infection**

Tumour-bearing mice were infected with SL7207 or PBS, and tumours were harvested at 7 dpi for flow cytometry analysis of immune cell populations. **A.** Representative flow cytometry plots showing the CD11c expression on  $\text{Ly6C}^+\text{MHCII}^+$  monocytes. Cells were gated on single, live,  $\text{CD45}^+$ ,  $\text{CD11b}^+$ ,  $\text{SiglecF}^-$ ,  $\text{F4/80}^+$ ,  $\text{Ly6G}^-$ ,  $\text{Ly6C}^+$ ,  $\text{MHCII}^+$ . **B.** Data shown as  $\text{CD11c}^+$  cells as a percentage of total  $\text{Ly6C}^+\text{MHCII}^+$  monocytes. Error bars SEM. Statistical analysis performed using Student's t test where  $p < 0.05^*$ .

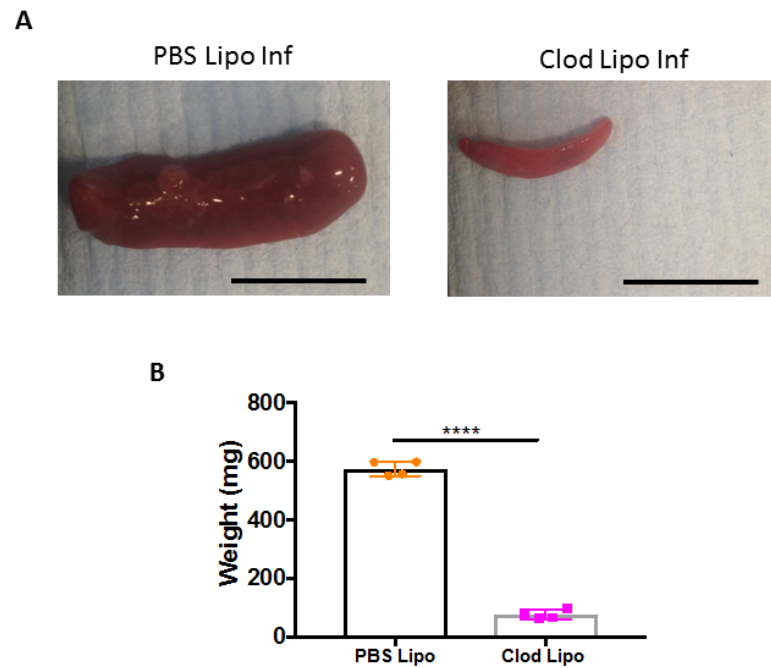


**Figure 9.5 Effects of Clod Lipo on spleens from infected tumour-bearing mice**

Tumour-bearing mice, intravenously injected with either PBS Lipo or Clod Lipo were also infected with SL7207. At 7 dpi, spleens were harvested. **A.** Representative images of tumours at 7 dpi following either PBS Lipo or Clod Lipo treatment. Scale bars 1 cm. **B.** Weights of spleens recovered from infected PBS Lipo and Clod Lipo-treated mice. Error bars SEM. Statistical analysis performed using Student's t test where  $p < 0.05^*$ ,  $p < 0.01^{**}$ ,  $p < 0.001^{***}$ ,  $p < 0.0001^{****}$ .